The application of geophysical modelling techniques to understand the subsurface morphology, eruptive history and magma volumes of maar volcanoes within the Newer Volcanics Province, South-Eastern Australia

By

Teagan N. Blaikie

A thesis submitted for the degree of

Doctor of Philosophy

Supervisors:

Dr. Laurent Ailleres

Associate Professor Peter G. Betts

School of Earth, Atmosphere and Environment

Monash University, Clayton, Victoria, Australia

October, 2014

Monash University

Declaration for thesis based or partially based on conjointly published or unpublished work

General Declaration

In accordance with Monash University Doctorate Regulation 17.2 Doctor of Philosophy and Research Master's regulations the following declarations are made:

I hereby declare that this thesis contains no material which has been accepted for the award of any other degree or diploma at any university or equivalent institution and that, to the best of my knowledge and belief, this thesis contains no material previously published or written by another person, except where due reference is made in the text of the thesis.

This thesis includes 2 original papers published in peer reviewed journals and 2 unpublished publications. The core theme of the thesis is the application of geophysical modelling techniques to understanding the subsurface morphology of maar volcanoes. The ideas, development and writing up of all the papers in the thesis were the principal responsibility of myself, the candidate, working within the School of Earth, Atmosphere and Environment under the supervision of Laurent Ailleres and Peter Betts.

The inclusion of co-authors reflects the fact that the work came from active collaboration between researchers and acknowledges input into team-based research.

In the case of chapters 2, 3, 4 and 5 my contribution to the work involved the following:

Thesis chapter	Publication title	Publication status	Nature and extent of candidate's contribution
2	Interpreting subsurface volcanic structures using geologically constrained 3-D gravity inversions: Examples of maar-diatremes, Newer Volcanics Province, southeastern Australia.	Published	87.5 % - Majority of data collection, processing, interpretation and manuscript preparation
3	A geophysical comparison of the diatremes of simple and complex maar volcanoes, Newer Volcanics Province, south-eastern Australia.	Published	87.5 % - Majority of data collection, processing, interpretation and manuscript preparation
4	Calculating the erupted volumes of tephra from maar volcanoes and their VEI magnitude: Examples from the late Cenozoic Newer Volcanics Province, south-eastern Australia	In preparation	87.5 % - Majority of data collection, processing, interpretation and manuscript preparation
5	Using sensitivity analysis to assess the ambiguity and variability of potential field models of maar-diatremes from the Newer Volcanics Province	In preparation	95 % - Majority of data collection, processing, interpretation and manuscript preparation

I have not renumbered sections of submitted or published papers in order to generate a consistent presentation within the thesis.

Signed: **Date:**

Contents

Chapter 3.

Chapter 4.

Chapter 5.

Chapter 6.

Appendices.

Digital Appendices (enclosed on CD).

1. PDF copy of this thesis.
2. Supplementary material chapter 2.
3. Supplementary material chapter 4.
4. Supplementary material appendix 1.
5. Geophysical data (includes oasis montaj project files, grids and geophysical databases).
6. 3D models and inversion data (Gocad projects and raw inversion files).
7. Petrophysical data.
8. High-heat geodynamic setting during the Palaeozoic evolution of the Mount Painter Province, SA, Australia: evidence from combined field structural geology and potential-field inversions.

List of Figures

Chapter 1.

Chapter 2.

Chapter 3.

Chapter 4.

Chapter 5.

List of Tables

Chapter 2.

Chapter 3.

Chapter 4.

Chapter 5.

Acknowledgements

The work completed in this thesis would not be possible without the knowledge and assistance of many other people and organisations.

Firstly I wish to thank my two supervisors, Laurent Ailleres and Peter Betts for your guidance, support, and for all the time and effort you put into helping me achieve and publish this work. You both provided the encouragement I needed to pursue my research independently, but were always there to provide technical assistance and feedback. I also wish to thank Ray Cas, for all his guidance, support and feedback on the volcanological aspects of this work.

Thank you to the members of my review panel; Ian Cartwright, Ray Cas and Roberto Weinberg, who always listened enthusiastically, and provided feedback on my confirmation, mid-candidature review and pre-submission seminars.

Several organisations have provided financial support for this research, and for conference attendance. Thanks to Monash University and the Australian Government for awarding me an APA scholarship, to the AusIMM for their research grant, and to the IAS and IAVCEI who provided generous travel grants to attend various conferences and workshops.

This work would not have been possible without everyone who gave up their time to assist with fieldwork. To everyone who helped out, thanks for being so enthusiastic and supportive, even after spending a few days walking through a swamp, standing in the pouring rain, being chased by cows and shocked by electric fences! Special thanks go to Felicity Piganis and Jackson van den Hove who were not scared away the first time, and came out with me on many different occasions! Thanks also go to Lucas Holden for loaning me a Differential GPS from RMIT for fieldwork, without it, I could not have obtained accurate data, and none of this thesis would have been possible!

During my time as a PhD student, I was fortunate enough to be a part of two research groups within the school who contributed to the development of this thesis. Thanks to all the members of the Structural Geophysics Group. The informal meetings we held each week were a great benefit, keeping me on track and providing advice and inspiration for my work. Special thanks go to Robin Armit, Brenton Crawford, Antoinette Stryk, Tom Carmichael, Jackson van den Hove, Dave Moore, Alan Aitken and Mark Lindsay and for all your advice and technical assistance over the last few years. Special thanks to Caroline Venn for her support and help organising travel and sorting out receipts.

Thank you also to all the members of Volcanology Research Group, who were another great source of advice and inspiration. Special thanks to Jozua van Otterloo for his advice and assistance on volume calculations, and to the rest of the research group who have/are working in the Newer Volcanics Province for all your helpful discussions; Simone Jordan, Julie Boyce, Janine Kavanagh, Jackson van den Hove and Felicity Piganis.

Thanks to all the administrative staff at the school who have helped me organise fieldwork and overseas travel and sort out all the paperwork that goes with it! To all the academic staff in the department, thank you for inspiring me to take up geology in my undergraduate degree, and continue on with postgraduate research. Thank you also for providing me the opportunity to demonstrate in your lab classes and field camps (and for the extra cash that goes with it!).

To Tom Carmichael, Jim Driscoll, Lucas Holden, Morena Salerno, Islay Laird and Shirin Seirafi, thanks for being such great officemates over the past few years, and for all of your friendships, support, tea breaks, coffee runs, and for watering my plant when I was away! Thank you to all the postgraduate students in the department for your friendship and support over the past few years, you have made this a great environment to work in, and I hope our paths will continue to cross again in the future!

Finally, and most importantly, thank you to my family for all their support and encouragement, I couldn't have done this without you!!

Abstract

Maars are the second most common terrestrial volcano on Earth, and although small, can exhibit great complexity in their eruptive histories. Much of the structure of a maar volcano lies beneath the surface in the form of a diatreme, a pipe-like structure which underlies the crater and is infilled with a mixture of fragmented juvenile and country rock material. The structure of the maar-diatreme (depth and geometry) reflects processes occurring during the eruption, such as phreatomagmatic explosions occurring at deep, shallow or varied levels (reflected in depth of the diatreme), migration of vents (coalesced diatremes) and transitions between eruption styles (presence of dykes and magma ponds). To fully appreciate these volcanic systems, it is necessary to have some understanding of the structure of the maar-diatreme; however, especially in young volcanic fields, they are not always exposed.

The Newer Volcanics Province (4.6 Ma-4.5 ka) is an intraplate, basaltic volcanic province comprised of over 400 monogenetic volcanoes, of which approximately 10% are maar volcanoes with no exposures of their diatremes. High-resolution ground gravity and magnetic data is acquired across the volcanic craters to image the depth and geometry of the maar-diatremes. Four case studies representing a range of sizes and eruptive styles were selected, and include the Red Rock and Mt Leura Volcanic Complexes, Ecklin Maar and the Anakies.

The geophysical models of these volcanic centres were produced from interpretations of gridded gravity and magnetic data, and from using forward and inverse modelling techniques (in 2D and 3D). The models were constrained by integrating data about the maars eruptive styles with measurements of rock density and magnetic susceptibility. However, because potential field models are non-unique, the aim of our modelling technique was to produce multiple models that are consistent with the available geologic and geophysical information. Sensitivity analyses were conducted to assess uncertainty in these models, and to delineate a range of end-member models based on the upper and lower bounds of the petrophysical constraints.

Geophysical modelling results suggest these maar volcanoes have broad, shallow diatremes, which form when phreatomagmatic explosions occur at shallow levels of the subsurface. Often, multiple vents are identified within these diatremes, and are possibly related to the weakly lithified host rock collapsing into and blocking the vent, causing it to migrate laterally. Some of these vents are aligned and form multiple, or coalesced craters, indicating vent migration is occurring along the length of a dyke. Other vents appear to be randomly distributed within the maar-diatreme, suggesting that dykes are propagating through the loose debris of the diatreme, causing vertical and lateral variations in the point of fragmentation.

Several geophysical trends were identified that correlate to the different eruptive styles of the case studies (i.e., dominantly phreatomagmatic, fluctuating between magmatic and phreatomagmatic, transitional between phreatomagmatic and magmatic). Maars with fluctuating eruptive styles (e.g., Red Rock Volcanic Complex) are characterised by short-wavelength positive gravity and magnetic anomalies superimposed on longer-wavelength gravity and magnetic lows. The irregularly distributed short-wavelength anomalies were reproduced during modelling as dykes and magma ponds within the maar-diatremes. The presence of these intra-diatreme dykes, and observations of fluctuating

eruptive styles, suggest the developing diatremes were not completely saturated with water during the eruption, which allowed to magma to fragment by either magmatic or phreatomagmatic styles when conditions were appropriate.

Maar volcanoes exhibiting predominantly phreatomagmatic activity (e.g., Ecklin and Anakie maar) are characterised by gravity and magnetic lows across the crater, but may contain broader-wavelength, low amplitude positive gravity and magnetic anomalies in the centre of the crater. Modelling indicates that these anomalies are associated with regions containing higher volumes of juvenile material within the diatreme, which is interpreted to represent the entrainment of debris jets into the diatreme fill during the eruption. Volcanic centres experiencing a transition in eruptive style from phreatomagmatic to magmatic (e.g., Mt Leura Volcanic Complex), are characterized by long-wavelength gravity and magnetic highs indicating a large volume of ponded lava infilled the maar crater during the eruption.

The total tephra and magma volumes associated with the eruption of these volcanoes can be calculated from the final geophysical models. Based on the average componentry and vesicularity of deposits in the maars ejecta-rims, the dense rock equivalent magma volume of the Ecklin maar, the Red Rock and Mount Leura volcanic complexes is 0.04×10^9 m^3, 0.17×10^9 m^3 and 0.29×10^9 m^3 respectively. The Red Rock and Mount Leura volcanic complexes have magma volumes that are an order of magnitude higher than Ecklin maar, and exhibit far more complex eruptive histories with multiple vents and transitions between explosive phreatomagmatic, magmatic explosive and effusive styles. Based on the total tephra volume, the Volcanic Explosivity Index (VEI) was estimated for each eruption. A VEI magnitude of 2 is assigned to the Ecklin maar, and 3 is assigned to the Mount Leura and Red Rock volcanic complexes.

Chapter 1.

Introduction

A summary of research aims and methods, maar-diatreme volcanism, and the regional geologic and tectonic history of south-eastern Australia

Cover page: Mount Leura Volcanic Complex.

1. Introduction

Predicting how an active volcano will behave requires an understanding of how similar volcanoes have erupted in the past. Achieving this requires careful observation and analysis of the products of volcanism and its surface and subsurface architecture. However, especially in young volcanoes, observations of volcanic products can be largely restricted to surface exposures, with much of the volcano lying beneath the surface where it cannot be directly observed. Where a volcano has been deeply eroded, it is possible to examine its subsurface structure, however the edifice is often eroded away. When only part of the volcanic edifice is examined, it can be difficult to completely understand the volcano because features observed at the surface cannot be linked with structures in the subsurface. Geophysical modelling techniques offer a solution to this problem, and can be applied to young or partially eroded volcanoes to image their subsurface structures, providing details on the volcanoes feeder system, vent locations and conduit geometry.

As data acquisition and modelling techniques have improved, geophysical methods are being increasingly applied to active and inactive volcanoes to aid in monitoring activity and understanding the three-dimensional structure and morphology of the underlying vent system (e.g., Rout *et al.* 1993; Camacho *et al.* 1997; Brunner *et al.* 1999; Araña *et al.* 2000; Kauahikaua *et al.* 2000; Finn and Morgan 2002; Lindner *et al.* 2004; Schulz *et al.* 2005; Montesinos *et al.* 2006; Blanco-Montenegro *et al.* 2007; Cassidy *et al.* 2007; Gottsmann *et al.* 2008; Lopez Loera *et al.* 2008; Mrlina *et al.* 2009; Paoletti *et al.* 2009). A range of geophysical modelling techniques are available, with different methods being able to resolve different properties of the volcanic substrate. This research focusses on applying potential field modelling techniques to understand the subsurface architecture of monogenetic volcanoes, and in particular maar volcanoes, whose structure lies largely in the subsurface and is strongly influenced by external conditions such as host rock rheology and groundwater availability.

Monogenetic volcanoes are among the most common type of subaerial volcanoes found on Earth (Wood 1980; Cas and Wright 1987; Wohletz and Heiken 1992; Lorenz 2007), forming in clusters as a volcanic field (e.g., the Newer Volcanics Province, Auckland Volcanic Field) or on the flanks of larger polygenetic volcanoes (e.g., Mauna Kea, Hawaii) (Connor and Conway 2000). Monogenetic volcanoes only erupt once and are fed from small volumes of magma, but can exhibit great complexity in their surface and subsurface architecture. They evolve from a variety of eruptive styles (e.g., effusive, Hawaiian fire-fountaining, Strombolian to violent Strombolian, Phreatomagmatic and Surtseyan), which form different types of volcanic edifices (e.g., spatter cone, scoria cone, maar, tuff ring, tuff cone, lava shield). Often, many monogenetic systems form composite edifices as a result of fluctuations in their eruptive styles triggered by external factors such as magma and/or groundwater supply, conduit geometry and magma composition (Kereszturi and Németh 2012). Maar volcanoes, and their characteristic phreatomagmatic eruptive style are the most hazardous type of eruption within a monogenetic volcanic field (Lorenz 2007). They are highly explosive and capable of producing lethal base surges and ejecting fine ash into the atmosphere, which create volcanic hazards on the time frame of hours to weeks.

Maar volcanoes are the second most common volcano type in the world (Wohletz and Heiken 1992) and form when subsurface phreatomagmatic explosions excavate a deep crater cut below the pre-eruptive surface (Lorenz 1986, 2003; Lorenz and Kurszlaukis 2007; White and Ross 2011). A pipe-like structure, called a diatreme, underlies the crater and is filled with a mix of fragmented juvenile and country rock material (Lorenz 1986; White and Ross 2011). The structure of the diatreme reflects processes occurring in the subsurface, such as explosions occurring at deep, shallow or varied levels (reflected in depth of the diatreme), migration of vents (coalesced diatremes) and transitions between eruption styles (presence of dykes and magma ponds) (White and Ross 2011; Valentine and White 2012). There have been only several eruptions of maar volcanoes witnessed in modern history (e.g., Ukinrek; Kienle *et al.* (1980), Nilahue; Muller and Veyl (1957), Lake Taal; Moore *et al.* (1966), Ambrym; Németh and Cronin (2011) and Tarawera; Nairn (1979)), however they do represent the greatest hazard within monogenetic volcanic fields. With the encroachment of modern society onto the fringes of many of these fields (e.g., Auckland, Melbourne, Mexico-City), it is crucial to better understand how maar volcanoes have erupted in the past which will help predict how they might behave in future eruptions.

Due to the subsurface nature of phreatomagmatic explosions, much of a maar volcano (i.e., the diatreme) lies beneath the surface, so observations of both surface and subsurface features are required in order to fully understand the eruption of these volcanoes. In young volcanic fields, such as the Newer Volcanics Province, it is not possible to link surface observations with subsurface structures because the field has not eroded to a level where the subsurface structures can be observed.

To overcome this problem, high-resolution ground gravity and magnetic data is used to model the subsurface architecture of several maar volcanoes located within the Newer Volcanics Province of Western Victoria. The maar volcanoes surveyed represent a range of the different sizes and styles of eruptions observed within maar volcanoes of the Newer Volcanics Province and include the Red Rock Volcanic Complex, Mount Leura Volcanic Complex, Ecklin maar, and the Anakie maar. A workflow for applying two-dimensional forward and three-dimensional inverse modelling of gravity and magnetic data is developed to reveal details on the depth, geometry and petrophysical property distributions within subsurface volcanic structures. The ambiguity of these models are considered, and the aim of our modelling technique is to produce a range of geophysical models through different inversion styles that are both geologically meaningful and consistent with the available geologic information, rather than seeking a single 'ideal' solution. In addition to an improved understanding the subsurface morphology and eruptive history of these volcanoes, the geophysical models are used to estimate the total magma involved in the eruption which is an important constraint for future spatio-temporal studies and hazard assessment.

1.1 Thesis aims

The main aims and research questions of this thesis are:

- To determine if gravity and magnetic data is capable of imaging the root zone of a volcanic system.
- To develop a workflow for interpreting potential field data acquired across volcanoes.
- To determine the depth and geometry of maar-diatremes within the Newer Volcanics Province using forward and inverse potential field modelling techniques.
- To conduct a sensitivity analysis of the geophysical models to understand the ambiguity of the interpretations, and the range of geologically and geophysically possible models.

- To understand how the host rock is affecting the geometry of maar-diatremes within the Newer Volcanics Province.
- To reconstruct the eruptive history of the case studies and determine any relationships between the geophysical signature, subsurface structures and eruptive styles of the maars.
- To calculate the magma and erupted tephra volume of the case studies, and then estimate their Volcanic Explosivity Index.

1.2 Thesis Structure

This thesis has been structured into an introduction and geologic background chapter, four research chapters and a discussion and conclusions chapter. Monash University permits PhD theses to be structured as a collection of submitted research papers, and each research chapter has been structured as a scientific journal article. This results in the repetition of background material in each chapter (e.g., regional geology and method). Chapters 2 and 3 are published, and 3 and 4 are in preparation. The content within chapters 2 and 3 of this thesis is identical to the published version, however in order to maintain a consistent formatting throughout the thesis, referencing and grammatical styles may vary slightly.

Chapter 1 introduces the research topics and presents important background information for the rest of the thesis including summaries on monogenetic volcanism, the current understandings of maar-diatreme volcanism, previous works on the thesis research topics, and introduces the geologic, geophysical and tectonic setting of the Newer Volcanics Province. The geology of the four case studies: Ecklin maar, Red Rock Volcanic Complex, Mount Leura Volcanic Complex and the Anakie's is introduced in this chapter and expanded upon in the relevant research chapters.

Techniques for modelling the internal structures of volcanoes using gravity and magnetic data is the subject of Chapter 2, entitled '*Interpreting subsurface volcanic structures using geologically constrained 3D gravity inversions, examples of maar-diatremes from the Newer Volcanics Province, southeastern Australia*'. This chapter is published in the *Journal of Geophysical Research: Solid Earth*, and focuses on how different inversion styles can resolve subsurface volcanic structures, and what can be learned about their eruptive histories from geophysical modelling. Results are drawn from several case studies of maar volcanoes located within south-eastern Australia, where the subsurface morphology, including the diatreme, dykes and feeder vents were modelled to better understand eruptive processes and the volcanoes evolution. Geologic data is integrated into each stage of modelling to constrain the inversion process and ensure that results are geologically realistic. However since potential field models suffer from non-uniqueness, this chapter also presents techniques on how to assess model ambiguity and calculate a range of model geometries for properties varied between their upper and lower bounds.

Chapter 3 expands upon the results introduced in chapter 2 and presents the geophysical models of the four case studies: Ecklin maar, Red Rock Volcanic Complex, Mount Leura Volcanic Complex and the Anakie's. This paper is titled: '*A geophysical comparison of the subsurface morphology of simple and complex maar volcanoes*' and is published in the *Journal of Volcanology and Geothermal Research*. This chapter describes the eruptive history and subsurface morphologies of the case studies. The eruptive histories of the case studies were determined from the integration of geologic data and geophysical modelling. This chapter focuses on what was learned about eruptive processes from the interpretation of geophysical data, including lateral and vertical vent migration and fluctuations in eruptive styles. A guide is provided for recognizing different eruptive styles based upon the geophysical response for future interpretations of potential field data sets over maar volcanoes.

Chapter 4 is titled '*Calculating the erupted volumes of tephra from maar volcanoes and their VEI magnitude: Examples from the Late Cenozoic Newer Volcanics Province, south-eastern Australia*' and uses the results of the geophysical models presented in chapters 2 to 3 in order to calculate the volume of magma associated with an eruption of a maar volcano. The volume of country rock present in the ejecta rims versus that which remains in the diatreme is considered and helps validate the geophysical models. The volcanic explosivity index (VEI) of the case studies is estimated from the magma and deposit volumes.

Chapter 5 is titled: '*Using sensitivity analysis to assess the ambiguity and variability of potential field models of maar-diatremes from the Newer Volcanics Province*' and focuses on examining each of the models described in chapters 2 and 3, to assess each model for ambiguity and sensitivity to changes in its properties and geometry.

Chapter 6 links the results of the thesis in a discussion and conclusions chapter. The major results of each chapter are summarised and placed into a broader context where the implications of the results are considered. Areas requiring further research are identified and described at the end of this chapter.

Appendix 1 includes a paper entitled: '*Three-dimensional potential field modelling of a multi-vent maar-diatreme - the Lake Coragulac maar, Newer Volcanics Province, south-eastern Australia*' which was published in the *Journal of Volcanology and Geothermal Research*. This paper presents background material for this thesis, including a preliminary discussion on the geophysical methods used, as well as some geologic data and a geophysical interpretation of a maar within the Red Rock Volcanic Complex. Although this paper was prepared concurrently with this thesis, it is included in the appendices since the bulk of the research was conducted for the award of an honours degree.

1.3 Research Methods

The methods used to conduct this research are listed below and described in detail in the relevant chapters of the thesis:

- **Fieldwork**: includes the acquisition of gravity and magnetic measurements across the maar craters which will be used to model their subsurface structures, and the collection of samples for magnetic susceptibility and density measurements which will be used to constrain the geophysical models.
- **Data processing**: Corrections must be applied to the acquired gravity and magnetic data sets prior to interpretation to remove effects from sources (e.g., topography) unrelated to the geology. The corrected data is then gridded and interpreted alongside regional scale data sets including aeromagnetic, gravity, Lidar and digital elevation models.
- **Modelling**: involves 2.5D forward and 3D inverse modelling of the gravity and magnetic response to model the subsurface morphology of the maar-diatreme, and the distribution of properties (density/magnetic susceptibility) within it. These models can assist in identifying the number and location of vents within the maars which is important for understanding the

eruptive processes of maar volcanoes and the volcanic hazards of another maar eruption in the region.

- **Sensitivity Analysis**: The potential field models suffer from non-uniqueness, so a sensitivity analysis is conducted to understand how uncertainty in the models input parameters affects the final model. This involves testing the preferred geophysical models using forward and inverse modelling techniques to determine a range of models that satisfy the observed geophysical and geologic data.
- **Volume calculations**: The volumes of the maar-diatremes can be calculated from the 3D models produced during geophysical modelling, and the volume of the ejecta rim is estimated by integrating data from boreholes and high resolution digital elevation models. The total volume of magma involved in the eruption of each of the maar volcanoes can then be estimated based upon the componentry of the ejecta rims. This data will allow an estimation of the volcanoes VEI.

2. Introduction to maar-diatreme volcanism

Maars are a small, monogenetic volcano characterised by a crater cut below the pre-eruptive ground surface and surrounded by a low tephra ring (Lorenz 1986; White and Ross 2011). They are the second most common sub-aerial volcano after scoria cones, and are common to basaltic volcanic fields, but can form in a diverse range of settings from a variety of magma compositions (White and Ross 2011). Maars are the result of explosive magma-water interaction occurring in the subsurface, which excavates a deep crater and forms a diatreme, a pipe-like structure underlying the crater and are infilled with a mix of fragmented juvenile material and country rock debris (Lorenz 1986). A maar-diatreme can be subdivided into three zones; the upper diatreme, lower diatreme, and the root zone (Figure 1; White and Ross 2011). The upper diatreme is characterised by inwardly dipping bedded lapilli tuffs and tuff breccias. The lower diatreme is composed of massive tuff breccias, which may be cross-cut by subvertical tuff breccias with different clast compositions, and fragmented domains of country rock. The root zone consists of volcaniclastic deposits that may be cross-cut by irregularly shaped intrusions and surrounded by country rock breccias (White and Ross 2011).

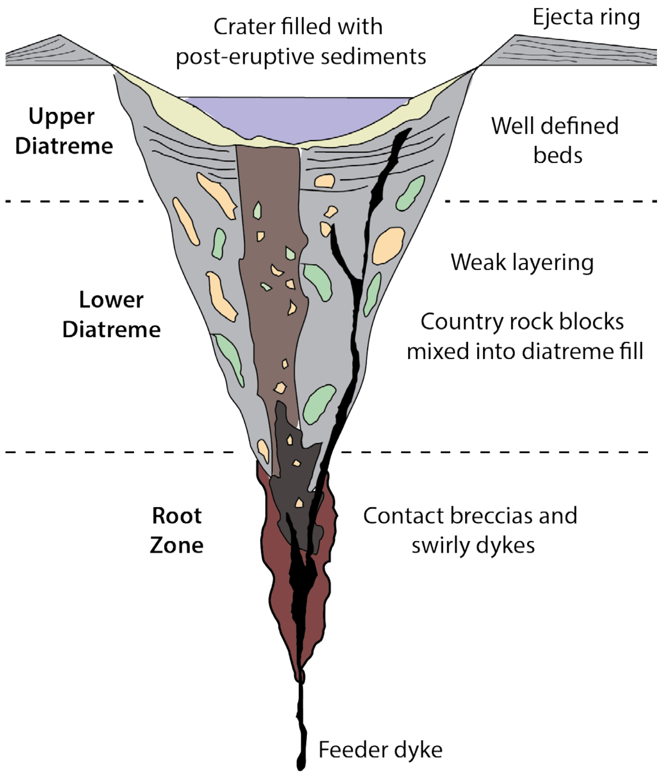

Figure 1. Structure of a maar-diatreme and the characteristics of the different zones recognised within it (Modified after White & Ross 2011).

There are only a few examples of historical maar eruptions (e.g., Ukinrek; Kienle *et al.* (1980), Nilahue; (Muller and Veyl 1957), Tarawera; (Nairn 1979), Lake Taal; (Moore *et al.* 1966), and Ambrym; (Németh and Cronin 2011)), but they represent the greatest hazard within monogenetic volcanic fields. It is therefore important to understand how they form and what influences the eruption of a maar volcano. A brief review of the most widely accepted models, and new developments in understanding the formation of maar volcanoes is provided below and expanded upon in later chapters.

2.1 The 'Lorenz Model'

A long-standing model on the formation of maar-diatreme volcanoes was established by Lorenz (1986) and refined by later works (e.g., Lorenz 2003; Lorenz and Kurszlaukis 2007). In this model, magma rises through the crust and interacts explosively with groundwater through molten fuel-coolant interaction (MFCL; Büttner and Zimanowski 2003) as it nears the water table (Figure 2a). These explosions are termed phreatomagmatic, which in this model are initially thought to occur at shallow levels close to the water table. Lorenz (1986) reports that the level at which magma can explosively interact with groundwater is restricted to a hydrostatic pressure barrier <20-30 bars, so at increasing depths, phreatomagmatic explosions are inhibited. The location of explosive activity will propagate downward as MFCL uses up shallow groundwater, and overlying rock is ejected from the crater which results in a lowering of the hydrostatic pressure and depth of the water table (Figure 2b-c).

Initial phreatomagmatic explosions will create a small crater with an ejecta rim and underlying diatreme (Figure 2a). As the eruption proceeds, large volumes of rock are excavated from above the point of magma-water interaction, and deposited in the surrounding ejecta rim or floor of the diatreme (Figure 2b-c). As the point of magma-water interaction deepens, the diatreme widens by subsidence and early deposits may collapse into the crater and contribute to the diatreme. The deepening of the location of magma-water interaction causes country rock lithics derived from progressively deeper levels to be ejected from the diatreme and deposited in the surrounding ejecta rim.

The Lorenz model explains many of the characteristics of diatremes and deposits in the ejecta rim, however, it fails to explain several key observations or processes that recent studies have shown to occur within maar-diatremes. Valentine and White (2012) summarise the flaws identified in the Lorenz model:

- Deep-seated lithics are sometimes present in ejecta rim deposits, however recent studies (e.g., Lefebvre *et al.* 2013) suggest most lithic material is derived from the upper few hundred metres.
- As explosions occur at progressively deeper levels, a pathway through the increasingly thick diatreme fill is required to eject material from the crater.
- The progressive drawdown of the water table must be balanced with the magma flux into the system.
- The geometry of the crater is a result of subsidence during the eruption.

2.2 Revised model

Valentine and White (2012) presented a new conceptual model for the formation of maar-diatreme volcanoes, building upon the strengths of the Lorenz model and addressing the flaws described above. This model is still being refined with new information from analogue experiments and studies of exposed diatremes (e.g., Lefebvre *et al.* 2013; Ross *et al.* 2013; Graettinger *et al.* 2014; Valentine *et al.* 2014).

Valentine and White (2012) suggest a new mechanism for diatreme formation (Figure 2d-f), where magma rises in a dyke, and explosive magma water interaction can occur at any depth where conditions for MFCL are met (i.e., water pressure is below a critical pressure; Büttner and Zimanowski (2003)), but are most efficient above a depth of 1 km. Shallow explosions are more likely to erupt, and will excavate a small crater which is underlain by a protodiatreme. The protodiatreme is comprised of the crater and debris fill in the upper few hundred metres, and below this, there may be small regions of breccia and peperite adjacent to the feeder dyke (Figure 2d).

As the eruption continues, the diatreme grows in both width and depth, typically growing faster at its top and relatively slower at its bottom because of the increased efficiency of MFCL and reduced rock strength at shallower depths. This results in more efficient explosions damaging larger volumes of the surrounding host rock. Additionally, collapse of diatreme and crater walls near the surface facilitates further widening of the crater and diatreme. Phreatomagmatic explosions may be occurring at any depth, but will typically only eject material from the crater when explosions are shallow (Figure 2e; Lefebvre *et al.* 2012; Lefebvre *et al.* 2013; Graettinger *et al.* 2014). Dykes may extend into the fill of the diatreme, which due to its heterogeneous and unconsolidated nature result in irregular shaped intrusions. These dykes form new sites for phreatomagmatic explosions in what is termed an ‘intra-diatreme fragmentation zone’ (White and Ross 2011). The observations of deeper lithics fragments in the ejecta rims of maar volcanoes (Lorenz 1975, 1986) must therefore have been driven upwards through the diatreme through progressive mixing due to explosion jets, and only ejected from the crater from shallow seated explosions.

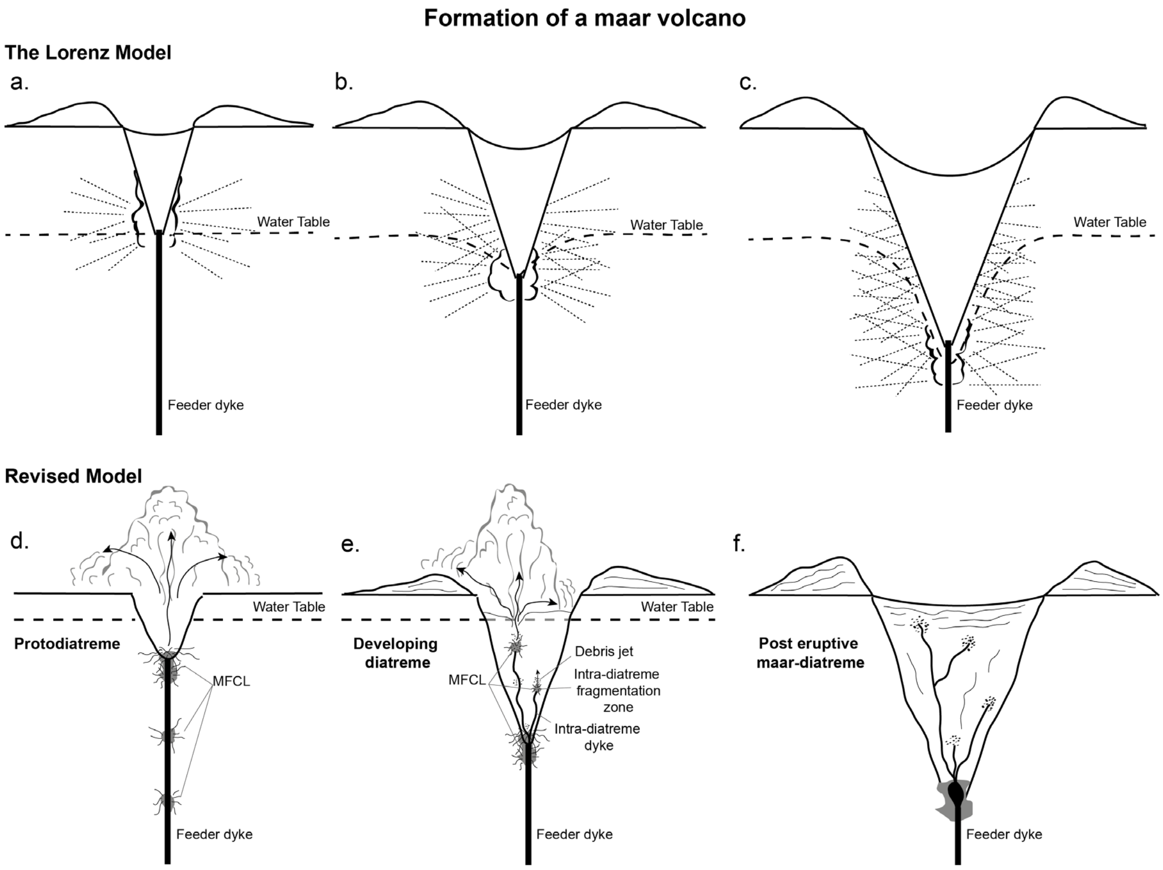

Figure 2. The Lorenz and revised model for the formation of maar-diatreme volcanoes (Modified after Lorenz 1986; Valentine & White 2012).

During the eruption, the diatreme fill which is comprised of country rock breccia and juvenile material, is mixed through the diatreme by two main processes. Firstly, explosions occurring within the root zone or at intra-diatreme fragmentation zones drive material upwards in debris jets, which is replaced by material flowing downwards. Secondly, material within the diatreme, or the diatreme walls can be disrupted by explosions, and may be temporarily liquefied where it can subside into the diatreme fill (Valentine and White 2012). Sometimes, larger slabs of country rock remain intact, forming 'floating reefs' within the diatreme (Lorenz and Kurszlaukis 2007), while others break apart and are progressively mixed into the diatreme by these processes. Any intra-diatreme dykes which were emplaced into the diatreme early in the eruption are usually broken up, and mixed through the diatreme by these processes. The only intra-diatreme dykes preserved intact are the ones typically emplaced later in the eruption (Valentine and White 2012).

Important contributions to this evolving model for the formation of maar volcanoes have recently been made through recent studies of exposed diatremes and analogue experiments. Studies of exposures of various levels of the diatreme and have recognised that fragmentation is occurring at any depth within the diatreme, and not every explosion will eject material from the vent to be deposited in the ejecta rim (White 1991; Lefebvre *et al.* 2012; Lefebvre *et al.* 2013). Recent analogue experiments simulating the formation of a maar crater support these results and demonstrate that maar-diatremes likely form from a combination of explosions occurring at various levels of the diatreme, and that material in the ejecta rim is typically only derived from shallow (above 200 m) explosions (Graettinger *et al.* 2014; Valentine *et al.* 2014).

2.3 Morphology of maar-diatremes in hard and soft rock settings

The structure of the maar-diatreme can be affected by the physical behaviours of the host rock when subjected to the forces of intense phreatomagmatic explosions. There are two distinct end-member environments relating to the formation of maar volcanoes and the availability of groundwater for phreatomagmatic explosions (Lorenz 2003). Hard rock environments, where groundwater is typically located within joints and fractures, and soft rock environments where groundwater is stored within the pores of the sediments. Commonly, these environments exist together where water-saturated, poorly consolidated sediments overly a crystalline basement (Lorenz 2003).

Maars formed in soft-rock environments, especially where sediments are unconsolidated, tend to have broad and shallow diatremes (Figure 3a), and commonly contain multiple vents. Broad shallow diatremes are a result of water saturated sediments allowing phreatomagmatic explosions to remain at shallow levels, rather than propagating downwards as groundwater dries up (Lorenz 2003; Auer *et al.* 2007; Ross *et al.* 2011). Additionally, the

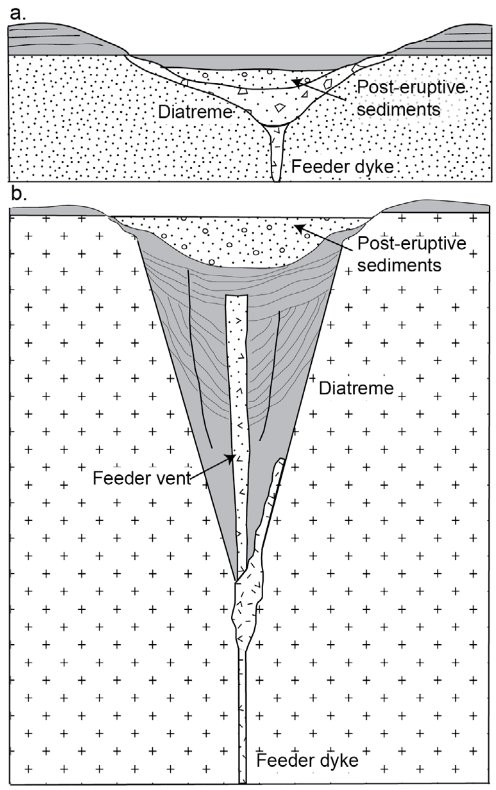

Figure 3 Different morphological structure of maars located within a) soft rock, and b) hard rock environments (Figures adapted from Németh & Martin (2007) and Lorenz (2003)).

shockwaves generated by phreatomagmatic explosions can cause liquefaction of the host sediments, which then flow into the diatreme, providing further influx of water and widening the crater in the process (Auer *et al.* 2007). The collapse of the host rock into the maar-diatreme can contribute to the formation of multiple vents within these volcanoes, as material flows into and blocks the vent, causing it to migrate and erupt in a new location (Martín-Serrano *et al.* 2009; Ort and Carrasco-Núñez 2009; Ross *et al.* 2011).

Maar-diatremes in hard rock environments tend to be deeper and narrower than those seen in soft rock settings (Figure 3b), which in the Lorenz model for diatreme growth, has been attributed to shallow groundwater drying out, resulting in the downward propagation of phreatomagmatic explosions (Lorenz 1986). The increased strength of the host rock means more steeply dipping diatreme walls can be sustained before they will collapse into the vent.

2.4 Application of geophysical techniques to understand maar-diatremes

The structure and morphology of maar volcanoes makes them well suited for geophysical modelling (Cassidy *et al.* 2007; Blaikie *et al.* 2012). They lend themselves to this application because they have suitable rock property contrasts with their surroundings, and typically have a relative flat topography which makes them accessible for high-resolution ground based surveys. A range of geophysical techniques, each with their pros and cons, have previously been applied to resolve different subsurface features of maar volcanoes, including electrical (conductivity, resistivity and self-potential), seismic, gravity and magnetics.

Potential field techniques are commonly applied to understand the subsurface architecture of maar volcanoes. The crater sediments and diatreme infill will usually have a density lower than the surrounding country rock, resulting in a gravity low (Cassidy *et al.* 2007; Blaikie *et al.* 2012), while the magnetic signature could consist of either magnetic highs or lows depending on componentry of the diatreme and susceptibility of the country rock. Heterogeneity in the composition of the diatreme, such as juvenile-rich zones and intra-diatreme dykes (e.g., Lefebvre *et al.* 2013) may exhibit a higher density and magnetic susceptibility than their surroundings, resulting in subtle gravity and magnetic highs, superimposed on the gravity and magnetic low due to the diatreme and crater.

Electrical methods have limited depth penetration (several to 10's of metres), but are a useful complement to other techniques, and are often applied in conjunction with gravity and magnetic surveys (e.g., Mrlina *et al.* 2009; Skacelova *et al.* 2010; Bolós *et al.* 2012). In an electrical survey, dykes and unweathered juvenile-rich breccias/volcanoclastics may stand out as highly resistive bodies whereas weathered volcanoclastics will have a low resistivity (Skacelova *et al.* 2010). Complementary gravity, magnetic and resistivity surveys were used by Skacelova *et al.* (2010) to image the upper most section of the partly preserved, Hnojnice and Rychnov maar-diatremes (northern Czech Republic) and distinguish the boundaries between volcanic breccia, dykes and the host rock of the maar. Bolós *et al.* (2012) applied self-potential and electrical resistivity methods to the La Crosa de Sant Dalmai maar in the Catalan Volcanic Zone (north-east Spain). Modelling of these data sets identified the depth to the maar-diatreme (below scoria cone and post-eruptive sediments), the presence of a buried lava flow, and identified a lineament which was interpreted as a fault that may have influenced the location of a nested scoria cone within the maar crater.

Seismic surveys are very effective at imaging lake sediments within the crater and horizontal layering in the upper parts of the maar-diatreme. Refraction and reflection surveys have been conducted over several maar volcanoes including the Baruth maar and the Messel Pit (Germany; Schulz *et al.* (2005)), and Laguna Potrok Aike (Argentina; Gebhardt *et al.* (2011)). The use of seismic methods in this application is limited due to its inability to image steep structures, which makes it difficult to define the lateral boundaries of the crater and steep edges of the maar-diatreme (Schulz *et al.* 2005; Buness *et al.* 2006).

The advantage of potential field techniques over electrical and seismic methods is its ability to image both deep, and steeply dipping structures, although it does has its disadvantages in that models are non-unique. Previous work modelling maar volcanoes using potential field data has utilised ground or airborne magnetic data combined with high resolution gravity data (Rout *et al.* 1993; Lindner *et al.* 2006; Cassidy *et al.* 2007; Lopez Loera *et al.* 2008; Mrlina *et al.* 2009; Skacelova *et al.* 2010; Bolós *et al.* 2012). For example, Cassidy *et al.* (2007) was able to model shallow diatremes and basaltic magma ponds of several volcanoes within the Auckland Volcanic Field. Skacelova *et al.* (2010) and Lindner *et al.* (2006) were able to produce slightly more complex models of maar-diatremes and their feeder dykes, however, these examples are restricted to interpretation of gridded data, and some 2D forward modelling. The work of Blaikie *et al.* (2012) represents the first attempt using three-dimensional inversion techniques to model the internal structures of maar-diatremes.

The techniques described above are being increasingly applied to understand the morphology of maar-diatremes. However, they are routinely applied in the exploration for kimberlite pipes which show similarities to maar-diatremes (Lorenz 1986; White and Ross 2011). Airborne methods such as electromagnetics, magnetics, radiometrics and more recently gravity gradiometry are the most common techniques used during exploration, while ground-based gravity, magnetics, resistivity and occasionally seismic refraction and reflection are used to follow up on targets identified in regional scale surveys (Macnae 1995; Smith *et al.* 1996; Rajagopalan *et al.* 2007).

The geophysical response of kimberlites can be highly variable depending on age and degree of weathering. They typically display roughly circular magnetic anomalies, but exhibit a strong remanent component and could have either a normal or reversed polarity (Kamara 1981; Macnae 1995). Heavily weathered kimberlites may have a low to non-magnetic response, but will typically exhibit a high conductivity, especially in the upper section of the pipe (Macnae 1979, 1995; Smith *et al.* 1996). Unweathered diatremes can be quite resistive and exhibit large magnetic responses. The density, and therefore gravity response of a kimberlite can also vary with weathered kimberlites typically having a density lower than its host rock, resulting in a gravity low. Unweathered kimberlites can have a higher density than its host rock, resulting in a gravity high (Macnae 1995).

3. Regional geologic and tectonic setting of south-eastern Australia and the Newer Volcanics Province

This section discusses the occurrence of volcanism within eastern Australia, the regional tectonic setting and evolution of the basement to the Newer Volcanics Province, and introduces the case studies examined in more detail in later chapters.

3.1 Volcanism in Eastern Australia

The eastern margin of Australia has experienced episodic intraplate volcanic activity since the break-up of Gondwana and rifting of Australia from Antarctica and the Lord Howe Rise between 95-50 Ma (Johnson 1989; Cas *et al.* 1993; Cas *et al.* 2011). Volcanic products extend 4400 km along the eastern margin of Australia, from the Maer Islands, through the Cape York Peninsula and Great Dividing Range to Victoria, Bass Straight and Tasmania (Figure 4; Johnson 1989). The youngest products of volcanism occur in Northern Queensland (~13 ka; Stephenson 1989), and South Australia (~5 ka, Mt Gambier; Van Otterloo and Cas 2013).

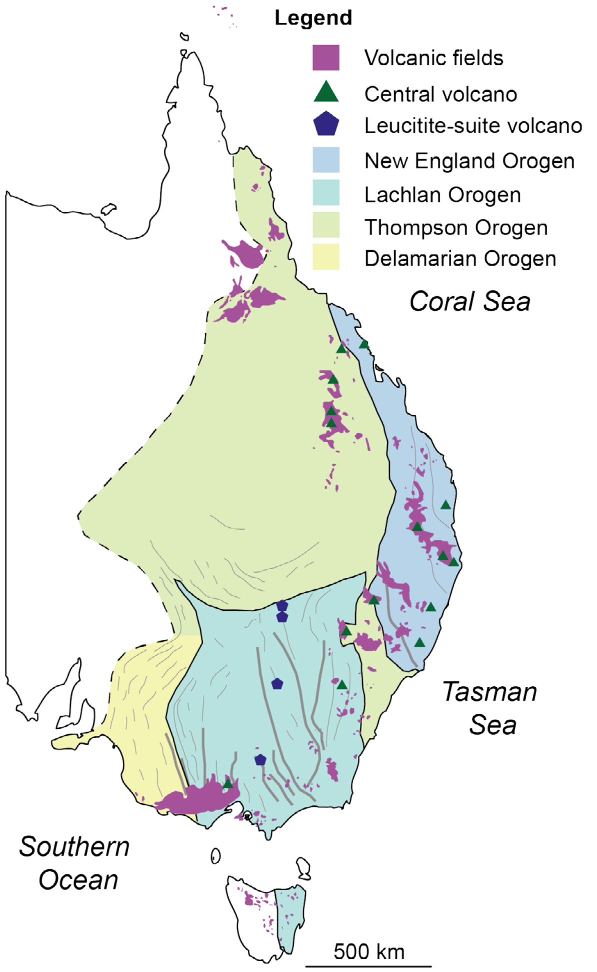

Figure 4. Distribution of volcanic fields, central and leucitite suite volcanoes along the eastern margin of Australia (modified after Johnson 1989), overlain on the Palaeozoic orogens (modified after Gray et al. 2003).

Volcanic activity along the eastern margin of Australia is interpreted to have initially originated due to close proximity to the active rifts within the Coral and Tasman Sea's and the Southern Ocean. However, as the Australian continent migrated away from the active spreading centres, volcanic activity occurring through to the Late Cenozoic could no longer be directly related to mantle activity associated with rifting. Wellman (1983) and Johnson (1989) proposed that volcanism could be related to intraplate hotspots or hotlines, which would account for the south-ward age progression of the central volcano systems. However; this model fails to account for the lava fields, which show no systematic age progression, and in some cases, the axis of volcanic activity is not aligned parallel to the proposed hotspot trail (Duncan and McDougall 1989; Price *et al.* 1997; Price *et al.* 2003).

Wellman and McDougall (1974) defined three main types of volcano occurring in eastern Australia; central volcanoes, lava fields and leucitite suite volcanoes. Central volcanoes, erupting from central or closely spaced vents are predominantly basaltic in composition, although some felsic examples have been recognised. The youngest central volcano system in eastern Australia is the Macedon-Trentham group of central Victoria (Wellman and McDougall 1974; Duncan and McDougall 1989). Lava fields, such as the Newer Volcanics Province of western Victoria, consist of extensive but usually thin lava flows, derived from dyke and pipe conduit systems. Vents are spread over distances of 100's km, with fields also containing many small cones, tuff rings and maars. The leucitite-suite volcanics are confined to central New South Wales and northern Victoria, and consist of intrusions and rare lava flows.

The youngest lava fields and central volcano systems are located in south-eastern Australia where volcanism has occurred intermittently since the Late Cretaceous. Three main periods of volcanism are recognised which form the Older Volcanics, Macedon-Trentham Group, and Newer Volcanics Province (Price *et al.* 2003).

The Older Volcanics (95-19 Ma, peaking between 42-57 Ma) are mostly located within Eastern Victoria, although a few occurrences have been recognised within the Otway Ranges. Products of volcanism are mostly eroded and weathered lava cones, fields and valley flows with compositions varying from nephelinites to qz-tholeiites (Day 1989).

Located northwest of Melbourne, the Macedon-Trentham Province (7-6 Ma) represents the second youngest peak in volcanism. Volcanic products consist of sub-aerial lava flows, domes and plugs with compositions ranging between K-rich basanite, alkali basalt, trachybasalt, basaltic trachy-andesite and trachyte, and includes the only occurrence of Cainozoic felsic rocks in Victoria (Knutson and Nicholls 1989).

The Newer Volcanics Province (4.6 Ma – 5 ka) represents the youngest peak of volcanism to occur within south-eastern Australia and is comprised of well-preserved lava plains and over 400 monogenetic volcanic edifices (Joyce 1975; Cas 1989; Knutson 1989; Cas *et al.* 1993; Cas *et al.* 2011). Volcanic products range in composition from subalkaline tholeiites and icelandites to alkaline hawaiites and basanites (Nicholls and Joyce 1989). Volcanism within the region shows no systematic age progression and interestingly, volcanism commenced and has continued to occur while the crust of south-eastern Australia is being shortened, suggesting that tectonic triggers could be the cause of volcanism (Lesti *et al.* 2008).

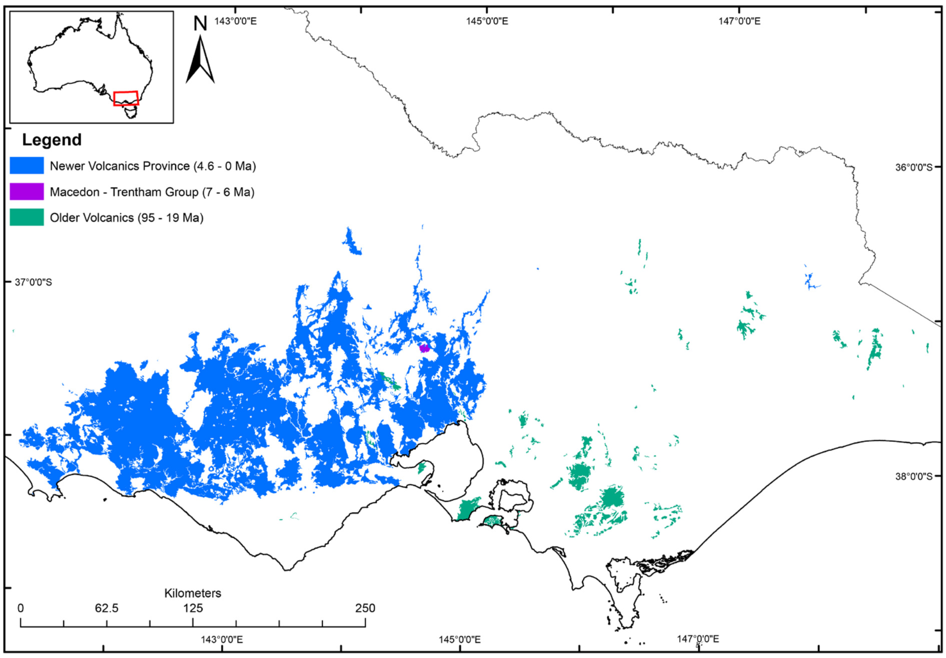

Figure 5. Distribution of Late Cretaceous-Late Cenozoic volcanism in Victoria.

3.2 Geologic setting of the Newer Volcanics Province

The Newer Volcanics Province is an intraplate, basaltic volcanic field that spans ~400 km in the east-west direction and ~180 km in the north-south direction with an aerial extent of >23,000 km^2. It is host to over 400 volcanic centres consisting of maars, tuff rings, shields, scoria cones, lava plains and volcanic complexes. Volcanism within the region is strongly influenced by the basement geology and structural trends, which causes an alignment of volcanic centres along pre-existing faults (Lesti *et al.* 2008), and where groundwater is abundant, can influence the eruptive style of the volcano (Joyce 1975). The Newer Volcanics Province was emplaced onto the Palaeozoic basement rocks of the Lachlan and Delamerian fold belts in the north, and the Otway Basin in the south.

3.2.1 The Palaeozoic Basement: the Delamerian and Lachlan Orogens

The Delamerian and Lachlan orogens lie within the Tasman Orogenic system along the eastern margins of the Australian continent, which was once part of the active margin of Gondwana (Birch and VandenBerg 2003). The Tasman Orogen formed part of a larger Orogenic system that evolved from the Neoproterozoic to the Triassic and extended 20,000 km from the northern Andes, through Antarctica and across eastern Australia (Figure 6a; Gray *et al.* 2003). Within Australia, this system is defined by the Delamerian, Tyennan, Lachlan/Thompson and New England Orogens (Figure 6b).

The Delamerian (early Palaeozoic) and the Lachlan orogens (early-middle Palaeozoic) are dominated by fold and thrust sequences of oceanic rocks, largely deep-marine turbidites and mafic volcanics that have been variably deformed, metamorphosed and intruded by granites (Coney *et al.* 1990; Fergusson and Coney 1992; Gray *et al.* 1997; Foster and Gray 2000). These systems are divided into nine structural zones, each exhibiting a particular deformation and metamorphic style, and bounded by major faults (e.g., Moyston, Avoca, Mt Williams faults; Figure 9) trending N-S and NNW-SSE (Gray and Foster 1998). The boundary between the Delamerian and Lachlan orogens is defined by the east-dipping Moyston Fault (Birch and VandenBerg 2003; Cayley *et al.* 2011), which also coincides with a geochemical transition within the Newer Volcanics Province known as the Mortlake discontinuity (Price *et al.* 1997).

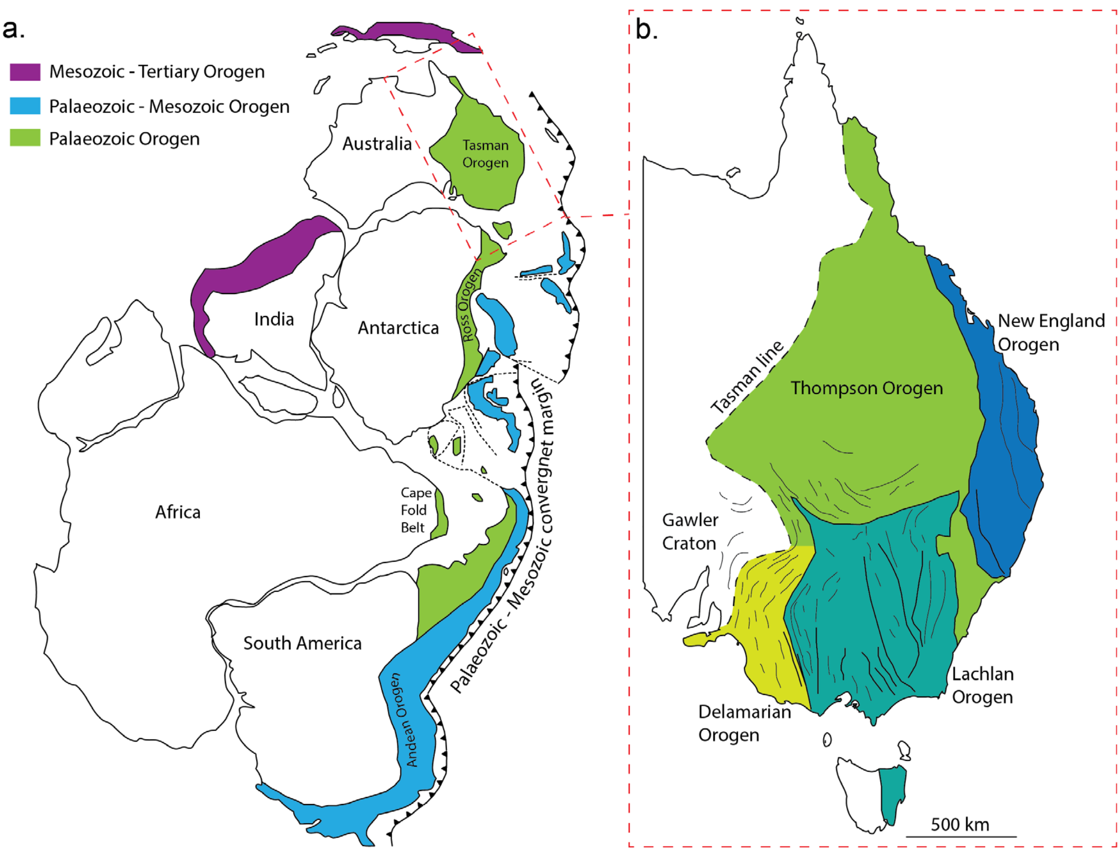

Figure 6 a) Reconstruction of Gondwana showing the location of the Tasman Orogenic system along the active margin (modified after Birch & VandenBerg 2003) b) The Tasman Orogenic system consisting of the Delamerian, Lachlan/Thompson and New England Orogens (modified after Gray et al. 2003).

3.2.2 The Otway Basin

The Otway Basin formed as a consequence of rifting between Australia and Antarctica during the break-up of Gondawana. The onset of rifting began in the Late Cretaceous with north-south tension which caused the development of major east-west trending rift basins across the southern margins of Australia, including the Great Australian Bight, Duntroon, Otway, Bass and Gippsland basins (Stagg *et al.* 1990). The Otway Basin extends across south-western Victoria into south-eastern South Australia and was formed from several episodes of extension and compression, and has now evolved into a passive continental margin that still consists of active sub-aerial and marine erosional and depositional environments. The stratigraphy, depositional environments and tectonic history of the Otway Basin is briefly summarised below and in Figure 8.

The onset of rifting between Australia and Antarctica began in the Late Jurassic. Within the Otway Basin, rifting resulted in the development of north-west to south-east, and east-west trending half grabens which formed major depocentres within the basin (Figure 7; Bernecker *et al.* 2003). Sedimentation commenced during this first phase of rifting with the deposition of the Otway Group (157-95 Ma), consisting of fluvial, lacustrine and delta plain sedimentary rocks (Bernecker *et al.* 2003). Rifting continued until the Mid-Cretaceous where a brief period of compression caused uplift and erosion of part of the Otway Group (Bernecker *et al.* 2003). Rifting recommenced before sea-floor spreading and the separation of Australia and Antarctica around ca 95 Ma (Veevers 1986). This second phase of extension resulted in the deposition of the Sherbrook Group (95-65 Ma) which consists of fluvial, delta plain and shallow marine sedimentary rocks (Edwards *et al.* 1996).

As the passive margin developed, a major transgression was initiated by subsidence and resulted in the deposition of the Wangerrip Group consisting of shallow marine and prograding deltaic sediments. An increase in spreading rate in the Southern Ocean during the mid-Eocene saw continued subsidence within the basin and the deposition of largely marine sediments within the Nirranda Group (45-29 Ma) (Yu 1988). As subsidence continued within the Otway Basin, and Australia and Antarctica drifted further apart, the increased width of the Southern Ocean saw the development of the circum-Antarctic current which provided enhanced conditions for the formation of carbonates (Edwards *et al.* 1996; Bernecker *et al.* 2003). This saw the rapid deposition of carbonates on the present-day shelf (Heytesbury Group 29-5 Ma).

Towards the end of the Miocene, the tectonic style of the region shifted from extensional faulting to compression as the Australia plate collided with the Pacific plate to the north and east (Perincek *et al.* 1994; Perincek and Cockshell 1995). This resulted in broad folding and regional uplift across the basin, coinciding with a regression of the sea. Regional uplift had ceased by the early Pliocene as the Otway Ranges reached their present day elevation (Perincek and Cockshell 1995). Volcanism associated with the Newer Volcanics Province resulted in extensive basaltic eruptions of lava flows, which cover the northern edges of the basin. These form large lakes where lava flows blocked pre-existing drainage systems (Edwards *et al.* 1996).

The faulting trend throughout the Otway Basin is important when considering the location of eruption points within the Newer Volcanics Province. Two dominant faulting trends are recognised in the Otways Basin, with faults striking in the WNW-direction in the western part of the basin (Perincek and Cockshell 1995), and in a NE-direction in the eastern part (Gilbert and Hill 1994).

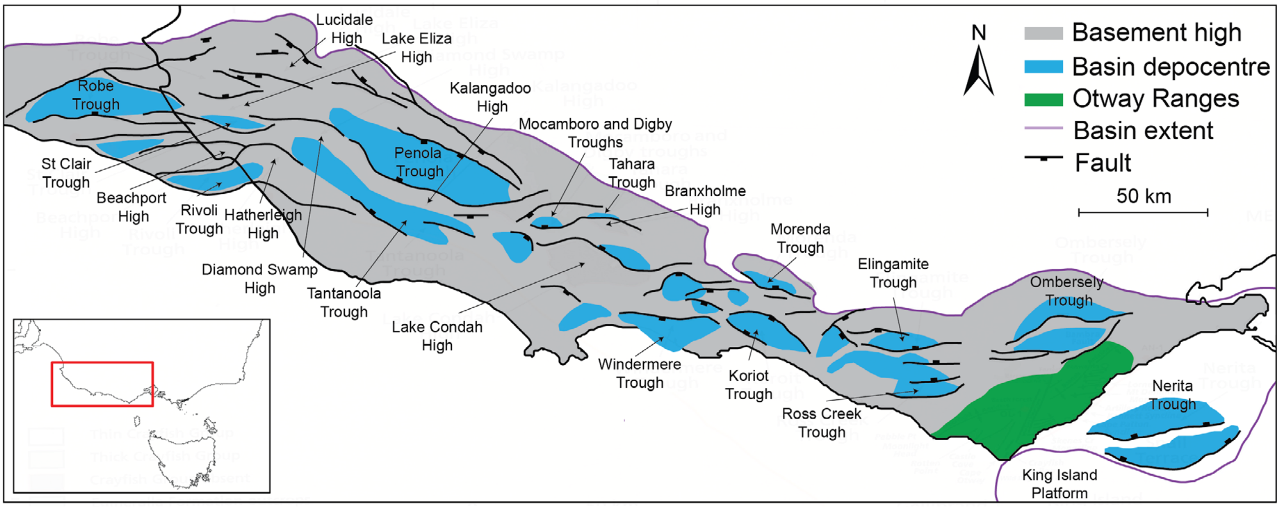

Figure 7 Major depocentres of the Otway Basin (modified after Duddy 2003).

3.3 Geology of the Newer Volcanics Province

The Newer Volcanics Province has been divided into three sub-provinces; the Central Highlands, Western Plains and Mt Gambier sub-provinces, which are defined based upon differences in eruptive styles and geochemistry; (Figure 9; Nicholls and Joyce 1989; Cas *et al.* 1993).

The Central Highlands sub-province overlies the Palaeozoic meta-sediments and granites of the Lachlan Orogen (Nicholls and Joyce 1989; Cas *et al.* 1993; Price *et al.* 2003) and is comprised of over 250 eruptive centres consisting dominantly of lava shields, lava flows and scoria cones. Volcanism within this region is dated between 4.5 and 2.0 Ma (Cas *et al.* 1993; Price *et al.* 2003).

The Western Plains is the largest of the three sub-provinces, comprised of extensive lava plains sourced from shield volcanoes and fissure systems. The topography of the Western Plains is relatively flat due to the depositional topography of the Otway Basin, and extensive lava flows which have filled in and blanketed the pre-existing topography. Superimposed on the flat to hummocky topography of the lava plains are the volcanic edifices of maars, tuff rings and scoria cones (Lesti *et al.* 2008). Numerous lakes are observed within the Western Plains, with most associated with lava flows blocking pre-existing drainage channels (e.g., Lake Corangamite), while others are crater lakes and associated with the eruption of maar volcanoes.

The Mt Gambier sub-province is the smallest of the three sub-provinces and is located 60 – 80 km west of the main section of the Newer Volcanics Province. This area is associated with clusters of maars, scoria cones and minor associated lavas which overlie a karst limestone terrain (Nicholls & Joyce 1989; Sheard 1990; Cas *et al.* 1993). Mt Gambier and Mt Schank, located within this sub-province represent the most recent eruptions within the Newer Volcanics Province (Sheard 1990).

3.4 Nature and dimension of volcanic features

Over 400 eruption points have been identified within the Newer Volcanics Province including low-angle shield volcanoes, scoria cones, spatter cones, tuff rings, maars, composite volcanoes and extensive plains lavas; volcanoes that are typical of intraplate, basaltic volcanic plains provinces (Cas 1989). Initial periods of volcanism within the Newer Volcanics Province consisted of prolonged effusive eruptions forming basaltic pahoehoe and aa lava flows. Later eruptive phases consisted of dominantly explosive eruptions forming numerous scoria cones and maars (Cupper *et al.* 2003).

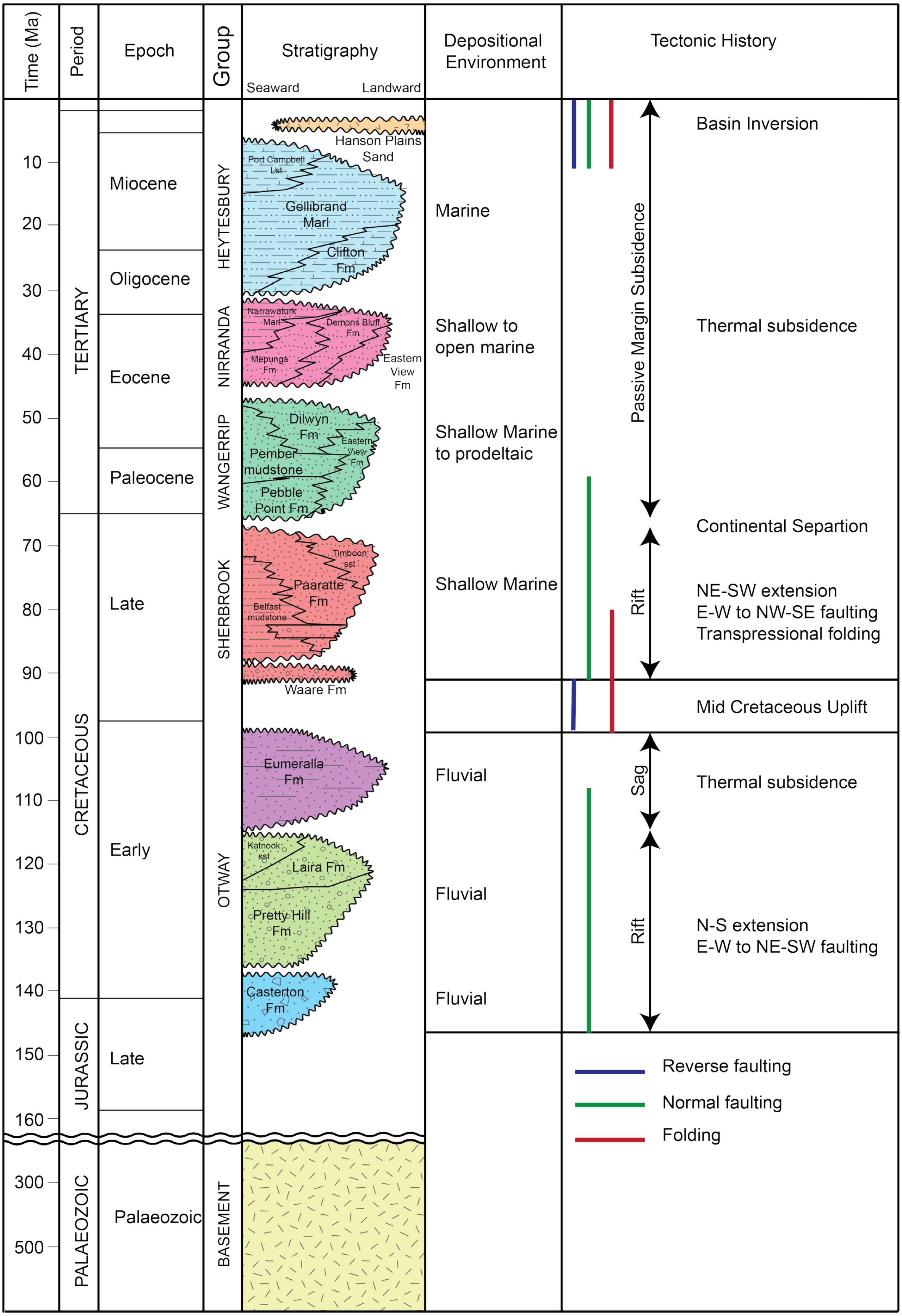

Figure 8 Stratigraphy, depositional environments and tectonic history of the Otway Basin (modified after Bernecker et al. 2003)

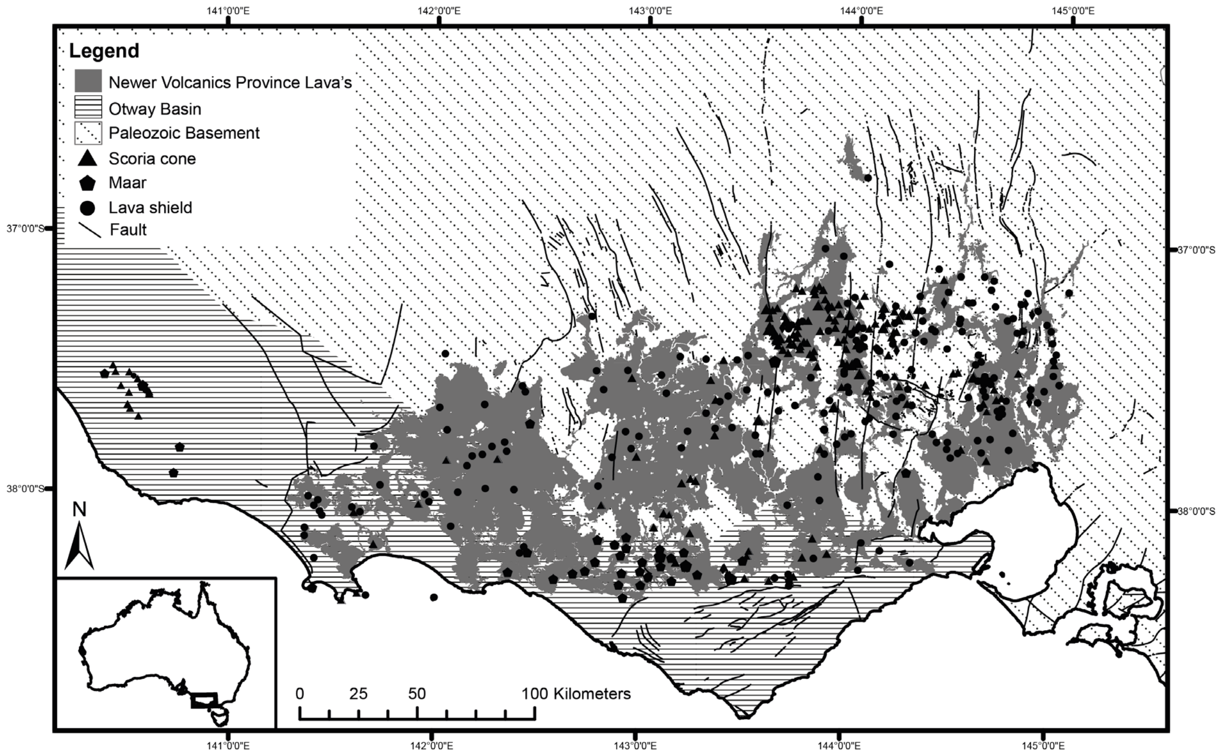

Figure 9 Simplified geologic map of Western Victoria showing the distribution eruptive centres and extent of lava flow fields.

The distribution of volcanoes within the Newer Volcanics Province is described by Joyce (1975). Almost two-thirds of the volcanoes are located within the Central Highlands sub-province, an area dominated by scoria cones and lava shields. Scoria cones are more common in the Western regions of the Central Highlands, while shield volcanoes are more common in the eastern regions. The remainder of volcanic centres are located within the Western Plains and Mt Gambier sub-provinces. Maar volcanoes are found predominantly along the southern margins of the Western Plains where phreatomagmatic volcanism has been influenced by the aquifers of the Otway Basin, at least in the initial stages of the eruption (Joyce 1975; Cas *et al.* 1993; Price *et al.* 2003; Cas *et al.* 2011; Blaikie *et al.* 2012). Shield volcanoes and scoria cones are more common in the northern regions of the Western Plains.

3.4.1 Scoria and cinder cones

Scoria cones are scattered across the landscape of Western Victoria and are particularly common in the northern areas of the Western Plains and eastern areas of the Central Highlands sub-provinces (Figure 10a). They are usually not more than 150 m high, although the largest scoria cone within the province; Mt Elephant reaches a height of 190 m above the surrounding plains. The base of Mt Elephant is 1.25 km wide and its crater has a diameter of 500 m and a depth of 100 m (Price *et al.* 2003; Cas *et al.* 2011).

3.4.2 Lava shields and flows

Shield volcanoes are one of the major sources of lava within intraplate basaltic provinces (Figure 10b) and comprise approximately half of the identified eruption points within the Newer Volcanics. Both pahoehoe and aa textures can be identified on the surfaces of younger lava flows, which can extend well beyond the margins of the shield (e.g., flows from Mt Rouse extend 60 km from the vent; Figure 10c) (Cas *et al.* 2011; Boyce *et al.* 2014).

Valley flows are common in the Central Highlands sub-province and produce narrow, elongate flows confined to pre-existing valleys. Sheet flows have produced extensive lava plains, resulting in the flat-to-hummocky topography observed in the Western Plains sub-province. Columnar jointing is visible in a number of lava flows, the best example is observed within the Organ Pipes National Park. Several examples of lava caves and tumuli exist, including in the Harman Valley flow and at Mt Eccles (Cas *et al.* 2011).

3.4.3 Maars and tuff rings

Approximately 40 maars (~10 % of eruption centres) have been identified within the Newer Volcanics Province, ranging from small, simple maars several hundred metres across, to more complex maars up to 3 km in diameter, including Lake Purrumbete and Tower Hill which are among the largest in the world (Joyce 1975). Maars and tuff rings are largely confined to the southern areas of the Western Plains and Mt Gambier sub-provinces where magma has interacted explosively with groundwater contained within aquifers of the Otway Basin (Figure 10d-e; Joyce 1975; Cas *et al.* 2011). There are several examples of maar volcanoes in the northern regions of the Newer Volcanics Province, which are hosted within granites where groundwater is available in joints and fractures (e.g., Anakie and Lake Burrumbete).

3.4.4 Complex volcanic centres

Many eruption centres within the Newer Volcanics Province may not be simply classified as one type or another, and instead consist of a combination of eruptive styles forming a complex volcanic edifice. Complex volcanic centres are usually comprised of multiple vents which exhibit different eruptive styles. Examples include the Red Rock Volcanic Complex, Mt Leura, Mt Noorat, Mt Eccles, Tower Hill, Mt Napier, Mt Gambier and Mt Schank (Figure 10d-e).

3.5 Origins of volcanism

Several tectonic and petrogenetic models exist for the Newer Volcanics Province and attempt to explain the causes and sources of volcanic activity within south-eastern Australia. However, each of these models are unable to explain every aspect of volcanism within the region, with many of the models still being tested and refined as new petrological, geochemical and geophysical data is obtained. The different models are:

3.5.1 Hotspot model

Wellman & McDougall (1974) and Duncan & McDougall (1989) attributed the origin of the Newer Volcanics Province to a hotspot or hotline that migrated along the Great Dividing Range from north to south. The hotspot model explains the enrichment of the sub-continental mantle in light rare earth (LRE), large-ion lithophiles (LIL) and high field strength (HFS) elements and the ocean island basalt (OIB) signature observed in different basalts within the Newer Volcanics Province. However, this model is no longer considered valid since the location of the Newer Volcanics Province is inconsistent with the proposed hotspot trace, volcanism has occurred sporadically in Victoria for at least 60 Ma, and there is an absence of the time related migration of eruption points usually associated with a hotspot (Price *et al.* 1997; Lesti *et al.* 2008).

Figure 10. Examples of different types of volcanoes within the Newer Volcanics Province. a) Scoria cone; Mount Elephant, b) Lava shield; Mt Napier, c) Lava flow; Mt Rouse, d) Tuff cone; Mount Schank, e) Maar; Mount Gambier.

3.5.2 Post-rift diapirism

Lister & Etheridge (1989) and Price *et al.* (1997) suggest that the presence of the Newer Volcanics Province is related to continental extension associated with the break-up of Gondwana, which initiated thermal instability within the mantle. This instability resulted in asthenospheric upwelling, which interacted with the overlying lithosphere to generate enriched melts which stalled within a sub-crustal environment. During different periods, these melts rise as clusters of diapirs through the shallow mantle. This model is supported by the east-west distribution of volcanism, parallel to the plate boundary, and the otherwise lack of any geographic/temporal patterns in volcanism. However, this model is questioned by Lesti *et al.* (2008) since volcanism does not span the entire southern margins of Australia and is instead localised within the Newer Volcanics Province of Western Victoria and South Australia. Additionally, this form of diapirism requires that the crust be under extension, whereas south-eastern Australia has been under NE-SW directed compression over the last ~10 Myrs (Sandiford *et al.* 2004).

3.5.3 Edge-driven convection

Based upon geophysical data of the sub-continental mantle, Demidjuk *et al.* (2007) suggested that the origin of volcanism within the Newer Volcanics Province could be due to edge driven convection. Upwelling is induced in the asthenosphere by convection cells caused by irregularities in lithospheric thickness as the Australian plate moves northwards. This model is however still debated since magmatism in the area is not continuous over time, instead occurring in short lived intervals (Cas *et al.* 2011).

3.5.4 Transtensional decompression

Lesti *et al.* (2008) identified a tectonic control on magma emplacement within the Newer Volcanics Province, with eruption points aligned along major fracture zones. These fracture zones are primarily Mesozoic-Cenozoic north-west to south-east trending structures, Palaeozoic north – south structures and Later Cretaceous east – west structures. Lesti *et al.* (2008) proposes that magmatism occurred when the north-west to south-east compressive stress regime induced transtensional areas along these structures, possible inducing melting through a short lived period of decompression in the mantle, and providing a pathway for magma to rise to the surface.

3.6 Hazard implications

The Newer Volcanics Province is still considered an active volcanic province, with an eruption recurrence rate of approximately 10,800 years (Cas *et al.* 2011; Boyce 2013). It is therefore important to consider the implications of future eruptions in the area, and how they may impact on society and the economy. Eruptions in the area may occur rapidly with very little warning, however; the eruption of monogenetic volcanoes are fairly localised and will generally not pose any immediate danger to areas beyond a few kilometres from the vent.

Any style volcanic eruption is likely to cause localised damage to infrastructure and threat to human life in the vicinity of the eruption. However, the hazards and long term impacts arising from each of the eruption styles discussed above may vary. A lava flow generally moves slowly and can be outrun, posing little threat to humans provided a safe distance from the eruption centre and associated flows are maintained. Extensive lava flows may cause damage to major and minor infrastructure and its impact will be long-lasting, leaving the land un-useable for farming for many years.

Explosive eruptions pose a greater threat to human life, especially phreatomagmatic eruptions resulting in lethal base surges and pyroclastic flows, however these are generally confined to within a few kilometres from the vent. Although the eruption is localised and short-lived, explosive eruptions can have far reaching effects as ash is dispersed downwind from the eruption. Fine ash ejected from an explosive eruption within the Newer Volcanics Province could potentially affect Melbourne, Canberra and Sydney, impacting upon human health, infrastructure and disrupting air traffic.

4. Introduction to case studies

Four maar volcanoes were selected for this study and represent a range of the different eruptive styles and sizes of maars within the Newer Volcanics Province. The Red Rock and Mt Leura volcanic complexes show complex eruptive histories with fluctuating eruptive styles. Ecklin and Anakie maars are simple maar volcanos, exhibiting predominantly phreatomagmatic eruptive styles, although Anakie is also associated with a scoria cone complex and the eruption from the maar was likely very short lived.

Red Rock, Mt Leura and Ecklin maar are hosted within the Tertiary sedimentary sequences of the Otway Basin, while the Anakie maar is hosted within a Late Devonian granite. The areas surround these volcanoes are typical of the geomorphological character of the Western Plains sub-province, with the numerous scoria cones and rims of maars and tuff cones superimposed on the flat to slightly undulating topography of the extensive lava plains (Cas et al. 2011). This region of the Newer Volcanics Province is also marked by numerous lakes; either forming in the maar craters or as a result of lava flows blocking pre-existing drainage systems. The geology and previous works on each of the case studies is briefly described below and will be expanded upon in later chapters.

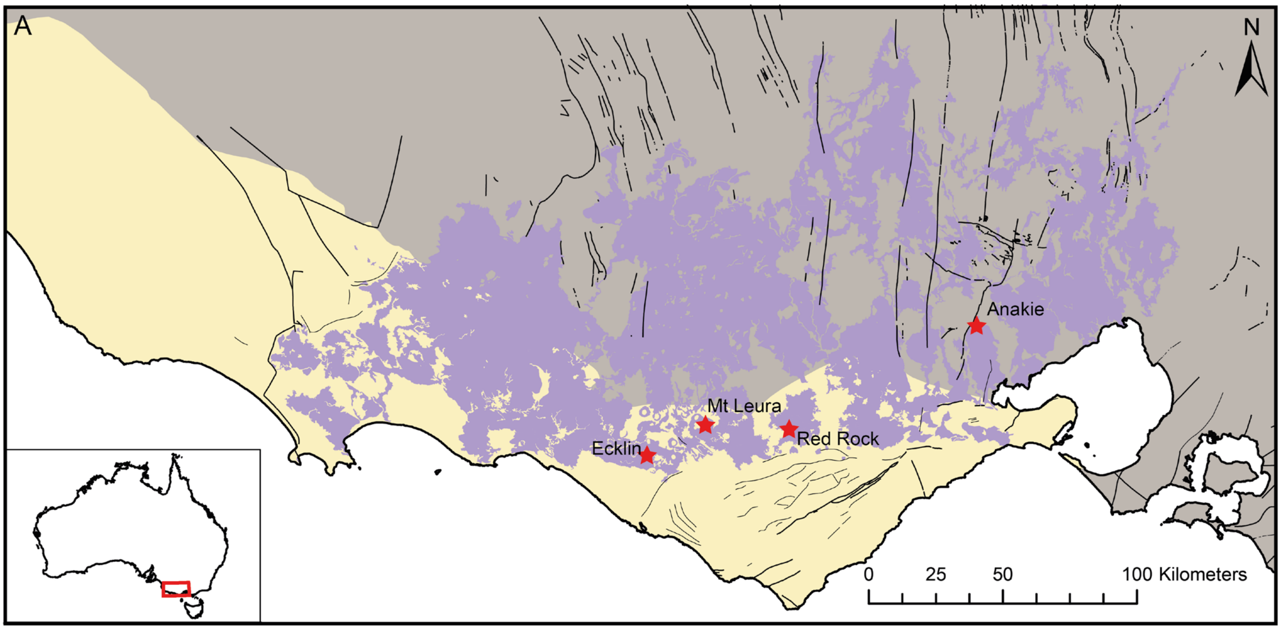

Figure 11. Location of the case studies within the Newer Volcanics Province.

4.1 The Ecklin Maar

The Ecklin maar volcano is located within the southern part of the Western Plains sub-province. It is a small maar, slightly elongated in the NNW-SSE direction and is approximately 800 m across its shortest axis (E-W) and 1000 m across it longest axis (NNW-SSE). The maar-rim deposits are thickest along the SW side of the maar, rising 40 m above the crater floor and are entirely absent in the NNW of the maar. The asymmetry in deposition is likely related to the prevailing wind direction during the eruption. Ecklin is a typical maar volcano, exhibiting predominantly phreatomagmatic behaviour with deposits derived from base-surge and fallout processes. Previous work on Ecklin maar is largely unpublished. The deposits of the maar were first described by Rosengren (1994) and the later studied by Roche (2011).

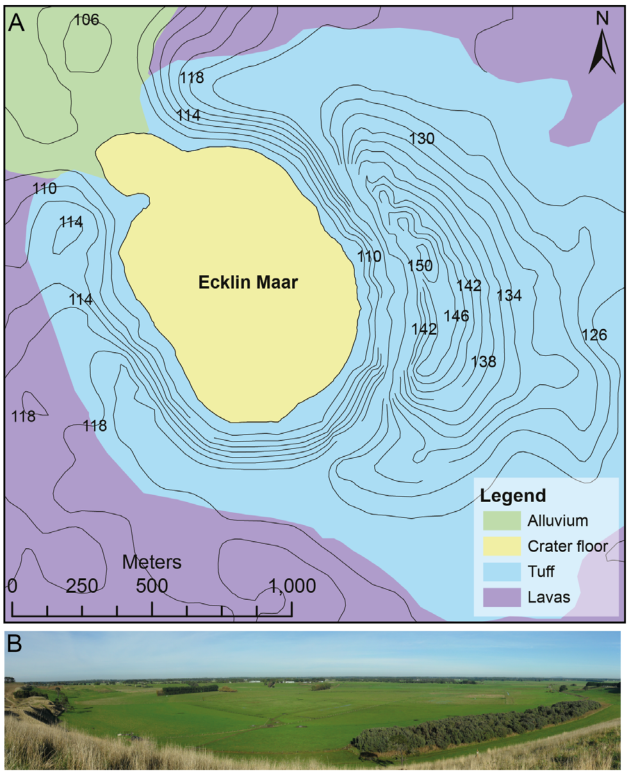

Figure 12. Geology of Ecklin maar

4.2 Red Rock Volcanic Complex

The Red Rock Volcanic Complex, located northwest of the township of Colac, is one of the most complex volcanic centres within the Newer Volcanics Province. It is the southern-most of three closely spaced volcanoes, including the Mt Alvie scoria cones (central) and the Warrion Hill lava shield (north). These closely spaced centres define a north-northeast trending lineament, and overlie the Avoca Fault. The Avoca Fault is a steep, west-dipping reverse fault which separates the Bendigo and Stawell zones of the Lachlan Orogen (Gray *et al.* 2003), and is presumed to have been exploited by magma as a conduit to the surface.

The chronology of volcanic eruptions within and surrounding the Red Rock Volcanic Complex in order are (Leach 1977, Piganis 2011):

1. Eruption of lavas from Warrion Hill, produces stoney rises.
2. Continued activity at Warrion Hill producing scoria and lava eruptions.
3. Formation of the Mt Alvie scoria cones.
4. Lava eruptions from the Red Rock Volcanic Complex (unknown vent).
5. Formation of maars within the Red Rock Volcanic Complex.
6. Formation of the scoria cone complex within the Red Rock Volcanic Complex.

The Red Rock Volcanic Complex consists of over 40 identifiable eruption points that have formed multiple poly-lobate maars and a scoria cone complex. At least 20 vents associated with the formation of the maar craters have been identified, (Cas *et al.* 1993; Cas *et al.* 2011; Piganis 2011; Blaikie *et al.* 2012), and there are at least another 28 eruption points associated with the scoria cone complex. Initial eruptive activity within the complex was dominantly phreatomagmatic, resulting in the formation of the scalloped shaped maars including Lakes Coragulac, Purdigulac, Gnalinegurk and Werowrap.

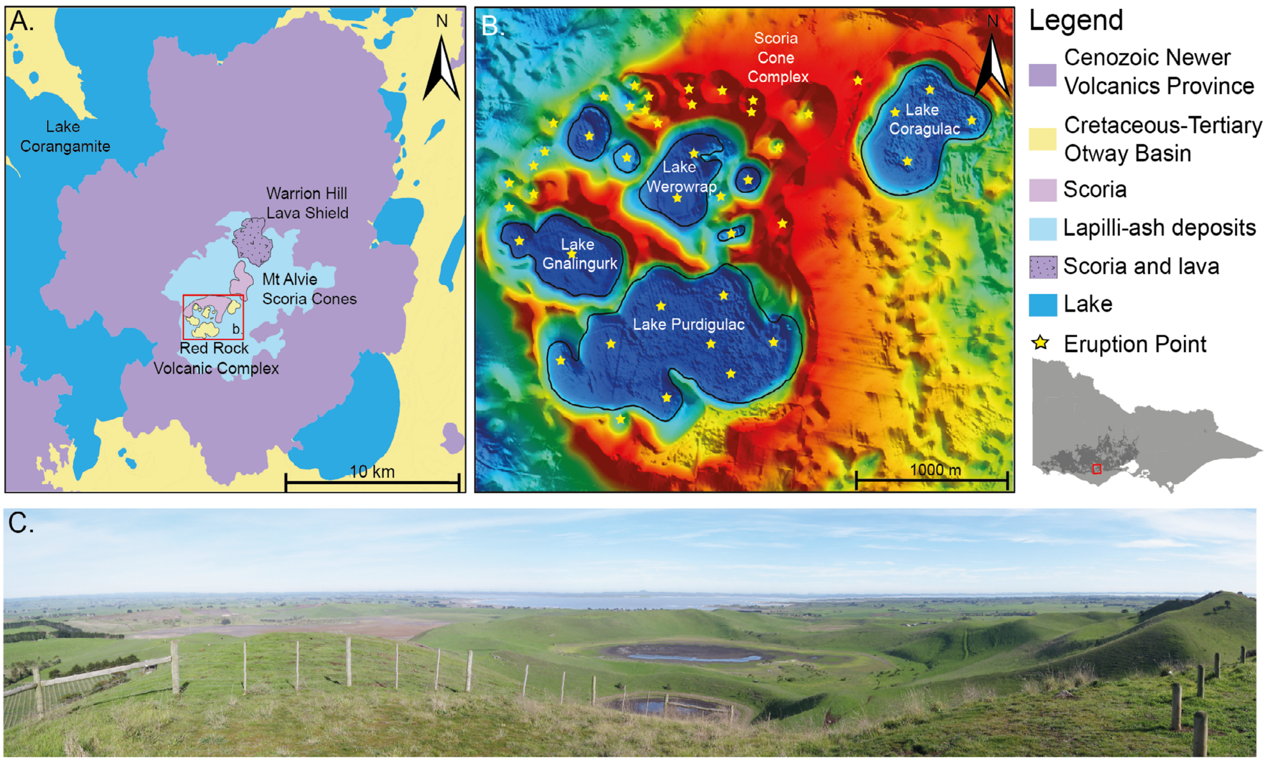

Figure 13. Geology of the Red Rock Volcanic Complex

Eruptive activity within the Red Rock Volcanic Complex then shifted to dominantly magmatic, producing the scoria cone complex in the northern region of the complex. The superposition of volcanic land forms suggests the scoria cone complex formed after the maars, however strombolian scoria fall deposits have been observed interbedded with phreatomagmatic fall/surge deposits in the maar rim successions. This suggests either the strombolian cones were active simultaneously with phreatomagmatic maar volcanism, or eruptive styles within the maars regularly fluctuated between phreatomagmatic and magmatic.

Geochemical analysis of the complex by Piganis (2011) suggests that two different magma batches were sourced by the Red Rock Volcanic Complex. Geochemical variations were correlated spatially and stratigraphically across the complex and separate the lower lapilli-ash/tuff sequences of Lake Purdigulac maar to the upper lapilli-ash/tuff and scoria/spatter sequences of the other maars and scoria cone complex. The lower sequence from Lake Purdigulac are classified as 'basanites' with relatively higher total alkalies, REE and incompatible element concentrations compared to the upper sequences of the rest of the complex which are classified as alkali-olivine to trachy-basalts with relatively lower total alkalies, REE and incompatible elements.

Previous studies on the volcanic history, stratigraphy and geophysics of the Red Rock Volcanic Complex are largely unpublished and include the works of Leach (1977), who concentrated on regional stratigraphy and chronology of volcanism, Forster (1983), and Van Tatenhove (1983) who studied in detail the pyroclastic deposits and the modes of formation and deposition around parts of Lake Coragulac and Lake Purdigulac maars respectively. More recent research into the physical volcanology, geochemistry and geophysics of the complex have been conducted by Cheesman (2007), Blaikie (2009), Piganis (2011) and Blaikie et al. (2012) and are summarised in Cas et al. (2011).

4.3 Mount Leura Volcanic Complex

The Mount Leura Volcanic Complex is located near the town of Camperdown, within the Western Plains sub-province, and is a composite volcano comprised of a coalesced maar and tuff ring with a nested scoria cone complex. Mt Leura is one of five large volcanic centres that lie along a NW-SE lineament, presumed to be the edge of the Elingamite graben. The eruption at Mt Leura consisted of two phases of volcanism. The first, predominately phreatomagmatic formed a large maar and overlapping tuff ring. The second phase of activity varied from effusive, infilling the craters with lava, to explosive magmatic, forming the

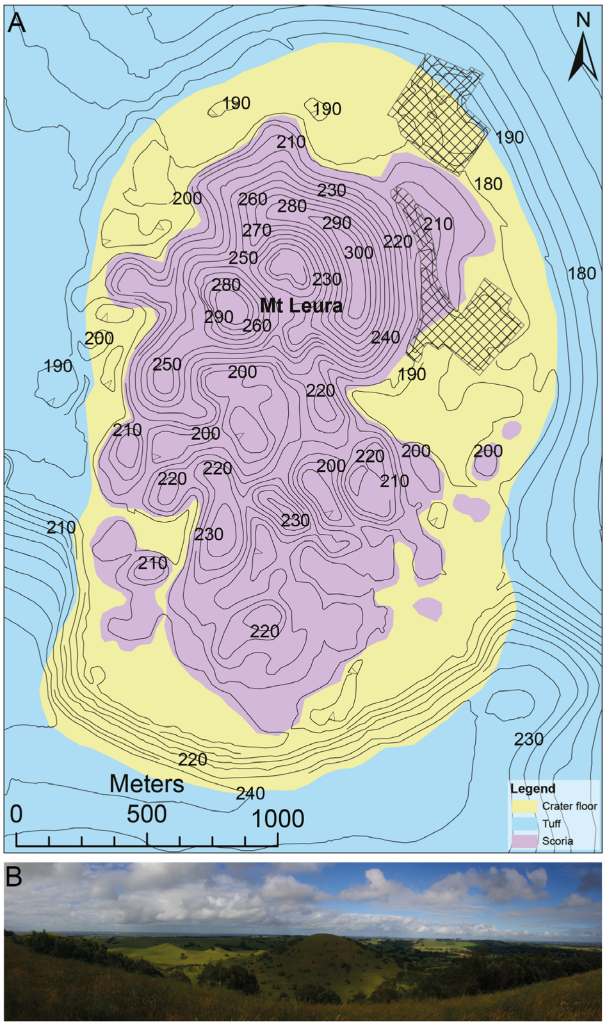

Figure 14. Geology of the Mount Leura Voclanic Complex

nested scoria cone complex which is mostly confined within the margins of the tuff ring. Mt Leura overlies the Tertiary sediments of the Otway Basin and earlier plains lavas of the Newer Volcanics Province.

The Mount Leura Volcanic Complex was described by Cas et al. (1993) and later work has focused on the physical volcanology and geochemistry of the complex, including the unpublished works of Shaw-Stuart (2005) and Uehara (2011).

4.4 Anakie Volcanic Complex

The Anakie Volcanic Complex is located on the Werribee Plains lava field, part of the Central Highlands Province and is comprised of three scoria cones (preserved basal diameters of ~1 km, and height of ~100 m) aligned in northwest-southeast direction, with a small maar nested between the two northern-most cones. The maar crater is elongate in the north-south direction and is 350 m wide and 600 m long, with a shallow crater that is 15 m deep. The complex is aligned along the Lovely Banks Monocline, which was likely exploited by magma as it rose to the surface.

The Anakie Volcanic Complex is located within a Late Devonian granite of the Lachlan Orogen, which is overlain by a thin layer (several metres) of unconsolidated sands and the lava flows of the Newer Volcanics Province. The source of water to fuel the phreatomagmatic explosions associated with the eruption of the maar is unclear, and is thought to have been derived either from fractures in the granite, or water contained within the pore spaces of a thin sandy layer overlying the granite.

Hare et al. (2005) attempted to correlate the volcanic stratigraphy of the Werribee plains, which constrains the age estimate of the Anakie Volcanic Complex to between 2.58-2.74 Ma (based on K-Ar and $^{40}Ar/^{39}Ar$ dates).

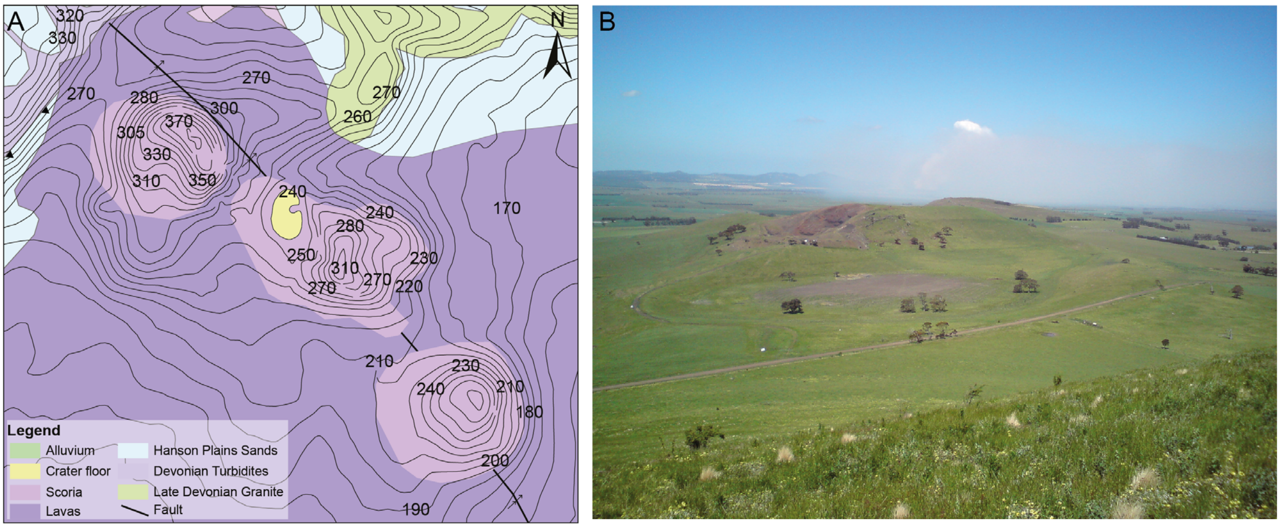

Figure 15. Geology of the Anakies

5. References

Araña V., Camacho A. G., Garcia A., Montesinos F. G., Blanco I., Vieira R. & Felpeto A. 2000. Internal structure of Tenerife (Canary Islands) based on gravity, aeromagnetic and volcanological data. *Journal of Volcanology and Geothermal Research* **103**, 43-64.

Auer A., Martin U. & Németh K. 2007. The Fekete-hegy (Balaton Highland Hungary) "soft-substrate" and "hard-substrate" maar volcanoes in an aligned volcanic complex - Implications for vent geometry, subsurface stratigraphy and the palaeoenvironmental setting. *Journal of Volcanology and Geothermal Research* **159**, 225-245.

Bernecker T., Smith M. A., Hill K. A. & Constantine A. E. 2003. Oil and gas. *In:* Birch W. D. ed. *Geology of Victoria*, pp. 470-487. Geological Society of Australia Special Publication **23**. Geological Society of Australia (Victoria Division).

Birch W. D. & VandenBerg A. H. M. 2003. Introduction. Continuing the advance of Victorian Geology. *In:* Birch W. D. ed. *Geology of Victoria*, pp. 1-14. Geological Society of Australia Special Publication **23.** Geological Society of Australia (Victoria Division).

Blaikie T. 2009. Determining the subsurace structure of a maar volcano, Lake Coragulac, Red Rock Volcanic Complex. Honours thesis, Monash University, Australia (unpubl.).

Blaikie T. N., Ailleres L., Cas R. A. F. & Betts P. G. 2012. Three-dimensional potential field modelling of a multi-vent maar-diatreme - the Lake Coragulac maar, Newer Volcanics Province, south-eastern Australia. *Journal of Volcanology and Geothermal Research* **235-236**, 70-83.

Blanco-Montenegro I., De Ritis R. & Chiappini M. 2007. Imaging and modelling the subsurface structure of volcanic calderas with high-resolution aeromagnetic data at Vulcano (Aeolian Islands, Italy). *Bulletin of Volcanology* **69**, 643-659.

Bolós X., Barde-Cabusson S., Pedrazzi D., Martí J., Casas A., Himi M. & Lovera R. 2012. Investigation of the inner structure of La Crosa de Sant Dalmai maar (Catalan Volcanic Zone, Spain). *Journal of Volcanology and Geothermal Research* **247-248**, 37-48.

Boyce J. 2013. The Newer Volcanics Province of southeastern Australia: a new classification scheme and distribution map for eruption centres. *Australian Journal of Earth Sciences* **60**, 449-462.

Boyce J. A., Keays R. R., Nicholls I. A. & Hayman P. 2014. Eruption centres of the Hamilton area of the Newer Volcanics Province, Victoria, Australia: pinpointing volcanoes from a multifaceted approach to landform mapping. *Australian Journal of Earth Sciences*, 1-20.

Brunner I., Friedel S., Jacobs F. & Danckwardt E. 1999. Investigation of a Tertiary maar structure using three-dimensional resistivity imaging. *Geophysical Journal International* **136**, 771-780.

Buness H. A., Wiederhold H. & Wonik T. 2006. Seismic reflection patterns of two Tertiary maars in Germany. *Zeitschrift der Deutschen Gesellschaft fur Geowissenschaften* **157**, 339-353.

Büttner R. & Zimanowski B. 2003. Phreatomagmatic Explosions in Subaqueous Volcanism. *In:* White J. D., Smellie J. L. & Clague D. A. eds. *Explosive Subaqueous Volcanism*, pp. 51-60. **140** American Geophysical Union Geophysical Monograph.

Camacho A. G., Montesinos F. G. & Vieira R. 1997. A three-dimensional gravity inversion applied to São Miguel Island (Azores). *Journal of Geophysical Research: Solid Earth* **102**, 7717-7730.

Cas R. A. F. 1989. Physical Volcanology. *In:* Johnson R. W., Knutson J. & Taylor S. R. eds. *Intraplate volcanism in eastern Australia and New Zealand*, pp. 55-88. Cambridge University Press.

Cas R. A. F., Blaikie T., Boyce J., Hayman P., Jordan S., Piganis F., Prata G. & van Otterloo J. 2011. VF01: Factors that influence varying eruption styles (from magmatic to phreato-magmatic) in intraplate continental basaltic volcanic provinces: the Newer Volcanics Province of south-eastern Australia. *IUGG 2011 Fieldtrip guide*.

Cas R. A. F., Simpson C. & Sato H. 1993. *Newer Volcanics Province - processes and products of phreatomagmatic activity.*

IAVCEI Canberra 1993: excursion guide, September, 1993. Record - Australian Geological Survey Organisation. Geoscience Australia, Canberra, A.C.T., Australia.

Cas R. A. F. & Wright J. V. 1987. *Volcanic successions : modern and ancient : a geologic approach to processes, products and successions*. Allen & Unwin, London.

Cassidy J., France S. J. & Locke C. A. 2007. Gravity and magnetic investigation of maar volcanoes, Auckland volcanic field, New Zealand. *Journal of Volcanology and Geothermal Research* **159**, 153-163.

Cayley R. A., Korsch R. J., Moore D. H., Costelloe R. D., Nakamura A., Willman C. E., Rawling T. J., Morand V. J., Skladzien P. B. & O'Shea P. J. 2011. Crustal architecture of central Victoria: results from the 2006 deep crustal reflection seismic survey. *Australian Journal of Earth Sciences* **58**, 113 - 156.

Cheesman A. 2007. The nature of transitions between magmatic and phreatomagmatic explosive volcanism at the Red Rock Volcanic Complex, Newer Volcanics Province, Southeastern Australia. Masters thesis, Monash University, Australia (unpubl.).

Coney P. J., Edwards A., Hine R., Morrison F. & Windrim D. 1990. The regional tectonics of the Tasman orogenic system, eastern Australia. *Journal of Structural Geology* **12**, 519-543.

Connor C. B. & Conway F. M. 2000. Basaltic Volcanic Fields. *In:* Sigurdsson H., Houghton B., McNutt S. R., Rymer H. & Stix J. eds. *Encyclopedia of Volcanoes*, pp. 331-343. Academic Press, San Diego, California.

Cupper M. L., White S. & Neilson J. L. 2003. Quaternary. *In:* Birch W. D. ed. *Geology of Victoria*, pp. 337-359. Geological Society of Australia Special Publication **23**. Geological Society of Australia (Victoria Division).

Day R. A. 1989. Victoria and South Australia - Volcanic Geology. *In:* Johnson R. W. ed. *Intraplate volcanism in eastern Australia and New Zealand*, pp. 132-135. Cambridge, Cambridge University Press.

Demidjuk Z., Turner S., Sandiford M., George R., Foden J. & Etheridge M. 2007. U-series isotope and geodynamic constraints on mantle melting processes beneath the Newer Volcanic Province in South Australia. *Earth and Planetary Science Letters* **261**, 517-533.

Duncan R. A. & McDougall I. 1989. Framework for Volcanism: Volcanic Space Time Relationships. *In:* Johnson R. W., Knutson J. & Taylor S. R. eds. *Intraplate volcanism in eastern Australia and New Zealand*, pp. 43-54. Cambridge University Press.

Edwards J., Leonard J. G., Pettifer G. R. & McDonald P. A. 1996. Colac 1:250 000 map geological report. *Geological Survey of Victoria Report* **98**.

Fergusson C. L. & Coney P. J. 1992. Convergence and intraplate deformation in the Lachlan Fold Belt of Southeastern Australia. *Tectonophysics* **214**, 417-439.

Finn C. A. & Morgan L. A. 2002. High-resolution aeromagnetic mapping of volcanic terrain, Yellowstone National Park. *Journal of Volcanology and Geothermal Research* **115**, 207-231.

Forster E. N. 1983. The eruptive history and eruptive mechanisms as determined by the deposits, sedimentary structures and structure of the Lake Coragulac deposits, a maar of the Red Rock Volcanic Complex, western Victoria. 3rd year project thesis, Monash University, Australia (unpubl.).

Foster D. A. & Gray D. R. 2000. Evolution and Structure of the Lachlan Fold Belt (Orogen) of Eastern Australia. *Annual Review of Earth and Planetary Sciences* **28**, 47-80.

Gebhardt A. C., De Batist M., Niessen F., Anselmetti F. S., Ariztegui D., Haberzettl T., Kopsch C., Ohlendorf C. & Zolitschka B. 2011. Deciphering lake and maar geometries from seismic refraction and reflection surveys in Laguna Potrok Aike (southern Patagonia, Argentina). *Journal of Volcanology and Geothermal Research* **201**, 357-363.

Gilbert M. B. & Hill K. A. 1994. Gippsland, a composite basin - A case study from the northern Strzelecki terrace, Gippsland Basin, Australia. *APEA Journal* **34**, 495-512.

Gottsmann J., Camacho A. G., Martí J., Wooller L., Fernández J., García A. & Rymer H. 2008. Shallow structure beneath the Central Volcanic Complex of Tenerife from new gravity data: Implications for its evolution and recent reactivation. *Physics of the Earth and Planetary Interiors* **168**, 212-230.

Graettinger A. H., Valentine G. A., Sonder I., Ross P. S., White J. D. L. & Taddeucci J. 2014. Maar-diatreme geometry and deposits: Subsurface blast experiments with variable explosion depth. *Geochemistry, Geophysics, Geosystems* **15**, 740-764.

Gray D. R. & Foster D. A. 1998. Character and kinematics of faults within the turbidite-dominated Lachlan Orogen: implications for tectonic evolution of eastern Australia. *Journal of Structural Geology* **20**, 1691-1720.

Gray D. R., Foster D. A. & Bucher M. 1997. Recognition and definition of orogenic events in the Lachlan Fold Belt. *Australian Journal of Earth Sciences* **44**, 489-501.

Gray D. R., Foster D. A., Morand V. J., Willman C. E., Cayley R. A., Spaggiari C. V., Taylor D. H., Gray C. M., VandenBerg A. H. M., Hendrickx M. A. & Wilson C. J. L. 2003. Structure, metamorphism, geochronolgy and tectonics of Palaeozoic rocks. Interpreting a complex, long-lived orogenic system. *In:* Birch W. D. ed. *Geology of Victoria*, pp. 15-72. Geological Society of Australia Special Publication 23 Geological Society of Australia (Victoria Division).

Johnson R. W. 1989. *Intraplate volcanism in eastern Australia and New Zealand*. Cambridge University Press, Cambridge.

Joyce E. B. 1975. Quaternary volcanism and tectonics in southeastern Australia. *Bulletin - Royal Society of New Zealand* **13**, 169-176.

Kamara A. Y. S. 1981. Review: Geophysical methods for kimberlite, prospecting. *Exploration Geophysics* **12**, 43-51.

Kauahikaua J., Hildenbrand T. & Webring M. 2000. Deep magmatic structures of Hawaiian volcanoes, imaged by three-dimensional gravity models. *Geology* **28**, 883-886.

Kereszturi G. & Németh K. 2012. Monogenetic Basaltic Volcanoes: Genetic Classification, Growth, Geomorphology and Degradation. *In:* Nemeth K. ed. *Updates in Volcanology - New Advances in Understanding Volcanic Systems*, pp. 1-86. InTech Open Publisher, Rijeka, Croatia.

Kienle J., Kyle P. R., Self S., Motyka R. J. & Lorenz V. 1980. Ukinrek Maars, Alaska, I. April 1977 eruption sequence, petrology and tectonic setting. *Journal of Volcanology and Geothermal Research* **7**, 11-37.

Knutson J. 1989. East Australian volcanic geology. *In:* Johnson R. W. ed. *Intraplate volcanism in eastern Australia and New Zealand*, pp. 89-155. Cambridge University Press, Cambridge.

Knutson J. & Nicholls I. A. 1989. Macedon-Trentham. *In:* Johnson R. W. ed. *Intraplate volcanism in eastern Australia and New Zealand*, pp. 136-137. Cambridge University Press, Cambridge.

Leach J. 1977. Geology of the eastern Corangamite region and the fossil fauna of Bald Hill, near Foxhow. Honours thesis, University of Melbourne, Australia (unpubl.).

Lefebvre N. S., White J. D. L. & Kjarsgaard B. A. 2012. Spatter-dike reveals subterranean magma diversions: Consequences for small multivent basaltic eruptions. *Geology* **40**, 423-426.

Lefebvre N. S., White J. D. L. & Kjarsgaard B. A. 2013. Unbedded diatreme deposits reveal maar-diatreme-forming eruptive processes: Standing Rocks West, Hopi Buttes, Navajo Nation, USA. *Bulletin of Volcanology* **75**, 1-17.

Lesti C., Giordano G., Salvini F. & Cas R. 2008. Volcano tectonic setting of the intraplate, Pliocene-Holocene, Newer volcanic province (southeast Australia); role of crustal fracture zones. *Journal of Geophysical Research* **113**.

Lindner H., Gabriel G., tze H.-J., rgen, Kaeppler R. & Suhr P. 2006. Geophysical and geological investigation of maar structures in the Upper Lusatia region (East Saxony). *Zeitschrift der Deutschen Gesellschaft fur Geowissenschaften* **157**, 355-372.

Lindner H., Kappler R., Pretzschner C. & Suhr P. 2004. Geophysical exploration of maar localities in Upper Lusatia, Germany. *Occasional Papers of the Geological Institute of Hungary* **203**, 70.

Lister G. S. & Etheridge 1989. Detachment Models for Uplift and Volcanism in the Eastern Highlands, and their Application to the Origin of Passive Margin Mountains. *In:* Johnson R. W., Knutson J. & Taylor S. R. eds. *Intraplate volcanism in eastern Australia and New Zealand*, pp. 297-313. Cambridge University Press.

Lopez Loera H., Aranda-Gomez J. J., Arzate J. A. & Molina-Garza R. S. 2008. Geophysical surveys of the Joya Honda Maar (Mexico) and surroundings; volcanic implications. *Journal of Volcanology and Geothermal Research* **170**, 135-152.

Lorenz V. 1975. Formation of phreatomagmatic maar-diatreme volcanoes and its relevance to kimberlite diatremes. *Physics and Chemistry of The Earth* **9**, 17-27.

Lorenz V. 1986. On the growth of maars and diatremes and its relevance to the formation of tuff rings. *Bulletin of Volcanology* **48**, 265-274.

Lorenz V. 2003. Maar-Diatreme Volcanoes, their Formation, and their Setting in Hard-rock or Soft-rock Environments. *Geolines* **15**, 72-83.

Lorenz V. 2007. Syn- and posteruptive hazards of maar-diatreme volcanoes. *Journal of Volcanology and Geothermal Research* **159**, 285-312.

Lorenz V. & Kurszlaukis S. 2007. Root zone processes in the phreatomagmatic pipe emplacement model and consequences for the evolution of maar-diatreme volcanoes. *Journal of Volcanology and Geothermal Research* **159**, 4-32.

Macnae J. 1979. Kimberlites and exploration geophysics. *Geophysics* **44**, 1395-1416.

Macnae J. 1995. Applications of geophysics for the detection and exploration of kimberlites and lamproites. *Journal of Geochemical Exploration* **53**, 213-243.

Martín-Serrano A., Vegas J., García-Cortés A., Galán L., Gallardo-Millán J. L., Martín-Alfageme S., Rubio F. M., Ibarra P. I., Granda A., Pérez-González A. & García-Lobón J. L. 2009. Morphotectonic setting of maar lakes in the Campo de Calatrava Volcanic Field (Central Spain, SW Europe). *Sedimentary Geology* **222**, 52-63.

Montesinos F. G., Arnoso J., Benavent M. & Vieira R. 2006. The crustal structure of El Hierro (Canary Islands) from 3-D gravity inversion. *Journal of Volcanology and Geothermal Research* **150**, 283-299.

Moore J. G., Nakamura K. & Alcaraz A. 1966. The 1965 eruption of Taal Volcano. *Science* **151**, 955-960.

Mrlina J., Kampf H., Kroner C., Mingram J., Stebich M., Brauer A., Geissler W. H., Kallmeyer J., Matthes H. & Seidl M. 2009. Discovery of the first Quaternary maar in the Bohemian Massif, Central Europe, based on combined geophysical and geological surveys. *Journal of Volcanology and Geothermal Research* **182**, 97-112.

Muller G. & Veyl G. 1957. The birth of Nilahue, a new Maar type volcano at Rininahue, Chile. *Chile Congreso Geológico Internacional* **1**, 375-396.

Nairn I. A. 1979. Rotomahana- Waimangu eruption, 1886: base surge and basalt magma. *New Zealand Journal of Geology and Geophysics* **22**, 363-378.

Németh K. & Cronin S. J. 2011. Drivers of explosivity and elevated hazard in basaltic fissure eruptions: The 1913 eruption of Ambrym Volcano, Vanuatu (SW-Pacific). *Journal of Volcanology and Geothermal Research* **201**, 194-209.

Nicholls I. A. & Joyce E. B. 1989. East Australian Volcanic Geology: Newer Volcanics. *In:* Johnson R. W., Knutson J. & Taylor S. R. eds. *Intraplate volcanism in eastern Australia and New Zealand*, pp. 137-141. Cambridge University Press.

Ort M. H. & Carrasco-Núñez G. 2009. Lateral vent migration during phreatomagmatic and magmatic eruptions at Tecuitlapa Maar, east-central Mexico. *Journal of Volcanology and Geothermal Research* **181**, 67-77.

Paoletti V., Di Maio R., Cella F., Florio G., Motschka K., Roberti N., Secomandi M., Supper R., Fedi M. & Rapolla A. 2009. The Ischia volcanic island (Southern Italy): Inferences from potential field data interpretation. *Journal of Volcanology and Geothermal Research* **179**, 69-86.

Perincek D. & Cockshell C. D. 1995. The Otway Basin: Early Cretaceous rifting to Neogene inversion. *APEA Journal* **35**, 451-466.

Perincek D., Simons B. & Pettifer G. 1994. The tectonic framework, and associated play types of the Western Otway Basin, Victoria, Australia. *APEA Journal* **34**, 460-477.

Piganis F. 2011. A volcanological investigation of the polymagmatic Red Rock Volcanic Complex and a 3D geophysical interpretation of the subsurface structure and geology of the poly-lobate Lake Purdigulac maar, Newer Volcanics Province, southeastern Australia. Masters thesis, Monash University, Australia (unpubl.).

Price R. C., Gray C. M. & Frey F. A. 1997. Strontium isotopic and trace element heterogeneity in the plains basalts of the Newer Volcanic Province, Victoria, Australia. *Geochimica et Cosmochimica Acta* **61**, 171-192.

Price R. C., Nicholls I. A. & Gray C. M. 2003. Cainozoic igneous activity. *In:* Birch W. D. ed. *Geology of Victoria*, pp. 361-375. Geological Society of Australia Special Publication **23**. Geological Society of Australia (Victoria Division).

Rajagopalan S., Carlson J. & Wituik D. 2007. Kimberlite exploration using integrated airborne geophysics. *ASEG Extended Abstracts* **2007**, 1-5.

Roche L. 2011. Volcanological evolution and subsurface structure of a maar. Honours thesis, Monash University, Australia (unpubl.).

Rosengren N. 1994. *Eruption Points of the Newer Volcanics Province of Victoria: An Inventory and Evaluation of Scientific Significance*. National Trust of Australia (Victoria) and the Geological Society of Australia (Victoria Division), Melbourne.

Ross P.-S., Delpit S., Haller M. J., Nemeth K. & Corbella H. 2011. Influence of the substrate on maar-diatreme volcanoes; an example of a mixed setting from the Pali Aike volcanic field, Argentina. *Journal of Volcanology and Geothermal Research* **201**, 253-271.

Ross P. S., White J. D. L., Valentine G. A., Taddeucci J., Sonder I. & Andrews R. G. 2013. Experimental birth of a maar–diatreme volcano. *Journal of Volcanology and Geothermal Research* **260**, 1-12.

Rout D. J., Cassidy J., Locke C. A. & Smith I. E. M. 1993. Geophysical evidence for temporal and structural relationships within the monogenetic basalt volcanoes of the Auckland volcanic field, northern New Zealand. *Journal of Volcanology and Geothermal Research* **57**, 71-83.

Sandiford M., Wallace M. & Coblentz D. 2004. Origin of the in situ stress field in south-eastern Australia. *Basin Research* **16**, 325-338.

Schulz R., Buness H., Gabriel G., Pucher R., Rolf C., Wiederhold H. & Wonik T. 2005. Detailed investigation of preserved maar structures by combined geophysical surveys. *Bulletin of Volcanology* **68**, 95-106.

Shaw-Stuart A. 2005. Transition from phreatomagmatic maar forming explosive activity to magmatic scoria cone complex forming activity in the Pleistocene Mt Leura Volcanic Complex, southeastern Australia. Masters thesis, Monash University, Australia (unpubl.).

Skacelova Z., Rapprich V., Valenta J., Hartvich F., Sramek J., Radon M., Gazdova R., Novakova L., Kolinsky P. & Pecskay Z. 2010. Geophysical research on structure of partly eroded maar volcanoes; Miocene Hnojnice and Oligocene Rychnov volcanoes (northern Czech Republic). *Journal of Geosciences* **55**, 333-345.

Smith R. S., Annan A. P., Lemieux J. & Pedersen R. N. 1996. Application of a modified GEOTEM system to reconnaissance exploration for kimberlites in the Point Lake area, NWT, Canada. *Geophysics* **61**, 82-92.

Stagg H. M. J., Cockshell C. D., Willcox J. B., Hill A. J., Needham D. J. L., Thomas B., O'Brien G. W. & Hough L. P. 1990. Basins of the Great Australian Bight region: geology and petroleum potential. Bureau of Mineral Resources Australia, Continental Margins Program Folio 5.

Stephenson P. J. 1989. Northern Queensland. *In:* Johnson R. W. ed. *Intraplate volcanism in eastern Australia and New Zealand*, pp. 89-97. Cambridge University Press, Cambridge.

Uehara D. 2011. Geophysical and volcanological study on the Mount Leura Volcanic Complex of the Newer Volcanics Province, south western Victoria. Honours thesis, Monash University, Australia (unpubl.).

Valentine G. A., Graettinger A. H. & Sonder I. 2014. Explosion depths for phreatomagmatic eruptions. *Geophysical Research Letters*, 2014GL060096.

Valentine G. A. & White J. D. L. 2012. Revised conceptual model for maar-diatremes: Subsurface processes, energetics, and eruptive products. *Geology* **40**, 1111-1114.

van Otterloo J. & Cas R. F. 2013. Reconstructing the eruption magnitude and energy budgets for the pre-historic eruption of the monogenetic ~5 ka Mt. Gambier Volcanic Complex, south-eastern Australia. *Bulletin of Volcanology* **75**, 1-18.

Van Tatenhove A. 1983. A girl and her volcano. 3rd year project thesis, Monash University, Australia (unpubl.).

Veevers J. J. 1986. Breakup of Australia and Antarctica estimated as mid-Cretaceous (95±5 Ma) from magnetic and seismic data at the continental margin. *Earth and Planetary Science Letters* **77**, 91-99.

Wellman P. 1983. Hotspot volcanism in Australia and New Zealand: Cainozoic and mid-Mesozoic. *Tectonophysics* **96**, 225-243.

Wellman P. & McDougall I. 1974. Cainozoic igneous activity in eastern australia. *Tectonophysics* **23**, 49-65.

White J. D. L. 1991. Maar-diatreme phreatomagmatism at Hopi Buttes, Navajo Nation (Arizona), USA. *Bulletin of Volcanology* **53**, 239-258.

White J. D. L. & Ross P. S. 2011. Maar-diatreme volcanoes: A review. *Journal of Volcanology and Geothermal Research* **201**, 1-29.

Wohletz K. & Heiken G. 1992. *Volcanology and geothermal energy*. Univ. Calif. Press, Berkeley, Calif. USA.

Wood C. A. 1980. Morphometric evolution of cinder cones. *Journal of Volcanology and Geothermal Research* **7**, 387-413.

Yu S. M. 1988. Structure and devolment of the Otway Basin. *APEA Journal*.

Chapter 2.

Interpreting subsurface volcanic structures using geologically constrained 3-D gravity inversions. Examples of maar-diatremes, Newer Volcanics Province, southeastern Australia

T. N. Blaikie, L. Ailleres, P. G. Betts, R. A. F. Cas,

School of Earth, Atmosphere and Enivronment, Monash University, Clayton, Victoria, 3800, Australia

Journal of Geophysical Research: Solid Earth, 119 (2014); doi: 10.1002/2013jb010751

Cover page: Early morning fog over the Lake Coragulac maar, Alvie Scoria Cones and Warrion Hill.

Monash University

Declaration for Thesis Chapter 2

Declaration by candidate

In the case of Chapter 2, the nature and extent of my contribution to the work was the following:

Nature of contribution	Extent of contribution (%)
Fieldwork, data and image processing, modelling, preparation of the manuscript	87.5 %

The following co-authors contributed to the work. If co-authors are students at Monash University, the extent of their contribution in percentage terms must be stated:

Name	Nature of contribution	Extent of contribution (%) for student co-authors only
L. Ailleres	Supervisory role	5
P. G. Betts	Supervisory role	5
R. A. F. Cas	Supervisory role	2.5

The undersigned hereby certify that the above declaration correctly reflects the nature and extent of the candidate's and co-authors' contributions to this work*.

Candidate's Signature **Date**

Main Supervisor's Signature **Date**

*Note: Where the responsible author is not the candidate's main supervisor, the main supervisor should consult with the responsible author to agree on the respective contributions of the authors.

Abstract

We present results and a method to geophysically image the subsurface structures of maar volcanoes to better understand eruption mechanisms and risks associated with maar-forming eruptions. High-resolution ground gravity and magnetic data were acquired across several maar volcanoes within the Newer Volcanics Province of south-eastern Australia, including the Ecklin maar, Red Rock Volcanic Complex, and Mount Leura Volcanic Complex. The depth and geometry of subsurface volcanic structures were determined by interpretation of gridded geophysical data, and constrained 2.5D forward and 3D inverse modelling techniques. Bouguer gravity lows identified across the volcanic craters reflect lower density lake sediments and pyroclastic debris infilling the underlying maar-diatremes. These anomalies were reproduced during modelling by shallow coalesced diatremes. Short-wavelength positive gravity and magnetic anomalies identified within the center of the craters suggest complex internal structures. Modelling identified feeder vents, consisting of higher proportions of volcanic debris, intrusive dykes, and ponded magma. Because potential field models are non-unique, sensitivity analyses were undertaken to understand where uncertainty lies in the interpretations, and how the models may vary between the bounds of the constraints. Rather than producing a single 'ideal' model, multiple models consistent with available geologic information are created using different inversion techniques. The modelling technique we present focuses on maar volcanoes, but there are wider implications for imaging the subsurface of other volcanic systems such as kimberlite pipes, scoria cones, tuff rings and calderas.

Key Words: Maar, diatreme, gravity, magnetics, forward modelling, 3D inverse modelling

1. Introduction

Understanding the subsurface architecture of a volcano is important in order to fully understand eruption histories and processes. Often, it is not possible to link eruptive processes recorded from a volcano's surface deposits with structures responsible for those processes in the subsurface because where the volcanic edifice is preserved, the underlying vent structure is not often exposed. When the vent is exposed, the edifice is often eroded away, making it difficult to link subsurface volcanic structures with observations of surface deposits (Valentine 2012). However, with the application of geophysical modelling techniques, it is possible to image the plumbing system of a volcano, and when the surface deposits of these volcanoes are fully or even partially exposed, link subsurface structures to surficial deposits to better understand the entire volcanic system (Blaikie *et al.* 2012; 2014).

The application of geophysical modelling techniques to volcanic systems is under-utilised given the potential to image the three-dimensional structure and morphology of the underlying vent system, but has become increasingly common in recent years as data acquisition and modelling techniques have improved (e.g., Rout *et al.* 1993; Camacho *et al.* 1997; Brunner *et al.* 1999; Araña *et al.* 2000; Kauahikaua *et al.* 2000; Finn and Morgan 2002; Lindner *et al.* 2004; Schulz *et al.* 2005; Montesinos *et al.* 2006; Blanco-Montenegro *et al.* 2007; Cassidy *et al.* 2007; Lopez Loera *et al.* 2008; Mrlina *et al.* 2009; Paoletti *et al.* 2009; Blaikie *et al.* 2012; 2014). A variety of geophysical methods have been applied to resolve different features of the volcanic substrate. Electrical methods have limited depth penetration, but are used to complement gravity and magnetic surveys and have been applied to map the boundaries between volcanic breccia, dykes, and the host rock of maar volcanoes based upon differences in their resistivities (Mrlina *et al.* 2009; Skacelova *et al.* 2010). Refraction and reflection seismic surveys are effective at imaging lake sediments within the crater and horizontal layering in the upper parts of the maar-diatreme (Schulz *et al.* 2005; Buness *et al.* 2006; Gebhardt *et al.* 2011). However, one of the limitations of seismic methods is its inability to image steep structures, making it difficult to define the lateral boundaries of the crater and steep edges of the diatreme (Schulz *et al.* 2005; Buness *et al.* 2006). Alternatively, the advantage of potential field methods is their capability to image steeply dipping structures.

Previous work modelling volcanic structures using potential field data has utilised aeromagnetic data to model the subsurface of large calderas (e.g., Vulcano, Italy; Finn and Morgan, 2002; Yellowstone Caldera, USA; Blanco-Montenegro *et al.*, 2007), and has been combined with high resolution gravity data to model the internal structures of maar volcanoes (Rout *et al.* 1993; Lindner *et al.* 2006; Cassidy *et al.* 2007; Lopez Loera *et al.* 2008; Mrlina *et al.* 2009; Skacelova *et al.* 2010). These examples are mostly restricted to 2D forward modelling techniques. Three-dimensional gravity inversion techniques have been previously applied to model volcanoes (e.g., Camacho *et al.* 1997; Kauahikaua *et al.* 2000; Montesinos *et al.* 2006; Paoletti *et al.* 2009), although these models do not utilise a geologic reference model. Blaikie *et al.* (2012) produced a 3D reference model of a maar volcano for constrained inversion from 2D modelling results. This approach can produce more geologically realistic results because the reference model is controlled by the user and is based upon a combination of geological and geophysical data. This work will expand upon the method of Blaikie *et al.* (2012; 2014) and will discuss different gravity and magnetic modelling techniques in 2D and 3D in order to realistically image the subsurface structures of maar volcanoes.

Maar volcanoes are common in monogenetic volcanic fields and are the second most common subaerial volcano type on Earth after scoria cones (Wohletz and Heiken 1992). Eruptions of maar volcanoes are short-lived, produce small volumes of erupted material, and are strongly influenced by external factors such as ground/surface water and host rock rheology (Ross *et al.* 2011). They form by subsurface explosive magma-water interaction which produces a low tephra ring surrounding a crater cut below the pre-eruptive surface. The volcanic crater is underlain by a pipe-like structure known as a diatreme, which can extend vertically over several hundred meters, up to 2 km depth, containing a mixture of fragmented and coherent volcanic and country rock (Lorenz 1975, 2003; Lorenz and Kurszlaukis 2007; White and Ross 2011; Valentine and White 2012). Due to the infrequent and violent nature of volcanic eruptions, work focussing on the subsurface structures of these volcanoes is conducted on the inactive and often partially eroded volcanic edifice (e.g., White 1991; Ross and White 2006; Keating *et al.* 2008; Hintz and Valentine 2012; Lefebvre *et al.* 2012; Valentine 2012) where observations cannot be linked with surface deposits because they are often eroded away.

This study focusses on maar volcanoes because they are generally easily accessible for ground-based geophysical surveys and the nature of the maar diatreme and its feeder vents will usually result in a high petrophysical contrast between the surrounding host rocks, making them good candidates for potential field modelling (Cassidy *et al.* 2007; Blaikie *et al.* 2012). However, the modelling technique described here is not just limited to maar volcanoes and may be applied to other volcanic or mineralised systems provided that adequate petrophysical variations exist within the subsurface. Results are drawn from several case studies within the Newer Volcanics Province of Western Victoria to illustrate different aspects of our modelling technique. This paper focusses on applying potential field modelling techniques to understand subsurface volcanic structures, and the broader volcanological implications of our results. A detailed discussion of the eruptive history of each case study is beyond the scope of this paper. Further discussion of our geophysical modelling results and the eruptive history of the case studies are addressed by Blaikie *et al.* (2014).

2. Regional Geological and Geophysical context

The Newer Volcanics Province is an intraplate basaltic plains province composed of over 400 different eruptive centres, including shield volcanoes, scoria cones, tuff rings, maars, composite volcanoes, and extensive lava plains (Joyce 1975; Cas 1989; 2011; Cas *et al.* 1993; Lesti *et al.* 2008). Volcanic products are Late Cenozoic in age (4.5 Ma-4.5 ka) and cover an area >23,000 km^2, with northern areas of the province overlying the Palaeozoic metasediments and granitic intrusions of the Lachlan and Kanmantoo Fold Belts and southern areas overlying the Mesozoic-Cenozoic sediments of the Otway Basin (Figure 1a) (Joyce 1975; Lesti *et al.* 2008; Cas *et al.* 2011).

Three volcanic centres located within the Newer Volcanics Province will be used as case studies in this paper, including several maars within the Red Rock Volcanic Complex, Ecklin maar, and the Mount Leura Volcanic Complex (Figure 1a). These volcanic centres are hosted in the weakly lithified sedimentary sequences of the Otway Basin where groundwater contained within aquifers facilitated phreatomagmatic activity in the initial stages of the eruptions (Joyce 1975; Cas *et al.* 2011; Blaikie *et al.* 2012). Ecklin maar is a simple maar volcano, formed predominantly by phreatomagmatic explosions which created a crater elongated in the NNW-SSE direction. The crater is 800 m across its shortest axis and 1000 m across its longest with tuff deposits rising 40 m above the crater floor, thickest in the

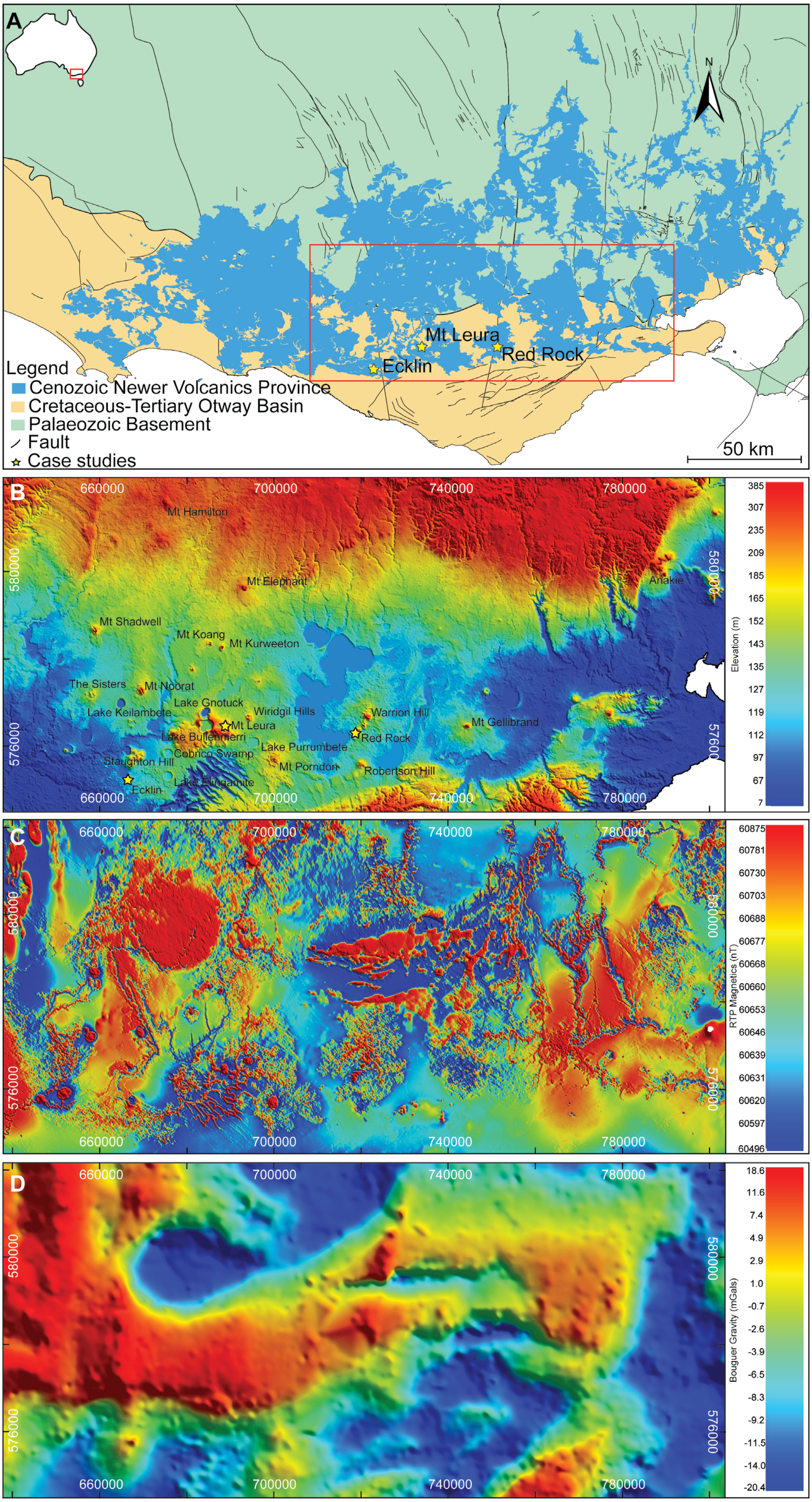
A
Mt Leura
Red Rock
Ecklin
Legend
Cenozoic Newer Volcanics Province
Cretaceous-Tertiary Otway Basin
Palaeozoic Basement
Fault
Case studies
50 km
N
B
Mt Hamilton
Mt Elephant
Anakie
Mt Shadwell
Mt Koang
Mt Kurweeton
The Sisters
Mt Noorat
Lake Gnotuck
Lake Keilambete
Wiridgil Hills
Warrion Hill
Mt Leura
Mt Gellibrand
Lake Bullenmerri
Red Rock
Lake Purrumbete
Cobrico Swamp
Staughton Hill
Mt Porndon
Robertson Hill
Ecklin
Lake Elingamite
Elevation (m)
RTP Magnetics (nT)
Bouguer Gravity (mGals)
C
D

south-east. The Mount Leura Volcanic Complex consists of a maar crater (1600 m in diameter) and a large overlapping tuff ring (2000 m), with up to 16 scoria cones contained within the two coalesced craters. The Red Rock Volcanic Complex is one of the most complex volcanic centres within the Newer Volcanics Province covering an area of 8.4 km^2 it is host to at least 40 separate eruption points forming seven polylobate maars and a scoria cone complex (Cas *et al.* 1993; 2011; Blaikie *et al.* 2012). Detailed descriptions on the geology and evolution of each of these volcanic centres, and further discussions of the geophysical results from this study can be found in Blaikie *et al.* (2014).

Relatively high-resolution geophysical data sets (sourced from Geoscience Australia) are available across the areas of interest. Aeromagnetic data with coverage over the volcanic centres have a flight spacing of 200 m and are gridded to 50 m. This is useful for imaging discrete eruptive centres and lava flow fields (Figure 1c) (Blaikie *et al.* 2012). Eruption points appear as near-circular positive magnetic anomalies. There are a few examples of negative anomalies which are interpreted to have erupted during a period of reversed polarity of the Earth's magnetic field. The extent of lava flow fields (both sheet and valley) within the Newer Volcanics Province is well defined by the aeromagnetic data displaying a short-wavelength mottled texture that obscures the underlying geophysical response. The geophysical signature of the province is superimposed on the smooth, low magnetic response of sediments within the Otway Basin in the south and the complex geophysical signature of the Palaeozoic basement in the north (Blaikie *et al.* 2012).

The regional Bouguer gravity grid (Figure 1d) is derived from data where the average station spacing is 1000 metres, so the resolution is insufficient to image individual volcanic centres, but is useful for examining larger regional-scale structures such as faults, plutons, and basin structures that may have controlled the location of eruptive points. Regional digital elevation models (DEMs) and local lidar data are available and assists in the mapping of eruption points, lava flows and pyroclastic deposits (Figure 1b), and is essential for gravity corrections.

2.1 Petrophysics

Samples from the three studied volcanic centres, and other nearby centres with similar features area were analysed for their petrophysical properties (density and magnetic susceptibility) in order to constrain the geophysical interpretations (Figure 2). Magnetic susceptibility measurements were acquired from exposed outcrops in the field. Susceptibility values range between 0.00001 – 0.083 SI for basalt, 0.00019 – 0.013 SI for scoria deposits and 0.00018 – 0.01 SI for tuff deposits; however, these were considered minimum values as they are often variably weathered and have undergone oxidation, which reduces magnetic susceptibility (Emerson 1979) and therefore may not be necessarily representative of rock petrophysics at depth.

The density of field samples was measured using an immersion technique based on the method of

Figure 1 (LEFT). Geologic and geophysical setting of the Newer Volcanics Province. (a) Simplified regional geologic map showing location of the three case studies and extent of images for Figures 1b–1d. (b) Digital elevation model highlighting the numerous volcanic centers of the region. (c) Reduced to the pole aeromagnetic data. Individual volcanic centers typically appear as magnetic highs, and lava flow fields appear as magnetic highs with a high-frequency mottled texture. (d) Bouguer anomaly. Gravity lows in the south of the image correspond to the sediments of the Otway Basin, while highs in the north correspond to the Palaeozoic metasediments and granites (circular low in northeast of image).

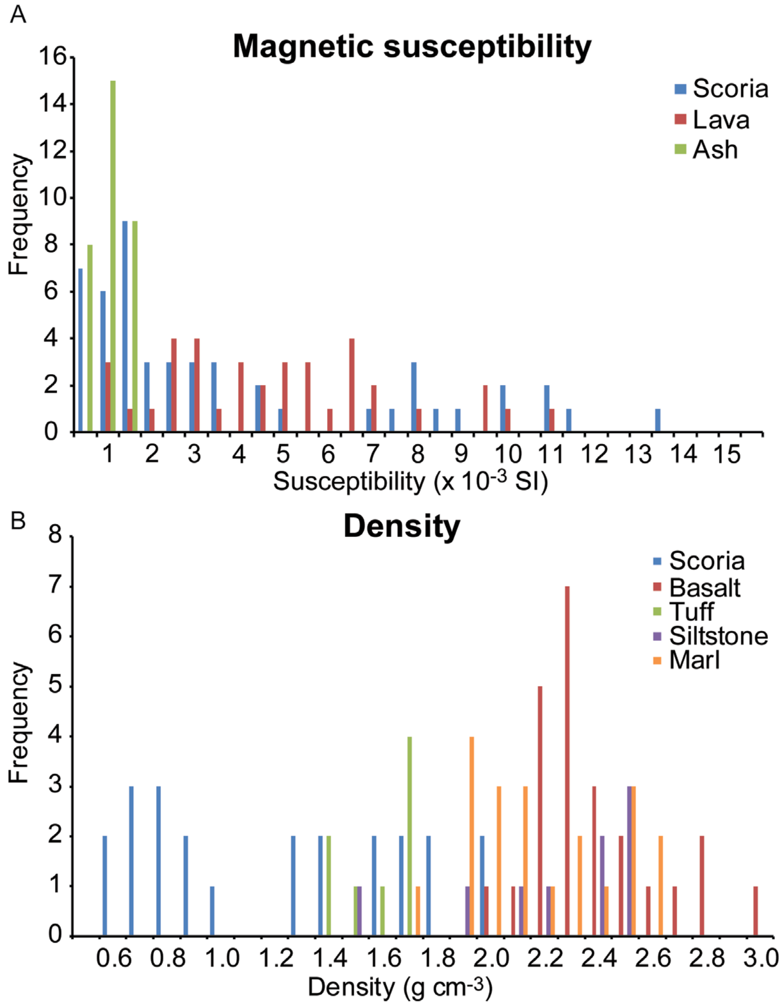

Figure 2. Density and magnetic susceptibility values of common rock types observed within the Newer Volcanics Province. Data are compiled from samples from the Ecklin maar, Red Rock Volcanic Complex, Mount Leura Volcanic Complex, Mount Noorat, Tower Hill, and Mount Rouse.

Houghton and Wilson (1989). Densities ranged between 1.9 – 2.9 g/cm^3 for basalts, 0.5 – 1.9 g/cm^3 for scoria and 1.34 – 1.67 g/cm^3 for tuff deposits. The density of basalt and scoria samples is variable depending on the level of vesiculation, and a range of samples with both high and low levels of vesicularity were taken. Denser clasts with low levels of vesiculation were considered representative of the volcanoes feeder conduits and/or lava flows, whereas the density of more vesicular clasts was considered representative of scoria deposits.

3. Data acquisition and processing technique

3.1 Survey design

Prior to commencing any geophysical survey, wavelengths of anomalies associated with different geologic bodies should be considered so that data may be acquired at a resolution suitable for imaging those structures. Several synthetic models of maar-diatremes with identical properties but variable geometries and internal structures were constructed (Figure 3a) to investigate the wavelength of anomalies associated with different subsurface structures, and to ensure that those structures are resolvable using our inversion technique. The calculated free-air gravity profile, sampled at 80 m intervals through the centre of each model is shown in Figure 3b. The gravity low observed across the maar crater in each model is related to the lower density pyroclastic debris within the diatreme.

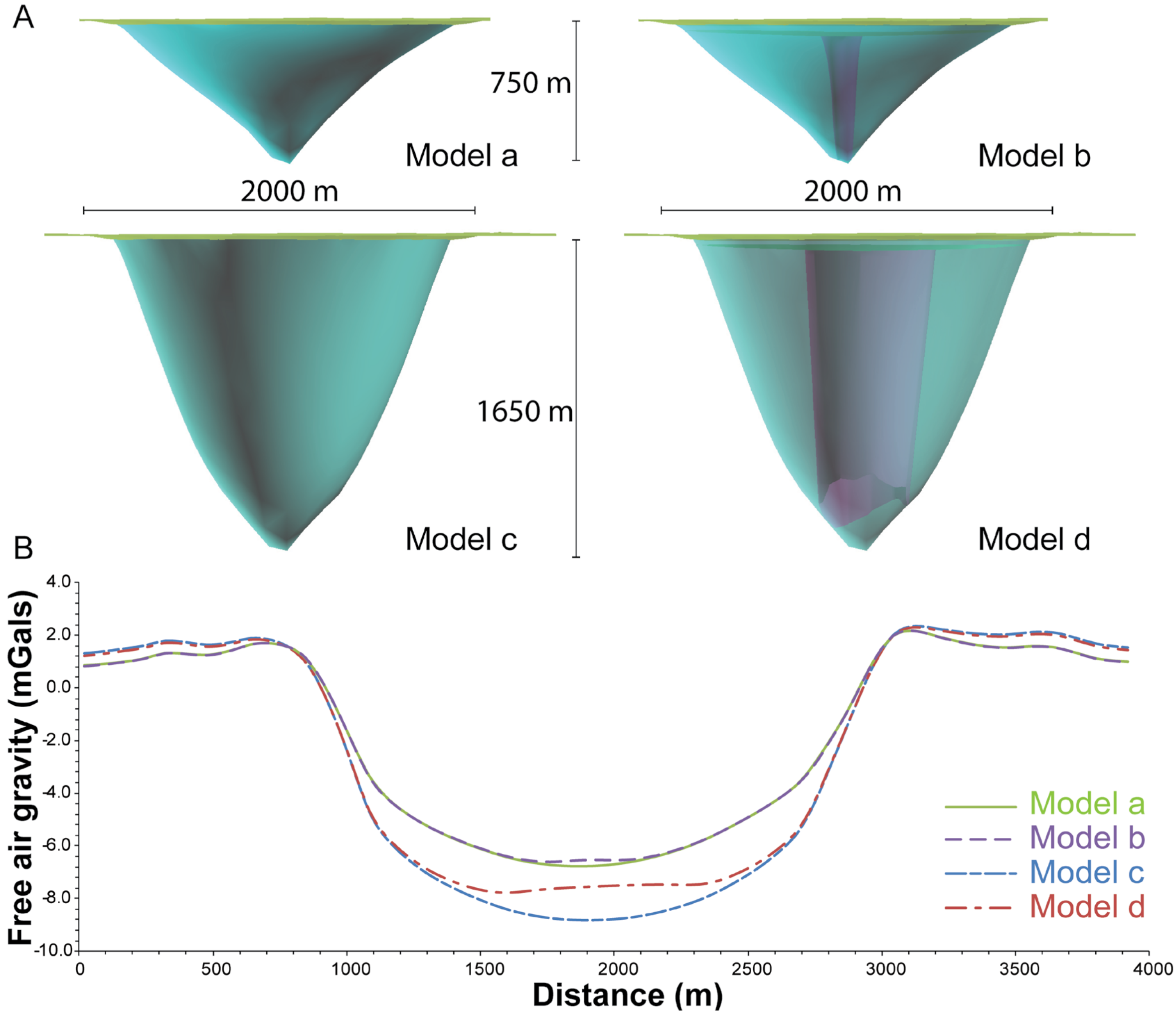

Figure 3. (a) Synthetic 3-D models of deep and shallow maar-diatremes, with (models a and c) and without (models b and d) a denser central conduit. (b) Free-air gravity profile through the center of the above 3-D models showing a gravity low over the lower density diatremes, with a gravity high located over the denser vents.

The wavelengths of the anomalies arising from the two diatreme geometries are similar; however, the deeper diatreme results in a greater negative amplitude. Short-wavelength anomalies are observed in the centre of the craters in models B and D (Figure 3b) and are related to the denser vents within the diatreme. Model D is closest to the expected subsurface structures within maar-diatremes of the Newer Volcanics Province. The anomaly related to the vent in model D is fairly subtle, and in order to detect such a structure in a survey the data resolution should be a minimum of half the distance of the hypothesised anomaly wavelength. If these structures are identified in field data, care must also be taken when selecting an appropriate model resolution to ensure these structures are resolvable during inversion.

The design of the geophysical survey is largely dependent on the volcano's size, complexity, and topography. For smaller volcanoes, data collected along orthogonal traverses are usually sufficient to model subsurface volcanic features, while for larger volcanoes several orthogonal traverses may be required. For a large maar, the geophysical signal of the diatreme has a longer wavelength compared to that of a small maar, which can be detected using a larger station spacing, however small-scale intrusions such as dykes within the diatreme may not be imaged. The distance between observation points may be reduced to image smaller maars, since the wavelengths of associated anomalies are shorter. Reducing the spacing allows detection of smaller-scale components of the volcanic plumbing system. The distance between gravity and magnetic observations is increased away from the vent at the periphery of the volcano because at this scale, only the longer wavelengths associated with the maar are being detected.

3.2 Geophysical data acquisition and correction

Ground gravity and magnetic surveys were conducted across the three volcanic centres, in a series of near orthogonal traverses. Instrument specifications, sample rates, resolution, and accuracy are summarised in table 1. Conditions at each field area varied, with swampy conditions present at Ecklin and the Red Rock Volcanic Complex and steep slopes present at Mount Leura and Red Rock. The parameters of the survey (e.g., station spacing and traverse orientation/location) were adjusted slightly to suit field conditions at each locality.

Gravity data were acquired using a high-precision Scintrex CG-3M gravity meter. A differential Global Positioning System (GPS) was used to obtain the position and elevation of each station to within 0.015 m (relative to a Global Navigation Satellite Systems (GNSS) differential GPS base station established within the survey area). The estimated uncertainty in gravity measurements from uncertainties in elevation is 0.005 mGal, which is equivalent to the accuracy of the gravity meter. Gravity data were acquired at intervals of 20 m inside the maar crater, increasing to 40 m outside. The gravity meter acquired each reading over a 30 s period (one reading per second), averaged the results, and applied the tidal correction. Swampy conditions in some areas of the craters resulted in gravity readings with high standard deviations (between 0.16-0.33 mGals). If conditions were particularly unfavourable, several readings were taken and the results averaged. To ensure high-quality data, results were thoroughly checked for noise prior to interpretation. Any anomalies defined by only one data point, and without a corresponding magnetic anomaly was assumed to be noise and removed.

Drift, latitude, free-air, Bouguer, and terrain corrections were applied to the raw data to correct for variations in gravity not arising from the underlying geology. A crustal density of 2400 kg/m^3 was applied for Bouguer and terrain corrections to reflect the lower density host sediments of the region; however, since free-air gravity data is used for two and three dimensional modelling the correction density does not influence the geophysical models. Free-air gravity data were selected for modelling because we include the volcanoes topography in each 2.5D and 3D model. The gravitational effects associated with topography along the plane of the 2.5D models are calculated and corrected for by GM-SYS during modelling. GM-SYS is an extension of Geosoft Oasis Montaj (www.geosoft.com) and allows forward modelling of gravity and magnetic data in 2.5D or 2.75D (Talwani *et al.* 1959; Talwani and Heirtzler 1964; Rasmussen and Pedersen 1979). The 3D modelling and inversion program VPmg (which stands for Vertical Prism magnetic and gravity; www.fullagargeophysics.com) is used for 3D inverse modelling and operates using free-air gravity; however, the gravitational effects of regional topography are corrected by importing a terrain model into VPmg during inversion (Fullagar *et al.* 2000; 2004; 2008).

Ground magnetic data were acquired across the maars, usually in grid-based pattern, except at the Red Rock Volcanic Complex where access to the maar craters was difficult with the instruments and data was acquired along the same traverses as the gravity survey. Magnetic data were acquired at 1-2 s intervals using a G858 Caesium-vapour magnetometer. A G856 proton-procession magnetometer set-up within the survey area was used as a base station. Magnetic data was despiked to remove noise (primarily arising from electric fences) and diurnal variations corrected for by base station readings. The International Geomagnetic Reference Field was removed before data and image processing.

Table 1. Summary of geophysical instruments used during surveys.

Instrument	Model	Resolution	Accuracy
Gravity meter	Scintrex CG-3M	0.001 mgal	0.005 mgal
Magnetometers	Caesium vapour G858	0.01 nT	> 2 nT – 1-2 second sampling
	Proton procession G856 (base station)	0.1 nT	> 0.5 nT – 3 minute sampling
Differential GPS	Trimble R8 GNSS base receiver	0.001 m	3-5 m Horizontal, 10 m Vertical
	Trimble R8 GNSS rover		10-15 mm
	Magellan Promark 500 base receiver		3-5 m Horizontal, 10 m Vertical
	Magellan Promark 500 rover		10-15 mm

3.3 Image processing

Processed gravity and magnetic data were gridded using the Geosoft Oasis Montaj minimum curvature algorithms. Magnetic data were reduced to the pole (RTP). Gridded data were selectively filtered to emphasise different features in the data which assists with the interpretation. High-pass filters were applied to remove effects of long-wavelength anomalies associated with deeper crustal structures. Upward continuation and low-pass filters were required to remove noise that was overlooked during the initial data despiking and emphasise longer-wavelength anomalies associated with deeper crustal structures.

A combination of filters is often applied to remove effects of a regional gradient and noise in order to obtain an image with better contrast between long- and short-wavelength features. Vertical derivatives, for example, tend to highlight short-wavelength anomalies which are associated with shallow structures, however they can emphasize noise in the data and are used in combination with a low-pass filter. Figures 4a-d show gridded gravity and magnetic data from the Ecklin maar with different filters applied. Figure 4a shows the Bouguer anomaly prior to any filtering. In Figure 4b the north-west to south-east regional gradient is removed. Figure 4c shows an image where the shorter-wavelength features associated with the maars vents have been enhanced by a high-pass filter. High pass filters are effective at enhancing subtle features within the maar as gravity anomalies with amplitudes between 0.43-0.73 mGal are imaged compared to the unfiltered data which only highlights a 2 mGal negative gravity anomaly. The subtle Bouguer gravity anomalies correlate well with the magnetic anomaly map (Figure 4d) indicating that they are not a result of the interpolation process during gridding and filtering.

4. Potential field modelling and interpretation

The processed gravity and magnetic data are subjected to 2.5D forward and 3D inverse modelling to understand the subsurface geologic features of the volcanic centres and the distribution of properties within them. Each model is constrained by the available geologic information including petrophysical properties, surface geology, and the interpretation of gridded geophysical data (both regional aeromagnetic and local survey data). The modelling workflow is summarised in figure 5 and uses

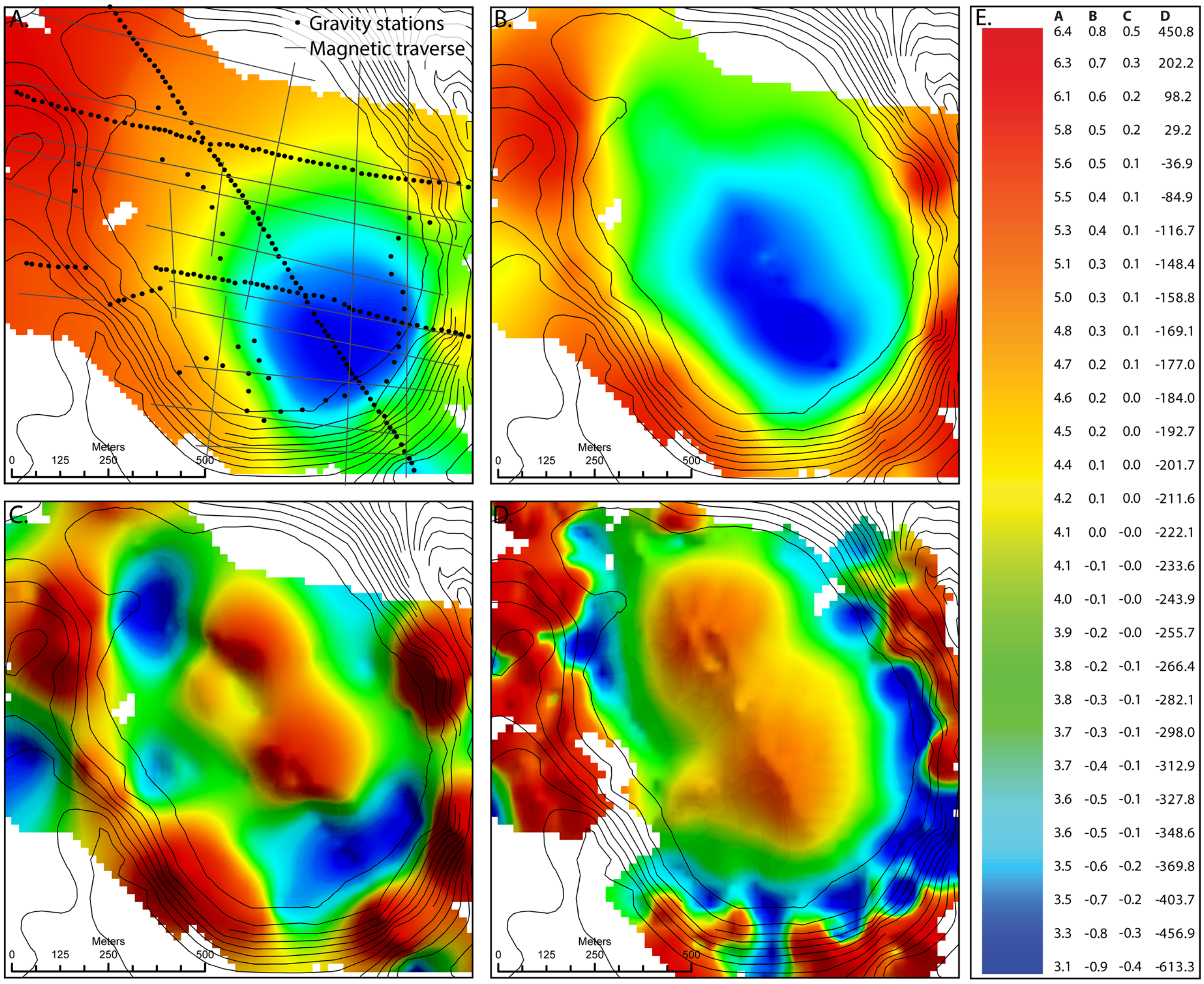

Figure 3. (a) Synthetic 3-D models of deep and shallow maar-diatremes, with (models a and c) and without (models b and d) a denser central conduit. (b) Free-air gravity profile through the center of the above 3-D models showing a gravity low over the lower density diatremes, with a gravity high located over the denser vents.

existing software packages (e.g., Oasis Montaj, www.geosoft.com; Gocad, www.gocad.org; and VPmg, www.fullagargeophysics.com). Our technique is based upon previous works focussing on modelling aeromagnetic and gravity data for large scale analysis of crustal architecture (e.g., McLean *et al.* 2008; Williams *et al.* 2009). Our modelling workflow was adapted from these works to be more suitable for imaging volcanic structures and will be discussed in detail below drawing from examples from the Red Rock Volcanic Complex, Mount Leura Volcanic Complex and Ecklin maar. This technique has not previously been applied in this type of setting, and our process of integrating interpretations from gridded data, 2D and 3D modelling, and using the results of earlier inverse models to drive the next inversion produces more robust and constrained models that have the potential to reveal new and more accurate information about the subsurface architecture of volcanic systems.

4.1 Joint 2.5D gravity and magnetic modelling

Two-dimensional forward modelling allows geologic cross sections to be constructed based upon geologic, petrophysical, and potential field data (Blakely 1995; McLean and Betts 2003; Williams *et al.* 2009; Blaikie *et al.* 2012). Multiple cross-cutting forward models of the surveyed maar volcanoes were produced using the *GM-SYS* module contained within the Geosoft Oasis Montaj software

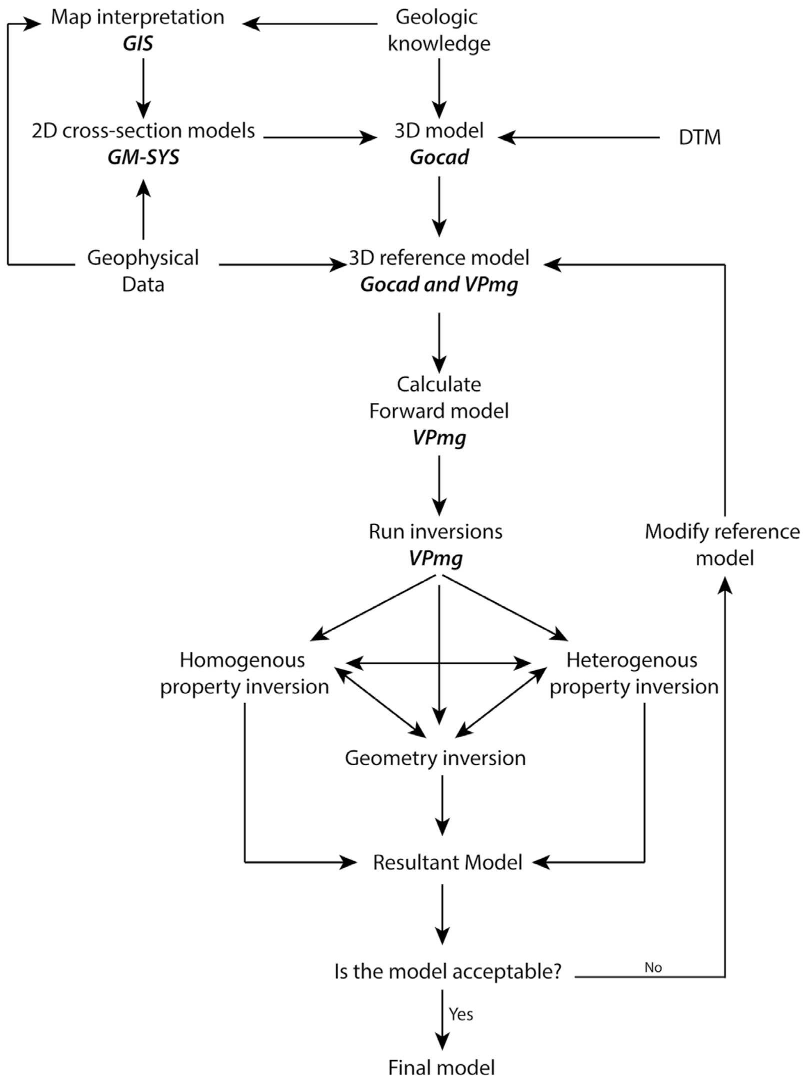

Figure 5. The geophysical modeling workflow applied to this research. Adapted from McLean et al. [2008].

package which allows gravity and magnetic data to be jointly modelled in two dimensions. GM-SYS is based on the methods of Talwani *et al.* (1959) and Talwani and Heirtzler (1964) and uses the algorithm described by Won and Bevis (1987). Geologic bodies are represented as 2.5D polygons (2.5D calculations based on Rasmussen and Pedersen (1979)) with the model extending ± 30 000 km in the x direction to eliminate edge effects and to ± infinity in the third dimension (y direction). The geometry and/or properties of the polygons are altered by the user until a geologically reasonable cross section with an acceptable fit between the observed and calculated data is obtained (Aitken *et al.* 2009).

The 2.5D forward models were constructed in GM-SYS incorporating the geology and petrophysical properties of the study area and an understanding of the structures expected within these types of volcanoes. The approximate depths of the diatremes were constrained based upon accessory lithic fragments observed in pyroclastic deposits; however, these represent minimum values as phreatomagmatic explosions occurring at deeper levels are often too weak to transport material to the surface and deposit it in the tuff ring (Valentine and White 2012; Lefebvre *et al.* 2013; Ross *et al.* 2013). The free-air gravity anomaly is modelled, so topography can be included within the model, and the gravity value is calculated at the surface and compared to the observed data. The reduced to the pole (RTP) magnetic field is calculated at an elevation of 2 m which represents the height of the

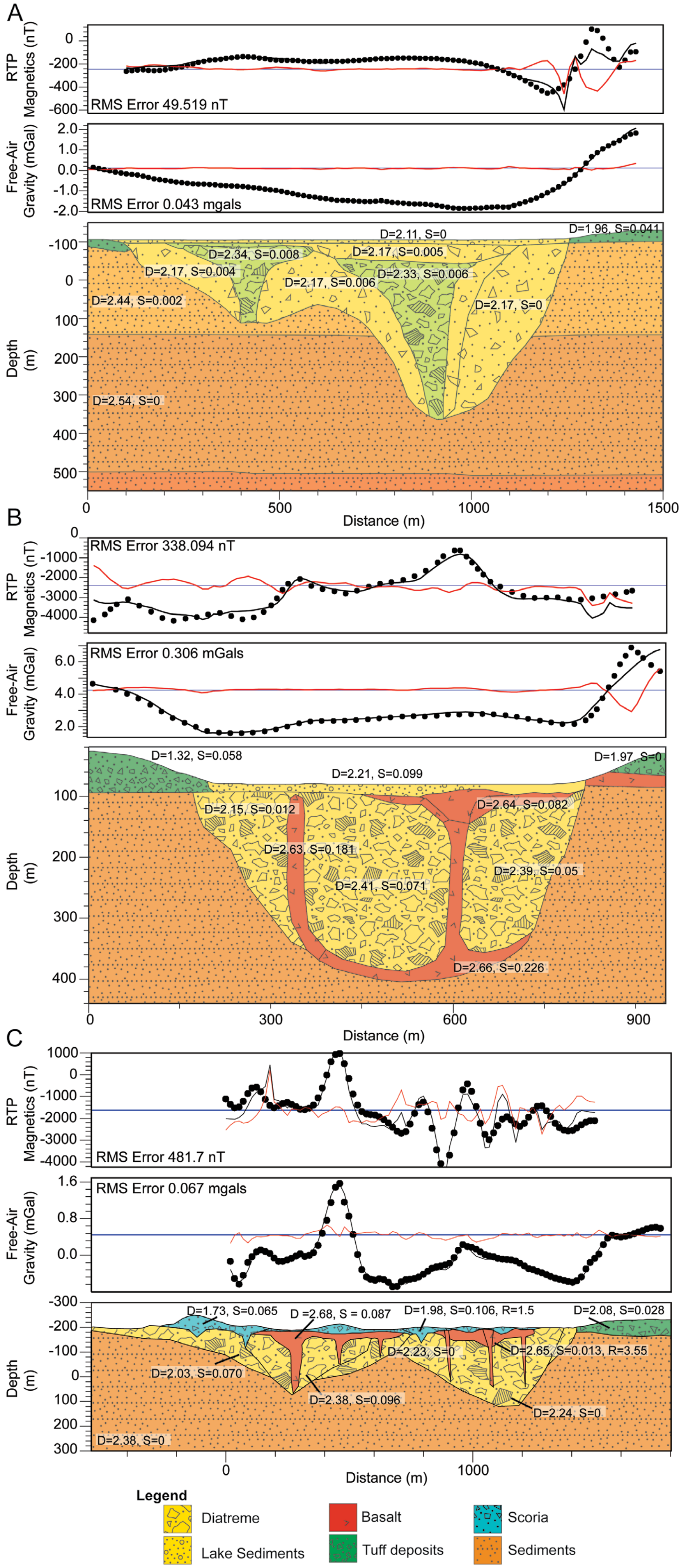
A
RTP Magnetics (nT)
RMS Error 49.519 nT
Free-Air Gravity (mGal)
RMS Error 0.043 mgals
D=2.11, S=0
D=1.96, S=0.041
D=2.34, S=0.008
D=2.17, S=0.005
D=2.17, S=0.004
D=2.33, S=0.006
D=2.17, S=0.006
D=2.44, S=0.002
D=2.17, S=0
D=2.54, S=0
Depth (m)
Distance (m)
B
RMS Error 338.094 nT
RTP Magnetics (nT)
RMS Error 0.306 mGals
Free-Air Gravity (mGal)
D=1.32, S=0.058
D=1.97, S=0
D=2.21, S=0.099
D=2.64, S=0.082
D=2.15, S=0.012
D=2.63, S=0.181
D=2.39, S=0.05
D=2.41, S=0.071
D=2.66, S=0.226
Depth (m)
Distance (m)
C
RTP Magnetics (nT)
RMS Error 481.7 nT
RMS Error 0.067 mgals
Free-Air Gravity (mGal)
D=1.73, S=0.065
D =2.68, S = 0.087
D=1.98, S=0.106, R=1.5
D=2.08, S=0.028
D=2.23, S=0
D=2.65, S=0.013, R=3.55
D=2.03, S=0.070
D=2.38, S=0.096
D=2.24, S=0
D=2.38, S=0
Depth (m)
Distance (m)
Legend
Diatreme
Basalt
Scoria
Lake Sediments
Tuff deposits
Sediments

sensor during ground surveys. As measured magnetic susceptibility values represent minimum values, the susceptibility of the model was increased (within the maximum range expected for basaltic rocks) (see Clark 1983; 1997) when an acceptable fit to the magnetic data could not be obtained within the range of measured values. An automatic DC shift is applied to the calculated gravity and magnetic response in order to provide the lowest misfit to the data.

Several examples of 2.5D models produced across the three study areas are shown in Figure 6. In each example the gravity lows observed across the volcanic crater can be reproduced by shallow diatreme structures with a lower density than their surroundings. Local positive gravity anomalies, with corresponding magnetic anomalies of a similar wavelength are observed in the centre of the Lake Werowrap maar crater at the Red Rock Volcanic Complex (Figure 6b) and the Mount Leura Volcanic Complex (Figure 6c). These anomalies can be reproduced by intrusive dykes with a higher density and magnetic susceptibility than the surrounding diatreme and host rock. Ecklin maar (Figure 6a) also exhibits two positive gravity and magnetic anomalies in the centre of the maar crater which have a longer wavelength (350 m) and smaller amplitude (0.36 mGal) than the anomalies thought to be related to intrusive dykes detected in Lake Werowrap (0.5 mGal, 100 m). These anomalies suggest that broader and deeper vents with a smaller density contrasts are present in the centre of the Ecklin diatreme. The subtle density contrast suggests vents of a similar composition to the diatreme, but containing higher proportions of volcanic debris. The Red Rock and Mount Leura Volcanic Complexes show morphological evidence for multiple coalesced diatremes and this is supported by the geophysical models, while the multiple vents modelled within the Ecklin maar were not apparent based on the surface morphology, and were only identified after geophysical modelling (Blaikie *et al.* 2014).

4.2 Three-dimensional modelling and potential field inversions

The 2.5D forward models produced in GM-SYS were imported into Gocad where they could be observed in three dimensions and serve as initial geometric constraints for the construction of a 3D model. Lithological boundaries within the model are defined by surfaces and are interpolated using a discrete smooth interpolation (DSI) algorithm which smooths surfaces whilst honouring fixed data points (i.e. boundaries defined by the 2D models) (Mallet 1992; 1997). A topography surface defines the upper boundary of the model and is interpolated from LIDAR, SRTM (Shuttle Radar Topography Mission), or differential GPS data. Three-dimensional models for each of the case studies, which serve as an initial reference models for 3D inversion, are shown in Figure 7.

In preparation for inversion, the 3D models are discretised into cells, referred to as voxels, to create a voxet model with a resolution of 20 m in the x and y directions and 10 m in the z direction. The model dimensions and number of voxels within it are constrained by the resolution of the geophysical data and computational capacity. Regions in the voxet model are defined by the surface model, and have a density or susceptibility value applied to them prior to inversion.

Inversions help improve the 3D geometry and property distribution within modelled structures and are

Figure 6 (LEFT). The 2.5-D forward models showing the observed and calculated free-air gravity and reduced to the pole magnetic responses and the misfit of the models from (a) Ecklin maar, (b) Lake Werowrap, Red Rock Volcanic Complex, and (c) Mount Leura Volcanic Complex.

performed using VPmg (Fullagar *et al.* 2000, 2004, 2008) which can sequentially perform homogeneous and heterogeneous property inversions and geometry inversions, but relies upon a reference mode,l so geologically meaningful results are obtained (Williams *et al.* 2009). The parameters of the reference model are numerically adjusted by software algorithms, using the method of steepest descent until an acceptable fit between the observed and calculated data is obtained (based on a chi-squared condition, where the fit is acceptable when , where and are the observed and calculated data and is the data uncertainty) (Fullagar and Pears 2007; Fullagar *et al.* 2008). During an inversion, VPmg numerically calculates the optimum property values, property distribution or geometry of a model within the bounds of constraints set by the user. The final model can be imported into Gocad for visualisation.

Gravity inversions are initially applied to obtain a best-fit geologic model of these volcanic centres, as there is greater confidence in the measured density values. Magnetic inversions are applied to the best-fit gravity model for the Ecklin maar to compare how well the magnetic signal of the reference model matches the observed data; however, inversion constraints are relaxed since the magnetic susceptibility measurements are taken from variably weathered surface deposits may not reflect the true susceptibility at depth. Magnetic inversions are not applied to the Red Rock or Mount Leura Volcanic Complexes because it became apparent through 2.5D modelling that these centres may have some degree of remnant magnetisation. Since exact remanence values are not available and the modelled values are only estimates, any magnetic inversion applied would be largely unconstrained and may not yield realistic results.

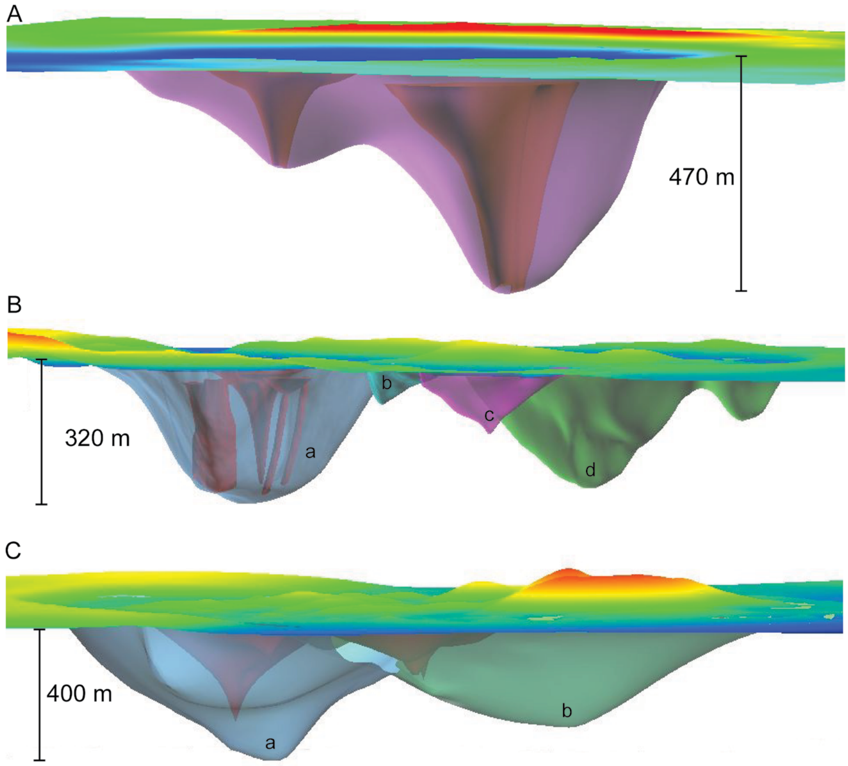

Figure 7. Three-dimensional models of the maar diatremes derived from 2.5-D cross sections. In each image, the colored surfaces represent topography (reds are topographic highs; blues are topographic lows). (a) The Ecklin maar (purple surface is the diatreme (region 4 in Table 2); orange surfaces are the vents (regions 5 and 6 in Table 2)). (b) The Red Rock Volcanic Complex (Blue, green, and pink surfaces represents the diatremes; red surfaces are the dikes and magma ponds). Small letter a is the Lake Werowrap maar which corresponds to region 4 in Table 2. The maar-diatremes (small letters b–d) correspond to regions 2, 8, and 9 in Table 2, respectively. (c) The Mount Leura Volcanic Complex (blue surface is the maar diatreme (region 1 in Table 2), green surface is the diatreme of the tuff ring (region 2 in Table 2), and red surfaces are vents and lava flows (region 3 in Table 2)).

4.3 Inversion Constraints

Constraints must be applied during inversion, so results remain geologically reasonable. Constraints may be set so parts of the model are prevented from changing (e.g., when constraints from drill core, seismic or topography data exist), may only change within bounds set by the user (e.g., maximum and minimum values for the petrophysical properties), or can only change by a certain amount per iteration (Fullagar and Pears 2007; Fullagar *et al.* 2008). Applying strict constraints will increase the chance of a stalled inversion (where the misfit does not improve after two iterations), and the target misfit may not be achieved unless the constraints are relaxed (Fullagar and Pears 2007).

Strict petrophysical constraints are applied to these case studies, and certain regions such as the host rock are often prevented from being modified during geometric and heterogeneous inversion. As a result of these tight constraints, the inversion will often stall before the target misfit is reached. When this occurs, the misfit is reduced by inverting the modified model file using a different inversion style. By running sequential inversions, an acceptable model is generally obtained without needing to relax the constraints.

4.4 Inversion technique

VPmg calculates a forward model prior to inversion, and the results can be examined numerically as the root mean aquare (RMS) and/or visually as the residual of the observed and calculated data (e.g., the coloured spheres in Figures 8a-b represent the residual calculated at each point). This allows the initial misfit of the reference modelled to be assessed, and identifies areas within the model that may need to be modified through inversion. The 3D reference model is constructed from 2D profiles that already match the observed data, so the 3D model should have a relatively low misfit. However, 3D inverse modelling accounts for the gravitational effect of terrain beyond the main profiles and the 3D geometry of structures within the model, so some misfit is expected and is reduced through inversion. VPmg targets a theoretical optimum misfit of 0.1 mgals during inversion, which equates to less than 5% of the total dynamic range for the gravity data at each volcanic centre.

Figure 8a shows the gravity misfit for the reference model of the Ecklin maar-diatreme (RMS misfit of 0.33 mGals). High levels of misfit correlate to the edges of the model where there is high topographic relief (i.e., maar rim) and around the maars vent where the 3D geometry was interpolated between the 2D cross-sections. A positive misfit indicates that the underlying regions within the model are too dense/magnetic while a negative misfit indicates regions of the model where the density/susceptibility should be increased. Alternatively, if the petrophysical properties are well constrained, the geometry of the model may need to be altered. In the Ecklin example, a negative misfit of the gravity data over the vent of the maar suggests that structure needs to be deeper and/or denser than the initial reference model (Figure 8a).

Once areas of misfit have been identified, inversions are performed to improve the property contrasts, property distribution, and/or the geometry of selected lithological regions and/or boundaries within the model in order to reduce the misfit. Three styles of inversion are applied to these examples:

1. Homogeneous inversions calculate the optimum property of all or specific regions of the model (Fullagar and Pears 2007). Upper and lower constraints on model densities/susceptibilities are set so properties remain within the range of observed values. A homogeneous inversion is an

initial step towards reducing a models misfit. The modified model file is used as the reference model for subsequent heterogeneous property and geometry inversion as the strict constraints applied in these examples result in the inversion stalling before reaching the target misfit.

2. Geometry inversions are applied to optimise the geometry of boundaries within the model while the petrophysical properties remain fixed to a value specified by the user. The geometry of lithological boundaries are altered by allowing the interfaces between vertical prisms (voxels) corresponding to the boundaries of selected model regions to move up or down, therefore optimising the distribution of density or magnetic susceptibility in selected regions of the model (Fullagar and Pears 2007). In these examples, a geometry inversion is applied after a homogenous inversion, and if the target misfit cannot be obtained, the results of the geometry inversion serve as the reference model for heterogeneous inversions.

3. Heterogeneous inversions calculate the optimum property distribution within all or selected model regions. There are different types of heterogeneous inversion, producing either smoothly (conventional style) or randomly (stochastic style) varying property distributions (Fullagar and Pears 2007). Stochastic inversions apply a random property distribution within the model with the size of each perturbation controlled by a statistical distribution set by the user and accepted if it produces a reduction in the misfit (Fullagar and Pears 2007). This is the preferred technique for these examples, as they are better at resolving vertical structures than the conventional style, which will tend to concentrate dense material at the surface of the model regardless of the depth of the original causative body (Li and Oldenburg 1996, 1998), although a depth weighting can be introduced to help counteract this (Oldenburg and Pratt 2007).

4.5 Results

The initial and optimised densities after homogenous inversion, and the RMS misfits of the reference and modified model of Red Rock, Mount Leura and Ecklin maar are shown in Table 2. Each inversion decreased the misfit of the reference model but did not reach the target misfit of 0.1 mGals and the modified model file was used as the reference model for further geometric and heterogeneous inversions.

Results of geometric and heterogeneous inversions are drawn from the Ecklin maar example and are shown in Figures 8b-d. The geometry of the Ecklin maar-diatreme was modified first, with results suggesting that the southern diatreme is deeper than the initial model and the northern diatreme is shallower (Figure 8b). This is consistent with observations of a negative misfit over the southern diatreme and positive misfit over the northern. These results have implications for understanding the evolution of the maar-diatreme as broad shallow diatremes indicate an abundant supply of water, and/or weakly lithified sediments, while deeper diatremes suggest downward propagation of the depth of magma-water interaction due to groundwater drying up at shallow levels (Lorenz 2003; Auer *et al.* 2007; Ross *et al.* 2011). This suggests that explosive magma-water interaction initially occurred with shallow, weakly lithified, and water-saturated sediments, before propagating downwards into more consolidated sediments.

Figure 8c shows results of a stochastic heterogeneous inversion of the modified model geometry, optimising the density distribution throughout the diatreme and the two vents. The rest of the model was not inverted, and densities were retained from the initial homogenous inversion. The property distribution throughout the diatreme supports previous interpretations of the data, and indicates two denser vents located within the centre of each diatreme, surrounded by lower density material. The southern diatreme is slightly less dense than the north which may be a result of a slightly different composition (i.e., higher proportion of pyroclastic debris) or a higher degree of fragmentation within the diatreme material.

To help verify these results, homogenous and heterogeneous inversions of the magnetic data are applied to the geometry of the best fit gravity model in attempt to achieve an acceptable model consistent with both data sets. Because the susceptibility data are not as well constrained and may vary over several orders of magnitude, the upper and lower model constraints are relaxed; however, the model geometry remains fixed. Figure 8d shows a stochastic heterogeneous inversion of the diatremes magnetic susceptibility, which has a RMS misfit of 114.87 nT. Although the target misfit of 70 nT (approximately 5% of total dynamic range) was not achieved with this inversion, areas of misfit occur largely outside the maar crater. The misfit over the crater is within an acceptable range, so the results of the inversion are considered valid.

Magnetic inversions support previous results obtained through density inversions and indicate two vents with higher proportions of magnetic minerals (corresponding to higher volumes of basalt),

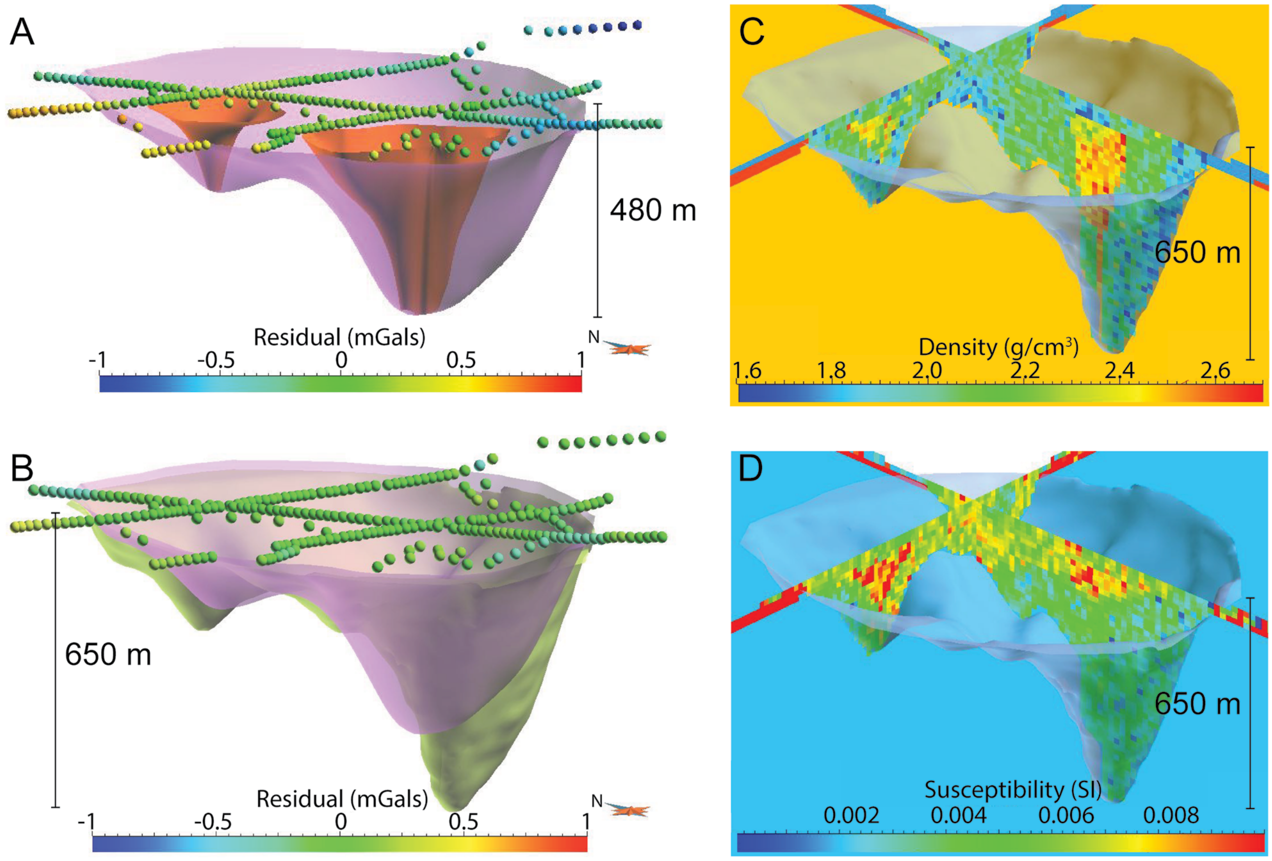

Figure 8. (a) Three-dimensional reference model of the Ecklin maar-diatreme showing the residual gravity anomaly calculated at each observation point (colored spheres; blues/reds = high levels of misfit and green = low levels of misfit). (b) Original (purple) and optimized (green) diatreme geometry showing reduced misfit. (c) Vertical slices showing optimized density distribution after stochastic heterogeneous inversion (colors represent density of vertical slices; optimized diatreme geometry surface overlain for reference). (d) Vertical slices showing optimized magnetic susceptibility distribution after stochastic heterogeneous inversion (colors represent magnetic susceptibility of vertical slices; optimized diatreme geometry surface overlain for reference).

surrounded by a material with a lower magnetic susceptibility. The southern vent is less well defined than the density models, with the majority of magnetic material being more broadly distributed closer to surface, rather than concentrated within the vent.

Table 2. Initial and optimised model densities and RMS misfits for the Ecklin maar, the Red Rock Volcanic Complex and the Mt Leura Volcanic Complex after homogeneous inversion.

Initial misfit	Optimised misfit	Model region	Initial Density	Optimised Density
		Ecklin		
0.33	0.25	1 – Sediments	2.420	2.485
		2 – Lava flow	2.610	2.623
		3 – Tuff	1.890	1.783
		4 – Diatreme	2.050	1.946
		5 – North vent	2.150	2.290
		6 – South vent	2.150	2.397
		Red Rock Volcanic Complex		
0.42	0.35	1 – Basement	2.670	2.670
		2 – Diatreme	2.100	2.299
		3 – Sediments	2.200	2.409
		4 – Diatreme	2.100	2.560
		5 – Dykes	2.500	2.809
		6 – Feeder Dyke	1.800	2.097
		7 – Lake sediments	2.000	2.192
		8 – Diatreme	2.000	2.274
		9 – Diatreme	1.800	1.817
		10 – Tuff	1.950	2.546
		Mt Leura Volcanic Complex		
1.14	0.65	1 – Diatreme (maar)	2.140	2.339
		2 – Diatreme (tuff ring)	2.300	2.500
		3 – Lava	2.700	2.800
		4 – Scoria	1.650	1.819
		5 – Tuff	1.800	1.658
		6 – Sediments	2.340	2.451

4.6 Sensitivity analysis

Ambiguity exists in any geophysical interpretation because an infinite number of solutions can explain the observed geophysical data (Whiting 1986; Valenta *et al.* 1992; Jessell *et al.* 1993; McLean and Betts 2003). Incorporating as much geologic and petrophysical information as possible into a model can reduce ambiguity by limiting the number of potential solutions. However, a degree of ambiguity still exists within a model, and a sensitivity analysis is needed in order to fully assess how the structures and properties within a model may be varied and still produce an acceptable fit to the data.

Model sensitivity is assessed during each stage of modelling to ensure results are realistic. Every change to a 2.5D model and every new inversion are prompted by the previous model being unable to achieve an acceptable result within the current constraints on model parameters, suggesting that part of the model needs to be refined. How much the model needs to change in order to obtain an acceptable result depends on how sensitive the data are to changes in the physical properties and/or geometry of a particular region.

Sensitivity can be qualitatively assessed by systematically altering the properties or geometry of the model in order to identify how the data responds to model changes and which regions of the model have the most/least influence. Structures with a high sensitivity strongly influence the data, and small changes in their properties/geometry can significantly alter the calculated response. The number of possible solutions (that are still geologically reasonable) pertaining to a structure with a high sensitivity is small, meaning that region of the model is better constrained than a structure with a low sensitivity, which can display a wider range of possible solutions.

The sensitivity of the data to changes in the density of selected regions can be modelled in 2.5D using GM-SYS. An example is drawn from the Mount Leura model (Figure 6c; oriented in an north-west to south-east direction) where the density of different regions within the model (diatreme, vents, lava flow and scoria cones) are altered to the upper and lower bounds of the constraints to observe how the calculated gravity response changes and identify which regions of the model have the greatest sensitivity (Figure 9).

The density of the diatreme in the reference model is already close to the upper bounds of the constraints so only a small variation to the calculated data was observed when the density was increased to its maximum bound. Decreasing the diatreme density to the lower bound of the constraints produced a significant change to the calculated data over the diatreme in the south-east of the cross-section, causing the amplitude of the anomaly to decrease by 1.5 mGal. A minor change in the range of 0.5 mGal was observed over the diatreme in the north-west of the section. This suggests that the geophysical signature of the northern diatreme is being masked by the thick lava flows and scoria cones that have infilled the maar crater.

Similar to the diatreme, the density of the lava is already close to the maximum bound of the constraints and so only a small variation to the calculated anomalies were observed (+0.5 mGal). Decreasing the density to the lower bound however, had a significant influence across the whole model (anomalies varied between –0.5 and –1 mGal) and the calculated data no longer fits within a range that may be considered acceptable. Changes to the density of the scoria cones only had a minor influence on the calculated data (anomalies varied by ±0.5 mGal).

These results suggest that the diatreme structures have a moderate to strong sensitivity, unless covered by thick lava flow sequence which can mask the geophysical response of any underlying structures. While a geometric sensitivity analysis can be performed in 2.5D (e.g., McLean and Betts 2003; Aitken *et al.* 2009; Blaikie *et al.* 2012), 3D geometry inversions offer a faster and more effective method of assessing how the geometry of a model can vary when the properties are varied. Once the parameters of the model have been defined, inversion allows multiple models to be rapidly calculated and easily visualised. Achieving the same outcome through 2.5D modelling requires the user to manually modify each model, subjecting it to user bias in the process.

4.7 Three-dimensional geometric sensitivity analysis

Three-dimensional geometry inversions are applied to test the variability in the models geometry when the density is varied within the bounds of the constraints. Density values observed for the surrounding tuff deposits (Figure 5) were used as an analogue for the diatreme; however, the properties of surface deposits may vary considerably to the diatreme due to compositional variations, diagenetic compaction, saturation with water, and weathering.

An example from the Ecklin maar-diatreme is shown in Figure 10. In order to test variations in the geometry of the diatreme, densities were kept homogeneous within each lithological region and it

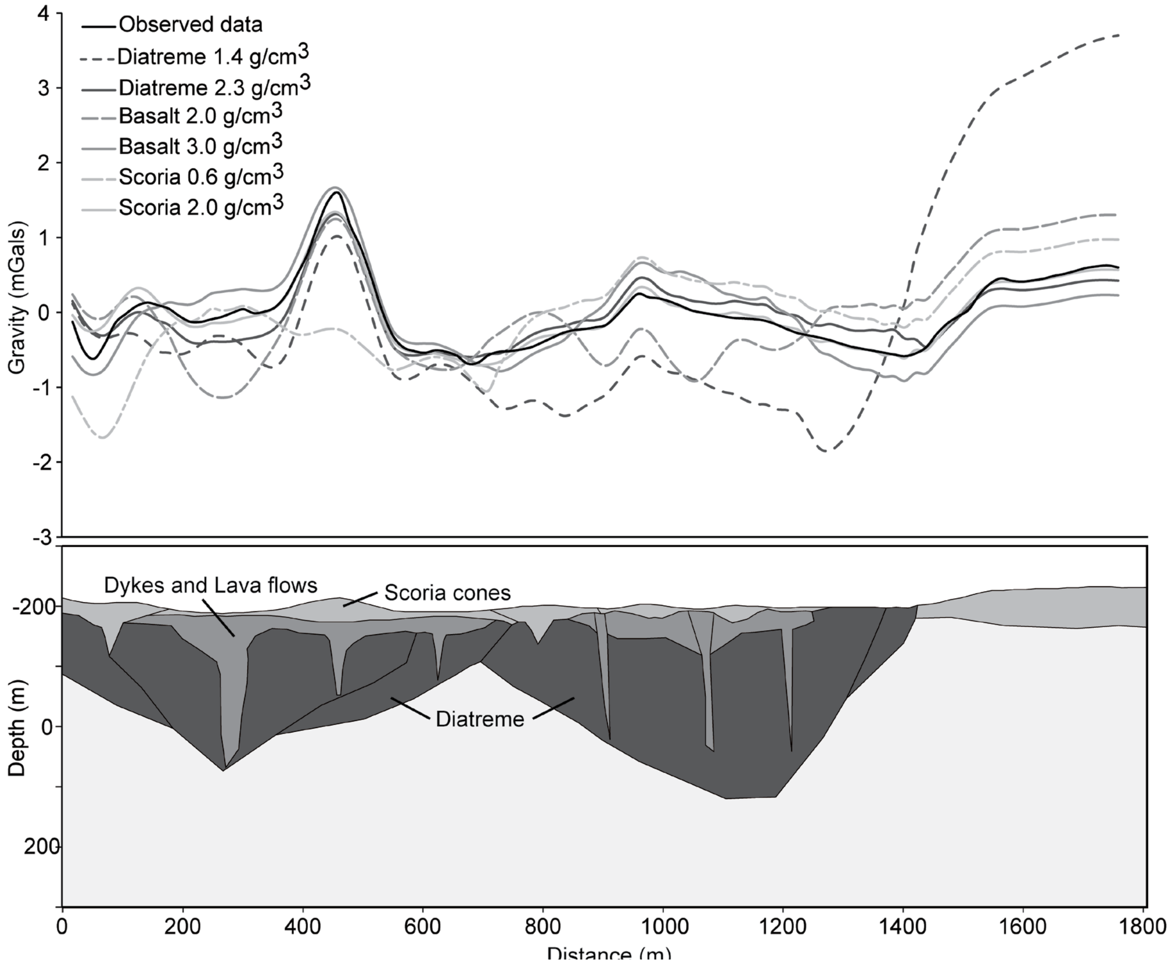

Figure 9. Two-dimensional petrophysical sensitivity analysis of the Mount Leura maar-diatreme model where the properties of the diatreme, lava flows, and scoria cones were altered to the upper and lower boundaries of the constraints.

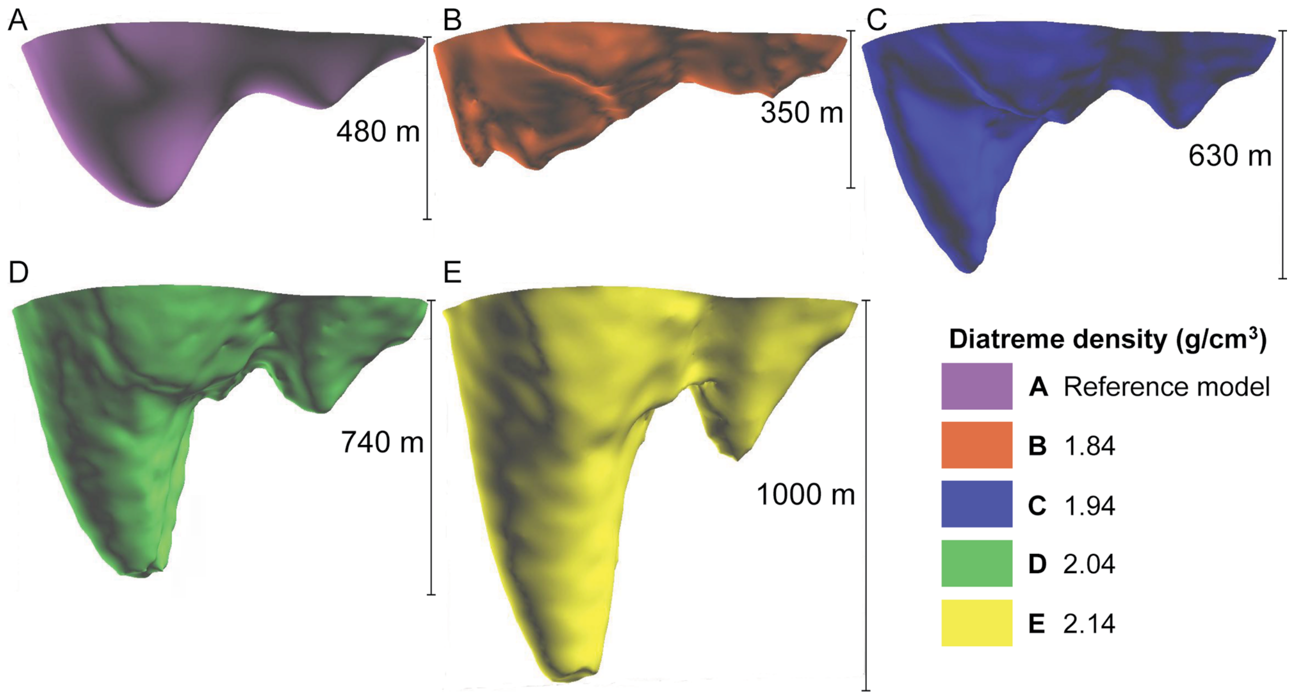

Figure 10. Results of geometric inversions of the Ecklin maar-diatreme model for variable diatreme densities. Model A shows the original reference models. Models B–E show the inverted diatreme geometries. The lowest density model (B) results in a broad shallow diatreme. Model C has the same properties as the reference model and is the preferred model (see inversion results in Figure 8). Models D and E are the higher-density models and show deeper diatremes with steeply dipping walls.

was assumed that the applied density represents an average of any density heterogeneities that may exist within the Ecklin diatreme and its vents. Both the density of the diatreme and its internal vents were altered; however, the density contrast (determined from homogeneous inversion) between them remained the same (north vent: +0.36 g cm^{-3}; south vent: +0.26 g cm^{-3}). Inversions were run for diatreme densities of 1.84, 1.94 (reference model density), 2.04, and 2.14 g cm^{-3}. Each inversion was allowed to proceed until an acceptable model was achieved (i.e., RMS misfit equal or lower than 0.1 mGal). Inversions that applied a diatreme density greater than 2.1 g cm^{-3} did not achieve a successful result, and the RMS misfit increased from the initial forward model. The optimum diatreme geometries for each of the densities listed above are shown in Figure 10.

When the density of diatreme was less than the initial reference model, the inverted diatreme structure became shallower than the initial model, and the two coalesced diatreme structures are less well defined. In each of the other models, the density was greater than the reference model and the inverted diatremes became deeper as the density increased. The two coalesced diatremes are still well defined in each of these inverted models. Without further information (e.g., from drill hole), it is not possible to confirm which model is closest to reality as each model fits within the bounds of the geologic constraints; however, understanding how much the geometry of a particular structure may vary if the properties were over or under estimated is important when targeting an area for drilling.

5. Discussion

Gravity and magnetic methods are one of the most commonly applied techniques to image maar volcanoes and the geophysical anomalies observed across the case studies presented are similar to anomalies documented across maar volcanoes elsewhere in the world (e.g., Rout *et al.* 1993; Schulz *et al.* 2005; Cassidy *et al.* 2007; Lopez Loera *et al.* 2008; Mrlina *et al.* 2009; Skacelova *et al.* 2010). Previous works that have applied potential field modelling to understand subsurface maar structures (eg. Rout *et al.* 1993; Schulz *et al.* 2005; Cassidy *et al.* 2007; Lopez Loera *et al.* 2008; Mrlina *et al.* 2009; Matthes *et al.* 2010; Skacelova *et al.* 2010; Blaikie *et al.* 2012) were largely restricted to forward modelling. While greater complexity can be gained from forward modelling, the advantage of the technique presented here is that the inverse models are built upon the results of the forward models, as well as previous inversion results, and are constrained by geological data at every stage. The resulting inverse models are therefore more robust because all the available geophysical and geologic data have been integrated into the model, creating a higher degree of confidence in the interpretation. Although some uncertainty remains regarding the chosen petrophysical properties because the subsurface was not sampled, the inversion process allows properties to be varied and multiple models calculated to examine how the model geometry may vary under different geologic conditions.

5.1 Limitation of geophysical models

Potential field models are limited because results are non-unique (Whiting 1986; Valenta *et al.* 1992; Jessell *et al.* 1993; McLean and Betts 2003). Applying constraints (e.g., petrophysics, surface, and drill hole observations) to the model limits the number of solutions and ensures that they remain geologically plausible. Although the examples presented here are well constrained, several assumptions were made throughout the modelling process and must be acknowledged.

Prior to modelling, when longer-wavelength anomalies are identified, it is assumed that they are related to the basement morphology and this trend is removed, all other anomalies are assumed to be associated with the maars subsurface structures. The geophysical models are kept relatively simple, with modelling focussing on the geometry of the diatreme and its vents. Smaller-scale structural and/or compositional variations within and surrounding the maar-diatreme such as ring faults and even larger-scale features such as a dyke and sill complex beneath the level of the diatreme are not modelled because these structures are beyond the resolution of the data and including them would only add to model ambiguity. The models voxel size is limited by the resolution of the observed data, therefore restricting the inversions ability to model these smaller-scale structures within the diatreme.

In the early stages of modelling the user must make decisions on the geometry and property distributions within the model which will bias the modelling process. In each 2.5D model and 3D model subject to a geometric or homogenous inversion, a homogenous density distribution within each region is applied assuming that density represents the mean value for that region and the density contrast between adjacent regions is greater than any density heterogeneities within it. This assumption means that any variations in the observed anomalies are accounted for by modifying the geometry of different structures. However, as seen in field examples of maar-diatremes (e.g., Coombs Hill (McClintock and White 2006; Ross and White 2006); Hopi Buttes (White 1991; White and Ross 2011)) complete homogeneity within the diatreme is unlikely to be the case, and the larger-scale variability in density is assessed and modelled by applying a heterogeneous property inversion.

During modelling it was necessary to assume that a petrophysical contrast exists between the margins of the diatreme and the host rock; however, it is sometimes observed that the margins of maar-diatremes are composed of debris flow deposits derived from the collapse of host rock material (Auer *et al.* 2007; Ross *et al.* 2011). As a result, there may be very little to no petrophysical contrast between the diatreme margins and the host rock. Heterogeneous inversions can be useful in identifying areas of the diatreme that have a gradational density contrast with the host rock; however, the modelled margin of the diatreme is highly ambiguous and could vary significantly from the best fit models (Blaikie *et al.* 2012).

Although the above assumptions were made during the modelling process, the aim of this work is not to produce a single 'ideal' model, rather a whole suite of models are produced that are all consistent with the available geologic information. In each case different parameters and/or inversion styles can be applied, yielding very different resultant models. Each model is a valid representation of the subsurface and allows uncertainty in model properties and geometry to be assessed.

5.2 Results and implications for maar-diatreme volcanism

The application of geophysical modelling techniques has improved our understanding of the subsurface morphology of these volcanic centres, which provides insight into their eruptive histories, and processes occurring in the subsurface during the eruption. This has implications for understanding the hazards associated with future phreatomagmatic eruptions in the Newer Volcanics Province and elsewhere. Modelling results suggest that the subsurface morphology of these maar-diatremes are highly complex and can vary greatly between different eruptive centres, even if surface morphology and eruptive styles are similar. Similarities are observed in the general structure of the case studies diatreme's (i.e., coalesced, shallow, and broad structures); however the internal structures within the diatremes (vents, dykes, and magma ponds) are highly variable and reflect differences in the eruptive history of each volcanic centre.

Shallow diatremes suggest an eruption where magma-water interaction remained at shallow levels, rather than propagating downwards, and are often an indication of a water-saturated weakly lithified to unconsolidated host rock (Lorenz 2003; Auer *et al.* 2007; Ross *et al.* 2011), which is consistent with the setting for each of these volcanic centres. Multiple vents are observed in these case studies and are another indication of an eruption hosted in a soft-substrate (White and McClintock 2001; Sohn and Park 2005; Ort and Carrasco-Núñez 2009) as weakly lithified sediments are unable to support steeply dipping diatremes walls and will collapse onto and block the vent, causing it to migrate and erupt at a new location (Martín-Serrano *et al.* 2009; Ort and Carrasco-Núñez 2009; Ross *et al.* 2011). Multiple vents are common to many other volcanic centres within the Newer Volcanics Province (e.g., Cas *et al.* 2011; Jordan *et al.* 2013; Van Otterloo *et al.* 2013; Blaikie *et al.* 2014), suggesting this processes is occurring frequently in the region. Often these vents are obvious, based upon the surface morphology of the maar crater (e.g., the Red Rock Volcanic Complex) and are confirmed by geophysical modelling, and other times simple crater morphologies hide the complexity of the underlying diatreme, and it is only through geophysics that multiple vents can be identified (e.g., Ecklin maar).

Geophysical surveys across the Red Rock and Mount Leura Volcanic Complexes both identified positive short wavelength gravity and magnetic anomalies over the crater which were modelled as dykes and magma ponds within the diatreme. Crater rim deposits indicate that the maars within the Red Rock Volcanic Complex frequently fluctuated between magmatic and phreatomagmatic eruptive styles (Cas *et al.* 2011; Blaikie *et al.* 2012; 2014), which is an indication of variations in groundwater supply, and/or a variable magma flux (Houghton *et al.* 1999). The model of the Lake Werowrap maar suggests dykes are preserved within the diatreme with diameters between to 10 – 30 m which flare outwards closer to the surface and have produced magma ponds up to 100 m across. These dykes (including ponded magma) have a total volume of 0.002 km^3 and represent 6.4% of the total volume of the diatreme (0.03 km^3). The preservation of dykes within the diatreme means they had to be emplaced in the later stages of the eruption, or they would have been destroyed by the gradual mixing of the diatreme as deeper explosions transport material upwards (Valentine and White 2012; Blaikie *et al.* 2014). This suggests that in the later stages of the eruption, explosive fragmentation may have been largely confined to shallow levels and was probably dominantly magmatic, which is consistent with the observation of a spatter cone partly buried within the lake sediments of the Lake Werowrap maar (Blaikie *et al.* 2014).

Rather than the frequent fluctuations in eruption style observed at Red Rock, the Mount Leura Volcanic Complex shows a transition from phreatomagmatic to magmatic activity, resulting in later stage intrusions into the diatreme which produced lava flows with an approximate volume of 0.08 km^3, and the formation of a scoria cone complex with a volume of 0.07 km^3 (Blaikie *et al.* 2014). The diatreme's of the maar and tuff ring have a combined volume of 0.58 km^3, although this is a rough estimate since the geometry of the diatremes are less well defined because the overlying lava flows are masking their geophysical response.

Eruptive styles at the Ecklin maar were dominantly phreatomagmatic, and its geophysical response is characterised by more subtle gravity and magnetic anomalies. These anomalies correlate to the maars vents which have maximum diameters of 30 and 100 m at the base of the diatreme, and 260 m and 470 m at the top of the north and south vents respectively. These vents have a combined volume of 0.012 km^3, representing 9.4% of the total volume of the diatreme (0.13 km^3; based on the optimised geometry model (Figure 8b)). The vents are interpreted to consist of higher proportions of juvenile material compared to the rest of the diatreme, based upon the increased density and magnetic susceptibility of these regions (average density of 2.37 g/cm^3 and 2.46 g/cm^3 and susceptibility of 0.005 SI and 0.01 SI for the north and south vents respectively) compared to the diatreme (average density of 2.0 g/cm^3 and susceptibility of 0.004 SI) (Blaikie *et al.* 2014).

Several models of the Ecklin diatreme were calculated for variable densities (Figure 10). The two end-member models had densities of 1.84 and 2.14 g/cm^3 and volumes of 0.1 km^3 and 0.23 km^3, for the shallowest and deepest diatreme respectively, and have slightly different implications for the hazards associated with the eruption. Phreatomagmatic explosions occurring at shallow levels within the diatreme are more likely to eject material from the vent and deposit it outside of the developing crater, whereas explosions occurring within deep levels of the diatreme may be too weak to transport material to higher levels within the diatreme and eject it from the crater (Valentine and White 2012; Lefebvre *et al.* 2013; Ross *et al.* 2013). The eruption of Ecklin likely involved phreatomagmatic explosions initially confined to shallow levels, particularly in the northern vent, before propagating downwards, forming the deeper southern diatreme.

The bulk diatreme volumes calculated from inversion results are consistent with other documented volumes of maar-diatremes and kimberlite pipes which can range between 0.01 – 1 km^3 (Brown and Valentine 2013; Lefebvre *et al.* 2013). Further analysis of deposit volume and composition is required to estimate the volumes of erupted magma. Due to limited exposures of maar-diatremes, most of which are partly eroded, previous bulk diatreme volume estimates are sparse, and largely determined by calculating the volume of an inverted cone (Kereszturi *et al.* 2013; Lefebvre *et al.* 2013). Our results show that diatremes can have complex geometries, and the inverted cone model may not always be representative of the subsurface, particularly in situations where multiple vents are identified. Further application of our modelling technique to partly exposed or unexposed maar-diatremes can help improve estimates of diatreme volumes, which is essential for understanding the relationships between magma volume, eruptive styles, and duration, therefore having important implications for hazard assessment (Kereszturi *et al.* 2013).

5.3 Application to other volcanic centres

Our inversion technique specifically focussed on modelling the 3D density/magnetic susceptibility distribution within the subsurface to understand the depth, geometry, and location of volcanic vents within maar volcanoes. These volcanic systems lend themselves to this approach because they have suitable rock property contrasts between the volcanic and host rock and relatively flat topography making them suitable for high resolution ground geophysical surveys. However, the modelling technique presented here is not limited to maar volcanoes and may be applicable to other volcano types.

The major difficulty for implementing the technique described is obtaining data of sufficiently high resolution, particularly over regions with rugged terrain, although this can be overcome by implementing airborne rather than ground-based surveys. This technique is most suited to modelling the internal structures of kimberlite pipes, scoria cones, tuff rings, and calderas, however it may be applied to most other types of volcanoes provided adequate petrophysical contrasts exists in the subsurface. For example, shield volcanoes composed predominantly of lava may not have the petrophysical contrast required to image their internal structures, although it may be possible to model the lower contact of the edifice and determine the total volume of the eruptive material through 3D modelling. In cases where a volcanic edifice is very large, the relatively short-wavelength anomalies associated with dykes and the volcanoes vents may be masked by the longer-wavelength and higher-amplitude anomalies associated with the volcanic edifice (e.g., lava shield or stratovolcano); however, it should be possible to model larger scale property variations within the volcano. It is hoped that with the application of this technique, advances can be made in understanding the subsurface architecture of volcanoes, so that eruptive processes are better understood and hazards associated with future eruptions can be assessed.

6. Conclusion

The application of geophysical modelling techniques can provide an improved understanding of maar-diatreme volcanism by constraining the depth, geometry, and property distributions within the diatreme and its feeder vents. Broad shallow diatremes are typically observed in the province and are common to maar-diatremes hosted within soft-substrates. These diatremes also contain multiple vents, suggesting the eruptive point frequently migrated during the course of the eruption, and in the case of the Red Rock and Mount Leura Volcanic Complexes, also fluctuated in eruptive style. Maars that show fluctuations in eruptive style typically have a more complex geophysical response consisting of short-wavelength gravity and magnetic highs superimposed on longer-wavelength gravity and magnetic lows. Maars which show predominantly phreatomagmatic activity (e.g., Ecklin) have a simpler geophysical signature, consisting of a gravity and magnetic low, but may contain broader, low-amplitude anomalies that indicate the location of vents within the diatreme.

The models presented represent best fit models obtained after a series of inversions; however, like all potential field models, they are non-unique with ambiguity existing in any interpretation. Strict geologic constraints are applied to ensure the number of plausible solutions is reduced; however, rather than seeking a single 'ideal' solution, the aim of the technique presented here is to produce multiple models through different inversion styles that are all geologically meaningful and consistent with available geologic information. When constraints are limited, uncertainty in model results will always exist; however, the uncertainty can be assessed by producing a range of models that examine possible solutions when initial constraints are varied to their upper and lower bounds.

7. Acknowledgements

Geophysical data for this paper are available in the supporting information. The regional geophysical data presented in Figure 1 are freely available from Geoscience Australia's Geophysical Archive Data Delivery System (GADDS; www.geoscience.gov.au/gadds). The 3D surface models shown in figure 7 are available in the supporting information as 3D pdfs.

This research was partially funded by the AusIMM Bicentennial Gold 88 Award. We wish to acknowledge the assistance provided in the field by Jackson van den Hove, Dan Uehara, Lisa Roche, and Felicity Piganis, and are grateful to all land owners who allowed us access to their properties to conduct fieldwork. The manuscript was greatly improved upon by the reviews of Cecilia Cadio, Patricia Gregg, Mark D. Behn and two anonymous reviewers.

8. References

Aitken A. R. A., Betts P. G., Weinberg R. F. & Gray D. 2009. Constrained potential field modeling of the crustal architecture of the Musgrave Province in central Australia: Evidence for lithospheric strengthening due to crust-mantle boundary uplift. *J. Geophys. Res.* **114**, B12405.

Araña V., Camacho A. G., Garcia A., Montesinos F. G., Blanco I., Vieira R. & Felpeto A. 2000. Internal structure of Tenerife (Canary Islands) based on gravity, aeromagnetic and volcanological data. *Journal of Volcanology and Geothermal Research* **103**, 43-64.

Auer A., Martin U. & Németh K. 2007. The Fekete-hegy (Balaton Highland Hungary) "soft-substrate" and "hard-substrate" maar volcanoes in an aligned volcanic complex - Implications for vent geometry, subsurface stratigraphy and the palaeoenvironmental setting. *Journal of Volcanology and Geothermal Research* **159**, 225-245.

Blaikie T. N., Ailleres L., Betts P. G. & Cas R. A. F. 2014. A geophysical comparison of the diatremes of simple and complex maar volcanoes, Newer Volcanics Province, south-eastern Australia. *Journal of Volcanology and Geothermal Research* **276**, 64-81.

Blaikie T. N., Ailleres L., Cas R. A. F. & Betts P. G. 2012. Three-dimensional potential field modelling of a multi-vent maar-diatreme - the Lake Coragulac maar, Newer Volcanics Province, south-eastern Australia. *Journal of Volcanology and Geothermal Research* **235-236**, 70-83.

Blakely R. 1995. *Potential field theory in gravity and magnetic applications*. Cambridge University Press.

Blanco-Montenegro I., De Ritis R. & Chiappini M. 2007. Imaging and modelling the subsurface structure of volcanic calderas with high-resolution aeromagnetic data at Vulcano (Aeolian Islands, Italy). *Bulletin of Volcanology* **69**, 643-659.

Brown R. J. & Valentine G. A. 2013. Physical characteristics of kimberlite and basaltic intraplate volcanism and implications of a biased kimberlite record. *Geological Society of America Bulletin* **125**, 1224-1238.

Brunner I., Friedel S., Jacobs F. & Danckwardt E. 1999. Investigation of a Tertiary maar structure using three-dimensional resistivity imaging. *Geophysical Journal International* **136**, 771-780.

Buness H. A., Wiederhold H. & Wonik T. 2006. Seismic reflection patterns of two Tertiary maars in Germany. *Zeitschrift der Deutschen Gesellschaft fur Geowissenschaften* **157**, 339-353.

Camacho A. G., Montesinos F. G. & Vieira R. 1997. A three-dimensional gravity inversion applied to São Miguel Island (Azores). *Journal of Geophysical Research: Solid Earth* **102**, 7717-7730.

Cas R. A. F. 1989. Physical Volcanology. *In:* Johnson R. W., Knutson J. & Taylor S. R. eds. *Intraplate volcanism in eastern Australia and New Zealand*, pp. 55-88. Cambridge University Press.

Cas R. A. F., Blaikie T., Boyce J., Hayman P., Jordan S., Piganis F., Prata G. & van Otterloo J. 2011. VF01: Factors that influence varying eruption styles (from magmatic to phreato-magmatic) in intraplate continental basaltic volcanic provinces: the Newer Volcanics Province of south-eastern Australia. *IUGG 2011 Fieldtrip guide*.

Cas R. A. F., Simpson C. & Sato H. 1993. *Newer Volcanics Province - processes and products of phreatomagmatic activity. IAVCEI Canberra 1993: excursion guide, September, 1993*. Record - Australian Geological Survey Organisation. Geoscience Australia, Canberra, A.C.T., Australia.

Cassidy J., France S. J. & Locke C. A. 2007. Gravity and magnetic investigation of maar volcanoes, Auckland volcanic field, New Zealand. *Journal of Volcanology and Geothermal Research* **159**, 153-163.

Clark D. A. 1983. Comments on magnetic petrophysics. *Australian Society of Exploration Geophysicists, Bulletin* **14**, 49-62.

Clark D. A. 1997. Magnetic petrophysics and magnetic petrology: aids to geological interpretation of magnetic surveys.

AGSO Journal of Australian Geology and Geophysics **17**, 83-103.

Emerson D. W. 1979. Comments on applied magnetics in mineral exploration. *Exploration Geophysics* **10**, 3-5.

Finn C. A. & Morgan L. A. 2002. High-resolution aeromagnetic mapping of volcanic terrain, Yellowstone National Park. *Journal of Volcanology and Geothermal Research* **115**, 207-231.

Fullagar P. K., Hughes N. A. & Paine J. 2000. Drilling-constrained 3D gravity interpretation. *Exploration Geophysics* **31**, 17-23.

Fullagar P. K., Pears G., Hutton D. & Thompson A. D. 2004. 3D gravity and aeromagnetic inversion for MVT lead-zinc exploration at Pillara, Western Australia. *Exploration Geophysics (Melbourne)* **35**, 142-146.

Fullagar P. K. & Pears G. A. 2007. Towards geologically realistic inversion. *In:* Milkereit B. ed. *Proceedings of Exploration 07: Fifth Decennial International Conference on Mineral Exploration*, pp. 444-460.

Fullagar P. K., Pears G. A. & McMonnies B. 2008. Constrained inversion of geologic surfaces--- pushing the boundaries. *The Leading Edge* **27**, 98-105.

Gebhardt A. C., De Batist M., Niessen F., Anselmetti F. S., Ariztegui D., Haberzettl T., Kopsch C., Ohlendorf C. & Zolitschka B. 2011. Deciphering lake and maar geometries from seismic refraction and reflection surveys in Laguna Potrok Aike (southern Patagonia, Argentina). *Journal of Volcanology and Geothermal Research* **201**, 357-363.

Hintz A. R. & Valentine G. A. 2012. Complex plumbing of monogenetic scoria cones: New insights from the Lunar Crater Volcanic Field (Nevada, USA). *Journal of Volcanology and Geothermal Research* **239–240**, 19-32.

Houghton B. F. & Wilson C. J. N. 1989. A vesicularity index for pyroclastic deposits. *Bulletin of Volcanology* **51**, 451-462.

Houghton B. F., Wilson C. J. N. & Smith I. E. M. 1999. Shallow-seated controls on styles of explosive basaltic volcanism: a case study from New Zealand. *Journal of Volcanology and Geothermal Research* **91**, 97-120.

Jessell M. W., Valenta R. K., Jung G., Cull J. P. & Geiro A. 1993. Structural geophysics. *Exploration Geophysics* **24**, 599-602.

Jordan S. C., Cas R. F. A. & Hayman P. C. 2013. The origin of a large ([>3]km) maar volcano by coalescence of multiple shallow craters, not deep excavation: The late Pleistocene Lake Purrumbete maar, Newer Volcanics Province, southeastern Australia. *Journal of Volcanology and Geothermal Research* **254**, 5-22.

Joyce E. B. 1975. Quaternary volcanism and tectonics in southeastern Australia. *Bulletin - Royal Society of New Zealand* **13**, 169-176.

Kauahikaua J., Hildenbrand T. & Webring M. 2000. Deep magmatic structures of Hawaiian volcanoes, imaged by three-dimensional gravity models. *Geology* **28**, 883-886.

Keating G., Valentine G., Krier D. & Perry F. 2008. Shallow plumbing systems for small-volume basaltic volcanoes. *Bulletin of Volcanology* **70**, 563-582.

Kereszturi G., Németh K., Cronin S. J., Agustín-Flores J., Smith I. E. M. & Lindsay J. 2013. A model for calculating eruptive volumes for monogenetic volcanoes — Implication for the Quaternary Auckland Volcanic Field, New Zealand. *Journal of Volcanology and Geothermal Research* **266**, 16-33.

Lefebvre N. S., White J. D. L. & Kjarsgaard B. A. 2012. Spatter-dike reveals subterranean magma diversions: Consequences for small multivent basaltic eruptions. *Geology* **40**, 423-426.

Lefebvre N. S., White J. D. L. & Kjarsgaard B. A. 2013. Unbedded diatreme deposits reveal maar-diatreme-forming eruptive processes: Standing Rocks West, Hopi Buttes, Navajo Nation, USA. *Bulletin of Volcanology* **75**, 1-17.

Lesti C., Giordano G., Salvini F. & Cas R. 2008. Volcano tectonic setting of the intraplate, Pliocene-Holocene, Newer volcanic province (southeast Australia); role of crustal fracture zones. *Journal of Geophysical Research* **113**.

Li Y. & Oldenburg D. W. 1996. 3-D inversion of magnetic data. *Geophysics* **61**, 394-408.

Li Y. & Oldenburg D. W. 1998. 3-D inversion of gravity data. *Geophysics* **63**, 109-119.

Lindner H., Gabriel G., tze H.-J., rgen, Kaeppler R. & Suhr P. 2006. Geophysical and geological investigation of maar structures in the Upper Lusatia region (East Saxony). *Zeitschrift der Deutschen Gesellschaft fur Geowissenschaften* **157**, 355-372.

Lindner H., Kappler R., Pretzschner C. & Suhr P. 2004. Geophysical exploration of maar localities in Upper Lusatia, Germany. *Occasional Papers of the Geological Institute of Hungary* **203**, 70.

Lopez Loera H., Aranda-Gomez J. J., Arzate J. A. & Molina-Garza R. S. 2008. Geophysical surveys of the Joya Honda Maar (Mexico) and surroundings; volcanic implications. *Journal of Volcanology and Geothermal Research* **170**, 135-152.

Lorenz V. 1975. Formation of phreatomagmatic maar-diatreme volcanoes and its relevance to kimberlite diatremes. *Physics and Chemistry of The Earth* **9**, 17-27.

Lorenz V. 2003. Maar-Diatreme Volcanoes, their Formation, and their Setting in Hard-rock or Soft-rock Environments. *Geolines* **15**, 72-83.

Lorenz V. & Kurszlaukis S. 2007. Root zone processes in the phreatomagmatic pipe emplacement model and consequences for the evolution of maar-diatreme volcanoes. *Journal of Volcanology and Geothermal Research* **159**, 4-32.

Mallet J. 1997. Discrete modeling for natural objects. *Mathematical Geology* **29**, 199-219.

Mallet J. L. 1992. Discrete smooth interpolation in geometric modelling. *Computer-Aided Design* **24**, 178-191.

Martín-Serrano A., Vegas J., García-Cortés A., Galán L., Gallardo-Millán J. L., Martín-Alfageme S., Rubio F. M., Ibarra P. I., Granda A., Pérez-González A. & García-Lobón J. L. 2009. Morphotectonic setting of maar lakes in the Campo de Calatrava Volcanic Field (Central Spain, SW Europe). *Sedimentary Geology* **222**, 52-63.

Matthes H., Kroner C., Jahr T. & Kämpf H. 2010. Geophysical modelling of the Ebersbrunn diatreme, western Saxony, Germany. *Near Surface Geophysics* **8**, 311-319.

McClintock M. & White J. 2006. Large phreatomagmatic vent complex at Coombs Hills, Antarctica: Wet, explosive initiation of flood basalt volcanism in the Ferrar-Karoo LIP. *Bulletin of Volcanology* **68**, 215-239.

McLean M. A. & Betts P. G. 2003. Geophysical constraints of shear zones and geometry of the Hiltaba Suite granites in the western Gawler Craton, Australia. *Australian Journal of Earth Sciences* **50**, 525-541.

McLean M. A., Rawling T. J., Betts P. G., Phillips G. & Wilson C. J. L. 2008. Three-dimensional inversion modelling of a Neoproterozoic basin in the southern Prince Charles Mountains, East Antarctica. *Tectonophysics* **456**, 180-193.

Montesinos F. G., Arnoso J., Benavent M. & Vieira R. 2006. The crustal structure of El Hierro (Canary Islands) from 3-D gravity inversion. *Journal of Volcanology and Geothermal Research* **150**, 283-299.

Mrlina J., Kampf H., Kroner C., Mingram J., Stebich M., Brauer A., Geissler W. H., Kallmeyer J., Matthes H. & Seidl M. 2009. Discovery of the first Quaternary maar in the Bohemian Massif, Central Europe, based on combined geophysical and geological surveys. *Journal of Volcanology and Geothermal Research* **182**, 97-112.

Oldenburg D. W. & Pratt D. A. 2007. Geophysical Inversion for Mineral Exploration: a Decade of Progress in Theory and Practice. Paper presented at Proceedings of Exploration 07: Fifth Decennial International Conference on Mineral Exploration(unpubl.).

Ort M. H. & Carrasco-Núñez G. 2009. Lateral vent migration during phreatomagmatic and magmatic eruptions at Tecuitlapa Maar, east-central Mexico. *Journal of Volcanology and Geothermal Research* **181**, 67-77.

Paoletti V., Di Maio R., Cella F., Florio G., Motschka K., Roberti N., Secomandi M., Supper R., Fedi M. & Rapolla A. 2009. The Ischia volcanic island (Southern Italy): Inferences from potential field data interpretation. *Journal of Volcanology and Geothermal Research* **179**, 69-86.

Rasmussen R. & Pedersen L. B. 1979. End corrections in potential field modeling. *Geophysical Prospecting* **27**, 749-760.

Ross P.-S., Delpit S., Haller M. J., Nemeth K. & Corbella H. 2011. Influence of the substrate on maar-diatreme volcanoes; an example of a mixed setting from the Pali Aike volcanic field, Argentina. *Journal of Volcanology and Geothermal Research* **201**, 253-271.

Ross P.-S. & White J. D. L. 2006. Debris jets in continental phreatomagmatic volcanoes; a field study of their subterranean deposits in the Coombs Hills vent complex, Antarctica. *Journal of Volcanology and Geothermal Research* **149**, 62-84.

Ross P. S., White J. D. L., Valentine G. A., Taddeucci J., Sonder I. & Andrews R. G. 2013. Experimental birth of a maar–diatreme volcano. *Journal of Volcanology and Geothermal Research* **260**, 1-12.

Rout D. J., Cassidy J., Locke C. A. & Smith I. E. M. 1993. Geophysical evidence for temporal and structural relationships within the monogenetic basalt volcanoes of the Auckland volcanic field, northern New Zealand. *Journal of Volcanology and Geothermal Research* **57**, 71-83.

Schulz R., Buness H., Gabriel G., Pucher R., Rolf C., Wiederhold H. & Wonik T. 2005. Detailed investigation of preserved maar structures by combined geophysical surveys. *Bulletin of Volcanology* **68**, 95-106.

Skacelova Z., Rapprich V., Valenta J., Hartvich F., Sramek J., Radon M., Gazdova R., Novakova L., Kolinsky P. & Pecskay Z. 2010. Geophysical research on structure of partly eroded maar volcanoes; Miocene Hnojnice and Oligocene Rychnov volcanoes (northern Czech Republic). *Journal of Geosciences* **55**, 333-345.

Sohn Y. K. & Park K. H. 2005. Composite tuff ring/cone complexes in Jeju Island, Korea: possible consequences of substrate collapse and vent migration. *Journal of Volcanology and Geothermal Research* **141**, 157-175.

Talwani M. & Heirtzler J. 1964. Computation of magnetic anomalies caused by two-dimensional bodies of arbitrary shape. *In:* GA P. ed. *Computers in the mineral industries*, pp. 464-480. Stanford Univ Publ Geological Sciences, Palo Alto, California.

Talwani M., Worzel J. L. & Landisman M. 1959. Rapid gravity computations for two-dimensional bodies with application to the Mendocino submarine fracture zone. *Journal of Geophysical Research* **64**, 49-59.

Valenta R. K., Jessell M. W., Jung G. & Bartlett J. 1992. Geophysical interpretation and modelling of three-dimensional structure in the Duchess area, Mount Isa, Australia. *Exploration Geophysics (Melbourne)* **23**, 393-339.

Valentine G. A. 2012. Shallow plumbing systems for small-volume basaltic volcanoes, 2: Evidence from crustal xenoliths at scoria cones and maars. *Journal of Volcanology and Geothermal Research* **223–224**, 47-63.

Valentine G. A. & White J. D. L. 2012. Revised conceptual model for maar-diatremes: Subsurface processes, energetics, and eruptive products. *Geology* **40**, 1111-1114.

van Otterloo J., Cas R. A. & Sheard M. J. 2013. Eruption processes and deposit characteristics at the monogenetic Mt. Gambier Volcanic Complex, SE Australia: implications for alternating magmatic and phreatomagmatic activity. *Bulletin of Volcanology* **75**, 1-21.

White J. D. L. 1991. Maar-diatreme phreatomagmatism at Hopi Buttes, Navajo Nation (Arizona), USA. *Bulletin of Volcanology* **53**, 239-258.

White J. D. L. & McClintock M. K. 2001. Immense vent complex marks flood-basalt eruption in a wet, failed rift: Coombs Hills, Antarctica. *Geology* **29**, 935-938.

White J. D. L. & Ross P. S. 2011. Maar-diatreme volcanoes: A review. *Journal of Volcanology and Geothermal Research* **201**, 1-29.

Whiting T. H. 1986. Aeromagnetics as an aid to geological mapping - a case history from the Arunta Inlier, Northern Territory. *Australian Journal of Earth Sciences* **33**, 271-286.

Williams H. A., Betts P. G. & Ailleres L. 2009. Constrained 3D modeling of the Mesoproterozoic Benagerie Volcanics, Australia. *Physics of the Earth and Planetary Interiors* **173**, 233-253.

Wohletz K. & Heiken G. 1992. *Volcanology and geothermal energy*. Univ. Calif. Press, Berkeley, Calif. USA.

Won I. & Bevis M. 1987. Computing the gravitational and magnetic anomalies due to a polygon: Algorithms and Fortran subroutines. *Geophysics* **52**, 232-238.

Chapter 3.

A geophysical comparison of the diatremes of simple and complex maar volcanoes, Newer Volcanics Province, south-eastern Australia

T. N. Blaikie, L. Ailleres, P. G. Betts, R. A. F. Cas,

School of Earth, Atmosphere and Environment, Monash University, Clayton, Victoria, 3800, Australia

Journal of Volcanology and Geothermal Research, 276 (2014); doi: 10.1016/j.jvolgeores.2014.03.001

Cover page: Mt. Sugarloaf, Mount Leura Volcanic Complex

Monash University

Declaration for Thesis Chapter 3

Declaration by candidate

In the case of Chapter 3, the nature and extent of my contribution to the work was the following:

Nature of contribution	Extent of contribution (%)
Fieldwork, data and image processing, modelling, preparation of the manuscript	87.5 %

The following co-authors contributed to the work. If co-authors are students at Monash University, the extent of their contribution in percentage terms must be stated:

Name	Nature of contribution	Extent of contribution (%) for student co-authors only
L. Ailleres	Supervisory role	5
P. G. Betts	Supervisory role	5
R. A. F. Cas	Supervisory role	2.5

The undersigned hereby certify that the above declaration correctly reflects the nature and extent of the candidate's and co-authors' contributions to this work*.

Candidate's Signature **Date**

Main Supervisor's Signature **Date**

*Note: Where the responsible author is not the candidate's main supervisor, the main supervisor should consult with the responsible author to agree on the respective contributions of the authors.

Abstract

Geophysical modelling techniques are applied to examine and compare the subsurface morphology of maar volcanoes within the Newer Volcanics Province to better understand their eruptive histories and the hazards associated with future eruptions within the province. The maar volcanoes under investigation include the Ecklin and Anakie maars, and the Red Rock and Mount Leura Volcanic Complexes, which vary in their complexity, morphology, eruptive styles and host rock type. The Ecklin and Anakie maars display relatively simple geophysical signatures. Long wavelength gravity lows with corresponding magnetic highs are observed across the craters and were reproduced during modelling with the presence of a shallow maar-diatreme structure at Anakie and two coalesced diatreme structures containing a denser central vent at Ecklin. Red Rock and Mount Leura have more complex geophysical signatures, consisting of short wavelength gravity and magnetic highs superimposed on longer wavelength gravity lows. These anomalies are reproduced during modelling with coalesced 'bowl shaped' diatremes containing dykes and magma ponds. The complex diatreme geometries revealed from forward and inverse modelling suggest that the eruption histories of these volcanoes are more complex than their morphology would suggest. Multiple coalesced diatreme structures indicate an eruption involving vent migration, while preserved dykes within the diatreme suggest short-lived fluctuations between phreatomagmatic and magmatic eruption styles. The geometry of the diatremes are consistent with maars hosted in a soft-substrate, which likely contributed to the migration of vents observed at Ecklin, Red Rock, and Mt Leura. The shallow diatreme observed within the Anakie maar is attributed to a short-lived eruption and low water content within the granitic host rock.

Key Words: maar-diatreme, gravity, magnetics, inverse modelling, Newer Volcanics Province

1. Introduction

A maar volcano is the product of a series of small volume eruptions, forming as magma rising to the surface intersects either ground or surface water and excavates a deep crater cut below the pre-eruptive surface as sub-surface phreatomagmatic explosions fragment and mobilise country rock and magma. Underlying the maar crater is a diatreme, an inverted-cone shaped structure that can extend to depths of 2.5 km and is filled with a mixture of fragmented and coherent volcanic and country rock (Lorenz 1975, 1986, 2003, 2007; White & Ross 2011; Ross *et al.* 2013). The subsurface nature of this type of eruption means that these processes are unable to be observed directly during the eruption. Studies of exposed maar diatremes have led to an improved understanding of maar-diatreme volcanism by recognising the formation of bedded successions deep in the diatreme, and the role of individual explosive events which facilitate mixing and remobilisation of debris (White 1991; Ross & White 2006; Lefebvre *et al.* 2012; 2013). However, where diatremes are exhumed (e.g,. Hopi Buttes volcanic field, Arizona, White (1991); Coombs Hill, Antarctica, Ross and White (2006)), the ejecta rings are normally eroded away and linking the eruptive mechanisms observed in the diatreme to a long eroded ejecta ring can be problematic. Where the ejecta ring exists, the diatreme is not usually exposed, leading to an incomplete understanding of the eruptive history and evolution of the plumbing system.

Maar volcanoes are common in monogenetic volcanic fields, and it is important to understand the development of plumbing systems and volcanic processes that occur in the shallow subsurface of these fields, and how this impacts on the eruptive styles and intensities. Although only a few historical records of maar eruptions exist (e.g., Ukinrek; Kienle *et al.* (1980), Nilahue; Muller and Veyl (1957), Tarawera; Nairn (1979) Lake Taal; Moore *et al.* (1966), and Ambrym; Németh and Cronin (2011)), they represent significant volcanic hazards because of their proximity to major cities (e.g., Auckland; Nemeth *et al.* 2012; Kereszturi *et al.* 2013). In order to fully understand eruption processes, and assess volcanic hazards for future eruptions, it is necessary to examine the entire volcanic system, from the feeder dyke to the edifice. However, depending on the level of erosion, often it is only possible to examine one section of the volcanic edifice. The Suoana crater in the Miyakejima volcano in Japan is the only known example of a maar-diatreme where all structural levels are exposed, however the maar is small, and inaccessible (Geshi *et al.* 2011).

There are no exposures of maar-diatremes within the Newer Volcanics Province of south-eastern Australia. Therefore the only way to image the structure of the diatreme and gain a greater understanding of the volcanoes eruptive histories is to use geophysical techniques (Blaikie *et al.* 2012). The application of geophysical techniques to understand the subsurface morphology of maar volcanoes has become increasingly common (e.g., Rout *et al.* 1993; Brunner *et al.* 1999; Schulz *et al.* 2005; Lindner *et al.* 2006; Cassidy *et al.* 2007; Lopez Loera *et al.* 2008; Mrlina *et al.* 2009; Skacelova *et al.* 2010; Blaikie *et al.* 2012; Barde-Cabusson *et al.* 2013), however the link between the geophysical interpretations, observations of surface deposits and the eruptive histories of the volcanoes could be improved upon.

The results of geophysical studies of four different maar volcanoes from the Newer Volcanics Province of South-eastern Australia are examined in this paper. The case studies were selected as they represent a good range of the different eruptive histories (e.g., dominantly phreatomagmatic, fluctuating phreatomagmatic/magmatic and phreatomagmatic transitioning to magmatic) and crater sizes (between 450 m and 2000 m) observed in maar volcanoes within the province. The aim of this study is to apply geophysical modelling techniques to obtain a 3D geologic model of the subsurface structures of maar volcanoes of varying complexity and eruptive histories. Detailed comparisons will be made between the geophysical signatures of the maars, the modelled structures and how these are related to their eruptive histories and intensities.

The geometries of maar-diatremes can be highly variable, and related to the type of rock in which they are hosted, as well as variations in the supply of magma and groundwater (Lorenz 2003; Field *et al.* 2008; Ross *et al.* 2011; White & Ross 2011). Shallow 'bowl shaped' diatremes are typically considered to form in weakly lithified to unconsolidated sediments, have shallowly dipping diatreme walls and are confined to the shallow subsurface. Deep 'pipe or cone shaped' diatremes form in hard rock settings, have steeply dipping walls and can extend to depths >1.5 km (Auer *et al.* 2007; Ross *et al.* 2011). The description of diatremes as being deep or shallow is fairly arbitrary, likely due to diatremes being only partly exposed, limiting studies on their depths and geometries. In this paper, we define diatremes as being deep or shallow as a function of their aspect ratios. Diatremes are considered shallow if the ratio between the depth of the diatreme and the minimum crater width is less than 1:1 and deep if the ratio is greater than this.

The Newer Volcanics Province is a monogenetic intraplate volcanic field located in southeast Australia, and contains the youngest products of volcanism within Australia (Mt Gambier ~ 5ka; van Otterloo *et al.* (2013)). Volcanic edifices within the province are relatively well preserved, and have yet to reach a level of erosion where their internal structures may be physically examined. Current levels of erosion are estimated to be several metres, and up to 10's of metres in river channels cutting through some of the older (>2 Ma) lava flows. Previous studies in the Newer Volcanics Province have focussed largely on the stratigraphy, petrology and geochemistry of lava flows (Price *et al.* 1997; Hare & Cas 2005; Hare *et al.* 2005), and describing pyroclastic deposits associated with some of the more complex maar volcanoes (Cas *et al.* 2011; Jordan *et al.* 2013; van Otterloo *et al.* 2013). While providing a good understanding of eruptive processes within individual volcanoes, the morphology of the subsurface plumbing systems of these volcanoes is still unknown, although Jordan *et al.* (2013) used country rock xenolith populations to demonstrate that the Lake Purrumbete maar had a shallow diatreme. Geophysical modelling techniques are applied to gain an improved understanding of the entire volcano. If there is some understanding of the eruptive history of a volcano, geophysical data may be interpreted in light of an understanding of processes that may have occurred during the eruption, and it may be possible to link features observed in the deposits with structures modelled in the subsurface (Blaikie *et al.* 2012).

2. Regional geologic and geophysical setting of the Newer Volcanics Province

Volcanic activity within south-eastern Australia has continued to occur intermittently since the break-up of Gondwana, with the Newer Volcanics Province representing the most recent peak in volcanism (Johnson 1989; Cas *et al.* 2011). The Newer Volcanics Province is an intraplate basaltic volcanic province, with eruptions occurring from ~4.6 Ma to 5 ka (K-Ar ages; Gray and McDougall (2009)). Natural hot springs and CO_2 emissions indicate that the magmatic system is still active and eruptions can be expected in the future (Lesti *et al.* 2008). Eruptive products extend over 400 km

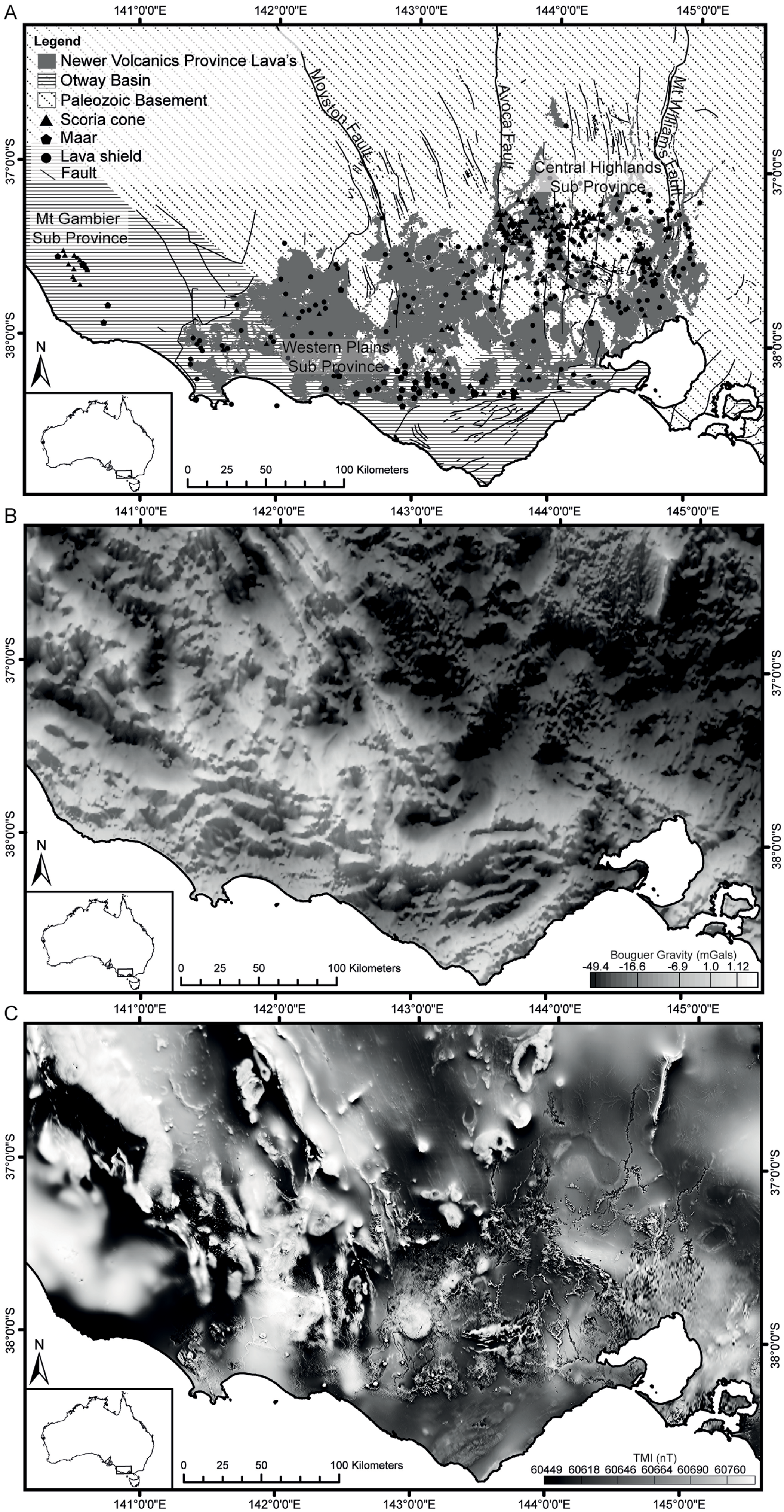
A
141°0'0"E
142°0'0"E
143°0'0"E
144°0'0"E
145°0'0"E
Legend
Newer Volcanics Province Lava's
Otway Basin
Paleozoic Basement
Scoria cone
Maar
Lava shield
Fault
Moyston Fault
Avoca Fault
Mt William Fault
Central Highlands Sub Province
Mt Gambier Sub Province
Western Plains Sub Province
37°0'0"S
38°0'0"S
N
0 25 50 100 Kilometers
B
Bouguer Gravity (mGals)
-49.4 -16.6 -6.9 1.0 1.12
C
TMI (nT)
60449 60618 60646 60664 60690 60760

from Melbourne to south-eastern South Australia with an aerial extent >23,000 km^2. At least 416 volcanoes have been identified within the province and include shield volcanoes, maars, scoria cones, tuff rings, lava flows and volcanic complexes (Hare *et al.* 2005; Cas *et al.* 2011; Boyce 2013). The youngest eruptive centre (~5 ka, radiocarbon dating; Blackburn 1966; Blackburn *et al.* 1982) identified within the province is the Mount Gambier Volcanic Complex located almost at the Western margin of the province (van Otterloo *et al.* 2013).

Three sub-provinces are identified within the Newer Volcanics Province and are defined based on differences in morphology and geochemistry (Figure 1; Nicholls & Joyce 1989; Cas *et al.* 1993). The Central Highlands sub-province to the north-east is comprised of approximately 250 eruptive centres that have produced scoria cones, lava shields and extensive lava flows between ca 4.5 and 2 Ma (Nicholls & Joyce 1989). The Western Plains sub-province consists of 175 eruptive centres which have produced extensive lava plains giving the region a flat to hummocky profile. Superimposed on the lava plains are the edifices of scoria cones, maars, shields and volcanic complexes (Cas *et al.* 2011; Boyce 2013). The Mt Gambier sub-province lies to the west of the Newer Volcanics Province, and consists of only 17 eruptive centres that have formed mainly scoria cones, tuff rings, maars and complexes (Sheard 1990).

The Western Plains and Mt Gambier sub-provinces overlie the sedimentary sequences of the Otway Basin, an east-west trending rift basin that formed during the late Jurassic to early Cretaceous as Australia and Antarctica broke apart (Figure 1; Price *et al.* 2003). The majority of maar volcanoes within the Newer Volcanics Province are located in this region where water saturated porous aquifers (predominately sandstones and limestone's) within the Otway Basin have influenced volcanism, resulting in phreatomagmatic activity, at least in the initial stages of the eruption (Joyce 1975; Cas *et al.* 1993; 2011). The basement to the Otway Basin, and directly underlying volcanic products of the Central Highlands and northern regions of the Western Plains sub-provinces are comprised of Palaeozoic meta-sedimentary, volcanic and granitic rocks of the Lachlan and Delamerian fold belts (Nicholls & Joyce 1989; Cas *et al.* 1993; 2011; Price *et al.* 2003). Eruptions in this area of the province are dominated by scoria cones, lava shields and lava flows.

3. Petrophysical state of the Newer Volcanics Province and Otway Basin

Relatively high resolution aeromagnetic data (200 m line spacing at a flying height of 80 m) is available across the NVP and is used to examine the magnetic relationship between different volcanic edifices and the country rock (Geophysical data is sourced from Geoscience Australia). The Otway Basin has a relatively neutral magnetic signature, offering high contrast against the more magnetic products of the Newer Volcanics Province. Aeromagnetic data is useful for identifying discrete eruptive centres and mapping of lava flows; however the resolution is insufficient to model short wavelength features associated with shallow structures within the volcano. Phreatomagmatic volcanic edifices (maars

Figure 1 (LEFT). Regional geological and geophysical data of the Newer Volcanic Province (modified after Hare and Cas (2005)) a) Simplified geological map highlighting the location of eruptive centres and distribution of lava within the Newer Volcanics Province, b) Greyscale image of the Bouguer gravity data, c) Greyscale aeromagnetic data.

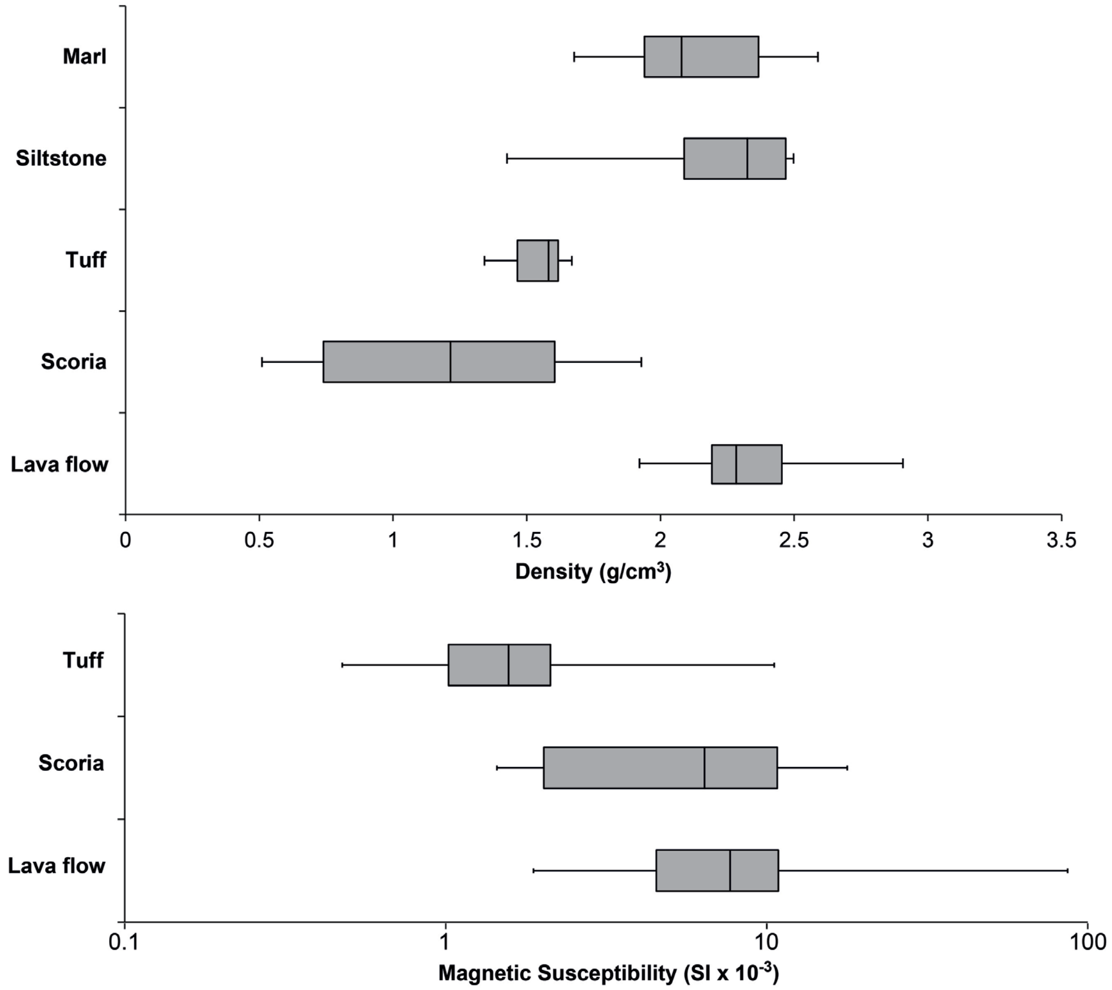

Figure 2. Petrophysics of common rock types of the Newer Volcanics Province. (Figure shows minimum, 2nd Quartile, mean, 3rd Quartile, maximum; Data is compiled from samples from the Red Rock Volcanic Complex, Ecklin Maar, Mt Leura Volcanic Complex, Anakie, Mt Noorat and Mt Rouse; Figure is modified after (Blaikie et al. 2012)).

and tuff rings) tend to have relatively neutral magnetic signatures, reflecting the higher proportions of country rock debris within the tephra rings. Magmatic edifices (shields, scoria cones, volcanic complexes) and lava flow fields tend to have a high magnetic signature since they are composed almost entirely of basalt. Petrophysical data has been compiled from a number of volcanic centres within the Newer Volcanics Province and assists in constraining the geophysical models (Figure 2).

4. Geology of the maar volcanoes

Four volcanic centres within the Newer Volcanics Province were selected for this study including the Red Rock Volcanic Complex, the Mount Leura Volcanic Complex, Anakie and Ecklin Maar (Figure 4). These centres were selected for geophysical studies because they exhibit a wide variety of eruption histories (phreatomagmatic, phreatomagmatic transitioning to magmatic, and fluctuating phreatomagmatic/magmatic; magmatic activity includes effusive, fire-fountaining and strombolian), have varying crater sizes and host rock types and are accessible for ground gravity and magnetic surveys.

The Rock Volcanic Complex, the Mount Leura Volcanic Complex and Ecklin maar are located within the Western Plains Sub-province of the Newer Volcanics Province and overlie the weakly lithified

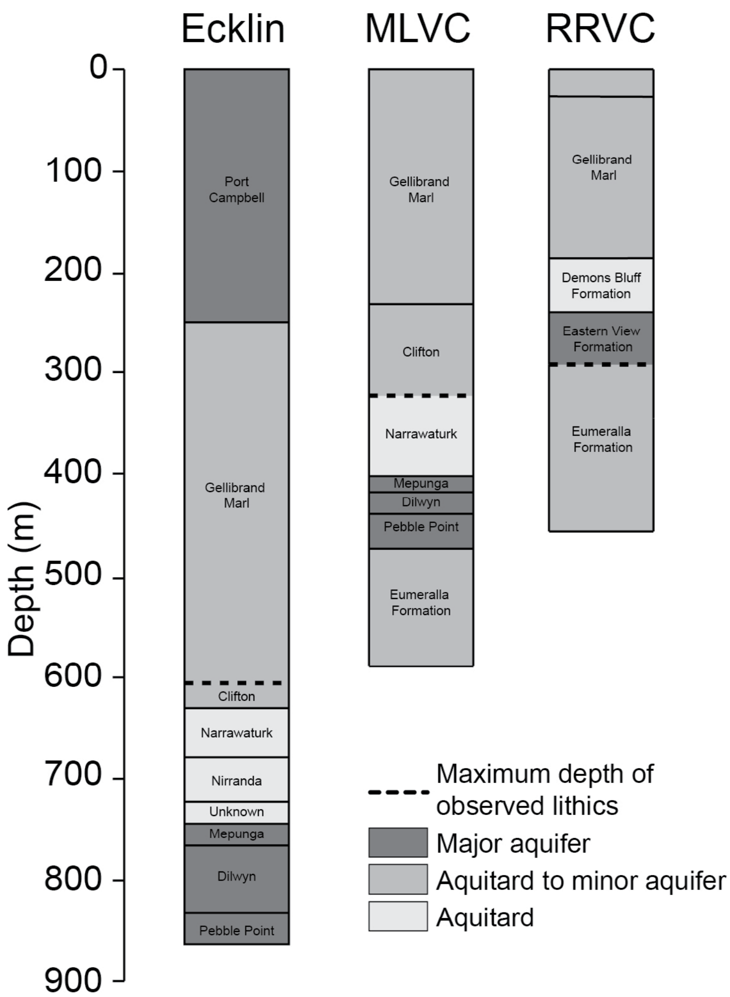

Figure 3. Stratigraphy underlying the Red Rock Volcanic Complex, Mt Leura Volcanic Complex and Ecklin maar (stratigraphic columns are based on well log reports from Constantine and Liberman (2001) and Leslie and Sell (1968)).

sedimentary sequences of the Otway Basin (Figure 1). The underlying stratigraphy at each volcanic centre is relatively well known due to nearby exploration drill holes and seismic surveys. This allows the quality of aquifers in the vicinity of the volcano to be assessed to better understand the levels at which phreatomagmatic fragmentation may have occurred. Although not necessarily representative of the stratigraphic level of a particular explosion, lithic fragments deposited in the maar-rim sequence are correlated with the underlying stratigraphy to give an indication of the depth of the maar-diatreme. However, lithic fragments derived from deeper levels of the stratigraphy are not always represented in the deposits of the ejecta ring (Valentine & White 2012; Lefebvre *et al.* 2013; Ross *et al.* 2013), so these constraints are used as a minimum estimate of diatreme depth for modelling. The stratigraphy and maximum depth of identified lithic fragments at Red Rock, Mt Leura and Ecklin maar are outlined in Figure 3.

4.1 Red Rock Volcanic Complex

The Red Rock Volcanic Complex (Figure 4a-b) consists of over 40 identifiable vents that have formed multiple maar and scoria cones over an area of 7-8 km^2. It is the youngest of three closely spaced, north-northeast trending volcanic centres and overlies the hummocky topography of the stony rises lava flows which originated from the Warrion Hill lava shield to the northeast (Cas *et al.* 2011; Blaikie *et al.* 2012). These three volcanic centres overlie the Avoca fault (Figure 1), a steep, west-dipping reverse fault that separates the Stawell and Bendigo zones of the Lachlan Fold Belt (Gray *et al.* 2003) and which may have been exploited by magma as a conduit to the surface (Cas *et al.* 1993; 2011).

The Rock Volcanic Complex is one of the most complex volcanic centres within the Newer Volcanics Province, with the highest number of vents of any volcanic centre and multiple eruptive styles. Eruptive activity can be separated into two different phases: an early dominantly phreatomagmatic phase that resulted in the formation of multiple scalloped shaped maars consisting of at least 18 vents, and a later dominantly magmatic phase that resulted in the formation of several scoria cones with at least 22 vents (Blaikie *et al.* 2012). However, interbedded magmatic fall deposits consistent with strombolian style activity (Walker 1973), and phreatomagmatic fall/surge deposits are observed in the ejecta rings of the Lake Coragulac maar (Cas *et al.* 1993; Piganis 2011; Blaikie *et al.* 2012). The interbedded nature of these deposits which are derived from very different eruptive styles suggests that some of the maars and scoria cones could be erupting contemporaneously. However, deposits are well stratified and do not show mixing which might be expected if the maars and cones were erupting simultaneously. This suggests that the maars eruptive style most likely fluctuated between magmatic and phreatomagmatic behaviour (Cas *et al.* 2011; Blaikie *et al.* 2012). Based upon country rock xenolith populations, Blaikie *et al.* (2012) determined that phreatomagmatic explosions were predominantly contained within the Gellibrand marl (26-186 m below surface; Figure 3) but could have propagated down as deep as the Eastern View Formation (238-290 m). The Gellibrand marl (comprised of marls, calcareous clays and silts) has a low hydraulic conductivity, and typically behaves like an aquitard, although there are more sandy facies variants with a higher porosity present in the upper part of the stratigraphy which act as an aquifer (Tickell *et al.* 1991) and could have provided the water to fuel phreatomagmatic explosions. The low hydraulic conductivity of the Gellibrand marl would have resulted in a slow recharge rate and likely contributed to the fluctuating eruptive styles observed within the Red Rock Volcanic Complex. The host sediments are also weakly lithified to unconsolidated, particularly in the upper part of the stratigraphy, and would have been prone to collapse into the developing diatreme, which would have provided further influx of water to fuel phreatomagmatic eruptions.

4.2 Ecklin

The Ecklin maar volcano is located within the southern part of the Western Plains sub-province (Figure 4a). It is a small maar, slightly elongated in the NNW-SSE direction and is approximately 800 m across its shortest axis (east-west) and 1000 m across its longest axis (north-northwest – south-southeast) (Figure 4b). The tuff-ring rises 40 m above the crater floor and is thickest along the northern and southeast sides of the maar and thins towards the western side of the crater where they are 10-15 m thick. Deposits are entirely absent along a small section of the north-northwest side of the maar, although this is likely due to land clearing to drain the maar lake for farmland. The asymmetry in deposition could be related to directed blasts, or due to the prevailing wind direction during the eruption, as is similarly observed in other volcanic centres in the area (e.g., Red Rock).

Deposits within the ejecta ring are of phreatomagmatic origin, deposited from base surge and fallout processes. Accidental lithic fragments are present in the form of blocks and bombs, as well as present in the matrix of the pyroclastic deposits. Fragments consist largely of basaltic blocks and bombs, likely derived from earlier lava flows, and clasts of the Gellibrand Marl (Rosengren 1994). Lithic fragments suggest that the depth of explosive magma-water interaction propagated downwards to the Gellibrand Marl, which is constrained between 240 and 600 m in depth by a nearby bore hole. The major aquifer for the region is the Port Campbell Limestone which has a high porosity and permeability (Edwards *et al.* 1996) and is present in the upper 240 m of the stratigraphy at the Ecklin maar, likely providing much of the water that fuelled the predominantly phreatomagmatic eruption. Underlying the Port Campbell limestone is the Gellibrand Marl, where similarly to the Red Rock Volcanic Complex, water was probably derived from more sandy facies variants within the stratigraphy (Tickell *et al.* 1991).

4.3 Mount Leura Volcanic Complex

The Mount Leura Volcanic Complex is a nested maar and scoria cone complex located within the Western Plains sub-province (Figure 4a). The complex forms one of several volcanoes aligned along northwest-southeast trending lineament; however vents within the complex are aligned in a north-south orientation.

The Mount Leura Volcanic Complex formed from an initial stage of phreatomagmatic activity that produced a maar crater 1600 m in diameter in the southern region of the complex, and a large overlapping tuff ring 2000 m in diameter in the north (Figure 4d). Eruptive activity then switched to more effusive and explosive magmatic styles, resulting in lava flows and 16 scoria/spatter cones infilling the two coalesced craters, the largest of which, Mt Sugarloaf, rises 115 m above the current crater floor. Lithic fragments derived from the Gellibrand marl (upper 240 m) and occasionally from the Clifton Formation (240 – 323 m; medium to course grained calcarenite and sandstones; Edwards *et al.* (1996)) are observed in the ejecta rim, and fragmentation was likely largely contained within these units, although Shaw-Stuart (2005) recognised fresh-water fossils in the deposits suggesting that fragmentation could have occurred as deep as the Mepunga, Dilwyn and Pebble point Formations (Figure 3). The aquifer properties of the Clifton Formation are not well known, although it is porous and likely to yield moderate amounts of water (Edwards *et al.* 1996). As previously described, the Gellibrand marl has low hydraulic conductivity, and its slow recharge rate likely contributed to the transition from phreatomagmatic explosions which formed the overlapping maar and tuff ring, to the magmatic effusive and explosive styles which produced lava flows and the cone complex.

4.4 Anakie

The Anakie's consist of three scoria cones (preserved basal diameters of ~ 1 km, and height of ~ 100 m) aligned in northwest-southeast direction, with a small maar nested between the two northern-most cones. The complex is aligned along the Lovely Banks Monocline, which was likely exploited by magma as it rose to the surface (Figure 4e). The Anakie's are located on the Werribee Plains lava field, part of the Central Highlands Province (Figure 4a). Hare *et al.* (2005) attempted to correlate the volcanic stratigraphy of the Werribee plains, which constrains the age estimate of the Anakies to between 2.58 and 2.74 Ma (based on K-Ar and $^{40}Ar/^{39}Ar$ dates).

The Anakies are hosted within a Late Devonian granite of the Lachlan fold belt, which is overlain by a thin layer (several metres) of unconsolidated sands and the lava flows of the Newer Volcanics

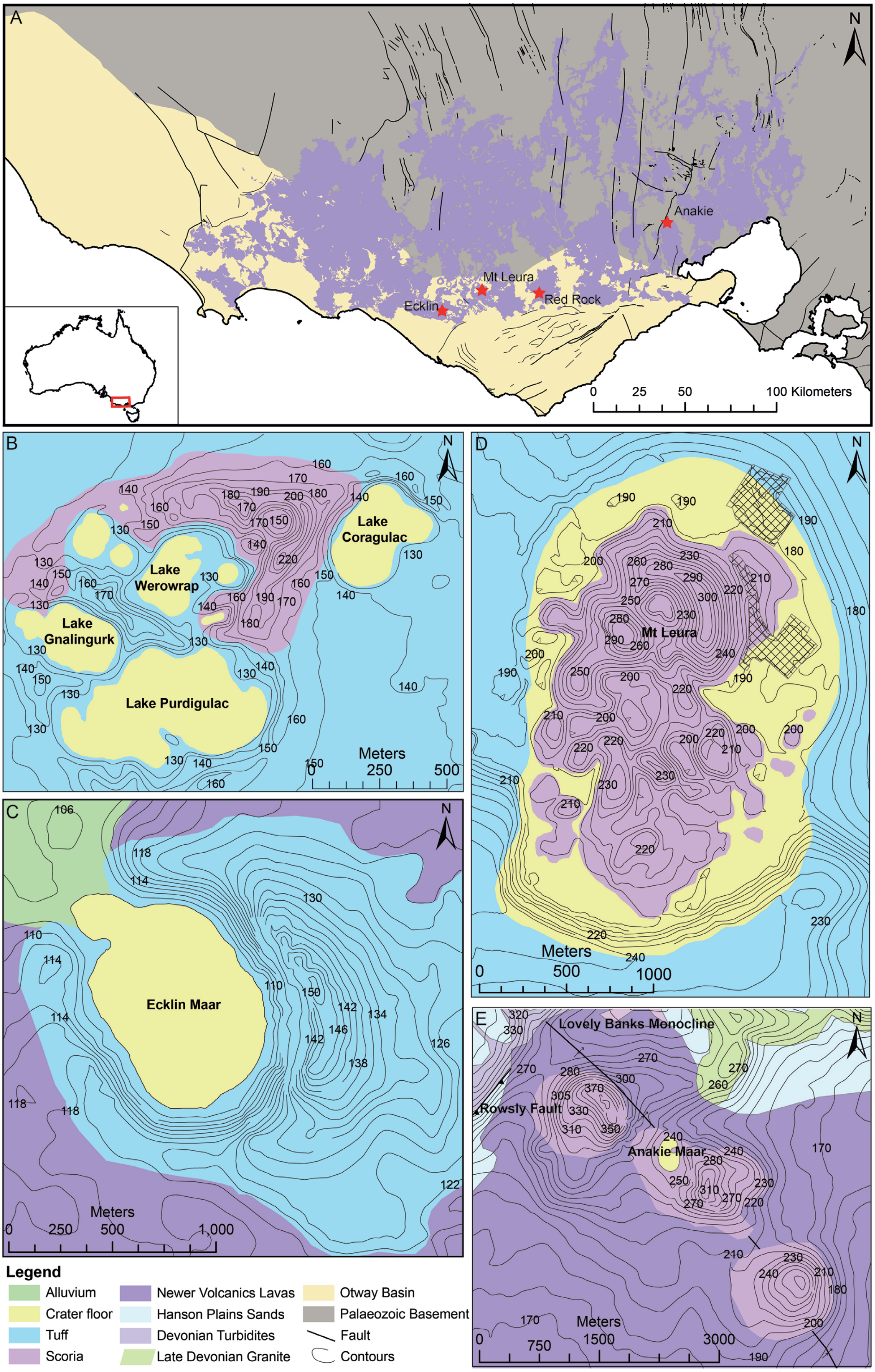

Figure 4. a) Simplified geology of the Newer Volcanics Province showing location of study areas. b) Red Rock Volcanic Complex, c) Ecklin maar, d) Mt Leura Volcanic Complex, e) The Anakie's. (Figures A and E are modified from Victorian shapefiles available from the Department of Primary Industries)

Province. The source of water to fuel the phreatomagmatic explosions associated with the eruption of the maar is unclear, and is thought to have been derived either from fractures in the granite, or the more likely scenario of water contained within the pore spaces of the thin sandy layer overlying the granite. The maar crater is elongated in the north-south direction and is 350 m wide and 600 m long, with a shallow crater that is 15 m deep.

5. Method: Geophysical data acquisition, processing and modelling

The effectiveness of applying geophysical modelling techniques to understand the subsurface structures of maar volcanoes has been demonstrated in recent years by Rout *et al.* (1993), Schulz *et al.* (2005), Cassidy *et al.* (2007), Lopez Loera *et al.* (2008), Mrlina *et al.* (2009) and Blaikie *et al.* (2012). The modelling technique applied to these case studies has been previously described by Blaikie *et al.* (2012) and is only briefly summarised below.

Very high resolution ground gravity and magnetic surveys were conducted at each of the maar volcanoes. Gravity data is acquired along several near orthogonal traverses with a station spacing of approximately 20 m. Magnetic data were acquired in a grid based pattern at Ecklin maar with a line spacing of approximately 100 m, and the southern half of Mt Leura with a line spacing of approximately 200 m. Access to the maar craters at Red Rock was difficult due to swampy conditions and magnetic data was acquired along the same traverses as the gravity data.

Gravity data were subject to tidal, drift, latitude, free-air, Bouguer and terrain corrections. Magnetic data were corrected for diurnal variations and the IGRF, and subjected to despiking and filtering to remove noise within the survey area before being reduced to the pole (RTP). Gravity and magnetic data were then gridded at a cell size appropriate for each survey using either minimum curvature or krigging algorithms, which are best suited to gridding irregularly spaced/oriented data. Additional processing of gridded data (e.g., vertical derivatives, band-pass filter) was performed to enhance contrast between long and short wavelength features in the data.

Following the examination of gridded data sets, 2.5D forward models were constructed to reveal information on the depth and geometry of the maars subsurface structures using the GM-SYS module within the Geosoft Oasis Montaj software package (www.geosoft.com). GM-SYS allows gravity and magnetic data to be jointly modelled with geologic bodies represented as 2.5 or 2.75D polygons (Talwani *et al.* (1959); Talwani and Heirtzler (1964); GM-SYS based upon the methods and calculations of Rasmussen and Pedersen (1979); Won and Bevis (1987)). Each model was constrained by the regional geology, pyroclastic deposits, petrophysical properties and the interpretation of gridded geophysical data. 2.5D interpretations are based upon free-air data so that topography could be included within the model.

Multiple cross cutting 2.5D forward models were produced across each volcanic centre and were used to construct a 3D geologic model of the volcanoes internal structures. The 3D models were built within Gocad (www.gocad.org) and used as a reference model for homogenous, heterogeneous and geometry inversions of the gravity data performed within VPmg (Fullagar *et al.* 2000; 2004; Fullagar & Pears 2007). Inversions were applied to minimise the misfit between the observed and calculated data and to understand the 3D structure and density distribution within the volcanoes underlying vent systems. This was achieved through sequential homogenous, geometry and heterogeneous property inversions.

Homogeneous and geometry inversions are applied to reduce the misfit between the observed and calculated data and optimise the density and geometry of select lithological regions. Heterogeneous inversions are then applied to understand the density distribution within the diatreme (Fullagar & Pears 2007). Constraints were applied so that the models remained geologically plausible and could only vary within the applied petrophysical and geological conditions. In addition to understanding the geometry and property distributions within the modelled maar diatremes, the 3D models also allow the bulk volumes of the diatremes to be calculated (Table 1).

Table 1. Geometric and volume information of best-fit geophysical models

	Max. crater diameter (m)	Min. crater diameter (m)	Max. diatreme depth (m)	Ratio of diatreme depth to minimum crater diameter	Dip of diatreme walls	Volume dykes and lava flows (km^3)	Volume vents (km^3)	Bulk diatreme volume (km^3)
Ecklin	1000	800	630	0.79	30 - 85	-	0.012	0.13
Mount Leura – maar	1700	1500	515	0.34	40 - 70	0.08	-	0.58
Mount Leura - tuff ring	2000	1800	355	0.20	20 – 30			
Red Rock – Lake Werowrap	720	370	320	0.86	60 - 75	0.002	-	0.03
Red Rock – west maar	365	260	140	0.79	30 - 60	-	-	0.0028
Red Rock – central maar	200	160	95	0.59	30 - 80	-	-	0.00077
Anakie	600	350	130	0.37	25 - 75	-	-	0.0053

6. Results

6.1 Red Rock Volcanic Complex

Blaikie *et al.* (2012) first presented data from the Lake Coragulac maar located within the northeast of the Red Rock Volcanic Complex. Gravity and magnetic data have since been acquired across a series of traverses through each of the other maar craters (Figure 5a-c). Data over the Lake Purdigulac maar was initially acquired and interpreted by Piganis (2011), and has been re-processed and levelled with new data acquired over the rest of the complex. The scoria cone complex was avoided as topography was too steep for geophysical surveying, and gravity data through the Lake Gnalingurk maar is sparse because the maar crater contained a small amount of water during the survey and was inaccessible for gravity measurements.

Red Rock exhibits a complex and highly varied geophysical response across each of the maars, reflecting the variable nature of the subsurface volcanic vent. The Bouguer gravity (terrain corrected with a crustal density of 2.4 g/cm^3) response of the complex is shown in Figure 5a, however a northwest-southeast regional gradient is present, obscuring the more subtle gravity responses of the maars. This gradient is removed by applying a band-pass filter to the data with a long-wavelength cut-off of 3000 m (Figure 5b). A short-wavelength cut-off of 50 m was applied to remove noise in the data which arose due to swampy conditions in some of the craters.

The Lake Werowrap maar is characterised by a Bouguer gravity high (1.5 mgal), which can be separated into several short-wavelength anomalies (100 m, 0.5 mgal) by a vertical derivative filter. These short-wavelength anomalies also correlate with magnetic anomalies within the crater (ranging between 1078 and 2540 nT in amplitude), and are interpreted to be dykes intruding into the maar diatreme. The Lake Purdigulac maar consists of a Bouguer gravity low, related to the lower density lake sediments and pyroclastic debris within the diatreme. A north-south trending linear gravity anomaly, with a correlating magnetic anomaly (Figure 5c) occurs in the centre of the maar. Given that the Lake Purdigulac maar is aligned in an east-west direction, it is interpreted that this anomaly may represent the deeper feeder system of the complex. The other maars within the complex have a relatively neutral response, comprised of longer wavelength anomalies characteristic of a well-mixed diatreme with little internal property contrast, suggesting that no dykes intruded them during the later stages of the eruption.

A total of seven 2.5D forward models were constructed over the northern region of the survey area, including Lake Werowrap, the two small maars to the west of it and Lake Gnalingurk. Six models were previously constructed over the Lake Purdigulac maar by Piganis (2011). These models were used to construct a 3D model of the complex which served as an initial constraint for 3D inversions (Figure 5e). The discussion of inversion results is focused on Lake Werowrap, and the two small maars to the west of it as data are too sparse over the Lake Gnalingurk maar to produce realistic results through 3D inversion. Geometric and volume information for these models are summarised in Table 1 and discussed below.

A 2.5D forward model of the free-air anomaly (with northwest-southeast trending regional gradient removed) that crosses the centre of three maar craters in the northwest region of the complex is shown in Figure 5d. The Lake Werowrap maar displays a complex gravity and magnetic signature, with several short wavelength positive gravity and magnetic anomalies located within the crater. One of these anomalies correlates with a small spatter cone (~60 m in diameter) protruding from the sediments in the northern part of the crater which formed in the later stage of the maars eruption. Other anomalies observed within the crater likely represent similar features buried under the maar lake sediments and are reproduced during forward modelling by the presence of dykes and spatter cones that likely produced the lava flows that infilled the crater in the later stages of the eruption. Forward modelling suggests that the Werowrap diatreme is shallow and 'bowl-shaped' (aspect ratio of 0.86), and is similar in structure to other diatremes observed within the Newer Volcanics Province (e.g., Lake Coragulac; Blaikie *et al.* (2012), Lake Purrumbete; Jordan *et al.* (2013), Ecklin maar and Mt Leura; see below) and elsewhere (e.g., Auckland (New Zealand), Cassidy *et al.* (2007), Kereszturi *et al.* (2013); and the Campo de Calatrava volcanic field (Spain), Martín-Serrano *et al.* (2009)). 3D modelling (Figure 5f) shows that the maar-diatreme is elongated in the north-south direction, with steeply dipping walls (~75°) on the east and west margins of the diatreme, dipping slightly shallower on the north and south margins (~60°), with a relatively flat bottom at a depth of 320 m. The intrusions within the diatreme (Figure 5f-g), some which reached the surface and formed small spatter cones and lava flows have a volume of 0.004 km^3 indicating a lack of available groundwater during the eruption, which allowed magma to rise to the surface without phreatomagmatic eruptions. The Werowrap diatreme has a bulk volume of 0.037 km^3, of which the dykes and magma ponds comprise 10%. This interpretation is analogous to the Pula maar, Hungary (Németh *et al.* 2008) and the Pali Aike volcanic field (Ross *et al.* 2011).

Forward and inverse modelling suggests that the two small maar craters on the western side of the traverse (Figure 5d) are underlain by small, shallow diatremes (Depths of 140 m and 95 m, dips ranging between of 30-60 and 30-80 degrees, and aspect ratio's of 0.79 and 0.59 for the western-most and central diatreme respectively). These diatremes have volumes of 0.0028 and 0.00077 km^3 for the western-most and central diatreme respectively. The western-most maar has a neutral gravity and magnetic response, which was reproduced by a simple diatreme structure. The central maar has a slightly higher gravity response than the maar crater to the west of it, and a large magnetic anomaly. The broader wavelength of the gravity/magnetic anomaly suggests a deeper source and was reproduced during modelling by a large feeder dyke below the maar crater. The absence of short-wavelength anomalies within the two western craters indicates that there are no shallow intrusions within the maar-diatremes, or they are too small to be detected within the current parameters of the survey, likely indicating an eruption that was dominantly phreatomagmatic, preventing dykes rising through the diatreme to shallow levels.

6.2 Ecklin

The Ecklin maar crater is characterised by a Bouguer gravity low (2 mgal). The negative anomaly is larger in the southern part of the crater, suggesting that the underlying diatreme is deeper in this area of the maar (Figure 6a). A high-pass filter with a cut-off bandwidth of 800 m was applied to the gravity data to remove long and emphasise short wavelengths in the data, and revealed two low amplitude gravity anomalies (0.43-73 mgal) within the centre of the maar (Figure 6b). The anomalies correlate with two magnetic high's (324 nT) aligned in the same direction as the long-axis of the maar (north-northwest - south-southeast; Figure 6c). The gravity and magnetic anomalies are broader and more subtle than the short wavelength anomalies observed at Red Rock, suggesting that the source is larger and has a smaller density and magnetic susceptibility contrast with the surrounding material. These anomalies are interpreted to represent the maars two vents which have a higher proportion of denser and more magnetic volcanic debris than the outer margins of the maar diatreme. This structure is similar to the juvenile enriched zones described for the Standing Rocks West diatreme in the Hopi Buttes volcanic field, (Arizona, USA; Lefebvre *et al.* (2013))

Three 2.5D forward models were constructed across the maar. Models A and B are shown in Figure 6d-e, model A-A' is aligned along the long axis of the maar, and model B-B' is aligned in an east-west direction and crosses the maars inferred southern vent. The observed data was reproduced by modelling two coalesced diatreme structures with central vents of a slightly different composition to the margins of the maar-diatreme. The greater density and magnetic susceptibility of these vents are interpreted to be due to higher proportions of volcanic juvenile material, and likely represent volcanic material that was entrained into the diatreme by debris jets that failed to reach the surface. The 3D geometry of the diatreme can be described as being broad and shallow (aspect ratio of 0.79), or 'bowl-shaped' (Figure 6f), with a depth of 480 m, and walls dipping at 20° in the north, increasing to 70° along the south-eastern margin of the diatreme where it is deepest. The two central vents have a combined volume of 0.01 km^3 which equates to 10% of the total bulk diatreme volume of 0.12 km^3. The geometry of the Ecklin diatreme is similar to other diatremes observed within the Newer Volcanic Province (Blaikie *et al.* 2012; Jordan *et al.* 2013) and characteristic of an eruption hosted within a weakly lithified host rock.

Inverse modelling supports the initial 2.5D models with two coalesced diatremes containing denser

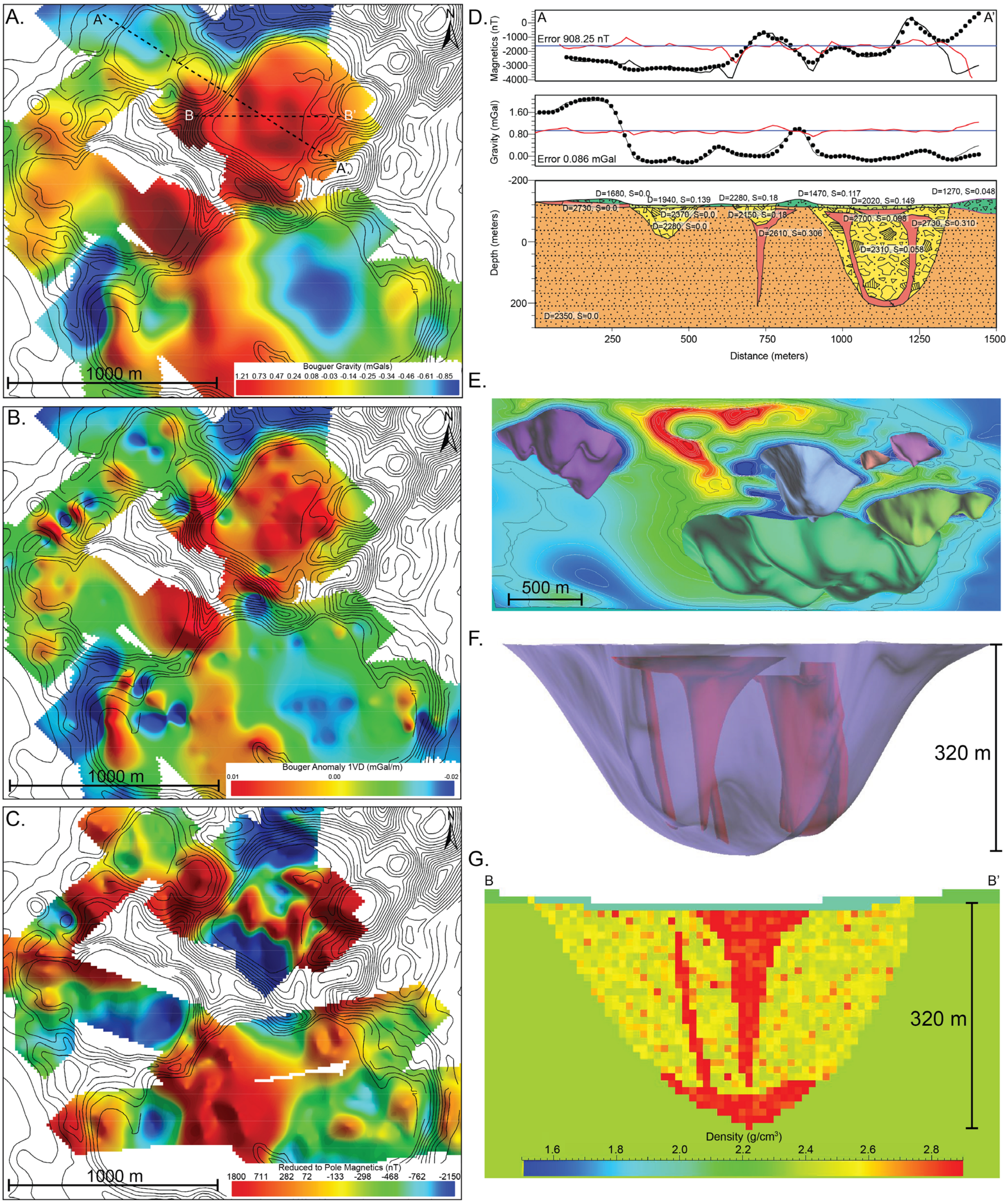

Figure 5. Geophysical response of the Red Rock Volcanic Complex a) Bouguer anomaly, regional trend removed, b) Bouguer anomaly, 1VD, c) RTP magnetic data, d) 2.5D forward model showing the structure of 3 maars within the complex, e) 3D model of the maar-diatremes underlying Red Rock (includes models from Blaikie et al. (2012) and Piganis (2011)). f) 3D model of the Lake Werowrap maar showing complex internal structures, g) heterogeneous inversion of the Lake Werowrap maar.

vents within their centres (Figure 6g-i). Three-dimensional gravity inversions do suggest, however, that the diatreme is deeper than initially modelled (630 m) in 2.5D, and is more steeply dipping (75-85°) below a depth of 300 m (Figure 6g). Above this depth, the diatreme is broader with shallowly dipping (30-45°) margins. This revised diatreme model has a bulk volume of 0.13 km^3 (Table 1). This change in diatreme geometry roughly coincides with a change in stratigraphy between the Gellibrand Marl (below 250 m depth) and the Port Campbell Limestone (above 250 m). A broader diatreme is observed in the weaker Port Campbell Limestone, while the relatively stronger Gellibrand Marl is able to support steeply dipping diatreme walls.

6.3 Mount Leura

The geophysical survey across the Mt Leura Volcanic Complex was limited to the southern area of the complex because active quarrying, steep slopes and thick vegetation over the Mt Sugarloaf scoria cone, the proximity of the town of Camperdown and a major highway mean that the area is unsuitable for gravity or magnetic surveying.

The Mt Leura Volcanic Complex exhibits a complex geophysical response that reflects its variable eruption styles. The maar crater in the south of the complex shows a neutral to low gravity response and a magnetic low, although a few small magnetic highs are present and were detected by the implementation of a higher resolution magnetic survey (Figure 7a-b). These magnetic anomalies reflect outcropping basaltic lava flows in the crater wall, and some infilling of scoria/lava in the crater during the later magmatic phases of the eruption. The gravity response of the tuff ring and crater reflects the lower density of phreatomagmatic pyroclastic deposits, consisting of highly fragmented country rock and juvenile material.

Confined mostly within the extent of the tuff ring is a Bouguer gravity high (~5 mgal), reflecting the infilling of the tuff ring with denser lava flows, welded spatter and scoria during the magmatic stage of the eruption. The high frequency, high amplitude (up to 2300 nT) magnetic response of the crater is characteristic of magmatic volcanic products such as lava flows within the Newer Volcanic Province. The highest amplitude magnetic anomalies are located over the peaks of the scoria cones, reflecting the thicker sequences of the more magnetic magmatic volcanic products.

2.75D forward modelling across the complex supports the initial interpretation of the data. Profiles A-A' and B-B' are shown in Figures 7c-d. Profile A-A' intersects the centre of the maar crater, and the south-western margin of the tuff ring. Profile B-B' is oriented in W-E direction and intersects the centre of the maar, and southern margin of the tuff ring. A regional gradient, increasing towards the north-west in A-A' was modelled by a sloping basement under the model (not seen in figure). Gravity and magnetic highs identified within the extent of the tuff ring are reproduced during modelling by the presence of ponded magma and lava flows up to 150 m thick, with a volume of 0.08 km^3 that infilled part of the maar and tuff ring craters. Overlying the centre of the two craters is a variably thick layer of scoria (50 m thick within the extent of cone complex, thinning to 1 m distal to cones), produced during the formation of the scoria/spatter cones within the craters. This interpretation of the data is analogous to the La Breña – El Jagüey maar complex (Mexico; Aranda Gomez *et al.* (1992)) and the Hoskietso maar in the Hopi Buttes volcanic field, (Arizona, USA; White (1991)).

Similarly to other diatremes modelled in the Newer Volcanic Province, the diatremes underlying the

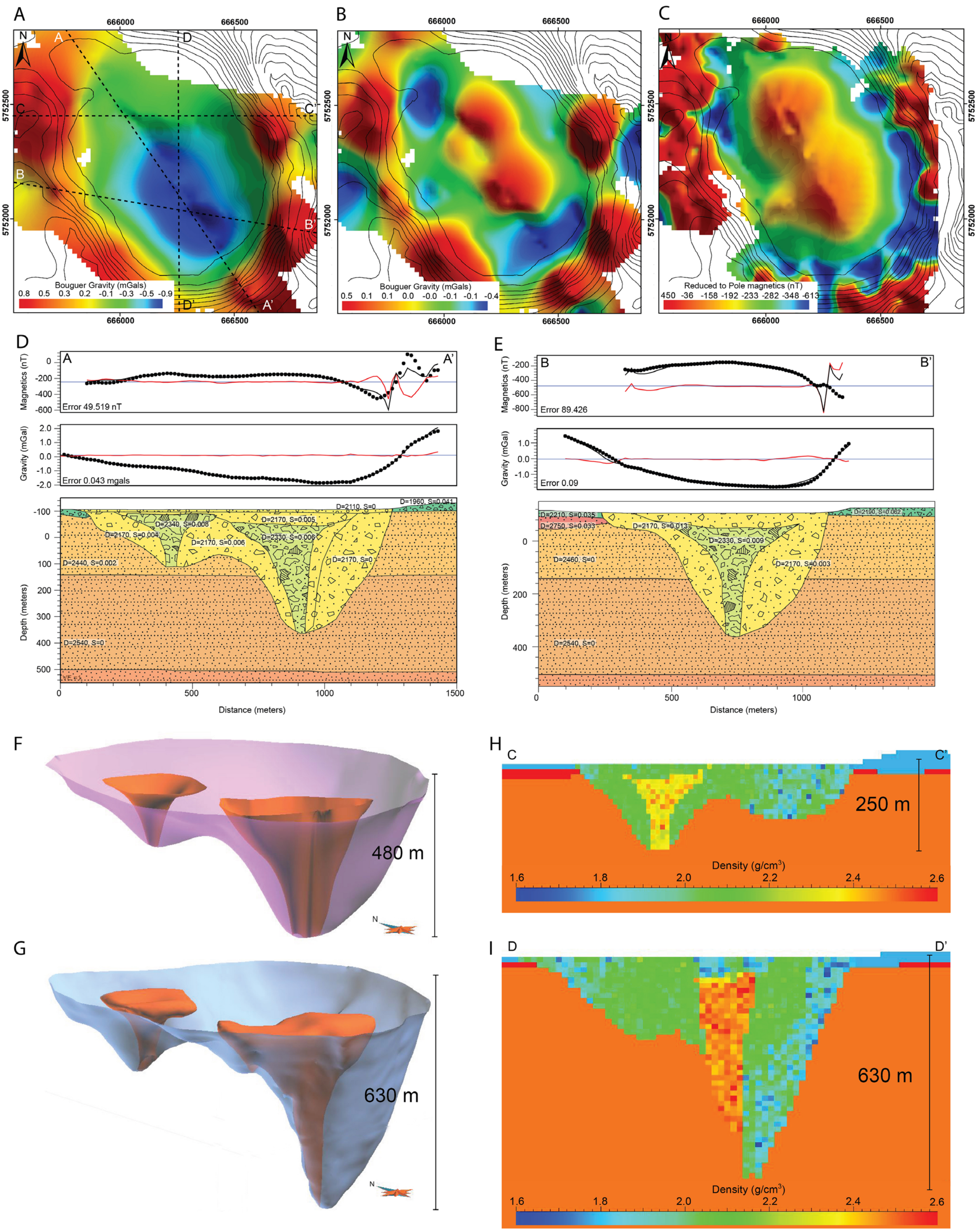

Figure 6. Geophysical response of the Ecklin maar a) Bouguer anomaly with regional trend removed showing gravity low over the crater b) Bouguer anomaly, HP filter 800m, showing two gravity anomalies in the centre of the maar, c) RTP magnetic data showing two magnetic anomalies which correlate with the gravity anomalies, d-e) 2.5D forward models showing structure of the maar diatreme, f) 3D model viewed from south-west, g) Optimised geometry of the Ecklin diatreme, h-i) Heterogeneous inversion of the optimised geometry showing denser vents in the centre of the diatreme surrounded by lower density material.

Mt Leura Volcanic Complex (Figure 7e) are broad (with diameters of 1500 m (maar) and 1900 m (tuff ring)) and shallow (with depths of 515 m (maar) and 355 m (tuff ring), giving aspect ratio's of 0.34 and 0.20 respectively) with diatreme walls dipping between 40° - 70° for the maar-diatreme and 20° - 30° under the tuff ring (Table 1). The diatremes have a combined volume of 0.58 km^3, although this is an estimate as the data is sparse across the northern areas of the complex so the model geometry is less well constrained. The centre of the maar and tuff ring diatremes are typically denser than the margins (Figure 7h)), possibly due to compaction induced porosity loss, and/or suggesting the existence of juvenile enriched zones (similar to Standing Rocks West, Hopi Buttes volcanic field, Arizona USA; Lefebvre *et al.* (2013)), which is likely given the corresponding magnetic anomalies. Three other 2.75D profiles produced through the maar crater and southern section of the tuff ring show similar results to profile A-A'. These models were imported in Gocad™ where a 3D model of the volcanic complex was produced in preparation for 3D gravity inversions (Figure 7d).

Inverse modelling indicates similar results to the 2.75D models. Initial geometry inversion indicates that the maar is deeper than the initial model, and lava flows are thicker (Figure 7f-g). However, during the inversion process, areas of the maar and the tuff ring diatremes that are overlain with lava were made shallower. This could be another indication that the thickness of the lava flows was under-estimated. These results also highlight the difficulties in modelling diatreme geometries when overlain by thick lava flows, as the signature of the lavas tends to mask the geophysical response of any underlying diatreme.

6.4 Anakie

The Anakie maar has a simple geophysical response, compared to Mt Leura and Red Rock which also exhibited magmatic phases during the eruption. The maar is characterised by a gravity and magnetic low (relative amplitudes of 1 mgal and 660 nT, Figure 8a-c). No shorter-wavelength anomalies were identified within the crater through data processing. 2.5D forward modelling results suggest that a shallow (130 m deep) maar-diatreme underlies the crater (Figure 8d). The diatreme is broad with shallowly dipping (~25°) diatreme walls in the north, which become more steeply dipping (~75°) in the south where the diatreme reaches its maximum depth of 130 m (Figure 8e) and has a volume of 0.0053 km^3 (Table 1). The simple geometry of the maar diatreme is attributed to a very short lived eruptive phase with relatively stable conduit conditions that prevented lateral and vertical vent migration. Most of the activity occurred at the cones to the northwest and southeast of the maar crater.

Geometry inversion suggests that the maar diatreme may be slightly deeper (190 m) than the initial model but of a similar geometry to the original interpretation (Figure 8f). However, during the inversion, the centre of the maar crater was forced upwards, bringing the denser granitic rock closer

Figure 7 (RIGHT) The geophysical response the Mt Leura Volcanic Complex showing the a) Bouguer anomaly b) RTP magnetic data overlain on Lidar data (2x vertical exaggeration; Lidar courtesy of the Corangamite Catchment Authority). Gravity and magnetic highs are confined mostly to the extent of the tuff ring (white ellipse) and while a smoother neutral to low gravity and magnetic response are observed over the maar (black ellipse). Geophysical models of Mt Leura; c-d) 2.75D forward models showing structure of the maar, tuff ring and infilled lava's. e) 3D model viewed from south-east, f) 2D section of 3D model g) Optimised geometry of 3D model h) heterogeneous inversion of inverted geometry. (Figures f-h) viewed from the north).

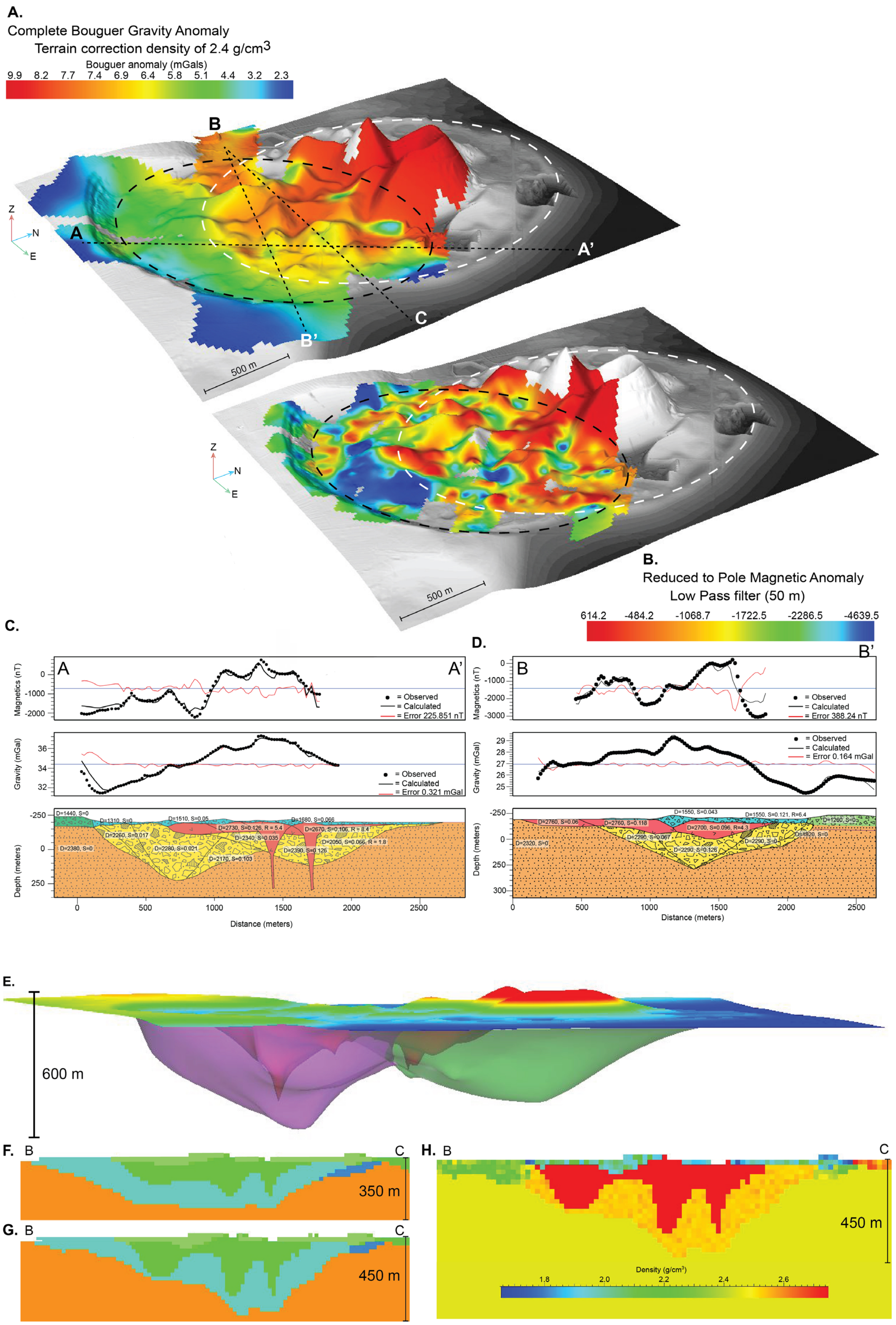
A.
Complete Bouguer Gravity Anomaly
Terrain correction density of 2.4 g/cm3
Bouguer anomaly (mGals)
9.9 8.2 7.7 7.4 6.9 6.4 5.8 5.1 4.4 3.2 2.3
B
A
A'
B'
C
Z
N
E
500 m
B.
Reduced to Pole Magnetic Anomaly
Low Pass filter (50 m)
614.2 -484.2 -1068.7 -1722.5 -2286.5 -4639.5
C.
D.
A
A'
B
B'
Magnetics (nT)
= Observed
= Calculated
= Error 225.851 nT
= Error 388.24 nT
Gravity (mGal)
= Error 0.321 mGal
= Error 0.164 mGal
Depth (meters)
Distance (meters)
E.
600 m
F. B
C
350 m
G. B
C
450 m
H. B
C
450 m
Density (g/cm³)
1.8 2.0 2.2 2.4 2.6

to the surface to increase the gravitational response. This could indicate the presence of a denser vent within the centre of the diatreme, or a deeper feeder dyke underlying the maar which was not previously identified through interpretation of gridded or profiled data. A heterogeneous inversion was applied to the granite region of the model to attempt to image this feature. Results indicate that a dense body dipping towards the east at an angle of 50° underlies the maar diatreme, most likely the feeder dyke for the complex (Figure 8g). The dip and orientation of the dyke is consistent with it having intruded along the along the Lovely Banks Monocline (Bolger 1977).

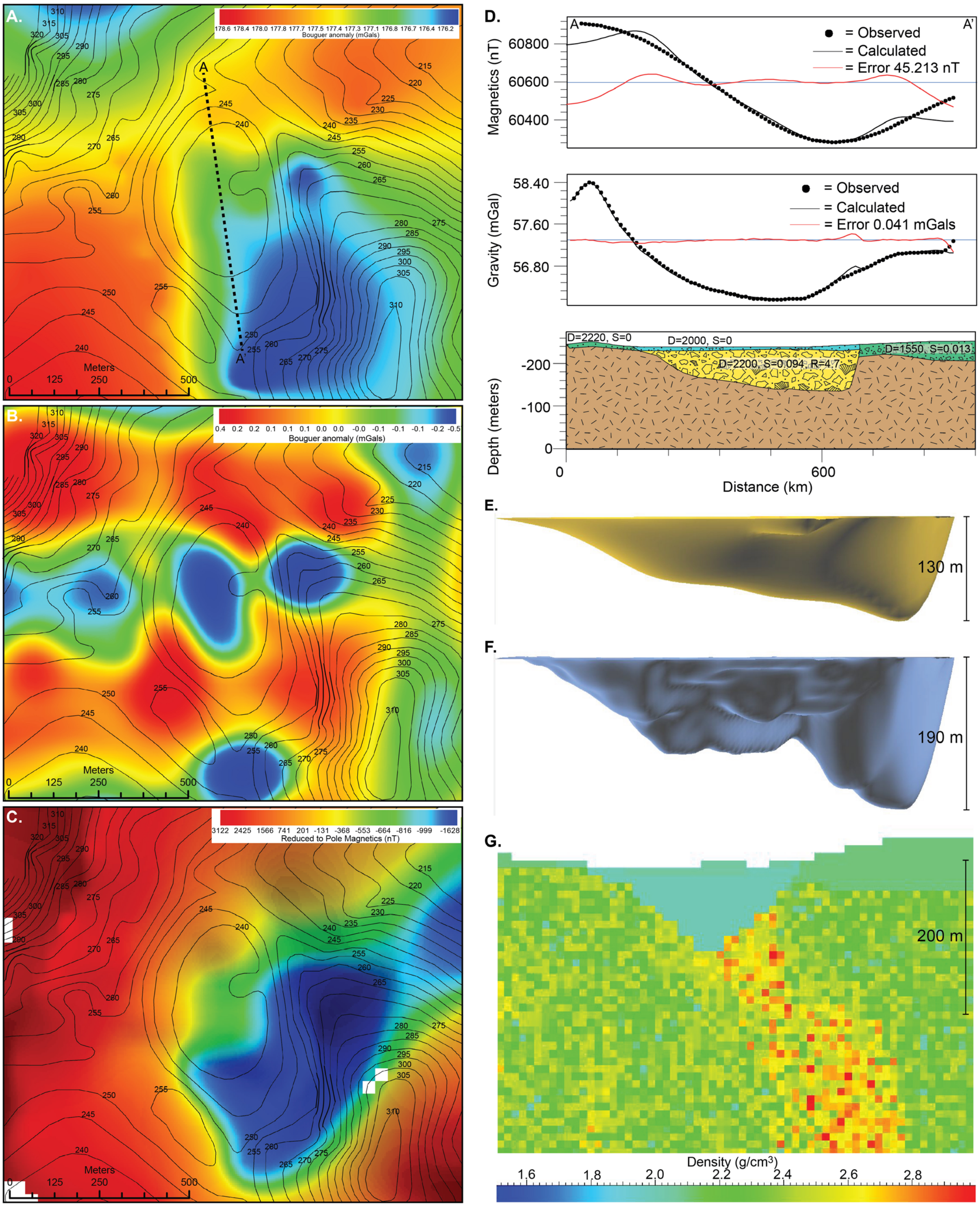

Figure 8 Geophysical response of the Anakie maar a) Bouguer anomaly, b) Bouguer anomaly, band-pass filter (cut-off wavelengths 40-700 m), c) RTP magnetic data. Data shows gravity low and neutral magnetic response. d) 2.5D forward model showing the shallow diatreme structure of the maar, e) 3D model, f) optimised geometry of the Anakie diatreme, g) heterogeneous inversion of host rock showing inclined feeder dyke (viewed from south).

7. Discussion

Monogenetic volcanoes can have complex eruptive histories, even when their morphologies are relatively simple. Without the application of geophysical modelling techniques it can be difficult to understand the evolution of an underlying vent system that is not exposed. The Ecklin maar is a good example of how complex a seemingly simple volcanic centre can be, and highlights the effectiveness of applying geophysical techniques to understand the entire volcano, from feeder dyke to the edifice. Although there is no drill hole data for any of our case studies that may help validate our interpretations, analysis of gridded gravity and magnetic data together with constrained geophysical modelling allows us to estimate the geometry and bulk volumes of underlying structures (Table 1), and identify vent numbers and locations within the crater, which is an important step towards fully understanding eruptive processes, how maars form and how they may evolve. By comparing the geophysical signature and eruptive histories of these case studies, and results from previous works of potential field modelling of maar volcanoes (e.g., Rout *et al.* 1993; Schulz *et al.* 2005; Lindner *et al.* 2006; Cassidy *et al.* 2007; Lopez Loera *et al.* 2008; Mrlina *et al.* 2009; Skacelova *et al.* 2010), several geophysical trends correlating to different eruptive histories have been identified and are summarised in Table 2. These trends are a guide only, as volcanoes hosted in different settings have differing petrophysical properties of the magma and host rock which may result in variable geophysical signatures. These results are for normally magnetised volcanics, any remanent magnetization may result in different magnetic signatures, or offset magnetic anomalies. Recognising these trends, and how they relate to the eruptive histories of the maars have assisted in understanding the evolution of these volcanoes, and may assist in future interpretations of potential field data.

Table 2. Summary of the geophysical signature and eruptive history of maar volcanoes

Anomaly	Eruptive history	Example
Gravity low and magnetic high or low over crater	Dominantly phreatomagmatic, homogeneous diatreme infill	Anakie maar Red Rock Volcanic Complex Pukaki, Auckland Volcanic Field (Cassidy et al., 2007) Baruth, Germany (Schulz et al., 2005)
Gravity and magnetic low over crater, superimposed low amplitude, broad positive gravity and magnetic anomaly	Dominantly phreatomagmatic with preserved vents containing higher proportions juvenile material	Ecklin maar
Gravity and magnetic low over crater, superimposed short wavelength, moderate to high amplitude, positive gravity and magnetic anomaly	Fluctuating phreatomagmatic/ magmatic. Preserved dykes within diatreme	Lake Coragulac and Purdigulac (Red Rock Volcanic Complex) Hnojnice diatreme, Czech Republic (Skacelova et al., 2010)
Gravity and magnetic high over crater, may be superimposed with short-wavelength higher amplitude gravity and magnetic anomalies	Early phreatomagmatic, late stage magmatic activity infilling maar crater with lava and preserving dykes within diatreme	Lake Werowrap (Red Rock Volcanic Complex) Mt Leura Volcanic Complex Pukekiwiriki, Waitomokia and Domain maars, Auckland volcanic field (Cassidy et al., 2007)

7.1 Model Limitations

Potential field models are limited because they always suffer from ambiguity. The models presented here were built with strict geologic constraints to ensure that they are geologically plausible, consistent with the geology of each volcanic centre, and maar-diatremes observed elsewhere. Although well constrained, our results are non-unique and other models that satisfy the observed data can be produced if different model properties are applied. Presenting end-member models for each case study here is beyond the scope of this paper, but will be addressed in the future. In each example presented, the model with the best fit between the observed and calculated data using the average density/susceptibility values and is the most consistent with geologic observations was presented. These models represent the intermediate between end-member models, and are consistent with previously described eruptive histories.

7.2 The formation and geometry of diatremes within the Newer Volcanics Province

The model first established for the formation of maar volcanoes by Lorenz (1986) proposes that maar craters are widened by the downwards propagation of the explosion focus and progressive downwards excavation of the country rock and pyroclastic debris, which are deposited in a surrounding ejecta ring. A revised model proposed by Valentine and White (2012) suggests that explosions may occur within any level of the diatreme at any time during the eruption, assuming the diatreme fill is fully saturated with water. The ejection of material from the maar crater occurs most effectively when explosions are near-surface, and progressive mixing within the diatreme occurs as debris jets transport material upwards through material that is subsiding downwards.

Elements of both the Lorenz (1986) model and the revised Valentine and White (2012) model are observed in our case studies. Geophysical modelling suggests that these maars are underlain with diatremes, which at least at the Ecklin maar, continued propagated downwards during the eruption (based on the geometry of the diatreme and observations of deeper lithic fragments in the ejecta rim). But in contrast to the deep pipe-like diatremes Lorenz (1986) describes, broad shallow diatremes are commonly observed within the Newer Volcanic Province. Evidence for these shallow diatremes comes from geophysical modelling (e.g., this study; Blaikie *et al.* (2012)) and from detailed studies on the physical volcanology of the eruptive centres, especially constraints provided by country rock xenolith populations (Jordan *et al.* 2013). Shallow diatreme structures are usually attributed to a water saturated, unconsolidated to weakly consolidated host rock, which slumps into the crater and provides a constant influx of water that allows phreatomagmatic explosions to remain at shallow levels (Lorenz 2003; White & Ross 2011), and this is consistent with the setting of Ecklin, the Red Rock and Mt Leura volcanic complexes.

Similarities are observed in diatreme structures across the Newer Volcanic Province (i.e. being coalesced, broad and shallow), however the internal structures within the diatremes (vents, dykes and magma ponds) are quite variable, and reflect differences in the eruptive histories and styles of the individual volcanoes. The revised model of Valentine and White (2012) can perhaps better explain the complex internal structures identified during geophysical modelling. The two denser vents observed within the centre of the Ecklin maar-diatreme are interpreted to represent an increased concentration of juvenile basaltic material by mixing from the injection of multiple debris jets into the diatreme. The multiple coalesced diatremes, presence of shallow dykes modelled within the diatremes, and the observed fluctuating eruptive styles at the Red Rock Volcanic Complex suggest that explosive fragmentation occurred at varied levels and migrated laterally along irregularly shaped intrusions within the diatremes. The low hydraulic conductivities of the host sediments mean that the diatremes were unlikely to be completely water-saturated during the eruption, likely contributing to the fluctuating eruptive styles of the maars.

The Red Rock, Mt Leura and Ecklin maars all exhibit multiple vents, suggesting that rather than the downward propagation of explosions, lateral vent migration is responsible for the widening of the crater. This process has been recognised as the cause for crater widening at several maar volcanoes (e.g., Németh *et al.* 2001; White & McClintock 2001; Sohn & Park 2005; Auer *et al.* 2007; Ort & Carrasco-Núñez 2009; Kereszturi & Németh 2011; Ross *et al.* 2011; Jordan *et al.* 2013). Multiple vents are a common occurrence within the volcanoes of the Newer Volcanic Province (e.g., Red Rock, Mt Leura, Ecklin maar, Anakie, Mt Gambier, Mt Rouse, Lake Purrumbete, Lake Bullen-Meri, Tower Hill, Mt Noorat, Mt Schank), and can perhaps be attributed to a weakly lithified host rock collapsing into, and blocking the vent, causing it to migrate elsewhere (Sohn & Park 2005). Sometimes these vents are aligned, suggesting that vent migration is occurring along the length of a dyke (e.g., Anakie, Mt Gambier, Mt Schank, cone-complexes at Red Rock and Tower Hill), which in some cases appear to be channelled along pre-existing faults (e.g., Anakie, Mt Gambier; van Otterloo *et al.* (2013)). Other times the vents are irregularly distributed within the crater (e.g., Lake Bullen-Meri, Lake Purrumbete, Lake Coragulac, and Lake Purdigulac) indicating that vent migration is occurring along irregularly shaped dykes propagating into the loose debris of the diatreme.

Shallow diatremes are typically attributed to a weakly lithified to unconsolidated host rock, however they could also be related to the formation of sills at a shallow depth (Németh & Martin 2007). Dykes may initiate from an established sill, and rise to a level where phreatomagmatic explosions occur. As the eruption proceeds the depth of magma-water interaction propagates downwards until the root zone of the diatreme reaches the level of the sill. Explosions may continue to occur within the root zone, or may propagate laterally along the sill, forming a new vent within the maar. However, it is difficult to determine if this is occurring in the Newer Volcanics Province because it is difficult to model horizontal structures such as sills using potential field techniques, and the detection of sills underlying each of the case studies presented here may be beyond the capabilities of the surveys. Seismic methods may be able to detect such structures, however strong reflections are observed from the lava flows at the surface so conditions are not ideal for seismic surveys in this region of the Newer Volcanic Province.

Our modelling results show that maar-diatremes can have complex geometries, especially when vent migration is occurring. This has important implications for understanding the bulk volumes of diatremes, which have previously been largely estimated by calculating the volume of an inverted cone based on (sometimes inferred) crater dimensions and limited exposures of the diatreme (Kereszturi *et al.* 2013; Lefebvre *et al.* 2013). Once a 3D model is constructed using our modelling technique, it is relatively simple to calculate the volume of different components of the model. The bulk diatreme volumes presented in this paper (Table 1) are fairly consistent with volumes previously calculated for maars and kimberlite pipes, which range between 0.01 and 1 km^3 (Brown & Valentine 2013; Lefebvre *et al.* 2013), with the exception of the very small maars at Anakie and Red Rock which have smaller volumes (however these represent small vents within larger complexes). By applying our modelling technique, together with a detailed study on the componentry and volume of the ejecta ring, it should be possible to calculate minimum magma volumes for the eruption of maar-volcanoes, which has important implications for understanding the relationships between magma volume, duration of an eruption and the eruptive style of the maar (Kereszturi *et al.* 2013).

Further work is required to achieve this for each of the case studies presented in this paper, as presently the size of our 3D models do not cover the entire extent of the ejecta ring so as to reduce the size of the model and increase the inversion computing time. In addition, drilling into the maars to provide important samples for petrophysical analysis is needed in order to help validate the geophysical interpretations.

7.3 Eruptive histories of the case studies

The application of geophysical modelling techniques has led to a better understanding of the eruptive history of each of these volcanic centres. Prior to modelling, some understandings of the eruptions were known from previous studies of the volcano's deposits (Cas *et al.* 1993; Cas *et al.* 2011), however often the complexity of the volcanoes eruptive histories was underestimated. Results suggest that the subsurface morphology of these maar-diatremes are highly complex and can vary greatly between different eruptive centres, even if their surface morphologies are similar. A schematic eruptive history for each volcanic centre is shown in Figure 9.

The Red Rock Volcanic Centre is one of the most complex volcanoes within the Newer Volcanic Province, and experienced frequently fluctuating eruption styles ranging from effusive to explosive magmatic and phreatomagmatic (Blaikie *et al.* 2012). Modelling of the complex identified multiple coalesced diatremes with complex internal structures consisting of dykes and magma ponds. Pyroclastic deposits indicate that the eruption style of the growing maars frequently fluctuated between magmatic and phreatomagmatic explosive activity, indicating a complex interplay between rising magma and groundwater availability, likely due to the low hydraulic conductivity and slow recharge of sediments underlying the complex. Fluctuating eruptive activity suggests that at some point during the eruption, dykes would have risen through the maar-diatreme to the near surface and are preserved within the diatreme where they were detected by the implementation of a high resolution survey (Blaikie *et al.* 2012).

Within the Red Rock Volcanic Centre, maar craters and scoria cones are aligned along several different orientations (east-west, northwest-southeast, north-northeast – south-southwest). However, multiple vents identified within individual maar craters do not tend to follow this alignment. The broad scale alignment of maar craters and scoria cones could represent magma being channelled along pre-existing bedrock structures, and/or being controlled by the regional stress orientation field (northwest-southeast; (Hillis *et al.* 1995)), with the random vent distribution within the maars being caused by the irregular intrusion of dykes within the loose debris of the diatreme. This would suggest that explosions are varying in lateral and vertical positions, however fragmentation is largely contained within the maar-diatreme and is not propagating down to deeper levels. The aligned craters at Red Rock suggest multiple near parallel dykes, possibly aligned along shallow subsurface structures. Vent migration along these dykes could be caused by variable magma flux (which could also explain the fluctuating eruption styles), or by lithification contrasts in the subsurface (Ort & Carrasco-Núñez 2009).

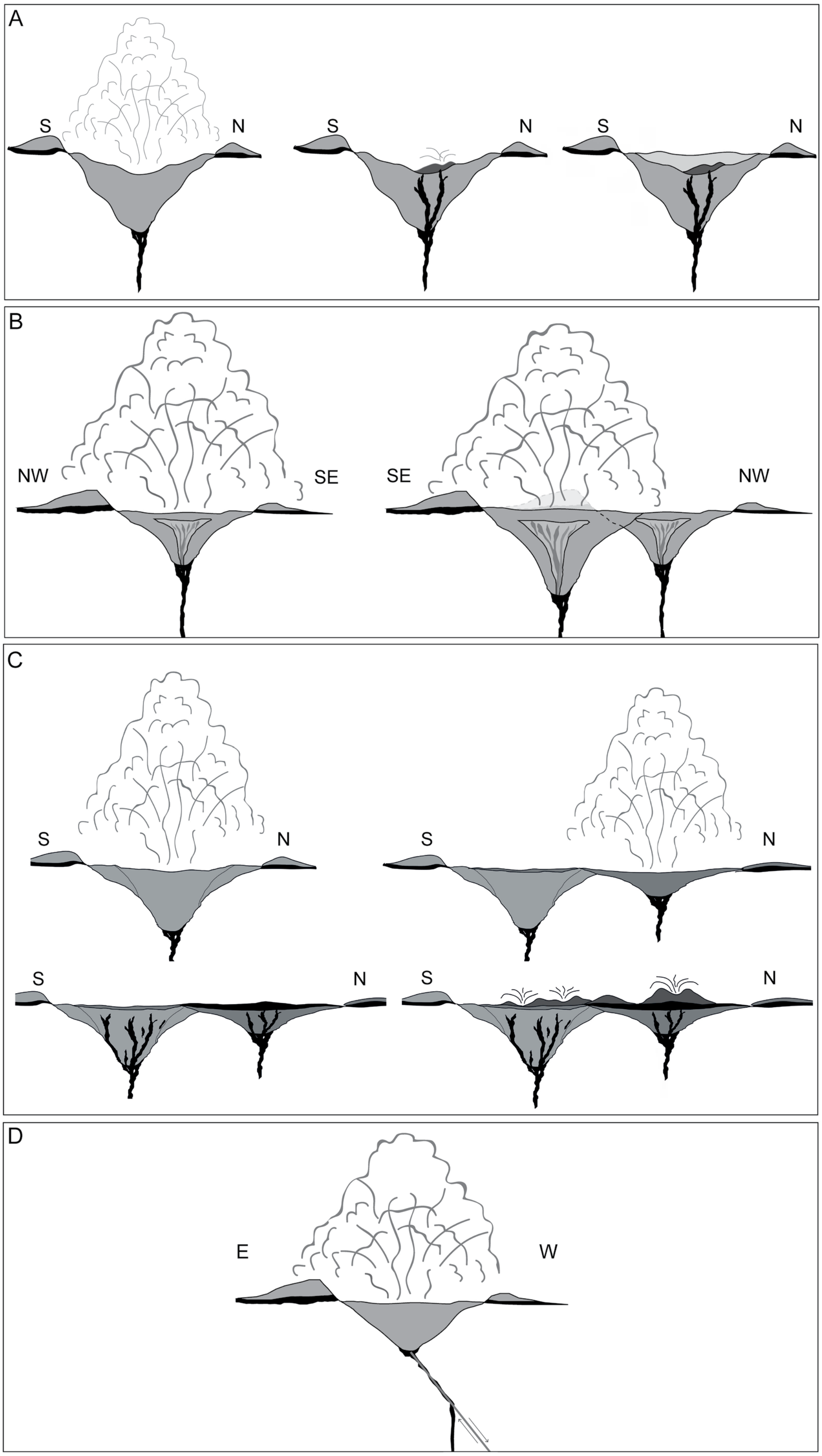

Figure 9. Eruptive histories of a) Lake Werowrap, Red Rock Volcanic Complex, showing formation of the maar, intrusion of dykes and spatter cone eruptions, deposition of lake sediments. b) Ecklin, showing the migration of eruption points and formation of coalesced diatremes. c) Mt Leura Volcanic Complex, showing formation of maar and tuff rings, infilling of the crater with lava and formation of the scoria cones. d) Anakie maar showing intrusion of dyke along a fault and eruption of the maar.

The Newer Volcanic Province is host to some of the largest maar volcanoes in the world which have crater diameters > 3 km (e.g., Lake Purrumbete, Tower Hill). Jordan *et al.* (2013) demonstrated that Lake Purrumbete (which is comparable in size to the Laguna Potrok Aike Maar, Argentina; Gebhardt *et al.* (2011)) was formed from multiple shallow vents, that coalesced to form a near circular crater after multiple eruptive phases. Evidence suggests these large craters form from the coalescence of multiple vents, and the Red Rock Volcanic Complex perhaps gives some insight into the intermediate stages of this process. If more water was available during the eruption at Red Rock, and the eruption style was dominantly phreatomagmatic instead of fluctuating, then perhaps there would be an increase in depth of phreatomagmatic explosions, which would result in the enlargement and coalescence of the craters. The other alternative is that a very large crater maar may be an erosional feature, where the gradual erosion of scoria cones and retreat of the crater rims produce one large crater (although this does not appear to be the case within large maars of the Newer Volcanics Province as newly obtained bathymetry and geophysical data over the Purrumbete maar (J. van den Hove, pers. comm) supports the interpretation of Jordan *et al.* (2013)).

Red Rock and Mt Leura exhibit a range of eruption styles that vary from phreatomagmatic to effusive and explosive magmatic. Mt Leura also consists of a broad shallow diatreme. Modelling however identified a thick lava flow, confined within the crater of the tuff ring. Small flows originating from the main scoria cone within the complex had been observed before, but the extent of lava flows infilling the crater had not previously been described by any volcanological studies. The structure modelled at Mt Leura is similar to the diatreme structure observed at the Hoskietso maar in the Hopi Buttes Volcanic Field, (Arizona, USA) (White 1991).

The Ecklin maar diatreme is comprised of two coalesced diatreme structures, with margins that are shallowly sloped and flared in the upper 300 m, and more steeply dipping below this. This change in diatreme geometry correlates with a change in lithology in the underlying sediments of the Otway Basin, and suggests that the diatreme propagated down into the more consolidated sediments which were able to support more steeply dipping diatreme walls. In contrast to Red Rock and Mt Leura, it is not thought that any dykes intruded into the Ecklin diatreme, or at least not to a level where they can be detected with the current parameters of the geophysical survey, and there is no evidence within the surrounding pyroclastic deposits that the maar exhibited short-lived magmatic phases that would have allowed dykes to rise to the surface and erupt in a magmatic style.

Maar volcanoes hosted in a hard-rock setting typically display deep, steeply dipping diatremes (Ross *et al.* 2011). It is thought that the shallow diatreme observed at Anakie is a result of a very short-lived eruption. The source of water that fuelled phreatomagmatic explosions within the Anakie maar is unclear, and may have been derived either from water contained with fractures in the granite or in the pore spaces of a thin layer of sand at the surface. If the thin sandy layer at the surface was the source of water fuelling phreatomagmatic explosions, then it is unlikely that the depth of magma-water interaction would have propagated down to deeper levels. The volcanic edifice is also quite degraded, being subject to quarrying for many years, and also due to the age of the complex. It is possible that what is being inferred as a maar crater, was actually a tuff-ring, however limited exposures of the deposits mean that this cannot be determined.

The most recent eruption within the Newer Volcanics Province was recently assigned a value of 4 on the Volcanic Explosivity Index (van Otterloo & Cas 2013). Any future eruption of a maar volcano within the region would represent a significant hazard. Recognising that many of the maars within the region have shallow diatremes has important implications for the assessment of volcanic hazards associated with future maar eruptions. Recent work suggests that explosions occurring within shallow levels of the diatreme may eject higher volumes of debris out of the crater, resulting in base surges and widespread distribution of tephra, while explosions occurring within deeper levels of the diatreme are largely confined by the crater walls, and are too weak to eject significant volumes of debris out of the crater (Valentine & White 2012; Lefebvre *et al.* 2013; Ross *et al.* 2013). If an eruption occurred in the future, it is likely that at least in the initial stages of the eruption, explosions would be located at a shallow level and result in the widespread distribution of tephra. This is observed for some maars in the province, (e.g., Tower Hill where deposits are identified ~12 km from the vent; Cas *et al.* (2011)). Whether the explosions would continue to occur at a shallow level, or propagate to deeper levels cannot be predicted, however based upon patterns of eruptions observed in the Newer Volcanic Province, and the weakly lithified nature of the country rock it is likely that phreatomagmatic explosions would be largely confined within the shallow subsurface.

8. Conclusions

Geophysical modelling techniques have been successfully applied to model the subsurface architecture of several maar volcanoes within the Newer Volcanics Province in order to gain an improved understanding of their eruptive histories. The depth, geometry and property distributions within the maar-diatremes were modelled to understand the subsurface morphology of the volcano, and how it relates to its eruptive styles. The Red Rock and Mt Leura Volcanic Complexes, Ecklin Maar and the Anakie's represent a range of the styles and sizes of maar volcanoes observed within the Newer Volcanic Province. Several geophysical trends were identified that correlate with the different eruptive histories of the maars (i.e., dominantly phreatomagmatic, fluctuating between magmatic and phreatomagmatic, transitional between phreatomagmatic and magmatic). Maars with fluctuating eruptive styles such as Red Rock are characterised by short wavelength positive gravity and magnetic anomalies superimposed on longer wavelength gravity and magnetic lows. The irregularly distributed short wavelength anomalies represent preserved dykes within the maar-diatremes, suggesting magma rose to and fragmented at variable depths within the diatreme. Maars such as Ecklin exhibiting predominantly phreatomagmatic activity are characterised by gravity and magnetic lows across the crater, but may contain broader wavelength, low amplitude positive gravity and magnetic anomalies in the centre of the crater. These anomalies are associated with preserved vents containing higher volumes of juvenile material compared to the rest of the diatreme. The Mt Leura Volcanic Complex experienced a transition in eruptive style from phreatomagmatic to magmatic and is characterized by long wavelength gravity and magnetic highs indicating a large volume of ponded lava infilled the maar crater during the eruption.

Multiple vents are associated with each of the volcanic centres, with some only identified after geophysical modelling. Multiple craters associated with a single eruptive centre are typically aligned, suggesting that at the larger scale, vent migration is occurring along a dyke. However, multiple vents within a single crater appear to be randomly distributed, suggesting that at the small scale, the loose debris of the diatreme are resulting in the irregular propagation of dykes within it, which is resulting in vertical and lateral variations of the point of fragmentation.

Results from this study highlight how geophysical data can improve our understanding of the eruptive histories and processes occurring in the shallow subsurface of volcanoes.

9. Acknowledgements

We wish to acknowledge assistance provided in the field by Jackson van den Hove, Felicity Piganis, Dan Uehara and Lisa Roche and are grateful to all land owners who allowed us access to their properties to conduct field work. This paper was greatly approved by comments from two anonymous reviewers.

10. References

Aranda Gomez J. J., Luhr J. F. & Pier J. G. 1992. The La Brena - El Jaguee Maar Complex, Durango, Mexico; 1, Geological evolution. Bulletin of Volcanology 54, 393-404.

Auer A., Martin U. & Németh K. 2007. The Fekete-hegy (Balaton Highland Hungary) "soft-substrate" and "hard-substrate" maar volcanoes in an aligned volcanic complex - Implications for vent geometry, subsurface stratigraphy and the palaeoenvironmental setting. Journal of Volcanology and Geothermal Research 159, 225-245.

Barde-Cabusson S., Bolós X., Pedrazzi D., Lovera R., Serra G., Martí J. & Casas A. 2013. Electrical resistivity tomography revealing the internal structure of monogenetic volcanoes. Geophysical Research Letters 40, 2544-2549.

Blackburn G. 1966. Radiocarbon dates relating to soil development and volcanic ash deposition in South-East South Australia. Australian Journal of Earth Sciences 29.

Blackburn G., Allison G. & Leaney F. 1982. Further evidence on the age of the tuff at Mount Gambier, South Australia. Royal Society of South Australia. Transactions 106, 163-167.

Blaikie T. N., Ailleres L., Cas R. A. F. & Betts P. G. 2012. Three-dimensional potential field modelling of a multi-vent maar-diatreme - the Lake Coragulac maar, Newer Volcanics Province, south-eastern Australia. Journal of Volcanology and Geothermal Research 235-236, 70-83.

Bolger P. 1977. Explanatory notes on the Meredith and You Yangs 1:50 000 geological maps. Geological Survey of Victoria Report. Department of Minerals & Energy, Victoria.

Boyce J. 2013. The Newer Volcanics Province of southeastern Australia: a new classification scheme and distribution map for eruption centres. Australian Journal of Earth Sciences 60, 449-462.

Brown R. J. & Valentine G. A. 2013. Physical characteristics of kimberlite and basaltic intraplate volcanism and implications of a biased kimberlite record. Geological Society of America Bulletin 125, 1224-1238.

Brunner I., Friedel S., Jacobs F. & Danckwardt E. 1999. Investigation of a Tertiary maar structure using three-dimensional resistivity imaging. Geophysical Journal International 136, 771-780.

Cas R. A. F., Blaikie T., Boyce J., Hayman P., Jordan S., Piganis F., Prata G. & van Otterloo J. 2011. VF01: Factors that influence varying eruption styles (from magmatic to phreato-magmatic) in intraplate continental basaltic volcanic provinces: the Newer Volcanics Province of south-eastern Australia. IUGG 2011 Fieldtrip guide.

Cas R. A. F., Simpson C. & Sato H. 1993. Newer Volcanics Province - processes and products of phreatomagmatic activity. IAVCEI Canberra 1993: excursion guide, September, 1993. Record - Australian Geological Survey Organisation. Geoscience Australia, Canberra, A.C.T., Australia.

Cassidy J., France S. J. & Locke C. A. 2007. Gravity and magnetic investigation of maar volcanoes, Auckland volcanic field, New Zealand. Journal of Volcanology and Geothermal Research 159, 153-163.

Edwards J., Leonard J. G., Pettifer G. R. & McDonald P. A. 1996. Colac 1:250 000 map geological report. Geological Survey of Victoria Report 98.

Field M., Stiefenhofer J., Robey J. & Kurszlaukis S. 2008. Kimberlite-hosted diamond deposits of southern Africa: A review. Ore Geology Reviews 34, 33-75.

Fullagar P. K., Hughes N. A. & Paine J. 2000. Drilling-constrained 3D gravity interpretation. Exploration Geophysics 31, 17-23.

Fullagar P. K., Pears G., Hutton D. & Thompson A. D. 2004. 3D gravity and aeromagnetic inversion for MVT lead-zinc exploration at Pillara, Western Australia. Exploration Geophysics (Melbourne) 35, 142-146.

Fullagar P. K. & Pears G. A. 2007. Towards geologically realistic inversion. In: Milkereit B. ed. Proceedings of Exploration 07: Fifth Decennial International Conference on Mineral Exploration, pp. 444-460.

Gebhardt A. C., De Batist M., Niessen F., Anselmetti F. S., Ariztegui D., Haberzettl T., Kopsch C., Ohlendorf C. & Zolitschka B. 2011. Deciphering lake and maar geometries from seismic refraction and reflection surveys in Laguna Potrok Aike (southern Patagonia, Argentina). Journal of Volcanology and Geothermal Research 201, 357-363.

Geshi N., Németh K. & Oikawa T. 2011. Growth of phreatomagmatic explosion craters: A model inferred from Suoana crater in Miyakejima Volcano, Japan. Journal of Volcanology and Geothermal Research 201, 30-38.

Gray C. M. & McDougall I. 2009. K-Ar geochronology of basalt petrogenesis, Newer Volcanic Province, Victoria. Australian Journal of Earth Sciences 56, 245-258.

Gray D. R., Foster D. A., Morand V. J., Willman C. E., Cayley R. A., Spaggiari C. V., Taylor D. H., Gray C. M., VandenBerg A. H. M., Hendrickx M. A. & Wilson C. J. L. 2003. Structure, metamorphism, geochronolgy and tectonics of Palaeozoic rocks. Interpreting a complex, long-lived orogenic system. In: Birch W. D. ed. Geology of Victoria, pp. 15-72. Geological Society of Australia Special Publication 23 Geological Society of Australia (Victoria Division).

Hare A. G. & Cas R. A. F. 2005. Volcanology and evolution of the Werribee Plains intraplate, basaltic lava flow-field, Newer Volcanics Province, southeast Australia. Australian Journal of Earth Sciences 52, 59-78.

Hare A. G., Cas R. A. F., Musgrave R. & Phillips D. 2005. Magnetic and chemical stratigraphy for the Werribee Plains basaltic lava flow-field, Newer Volcanics Province, southeast Australia; implications for eruption frequency. Australian Journal of Earth Sciences 52, 41-57.

Hillis R. R., Monte S. A., Tan C. P. & Willoughby D. R. 1995. The contemporary stress field of the Otway Basin, South Australia; implications for hydrocarbon exploration and production. The APEA Journal 35, Part 1, 494-506.

Johnson R. W. 1989. Intraplate volcanism in eastern Australia and New Zealand. Cambridge University Press, Cambridge.

Jordan S. C., Cas R. F. A. & Hayman P. C. 2013. The origin of a large ([>3]km) maar volcano by coalescence of multiple shallow craters, not deep excavation: The late Pleistocene Lake Purrumbete maar, Newer Volcanics Province, southeastern Australia. Journal of Volcanology and Geothermal Research 254, 5-22.

Joyce E. B. 1975. Quaternary volcanism and tectonics in southeastern Australia. Bulletin - Royal Society of New Zealand 13, 169-176.

Kereszturi G. & Németh K. 2011. Shallow-seated controls on the evolution of the Upper Pliocene Kopasz-hegy nested monogenetic volcanic chain in the Western Pannonian Basin (Hungary). Geologica Carpathica 62, 535-546.

Kereszturi G., Németh K., Cronin S. J., Agustín-Flores J., Smith I. E. M. & Lindsay J. 2013. A model for calculating eruptive volumes for monogenetic volcanoes — Implication for the Quaternary Auckland Volcanic Field, New Zealand. Journal of Volcanology and Geothermal Research 266, 16-33.

Kienle J., Kyle P. R., Self S., Motyka R. J. & Lorenz V. 1980. Ukinrek Maars, Alaska, I. April 1977 eruption sequence, petrology and tectonic setting. Journal of Volcanology and Geothermal Research 7, 11-37.

Lefebvre N. S., White J. D. L. & Kjarsgaard B. A. 2012. Spatter-dike reveals subterranean magma diversions: Consequences for small multivent basaltic eruptions. Geology 40, 423-426.

Lefebvre N. S., White J. D. L. & Kjarsgaard B. A. 2013. Unbedded diatreme deposits reveal maar-diatreme-forming eruptive processes: Standing Rocks West, Hopi Buttes, Navajo Nation, USA. Bulletin of Volcanology 75, 1-17.

Lesti C., Giordano G., Salvini F. & Cas R. 2008. Volcano tectonic setting of the intraplate, Pliocene-Holocene, Newer volcanic province (southeast Australia); role of crustal fracture zones. Journal of Geophysical Research 113.

Lindner H., Gabriel G., tze H.-J., rgen, Kaeppler R. & Suhr P. 2006. Geophysical and geological investigation of maar structures in the Upper Lusatia region (East Saxony). Zeitschrift der Deutschen Gesellschaft fur Geowissenschaften 157, 355-372.

Lopez Loera H., Aranda-Gomez J. J., Arzate J. A. & Molina-Garza R. S. 2008. Geophysical surveys of the Joya Honda Maar (Mexico) and surroundings; volcanic implications. Journal of Volcanology and Geothermal Research 170, 135-152.

Lorenz V. 1975. Formation of phreatomagmatic maar-diatreme volcanoes and its relevance to kimberlite diatremes. Physics and Chemistry of The Earth 9, 17-27.

Lorenz V. 1986. On the growth of maars and diatremes and its relevance to the formation of tuff rings. Bulletin of Volcanology 48, 265-274.

Lorenz V. 2003. Maar-Diatreme Volcanoes, their Formation, and their Setting in Hard-rock or Soft-rock Environments. Geolines 15, 72-83.

Lorenz V. 2007. Syn- and posteruptive hazards of maar-diatreme volcanoes. Journal of Volcanology and Geothermal Research 159, 285-312.

Martín-Serrano A., Vegas J., García-Cortés A., Galán L., Gallardo-Millán J. L., Martín-Alfageme S., Rubio F. M., Ibarra P. I., Granda A., Pérez-González A. & García-Lobón J. L. 2009. Morphotectonic setting of maar lakes in the Campo de Calatrava Volcanic Field (Central Spain, SW Europe). Sedimentary Geology 222, 52-63.

Moore J. G., Nakamura K. & Alcaraz A. 1966. The 1965 eruption of Taal Volcano. Science 151, 955-960.

Mrlina J., Kampf H., Kroner C., Mingram J., Stebich M., Brauer A., Geissler W. H., Kallmeyer J., Matthes H. & Seidl M. 2009. Discovery of the first Quaternary maar in the Bohemian Massif, Central Europe, based on combined geophysical and geological surveys. Journal of Volcanology and Geothermal Research 182, 97-112.

Muller G. & Veyl G. 1957. The birth of Nilahue, a new Maar type volcano at Rininahue, Chile. Chile Congreso Geológico Internacional 1, 375-396.

Nairn I. A. 1979. Rotomahana- Waimangu eruption, 1886: base surge and basalt magma. New Zealand Journal of Geology and Geophysics 22, 363-378.

Németh K. & Cronin S. J. 2011. Drivers of explosivity and elevated hazard in basaltic fissure eruptions: The 1913 eruption of Ambrym Volcano, Vanuatu (SW-Pacific). Journal of Volcanology and Geothermal Research 201, 194-209.

Nemeth K., Cronin S. J., Smith I. E. M. & Agustin Flores J. 2012. Amplified hazard of small-volume monogenetic eruptions due to environmental controls, Orakei Basin, Auckland volcanic field, New Zealand. Bulletin of Volcanology 74, 2121-2137.

Németh K., Goth K., Martin U., Csillag G. & Suhr P. 2008. Reconstructing paleoenvironment, eruption mechanism and paleomorphology of the Pliocene Pula maar, (Hungary). Journal of Volcanology and Geothermal Research 177, 441-456.

Németh K. & Martin U. 2007. Shallow sill and dyke complex in western Hungary as a possible feeding system of phreatomagmatic volcanoes in “soft-rock” environment. Journal of Volcanology and Geothermal Research 159, 138-152.

Németh K., Martin U. & Harangi S. 2001. Miocene phreatomagmatic volcanism at Tihany (Pannonian Basin, Hungary). Journal of Volcanology and Geothermal Research 111, 111-135.

Nicholls I. A. & Joyce E. B. 1989. East Australian Volcanic Geology: Newer Volcanics. In: Johnson R. W., Knutson J. & Taylor S. R. eds. Intraplate volcanism in eastern Australia and New Zealand, pp. 137-141. Cambridge University Press.

Ort M. H. & Carrasco-Núñez G. 2009. Lateral vent migration during phreatomagmatic and magmatic eruptions at Tecuitlapa Maar, east-central Mexico. Journal of Volcanology and Geothermal Research 181, 67-77.

Piganis F. 2011. A volcanological investigation of the polymagmatic Red Rock Volcanic Complex and a 3D geophysical interpretation of the subsurface structure and geology of the poly-lobate Lake Purdigulac maar, Newer Volcanics

Province, southeastern Australia. Masters thesis, Monash University, Australia (unpubl.).

Price R. C., Gray C. M. & Frey F. A. 1997. Strontium isotopic and trace element heterogeneity in the plains basalts of the Newer Volcanic Province, Victoria, Australia. Geochimica et Cosmochimica Acta 61, 171-192.

Price R. C., Nicholls I. A. & Gray C. M. 2003. Cainozoic igneous activity. In: Birch W. D. ed. Geology of Victoria, pp. 361-375. Geological Society of Australia Special Publication 23. Geological Society of Australia (Victoria Division).

Rasmussen R. & Pedersen L. B. 1979. End corrections in potential field modeling. Geophysical Prospecting 27, 749-760.

Rosengren N. 1994. Eruption Points of the Newer Volcanics Province of Victoria: An Inventory and Evaluation of Scientific Significance. National Trust of Australia (Victoria) and the Geological Society of Australia (Victoria Division), Melbourne.

Ross P.-S., Delpit S., Haller M. J., Nemeth K. & Corbella H. 2011. Influence of the substrate on maar-diatreme volcanoes; an example of a mixed setting from the Pali Aike volcanic field, Argentina. Journal of Volcanology and Geothermal Research 201, 253-271.

Ross P.-S. & White J. D. L. 2006. Debris jets in continental phreatomagmatic volcanoes; a field study of their subterranean deposits in the Coombs Hills vent complex, Antarctica. Journal of Volcanology and Geothermal Research 149, 62-84.

Ross P. S., White J. D. L., Valentine G. A., Taddeucci J., Sonder I. & Andrews R. G. 2013. Experimental birth of a maar–diatreme volcano. Journal of Volcanology and Geothermal Research 260, 1-12.

Rout D. J., Cassidy J., Locke C. A. & Smith I. E. M. 1993. Geophysical evidence for temporal and structural relationships within the monogenetic basalt volcanoes of the Auckland volcanic field, northern New Zealand. Journal of Volcanology and Geothermal Research 57, 71-83.

Schulz R., Buness H., Gabriel G., Pucher R., Rolf C., Wiederhold H. & Wonik T. 2005. Detailed investigation of preserved maar structures by combined geophysical surveys. Bulletin of Volcanology 68, 95-106.

Shaw-Stuart A. 2005. Transition from phreatomagmatic maar forming explosive activity to magmatic scoria cone complex forming activity in the Pleistocene Mt Leura Volcanic Complex, southeastern Australia. Masters thesis, Monash University, Australia (unpubl.).

Sheard M. J. 1990. A guide to Quaternary volcanoes in the lower south-east of South Australia. Mines and Energy Review - South Australia 157, 40-50.

Skacelova Z., Rapprich V., Valenta J., Hartvich F., Sramek J., Radon M., Gazdova R., Novakova L., Kolinsky P. & Pecskay Z. 2010. Geophysical research on structure of partly eroded maar volcanoes; Miocene Hnojnice and Oligocene Rychnov volcanoes (northern Czech Republic). Journal of Geosciences 55, 333-345.

Sohn Y. K. & Park K. H. 2005. Composite tuff ring/cone complexes in Jeju Island, Korea: possible consequences of substrate collapse and vent migration. Journal of Volcanology and Geothermal Research 141, 157-175.

Talwani M. & Heirtzler J. 1964. Computation of magnetic anomalies caused by two-dimensional bodies of arbitrary shape. In: GA P. ed. Computers in the mineral industries, pp. 464-480. Stanford Univ Publ Geological Sciences, Palo Alto, California.

Talwani M., Worzel J. L. & Landisman M. 1959. Rapid gravity computations for two-dimensional bodies with application to the Mendocino submarine fracture zone. Journal of Geophysical Research 64, 49-59.

Tickell S. J., Cummings S., Leonard I. G. & Withers J. A. 1991. Colac 1:50 000 map geological report. Geological Survey of Victoria Report 89.

Valentine G. A. & White J. D. L. 2012. Revised conceptual model for maar-diatremes: Subsurface processes, energetics, and eruptive products. Geology 40, 1111-1114.

van Otterloo J., Cas R. A. & Sheard M. J. 2013. Eruption processes and deposit characteristics at the monogenetic Mt. Gambier Volcanic Complex, SE Australia: implications for alternating magmatic and phreatomagmatic activity. Bulletin of Volcanology 75, 1-21.

van Otterloo J. & Cas R. F. 2013. Reconstructing the eruption magnitude and energy budgets for the pre-historic eruption of the monogenetic ~5 ka Mt. Gambier Volcanic Complex, south-eastern Australia. Bulletin of Volcanology 75, 1-18.

Walker G. 1973. Explosive volcanic eruptions — a new classification scheme. Geologische Rundschau 62, 431-446.

White J. D. L. 1991. Maar-diatreme phreatomagmatism at Hopi Buttes, Navajo Nation (Arizona), USA. Bulletin of Volcanology 53, 239-258.

White J. D. L. & McClintock M. K. 2001. Immense vent complex marks flood-basalt eruption in a wet, failed rift: Coombs Hills, Antarctica. Geology 29, 935-938.

White J. D. L. & Ross P. S. 2011. Maar-diatreme volcanoes: A review. Journal of Volcanology and Geothermal Research 201, 1-29.

Won I. & Bevis M. 1987. Computing the gravitational and magnetic anomalies due to a polygon: Algorithms and Fortran subroutines. Geophysics 52, 232-238.

Chapter 4.

Calculating the erupted volumes of tephra from maar volcanoes and their VEI magnitude: Examples from the late Cenozoic Newer Volcanics Province, south-eastern Australia

T. N. Blaikie, J. Van Otterloo, R. A. F. Cas, L. Ailleres, P. G. Betts

School of Earth, Atmosphere and Environment, Monash University, Clayton, Victoria, Australia

Cover page: The Lake Werowrap maar, Red Rock Volcanic Complex.

Monash University

Declaration for Thesis Chapter 4

Declaration by candidate

In the case of Chapter 4, the nature and extent of my contribution to the work was the following:

Nature of contribution	Extent of contribution (%)
Modelling, volume calculations, compilation of componentry data, preparation of the manuscript	87.5 %

The following co-authors contributed to the work. If co-authors are students at Monash University, the extent of their contribution in percentage terms must be stated:

Name	Nature of contribution	Extent of contribution (%) for student co-authors only
J. van Otterloo	Editing of manuscript, advisory role on calculation techniques	5
R. A. F. Cas	Supervisory role	2.5
L. Ailleres	Supervisory role	2.5
P. G. Betts	Supervisory role	2.5

The undersigned hereby certify that the above declaration correctly reflects the nature and extent of the candidate's and co-authors' contributions to this work*.

Candidate's Signature **Date**

Main Supervisor's Signature **Date**

*Note: Where the responsible author is not the candidate's main supervisor, the main supervisor should consult with the responsible author to agree on the respective contributions of the authors.

Abstract

Monogenetic volcanoes can exhibit complex eruptive histories with transitions from effusive and explosive behaviour. For maar volcanoes, calculations of magma volumes have often been hindered by the uncertainty of the volumes of maar-diatremes. We calculate the eruptive volumes of several complex monogenetic volcanic centres within the Newer Volcanics Province of south-eastern Australia including Ecklin maar, and the Red Rock and Mount Leura volcanic complexes. We use existing geophysical models to constrain the volumes of subsurface diatremes and conduits, and calculate the volume of the ejecta rims based on digital elevation models and drill hole data. Based on an average componentry of the ejecta-rim, we estimate a dense rock equivalent magma volume of 0.04 x 10^9 m^3, 0.17 x 10^9 m^3 and 0.29 x 10^9 m^3 for Ecklin maar, the Red Rock and Mount Leura volcanic complexes respectively. The Red Rock and Mount Leura volcanic complexes have magma volumes that are an order of magnitude higher than Ecklin maar, and exhibit far more complex eruptive histories with multiple vents and transitions between explosive phreatomagmatic, magmatic explosive and effusive styles. Based on the total tephra volume comparisons of observed eruptions, we estimate a VEI of 2 for Ecklin, and 3 for Mount Leura and Red Rock.

Key words: maar, diatreme, bulk volume, magma volume, Newer Volcanics Province

1. Introduction

Common to monogenetic volcanic fields, maar volcanoes are the second most abundant terrestrial volcano (Wohletz and Heiken 1992). They form as rising magma interacts explosively with ground water, resulting in subsurface phreatomagmatic explosions that excavate a deep crater cut below the pre-eruptive surface and surrounded by an ejecta ring comprised of base surge and fall out deposits (Lorenz 1975, 1986; White and Ross 2011). A diatreme underlies the maar crater, which is a 'pipe-like' structure filled with a mixture of fragmented country rock and juvenile clasts, and intrusions. Ongoing phreatomagmatic explosions result in the fragmentation and mobilisation of country rock and juvenile material within the maar diatreme, which can extend in depth from several hundreds of metres to ~ 2 km (Lorenz 1975, 1986, 2003, 2007; White and Ross 2011).

Eruptions of maars and other monogenetic volcanoes involve low volumes of magma, with eruptive activity occurring in short episodes (days to years). Eruptions in monogenetic fields are typically spatially and temporally linked, and are related to stress conditions in the crust during the time of eruption (Connor *et al.* 1992; Cebriá *et al.* 2011; Kereszturi *et al.* 2013). Recent work has attempted to calculate the magma volume of these fields, which is crucial for understanding long-term magma flux, and predicting future eruptive potential. However, these volumes are often difficult to determine because rapid erosion and the long lifespan of these volcanic fields means the edifices are not always well-preserved (Kereszturi *et al.* 2013; van Otterloo and Cas 2013). Additionally, one of the major unknowns in these calculations is the volume of magma contained within a maar-diatreme and its deposits. Although the number of occurrences of maar eruptions within monogenetic fields can vary depending on climate (Németh 2010), and range between 0-10% in arid volcanic fields, 20-30% in wetter climates, and up to 70% in partially marine settings (Brown and Valentine 2013), maars represent the greatest volcanic hazard in a monogenetic field. It is therefore important to understand their formation, and potential eruption duration; this requires an accurate assessment of the magma volume involved in the eruption.

Recently, Kereszturi *et al.* (2013) and Lefebvre *et al.* (2013) have attempted to calculate the bulk diatreme and magma volumes based on (sometimes inferred) crater dimensions and partial exposures of the diatremes. Van Otterloo and Cas (2013) also used a similar approach to estimate the diatreme and total magma volume of the Mt Gambier Volcanic Complex in the Newer Volcanics Province, and used the results to calculate the energy budget of the eruption. The estimates for diatreme volume in each of these works assume the diatreme can be approximated as an inverted cone. However, Blaikie *et al.* (2014a) demonstrates that the geometry of some maar-diatremes can be complex and can deviate from the simple 'inverted cone' structure assumed in the calculations by Kereszturi *et al.* (2013), Lefebvre *et al.* (2013) and van Otterloo and Cas (2013).

In order to understand the magma volumes associated with maar eruptions, it is important to first understand the depth and geometry of the maar diatremes and their internal structures. However, it is not always possible to examine the subsurface of an individual volcanic centre. Additionally, in most cases when it is possible, the ejecta rim and its relationship with subsurface deposits cannot be examined (Blaikie *et al.* 2012; Valentine 2012). Currently, the only known example of a maar–diatreme, where all structural levels are exposed, is the Suoana Crater of the Miyakejima volcano in Japan (Geshi *et al.* 2011). Only a partial understanding of an eruptive centre can be gained when only part of the system is examined, but when the subsurface structures are not exposed, geophysical methods can be employed to constrain the geometry of underlying structures. Once the geometry is constrained and the eruption history is reconstructed, an estimate of the diatreme and magma volume can be made. Although there is still some uncertainty relating to geophysical interpretations, the resultant models provide greater constraints on the geometry of the subsurface structures. This provides, and can lead to, more accurate estimates of the volumes of magma associated with these eruptions than inferring a particular geometry based upon a favoured model.

In this paper, we calculate the bulk volumes of the diatreme and ejecta ring of several maars located within the Newer Volcanics Province of south-eastern Australia based on the models of the maar-diatremes determined through the joint gravity and magnetic modelling of Blaikie *et al.* (2014a; 2014a). Using the componentry of the ejecta ring as a proxy for the componentry of the diatreme, the total magma volumes used in the eruptions are estimated. We also compare our bulk diatreme volumes to results obtained using the model proposed by Kereszturi *et al.* (2013) to evaluate the reliability of this technique when geophysical modelling is not possible.

2. Regional Geology

The Late Cenozoic (~4.6 Ma – 5ka) Newer Volcanics Province located in south-eastern Australia, extends ~400 km west from the city of Melbourne encompassing an area of ~23,000 km^2 (Hare and Cas 2005; Cas *et al.* 2011). It is an intraplate, basaltic volcanic province composed of approximately 416 volcanic centres that produced extensive lava flows, scoria cones, shields, maars, tuff rings, tuff cones and composite volcanic centres (Joyce 1975; Price *et al.* 1997; Price *et al.* 2003; Cas *et al.* 2011; Boyce 2013). Forming the basement to the Newer Volcanics Province, are the sedimentary successions of the Cretaceous-Tertiary Otway Basin in the south, and the Palaeozoic metasediments and granites of the Lachlan and Delamarian fold belts in the north.

Three sub-provinces are recognised within the Newer Volcanics Province, which were defined due to differences in morphology and geochemistry (Nicholls and Joyce 1989; Cas *et al.* 1993). These include the Central Highlands sub-province, comprised mainly of scoria cones, lava shields and extensive lava flows; the Western Plains sub-province consisting of lava plains, scoria cones, shields and maar volcanoes; and the Mt Gambier sub-province which lies in the west of the Newer Volcanics Province, and consists mainly of tuff rings, maars and scoria cones, including Australia's youngest volcano, the ~5ka Mt Gambier Volcanic Complex (van Otterloo and Cas 2013).

Approximately 40 maar volcanoes (~10 % of the entire field) have been identified within the Newer Volcanics Province, and are mostly restricted to the south of the province where aquifers within the Otway Basin have provided the water to fuel phreatomagmatism (Joyce 1975; Cas *et al.* 2011; Blaikie *et al.* 2012).

Recent work in the Newer Volcanics Province focussed on understanding the complex eruptive histories of very large maar volcanoes (Jordan *et al.* 2013; van Otterloo *et al.* 2013; van Otterloo and Cas 2013), that often exhibit multiple phases of eruptive activity that varies from phreatomagmatic to explosive and effusive magmatic activity. Gravity and magnetic modelling was applied to understand the subsurface morphology of some of these maar volcanoes, and infer processes occurring in the subsurface (Blaikie *et al.* 2012, 2014a). In addition there has been a focus in recent years to accurately define the number of eruption points (Boyce 2013), and the extent and volume of volcanic products associated with large maars (van Otterloo and Cas 2013), and the entire Newer Volcanics Province (van den Hove, in prep). However, there is always a large uncertainty in calculating the volume of subsurface volcanic structures, such as maar-diatremes, which at least in the Newer Volcanics Province comprise approximately 10% of the total number of volcanic centres.

2.1 Diatreme geometries and eruptive histories

Three volcanic centres were selected for this study: Ecklin maar, and the Red Rock and Mt Leura volcanic complexes. The selected case studies represent a good range of crater sizes and eruptive histories of maar volcanoes within the Newer Volcanics Province and are hosted within the southern part of the Western Plains sub-province, which overlies the sediments of the Otway Basin. The host sediments are unconsolidated to weakly lithified, consisting of marls, limestones and sandstones, which likely influenced the geometry of the maar-diatremes at each volcanic centre (Blaikie *et al.* 2012, 2014a).

These volcanoes have previously been the subject of geophysical investigations into the geometry of the underlying maar-diatreme and results from these studies are presented from a methodological point of view in Blaikie *et al.* (2014b) and from a volcanological point of view in Blaikie *et al.* (2012, 2014). Some statistical data reporting the bulk volumes of the maar diatremes was presented by (Blaikie *et al.* 2014a, b), but calculating the volumes of the ejecta rings and total magma volume was beyond the scope of those papers and is addressed here. Descriptions of the eruptive histories, and geometry of subsurface structures for these case studies are briefly summarised below; more detail is available in Blaikie *et al.* (2012, 2014a, b)

The Red Rock Volcanic Complex (Figure 1a) is one of the most complex volcanic centres within the Newer Volcanics Province, with the highest number of vents of any volcanic centre in the region. It is a complex volcano composed of multiple, poly-lobate maar craters and scoria cones. Studies of the deposits surrounding the maar craters suggest a complex eruptive history that involved frequent fluctuations between explosive magmatic and phreatomagmatic fragmentation (Cas *et al.* 2011; Blaikie *et al.* 2012). Geophysical modelling of the maar volcanoes within Red Rock suggests complex diatreme structures. Diatremes are typically broad and shallow, and formed from the coalescence of multiple vents (Figure 1d; Blaikie *et al.* 2014b). Dykes or plug-like structures were identified in the three largest maars within the complex and are consistent with the interpretation of fluctuating eruptive styles.

The Ecklin maar has a relatively simple surface morphology, consisting of a single elliptical crater (Figure 1b). However, geophysical results indicate a more complex subsurface structure comprised of two coalesced diatremes that contain central vents with higher proportions of juvenile material (Figure 1e). These structures were interpreted by Blaikie *et al.* (2014a) to have been partly filled in by the deposits of debris jets that were entrained into the diatreme fill during the eruption (cf. Ross and White 2006).

The Mt Leura Volcanic Complex is a composite volcanic centre that erupted during two phases: an early phreatomagmatic eruptive phase that formed a coalesced maar and a tuff ring, and a later effusive and explosive magmatic phase. The latter filled in the two coalesced craters with lava and formed a scoria and spatter cone complex comprising at least 16 separate vents (Figure 1c). Geophysical modelling of this volcanic centre was able to constrain the depth as well as the extent of lava flows contained within the craters, and determine the depth and geometry of the diatremes (Figure 1f).

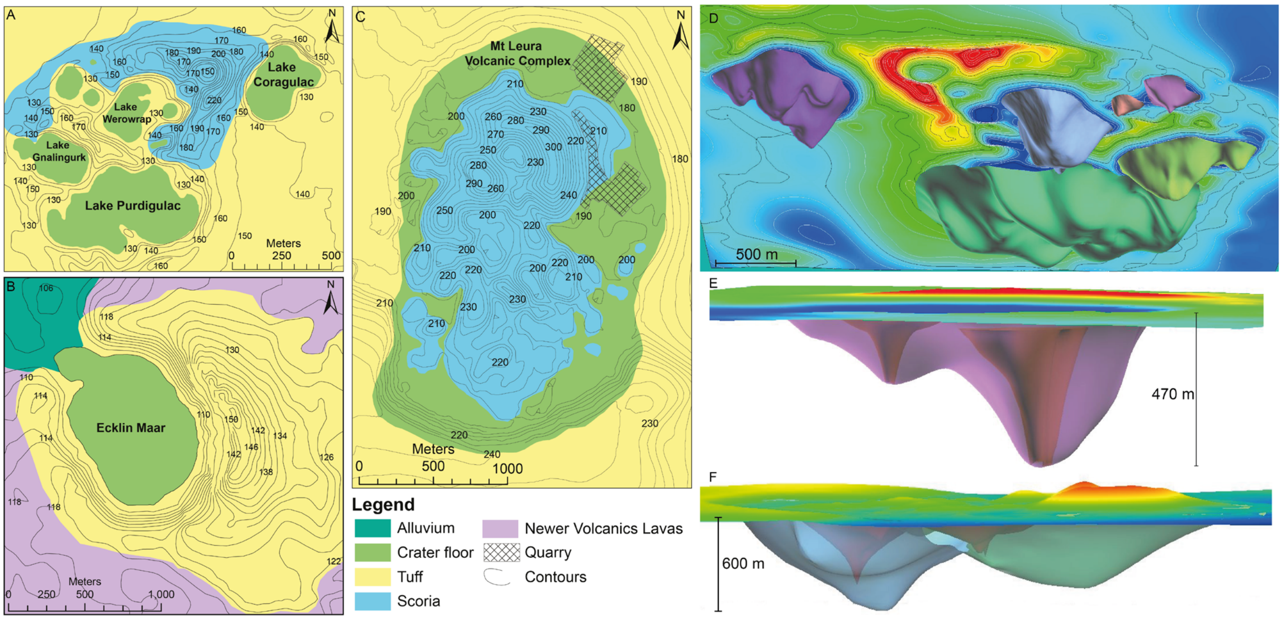

Figure 1. Surface geologic maps of a) Red Rock, b) Ecklin, c) Mount Leura; and 3D models of d) Red Rock, e) Ecklin, f) Mount Leura showing coalesced maar-diatremes.

3. Method

Calculating the volumes of magma involved in the eruption of monogenetic volcanoes can be complex, especially when a volcanic centre exhibits more than one eruptive style. To simplify the process, we split the calculations into several components; subsurface structures and surface deposits, which are further divided into their phreatomagmatic and magmatic components where possible. Magma volume calculations are constrained by the componentry of the ejecta rims, and geophysical models produced by Blaikie *et al.* (2014a, b).

3.1 Bulk and magma volume of subsurface structures

The bulk diatreme, and total magma volumes of maar diatremes are largely unknown due to their subsurface nature, but attempts have been made to estimate the volume of these components (e.g., Kereszturi *et al.* 2013; Lefebvre *et al.* 2013; van Otterloo and Cas 2013). However, these studies rely on an inverted cone model for the diatreme, and it has been demonstrated that the structure of a diatreme can be more complex (Blaikie *et al.* 2014a). It is therefore important to have some constraint on the geometries of the diatremes under investigation in order to obtain reliable volume estimates.

The geometry of the diatremes, for each of the case studies described above, was previously determined by Blaikie *et al.* (2012, 2014a, b) through two and a half-dimensional forward and three-dimensional inverse modelling of gravity and magnetic data. The inversion process required the discretisation of the three-dimensional surface model into prisms of a given dimension (usually 20 x 20 x 10 m in the *x*, *y* and *z* direction respectively). The volumes of the different regions within the models were calculated by multiplying the number of prisms within a region by their volume. The calculated volumes represent the bulk volumes of various structures within the subsurface; further calculation is required to obtain the total magma and country rock volumes. As a comparison, we calculate the bulk volume of the diatremes for each case study using the method of Kereszturi *et al.* (2013).

For these calculations, we assume that the componentry of the diatreme is similar to that observed in the maar's ejecta rim. In order to calculate the dense rock equivalent (DRE) volume of magma, the vesicularity of juvenile clasts and the porosity of the deposits within the diatreme must also be considered, and is also based upon observations of juvenile clasts and deposits within the ejecta rim and cone complexes from previous studies (e.g., Shaw-Stuart 2005; Cheesman 2007; Piganis 2011). The equations used to calculate bulk and DRE volumes are summarised in figure 2.

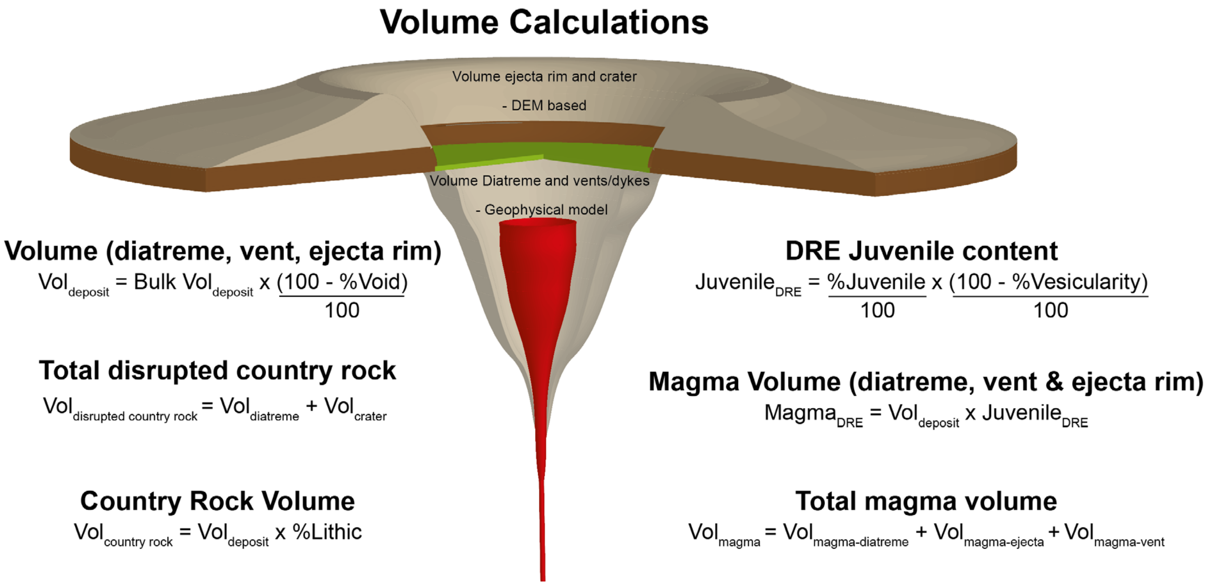

Figure 2. Summary of equations applied to each component of the maar-diatreme.

3.2 Volume of ejecta ring

The volume of the ejecta rings for these case studies was not calculated by Blaikie et al. (2014a, b) in order to reduce the model size and computing time required for inversion. Additionally, the resolution of the model used for inversion (20 x 20 x 10 m prisms), was too coarse to accurately calculate the volume of surface deposits because, in places, the deposits are thinner than the vertical resolution of the prisms. For this study, the volume of the ejecta ring was calculated by first defining the extent and thickness of the deposits, which required a digital elevation model (DEM) of the current and pre-eruptive topography.

The DEMs of the current topography (Figure 3a) were defined from 5 m Lidar data (Light Detection and Ranging; courtesy of the Corangamite catchment management authority) which was available for the Red Rock and Mount Leura volcanic complexes, and should be more than sufficient to accurately calculate volume. No Lidar data was available at Ecklin, so the DEM was derived from a combination of 90 m SRTM and differential GPS data acquired for the gravity survey conducted by Blaikie *et al.* (2014b).

The pre-eruptive surface was constrained largely by groundwater boreholes in the vicinity of each volcanic centre and interpolated between these points (data freely accessible from GeoVic; www.energyandresources.vic.gov.au/earth-resources). Lithological and location information for these boreholes is not always well defined, so there is some ambiguity regarding the pre-eruptive surface.

However, this region of the Newer Volcanics Province is marked by a relatively flat topography, so a flat-lying surface correlating with the depth of available and reliable boreholes should be sufficient to calculate deposit volume.

The same approach used for calculating the volume of the subsurface structures can be applied to the surface deposits (cf. van Otterloo and Cas 2013); however, the accurate calculation of deposit volume requires a higher resolution model (e.g., 1 x 1 x 1 m prisms as applied by van Otterloo and Cas (2013)) than what was used for the subsurface. The computation of this model can take several hours, and produces extremely large file sizes which are difficult to work with, even using computers with fast processors.

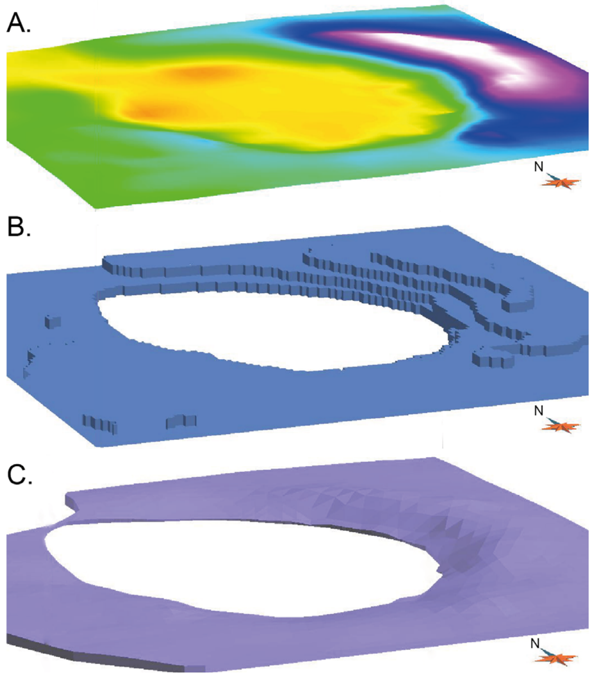

Figure 3. Examples of the different models which can be used to calculate volume. a) digital elevation model, b) rectangular prism model, c) solid model with triangular mesh.

We calculated the deposit volume using a slightly different approach where the extent and thickness of the deposits (calculated by subtracting the elevation of the pre-eruptive surface from the digital elevation), were defined by a 'solid' within Gocad. Aside from decreased computational time, the advantage of this process is it uses a triangular mesh, rather than rectangular prisms (Figure 3b), so can more accurately represent and account for slope information (Figure 3c).

Where there were multiple eruptive phases (e.g., Red Rock and Mount Leura), the deposits were split into a magmatic and phreatomagmatic component. In the case of Red Rock, where there are 7 maars containing at least 20 vents, it is difficult to separate the deposits derived from individual craters. The deposit volume was therefore calculated for the entire complex, and the diatreme volumes were summed prior to calculating the magma volume. This of course leads to the assumption that the componentry of the individual diatremes are similar.

Calculating the volume of deposits at Red Rock and Ecklin is relatively simple as the extent of deposits, and overprinting relationships with nearby volcanoes are fairly well defined. However, the southern ejecta ring of Mount Leura overprints the ejecta rings from several large maars (diameter of ~ 2 km), and based on magnetic anomalies, probably a buried scoria cone or lava shield. With relatively little exposure, it is difficult to separate deposits derived from Mount Leura and those from other centres. For these calculations we neglect the volume of the ejecta rim because we cannot confidently define the extent and thickness of deposits derived from the Mount Leura Volcanic Complex. Instead we focus on magma volume estimates for the cone complex, lava flows and the diatreme.

Once the deposit volume is determined, the magma volume can be estimated based upon the componentry of the deposits. Previous studies have examined the deposits of each of the volcanic centres in detail, and have used point counting and visual estimates to determine the juvenile content throughout the stratigraphy (Shaw-Stuart 2005; Piganis 2011). For these calculations, we use the average juvenile content and vesicularity (Table 1) to estimate the dense rock equivalent magma volume for each case study.

Table 1. Componentry and vesicularity of pyroclastic deposits

Volcanic centre	Lithic content	Juvenile content	Vesicularity	Porosity/Void space
		Phreatomagmatic deposits		
Red Rock	55 %	45 %	20 %	1 %
Ecklin	75 %	25 %	15 %	1 %
Mount Leura	60 %	40 %	20 %	1 %
		Magmatic deposits		
Red Rock	1	99 %	64%	60 %
Mount Leura – Scoria	1	99 %	60%	60 %
Mount Leura – Lava	0	100 %	10 %	0 %

4. Results and Discussion

4.1 Magma Volumes

The magma volumes for the Red Rock, Mount Leura and Ecklin volcanoes were calculated using the method described above using the componentry listed in table 1. The results are discussed below and summarised in figure 4. All volumes calculated represent minimum volumes that do not take account of the distal ash dispersed by base surges and wind beyond the visible limits of the maar tephra ring, and the volume of material contained within any dyke and sill complex beneath the maar-diatreme.

The Red Rock Volcanic Complex has a total deposit volume of 0.10×10^9 m^3, of which the phreatomagmatic and magmatic components make up 0.065×10^9 m^3 and 0.037×10^9 m^3 respectively. Based on the componentry and void spaces listed in table 1, the dense rock equivalent volume of erupted magma contained within the phreatomagmatic and magmatic deposits is approximately 0.023×10^9 and 0.005×10^9 m^3 respectively. This gives a total dense rock equivalent erupted magma volume of 0.029×10^9 m^3.

The diatremes of Red Rock have a combined volume of 0.38×10^9 (excluding intra-diatreme dykes and magma ponds which have a volume of 0.022×10^9 m^3). Assuming a similar composition and vesicularity to the surface pyroclastic deposits, and including the volume of intra-diatreme dykes, the total subsurface magma volume of the complex is 0.15×10^9 m^3. This yields a total dense rock equivalent magma volume for the complex of 0.18×10^9 m^3, although this is a conservative estimate since our calculations neglect the subsurface structures associated with the cone complex. In addition, any dykes and sills underlying the diatremes are not included because these structures were beyond the resolution of the geophysical models produced by Blaikie *et al.* (2014a).

The calculated volume of country rock within the ejecta rims is 0.04×10^9 m^3, which is equivalent to the combined volumes of the craters (from pre-eruptive surface to crater floors). The volume of country rock might be expected to be higher, considering geophysical modelling indicated there were substantial diatremes beneath the maar craters, and the total volume of disturbed country rock is 0.42×10^9 m^3. However, given that there are at least 40 separate vents within close proximity, much of the deposits from individual vents would have been destroyed when a new vent formed, and the material either lost to the eruption column, recycled within the developing diatremes or re-deposited proximal to the new vent. These calculations also do not consider the volume of deposits lost to erosion, or deposited distally to the complex.

Ecklin maar has a total deposit volume of 0.056 x 10^9 m^3, and a bulk diatreme volume of 0.13 x 10^9 m^3, of which 0.012 x 10^9 m^3 is contained with two vents with a higher juvenile content. Assuming an average juvenile content of 25 % and a vesicularity of 15 % within the juvenile pyroclasts in both the diatreme and the ejecta rim, and a juvenile clast content of 60% within the two vents, the subsurface and erupted DRE magma volume is 0.031 x 10^9 m^3 and 0.012 x 10^9 m^3 respectively, which gives a total DRE volume of magma for the eruption of approximately 0.043 x 10^9 m^3. The total country rock volume in the diatreme and the deposits of the Ecklin maar is 0.13 x 10^9 m^3, which is equivalent to the total volume of country rock disrupted during the eruption. It might be expected that there is a greater discrepancy between the calculated lithic volume, and the disrupted country rock when erosion, and material lost in the eruption column are considered. This could suggest that either the volume of the diatreme was under-estimated, or the volume of the ejecta rim over-estimated.

The diatremes of the Mount Leura Volcanic Complex have a combined bulk volume of 0.58 x 10^9 m^3, excluding the volume of intra-diatreme dykes, magma ponds and lava flows which have a volume of 0.095 x 10^9 m^3. Assuming the componentry of the diatremes are similar to the ejecta rim (juvenile content of 40 %, vesicularity of 20%; Shaw-Stuart 2005), the DRE magma volume is 0.18 x 10^9 m^3. Combined with the volume of intra-diatreme dykes and lava flows, the total subsurface magma volume is 0.28 x 10^9 m^3 DRE. The volume of the cone complex is estimated at 0.07 x 10^9 m^3, which based on a total vesicularity and void space of 60% and 40 % respectively (Shaw-Stuart 2005), yields a DRE volume of 0.011 x 10^9 m^3. The total magma volume of the complex (excluding the ejecta-rim) is therefore 0.29 x 10^9 m^3.

4.2 Comparison with other techniques for volume estimation

The results of our volume calculations are compared to results obtained using the method of Kereszturi *et al.* (2013) to assess their approach as an alternative when geophysical modelling is not possible (table 2). We calculate the bulk diatreme volume as a comparison, but do not attempt to compare magma volumes derived using this technique. Comparing such results would be unrealistic because our geophysical models allow an estimate of the volume of intrusions and vents contained within the diatremes, whereas the method of Kereszturi *et al.* (2013) was proposed to estimate volumes in the absence of such information.

The calculations of Kereszturi *et al.* (2013) are based on an inverted cone model, and therefore assume the crater is circular, and if not, recommend taking the minimum crater radius to avoid over estimating volume due to the erosional retreat of the crater rim. Since some of our case studies are very irregular in shape (Figure 1), we calculated the volume based on both the radii of the maar craters' short and long axes. To ensure a fair comparison, the depth of the diatreme remains equal to the maximum depth observed the geophysical models, which required that we vary the wall-rock angle in each calculation, rather than calculating a range of volumes for set wall-rock angles as suggested by Kereszturi *et al.* (2013).

Compared to volumes based on our geophysical models, the results suggest that estimates based on the minimum radius largely underestimate the volume of the diatreme (table 2). Values obtained for the

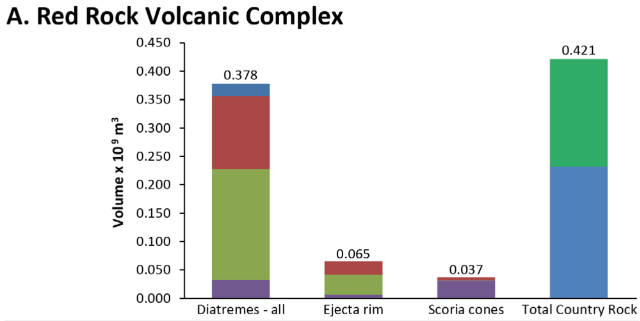

	Diatremes - all	Ejecta rim	Scoria cones	Total Country Rock
Magma - dykes and lavas	0.022	0.000	0.000	
Magma (DRE)	0.128	0.023	0.005	
Country rock	0.196	0.036	0.000	
Inter-particle void/vesicles	0.032	0.006	0.031	
Unaccounted country rock				0.189
Accounted country rock				0.232

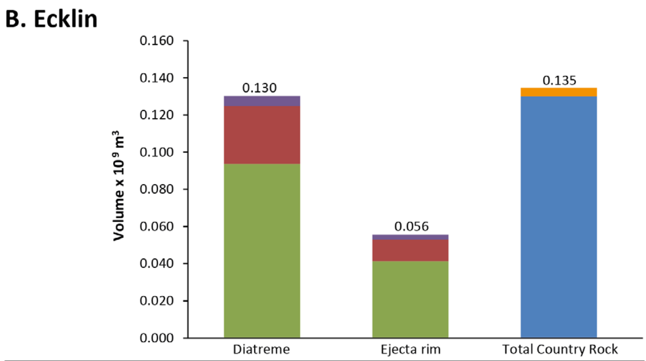

	Diatreme	Ejecta rim	Total Country Rock
Magma (DRE)	0.031	0.012	
Country rock	0.093	0.041	
Inter-particle void/vesicles	0.006	0.003	
Accounted country rock			0.130
Over-accounted country rock			0.005

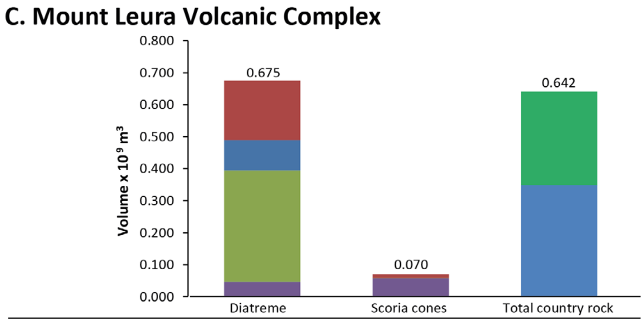

	Diatreme	Scoria cones	Total country rock
Magma (DRE)	0.186	0.011	
Magma - dykes and lavas	0.095	0.000	
Country rock	0.348	0.001	
Inter-particle void/vesicles	0.046	0.058	
Unaccounted country rock			0.293
Accounted country rock			0.349

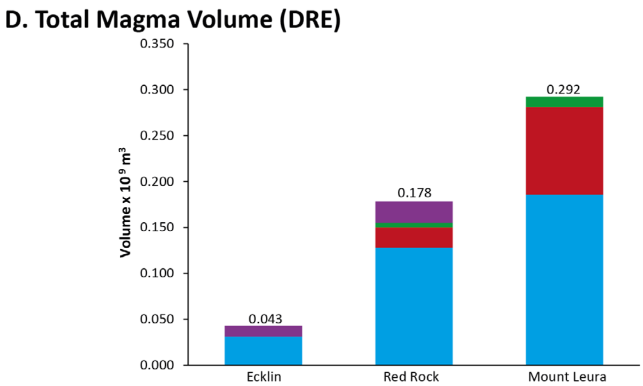

	Ecklin	Red Rock	Mount Leura
Ejecta rim	0.012	0.023	
Cones		0.005	0.011
Dykes and Lavas		0.022	0.095
Diatreme	0.031	0.128	0.186

Figure 4. Summary of diatreme, deposit and magma volumes for a) the Red Rock Volcanic Complex, b) Ecklin maar, and c) Mount Leura Volcanic Complex, and d) the total magma volume for each volcanic centre.

western-most and central maar in the Red Rock Volcanic Complex, and Ecklin maar are the closest to the observed value, accounting for 79, 65, and 75 % of the observed volumes respectively. All the other case studies accounted for less than 50 % of the observed volume, with the worst result observed for the Lake Purdigulac maar (Red Rock) with the minimum crater radius accounting for only 7 % of the observed volume; however this is not surprising since Lake Purdigulac is highly irregular in its shape.

Results obtained based on the maximum crater radius over-estimated the volumes of all the maars, excluding Lake Purdigulac, where results were within 4 % of the observed value. Results from the Ecklin maar, and the central maar from the Red Rock Volcanic Complex were closest to the observed value and only over-estimated the volume by approximately 20 %, while all the other maars overestimated the volume by 35-76 %.

The most consistent results for both the maximum and minimum volume estimates were obtained in situations where the crater morphology is relatively simple. Greater variation from the observed value is seen when the geometry of the crater becomes more complex. However, in these situations, averaging the maximum and minimum volume showed the results fall largely within a range of 15% from the observed value. This analysis suggests that the method of Kereszturi *et al.* (2013) may be useful to estimate bulk diatreme volumes where the geometry of the crater is relatively simple, however it is useful to have some initial constraint on the depth of the diatreme (e.g., from wall rock lithics). Results are less reliable in more complex situations, and averaging the range of results may produce a more reliable estimate.

Table 2. Results of bulk diatreme volume estimates using the method of Kereszturi *et al.* (2013). All estimates include the volume of post-eruptive crater infill except the observed value for Mt Leura which includes the volume of infilling lavas.

	Crater width		Depth	Volume	Wall rock angle		Volume	
	Short-axis (m)	Long-axis (m)	(m)	(x 10^9 m^3)	Minimum (°)	Maximum (°)	Minimum (x 10^9 m^3)	Maximum (x 10^9 m^3)
				Ecklin Maar				
Ecklin Maar	800	1000	630	0.13	59.57	53.28	0.0973	0.156
				Mount Leura Volcanic Complex				
Mt Leura	1500	2700	515	0.675*	39.39	22.39	0.305	1.08
				Red Rock Volcanic Complex				
Werowrap	370	720	320	0.03	64.16	44.12	0.0094	0.0421
West maar	260	365	140	0.0028	51.84	40.66	0.0022	0.00484
Central maar	160	200	95	0.00077	57.07	49.90	0.0005	0.000892
Purdigulac	450	1500	360	0.23	29.66	26.57	0.017	0.22
Coragulac	400	750	290	0.031	59.62	40.05	0.010	0.042
Gnalinegurk	400	750	300	0.025	30.96	41.01	0.011	0.044

4.3 Limitations of volume models

There are a number of uncertainties when calculating the deposit and magma volumes associated with each of these volcanic centres; therefore, the estimates are conservative. For these calculations we present diatreme volumes calculated based on the 'best-fit' geophysical models produced by Blaikie *et. al.*, (2012, 2014a, b), but we also acknowledge that these models are ambiguous, and there is a range of geophysically possible alternative models. Blaikie *et al.* (2014b) constrained the models with geological data, and undertook sensitivity analyses to demonstrate why these models are realistic, and are the best possible models based upon the data available. Questions still remain regarding the exact componentry of the diatreme for each method, but the composition of the ejecta rim offers a good proxy for that of the diatreme when drilling is not possible.

In spite of the ambiguities, volume calculations based upon geophysical models can offer more reliable results than the method suggested by Kereszturi *et al.* (2013) because it does not over-simplify the geometry of underlying structures, and can account for the volume intra-diatreme dykes, magma ponds and heterogeneities within the diatreme. Comparison of our volume calculations, and results obtained using the equations of Kereszturi *et al.* (2013) suggest that when geophysical modelling is not possible, this is a good alternative for estimating bulk diatreme and magma volumes provided that the crater morphology is relatively simple and there are some initial constraints on the depth of the diatreme. Results obtained using this technique on larger, complex maars with irregular crater geometries are less reliable, and caution should be taken if this technique is to be applied in these situations. However, in the absence of any information on the depth of the diatreme, this approach will always produce uncertain results, so in keeping with the conclusions of Kereszturi *et al.* (2013), a conservative approach to volume estimate is always advised.

For these case studies, we only consider the volume of proximal deposits, and do not account for the volume of deposits lost due to erosion or distal transport of material in the eruption column. This is because it is difficult to determine the origin of preserved distal deposits because of so many closely-spaced volcanic centres in the Newer Volcanics Province. The volume of ash produced by a scoria cone for example, can be up to 8 times the volume of the cone in violent strombolian and micro-plinian eruptions (Guilbaud *et al.* 2012), so our volume estimates are therefore conservative, and represent minimum values for these eruptive centres.

4.4 Comparisons with other volcanic centres

There is relatively little information on bulk diatreme volumes, and total magma volumes associated with the eruption of maar volcanoes. This is likely due to the uncertainty of the geometry of subsurface structures, the volume of magma contained within them, and relatively few historical eruptions. Volcanic fields also have a long lifetime, and individual volcanoes can be eroded rapidly, making it difficult to obtain accurate volume estimates of the edifice (Kereszturi *et al.* 2013).

Bulk volume estimates for the different components of maar volcanoes typically range between 10^6 and 10^8 m^3 for the diatreme (Brown and Valentine 2013), and up to 10^8 m^3 for the edifice (Sottili *et al.* 2012; Valentine and White 2012; Lefebvre *et al.* 2013). Reported magma volumes for maar volcanoes are limited and have been inferred based upon the observed volume of intrusions within maar-diatremes, ranging between 10^2 and 10^6 m^3 (Valentine *et al.* 2014), or calculated from partial diatreme exposures (e.g., a magma volume of the 72 x 10^5 m^3 for the Standing Rocks West maar-diatreme in the Hopi Buttes Volcanic Field, Arizona, USA was estimated by Lefebvre *et al.* (2013)).

The bulk diatreme and ejecta rim volumes of our case studies are consistent with these ranges, and magma volumes are consistent with estimates for Ecklin maar. However; our calculations show that eruption of Red Rock and Mount Leura involved larger magma volumes, in the order of 10^8 m^3. In these cases however, the eruption was comprised of multiple coalesced craters and also involved significant effusive/explosive magmatic components, and in the case of Red Rock, the eruption of two magma batches (Piganis 2011).

Similar magma volumes were also observed for the Mt Gambier Volcanic Complex where a minimum magma volume of 0.237 x 10^9 m^3 was calculated by van Otterloo and Cas (2013). Larger magma volumes are more likely to result in complex eruptions involving multiple phases of activity (i.e. phreatomagmatic followed by effusive and/or explosive magmatic activity; Kereszturi *et al.* (2013)), which was observed at each of these volcanic centres. Conversely, the eruption of the Ecklin maar involved a lower volume of magma (0.045 x 10^9 m^3), and was formed predominantly by phreatomagmatic activity.

4.5 Volcanic Explosivity Index

The size of these eruptions according to the Volcanic Explosivity Index (VEI; Newhall and Self 1982) can be determined from the calculated tephra volume and an estimate on the height of the eruption column based upon observations of eruptions producing similar deposit types. Modelling the height of the eruption column (e.g., using Tephra2 or similar codes; Bonadonna *et al.* 2005; Connor and Connor 2006) would be preferable, however many of the parameters required for these models cannot be met without further detailed analysis of the stratigraphy and distal ash dispersal of these volcanoes. Determination of these parameters is a very difficult process and beyond the scope of this work because there is no data on distal ash dispersal distances because of a lack of preserved distal deposits. Additionally, many other volcanic centres are located close to the volcanoes in this study, so it is a difficult task to determine the origin of any distal ash deposits that are preserved.

Ecklin maar falls into the category of a VEI of 2 based on a preserved tephra volume in the order of 10^7 m^3. Tephra within the ejecta rim is phreatomagmatic in origin, consisting of ballistic blocks ejected from the vent, and planar to cross-stratified fine to coarse ash deposited from both base-surge and fall-out processes (Blaikie *et al.* 2014a). Several examples of small volume basaltic eruptions that experienced phreatomagmatic activity, and their observed eruption column heights include Halemaumau crater (Kilauea); 2 km (1924), Ukinrek; 6 km (1977), and Taal; 15-20 km, (1965) (Moore *et al.* 1966; Kienle *et al.* 1980; White and Houghton 2000). It is unlikely the eruption of Ecklin was as large as Taal, but it is probably comparable to Ukinrek and Halemaumau crater, and could have produced an eruption column that ranged between the 1 – 5 km required for a classification of VEI 2 (Newhall and Self 1982).

Estimating the VEI of the Red Rock Volcanic Complex is more complex because it is comprised of multiple small maars and a scoria cone complex dispersed over > 40 vents. The eruption of individual maars, and the scoria cones likely did not produce tephra volumes that would exceed VEI 2. However, a total erupted tephra volume for the Red Rock Volcanic complex of 10^8 m^3 places it in the VEI 3 category. This raises the question, can an eruption of this type dispersed over > 40 vents sustain an eruption column of >3 km?

The individual maars at the Red Rock Volcanic Complex, formed from phreatomagmatic activity, but experienced frequent transitions to Strombolian activity. This produced a diverse range of deposits consisting of planar to cross stratified fine and coarse ash interbedded with thin beds of coarse, highly vesicular scoria (Blaikie *et al.* 2012). This is similar to observations of the eruption at Ukinrek (1977) where phreatomagmatic activity with some transitional Strombolian phases were also observed, producing two small maars with maximum diameters of 170 and 300 m (Self *et al.* 1980). These crater dimensions are comparable to diameters of individual vents within the maar craters at Red Rock. The eruption of the scoria cone complex produced deposits consisting of massive to diffusely stratified medium-coarse lapilli sized scoria deposits that are highly vesicular and dispersed over an area >500 m from the vent. Blaikie *et al.* (2012) suggested that the dispersal of these deposits away from the cone complex indicate that a sustained, low buoyant eruption column existed at the time of the eruption, the term microplinian (e.g., Francis *et al.* 1990) was applied to describe the eruption, although violent strombolian may be a more appropriate term. The eruption of the cone complex can be compared to Parícutin, where violent Strombolian activity produced eruption columns 2-6 km high (Pioli *et al.* 2008). Based on similarities in the vent size and eruption style between the maars of the Red Rock Volcanic Complex and Ukinrek, and the eruption style of the scoria cones with Parícutin, we can infer that the eruption column reached heights > 3 km during the eruption, and a VEI of 3 is appropriate.

The scoria cones contained within the Mt Leura Volcanic Complex produced a tephra volume in the order of 10^7 m^3, placing it in the VEI 2 category. However, because of the close proximity to other volcanic centres we neglected the volume of tephra in the ejecta rim because it could not be accurately calculated. If we consider the ejecta rim of the maar, and infer a volume that is similar or perhaps even slightly greater than Ecklin, or the larger maars at Red Rock, then the total tephra volume would be in the order of 10^8 m^3. Assuming that the phreatomagmatic and Strombolian activity was of a similar intensity to Red Rock, Mt Leura could have produce eruption columns > 3 km in height, which would place Mt Leura in the VEI 3 category.

Table 3. Summary of tephra volumes and VEI for each volcanic centre.

Volcano	Total erupted tephra x 10^9 m^3	DRE Erupted Tephra x 10^9 m^3	Total DRE Magma volume x 10^9 m^3	Erupted DRE magma volume x 10^9 m^3	VEI Index
Ecklin	0.056	0.05	0.043	0.012	2
Red Rock	0.10	0.06	0.17	0.029	3
Mt Leura	0.07 (cones only)	0.01	0.29	0.01	3

4.6 Implications for future eruptions

There has been an increased focus on understanding the complex monogenetic volcanic centres within the Newer Volcanics Province in recent years, especially focusing on those volcanoes that formed from prolonged phreatomagmatic activity, producing some of the largest maar volcanoes in the world (e.g., Cas *et al.* 2011; Blaikie *et al.* 2012; Jordan *et al.* 2013; van Otterloo *et al.* 2013). Although these kinds of eruptions may not cause widespread damage, they are capable of producing significant amounts of fine ash, to which the complex infrastructure of modern society is highly susceptible, as demonstrated by the 2010 eruption of Eyjafjallajokull, Iceland.

The sizes of these eruptions are comparable to 1977 eruption of the Ukinrek maars in Alaska, which produced eruption columns up to 6 km in height and deposited fine ash at least 160 km from the vent (Kienle *et al.* 1980). With winds predominantly coming from the west, a future phreatomagmatic eruption of a similar intensity in western Victoria, could significantly affect major cities such as Melbourne, Sydney, Canberra and perhaps even New Zealand by disrupting air travel to and from the region, and impacting upon the health of those living in the area. However, it is important to recognise that these are worst-case scenarios for the region, with only 10% of volcanoes within the province formed from prolonged phreatomagmatic activity, and research into individual eruptive centres biased towards the larger, more complex eruptions.

5. Conclusion

Understanding not only the subsurface geometry of maar-diatremes, but also the volume of magma is crucial when considering the volcanic hazards that may arise due to a future maar eruption in a populated area. Using geophysical models to constrain the geometry of the subsurface, we estimate that the total volume of magma involved in the eruption (surface and subsurface) ranges between 10^7-10^8 m^3, with an erupted magma volume in the range of 10^7 m^3. The total eruptive tephra volume ranges between 10^7-10^8 m^3, and based on this volume, we estimate a VEI of 2 for Ecklin, and a 3 for Mt Leura and Red Rock. Through this work, and other recent studies within the Newer Volcanics Province, we have the information to assess and understand the range of eruptive scenarios that might occur in a future eruption within the Newer Volcanics Province.

6. References

Blaikie T. N., Ailleres L., Betts P. G. & Cas R. A. F. 2014a. A geophysical comparison of the diatremes of simple and complex maar volcanoes, Newer Volcanics Province, south-eastern Australia. *Journal of Volcanology and Geothermal Research* **276**, 64-81.

Blaikie T. N., Ailleres L., Betts P. G. & Cas R. A. F. 2014b. Interpreting subsurface volcanic structures using geologically constrained 3-D gravity inversions: Examples of maar-diatremes, Newer Volcanics Province, southeastern Australia. *Journal of Geophysical Research-Solid Earth* **119**, 3857-3878.

Blaikie T. N., Ailleres L., Cas R. A. F. & Betts P. G. 2012. Three-dimensional potential field modelling of a multi-vent maar-diatreme - the Lake Coragulac maar, Newer Volcanics Province, south-eastern Australia. *Journal of Volcanology and Geothermal Research* **235-236**, 70-83.

Bonadonna C., Connor C. B., Houghton B. F., Connor L., Byrne M., Laing A. & Hincks T. K. 2005. Probabilistic modeling of tephra dispersal: Hazard assessment of a multiphase rhyolitic eruption at Tarawera, New Zealand. *Journal of Geophysical Research: Solid Earth* **110**, B03203.

Boyce J. 2013. The Newer Volcanics Province of southeastern Australia: a new classification scheme and distribution map for eruption centres. *Australian Journal of Earth Sciences* **60**, 449-462.

Brown R. J. & Valentine G. A. 2013. Physical characteristics of kimberlite and basaltic intraplate volcanism and implications of a biased kimberlite record. *Geological Society of America Bulletin* **125**, 1224-1238.

Cas R. A. F., Blaikie T., Boyce J., Hayman P., Jordan S., Piganis F., Prata G. & van Otterloo J. 2011. VF01: Factors that influence varying eruption styles (from magmatic to phreato-magmatic) in intraplate continental basaltic volcanic provinces: the Newer Volcanics Province of south-eastern Australia. *IUGG 2011 Fieldtrip guide*.

Cas R. A. F., Simpson C. & Sato H. 1993. *Newer Volcanics Province - processes and products of phreatomagmatic activity. IAVCEI Canberra 1993: excursion guide, September, 1993*. Record - Australian Geological Survey Organisation. Geoscience Australia, Canberra, A.C.T., Australia.

Cebriá J. M., Martín-Escorza C., López-Ruiz J., Morán-Zenteno D. J. & Martiny B. M. 2011. Numerical recognition of alignments in monogenetic volcanic areas: Examples from the Michoacán-Guanajuato Volcanic Field in Mexico and Calatrava in Spain. *Journal of Volcanology and Geothermal Research* **201**, 73-82.

Cheesman A. 2007. The nature of transitions between magmatic and phreatomagmatic explosive volcanism at the Red Rock Volcanic Complex, Newer Volcanics Province, Southeastern Australia. Masters thesis, Monash University, Australia (unpubl.).

Connor C. B., Condit C. D., Crumpler L. S. & Aubele J. C. 1992. Evidence of regional structural controls on vent distribution: Springerville Volcanic Field, Arizona. *Journal of Geophysical Research: Solid Earth* **97**, 12349-12359.

Connor C. B. & Connor L. J. 2006. Inversion is the solution to dispersion: understanding eruption dynamics by inverting tephra fallout. *In:* Mader H. M., Coles S., Connor C. B. & Connor L. J. eds. *Statistics in volcanology*, pp. 231-242. Geological Society of London, London.

Francis P. W., Glaze L. S., Pieri D., Oppenheimer C. M. M. & Rothery D. A. 1990. Eruption terms. *Nature* **346**, 519-519.

Geshi N., Németh K. & Oikawa T. 2011. Growth of phreatomagmatic explosion craters: A model inferred from Suoana crater in Miyakejima Volcano, Japan. *Journal of Volcanology and Geothermal Research* **201**, 30-38.

Guilbaud M.-N., Siebe C., Layer P. & Salinas S. 2012. Reconstruction of the volcanic history of the Tacámbaro-Puruarán area (Michoacán, México) reveals high frequency of Holocene monogenetic eruptions. *Bulletin of Volcanology* **74**, 1187-1211.

Hare A. G. & Cas R. A. F. 2005. Volcanology and evolution of the Werribee Plains intraplate, basaltic lava flow-field, Newer Volcanics Province, southeast Australia. *Australian Journal of Earth Sciences* **52**, 59-78.

Jordan S. C., Cas R. F. A. & Hayman P. C. 2013. The origin of a large ([>3]km) maar volcano by coalescence of multiple shallow craters, not deep excavation: The late Pleistocene Lake Purrumbete maar, Newer Volcanics Province, southeastern Australia. *Journal of Volcanology and Geothermal Research* **254**, 5-22.

Joyce E. B. 1975. Quaternary volcanism and tectonics in southeastern Australia. *Bulletin - Royal Society of New Zealand* **13**, 169-176.

Kereszturi G., Németh K., Cronin S. J., Agustín-Flores J., Smith I. E. M. & Lindsay J. 2013. A model for calculating eruptive volumes for monogenetic volcanoes — Implication for the Quaternary Auckland Volcanic Field, New Zealand. *Journal of Volcanology and Geothermal Research* **266**, 16-33.

Kienle J., Kyle P. R., Self S., Motyka R. J. & Lorenz V. 1980. Ukinrek Maars, Alaska, I. April 1977 eruption sequence, petrology and tectonic setting. *Journal of Volcanology and Geothermal Research* **7**, 11-37.

Lefebvre N. S., White J. D. L. & Kjarsgaard B. A. 2013. Unbedded diatreme deposits reveal maar-diatreme-forming eruptive processes: Standing Rocks West, Hopi Buttes, Navajo Nation, USA. *Bulletin of Volcanology* **75**, 1-17.

Lorenz V. 1975. Formation of phreatomagmatic maar-diatreme volcanoes and its relevance to kimberlite diatremes. *Physics and Chemistry of The Earth* **9**, 17-27.

Lorenz V. 1986. On the growth of maars and diatremes and its relevance to the formation of tuff rings. *Bulletin of Volcanology* **48**, 265-274.

Lorenz V. 2003. Maar-Diatreme Volcanoes, their Formation, and their Setting in Hard-rock or Soft-rock Environments. *Geolines* **15**, 72-83.

Lorenz V. 2007. Syn- and posteruptive hazards of maar-diatreme volcanoes. *Journal of Volcanology and Geothermal Research* **159**, 285-312.

Moore J. G., Nakamura K. & Alcaraz A. 1966. The 1965 eruption of Taal Volcano. *Science* **151**, 955-960.

Németh K. 2010. Monogenetic volcanic fields: Origin, sedimentary record, and relationship with polygenetic volcanism. *Geological Society of America Special Papers* **470**, 43-66.

Newhall C. G. & Self S. 1982. The volcanic explosivity index (VEI) an estimate of explosive magnitude for historical volcanism. *Journal of Geophysical Research: Oceans* **87**, 1231-1238.

Nicholls I. A. & Joyce E. B. 1989. East Australian Volcanic Geology: Newer Volcanics. *In:* Johnson R. W., Knutson J. & Taylor S. R. eds. *Intraplate volcanism in eastern Australia and New Zealand*, pp. 137-141. Cambridge University Press.

Piganis F. 2011. A volcanological investigation of the polymagmatic Red Rock Volcanic Complex and a 3D geophysical interpretation of the subsurface structure and geology of the poly-lobate Lake Purdigulac maar, Newer Volcanics

Province, southeastern Australia. Masters thesis, Monash University, Australia (unpubl.).

Pioli L., Erlund E., Johnson E., Cashman K., Wallace P., Rosi M. & Delgado Granados H. 2008. Explosive dynamics of violent Strombolian eruptions: The eruption of Parícutin Volcano 1943–1952 (Mexico). *Earth and Planetary Science Letters* **271**, 359-368.

Price R. C., Gray C. M. & Frey F. A. 1997. Strontium isotopic and trace element heterogeneity in the plains basalts of the Newer Volcanic Province, Victoria, Australia. *Geochimica et Cosmochimica Acta* **61**, 171-192.

Price R. C., Nicholls I. A. & Gray C. M. 2003. Cainozoic igneous activity. *In:* Birch W. D. ed. *Geology of Victoria*, pp. 361-375. Geological Society of Australia Special Publication **23**. Geological Society of Australia (Victoria Division).

Ross P.-S. & White J. D. L. 2006. Debris jets in continental phreatomagmatic volcanoes; a field study of their subterranean deposits in the Coombs Hills vent complex, Antarctica. *Journal of Volcanology and Geothermal Research* **149**, 62-84.

Self S., Kienle J. & Huot J.-P. 1980. Ukinrek Maars, Alaska, II. Deposits and formation of the 1977 craters. *Journal of Volcanology and Geothermal Research* **7**, 39-65.

Shaw-Stuart A. 2005. Transition from phreatomagmatic maar forming explosive activity to magmatic scoria cone complex forming activity in the Pleistocene Mt Leura Volcanic Complex, southeastern Australia. Masters thesis, Monash University, Australia (unpubl.).

Sottili G., Palladino D., Gaeta M. & Masotta M. 2012. Origins and energetics of maar volcanoes: examples from the ultrapotassic Sabatini Volcanic District (Roman Province, Central Italy). *Bulletin of Volcanology* **74**, 163-186.

Valentine G. A. 2012. Shallow plumbing systems for small-volume basaltic volcanoes, 2: Evidence from crustal xenoliths at scoria cones and maars. *Journal of Volcanology and Geothermal Research* **223–224**, 47-63.

Valentine G. A., Graettinger A. H. & Sonder I. 2014. Explosion depths for phreatomagmatic eruptions. *Geophysical Research Letters*, 2014GL060096.

Valentine G. A. & White J. D. L. 2012. Revised conceptual model for maar-diatremes: Subsurface processes, energetics, and eruptive products. *Geology* **40**, 1111-1114.

van Otterloo J., Cas R. A. & Sheard M. J. 2013. Eruption processes and deposit characteristics at the monogenetic Mt. Gambier Volcanic Complex, SE Australia: implications for alternating magmatic and phreatomagmatic activity. *Bulletin of Volcanology* **75**, 1-21.

van Otterloo J. & Cas R. F. 2013. Reconstructing the eruption magnitude and energy budgets for the pre-historic eruption of the monogenetic ~5 ka Mt. Gambier Volcanic Complex, south-eastern Australia. *Bulletin of Volcanology* **75**, 1-18.

White J. D. & Houghton B. 2000. Surtseyan and related phreatomagmatic eruptions. *In:* Sigurdsson H., Houghton B., McNutt S. R., Rymer H. & Stix J. eds. *Encyclopedia of Volcanoes*, pp. 495-512. Academic Press, San Diego, California.

White J. D. L. & Ross P. S. 2011. Maar-diatreme volcanoes: A review. *Journal of Volcanology and Geothermal Research* **201**, 1-29.

Wohletz K. & Heiken G. 1992. *Volcanology and geothermal energy*. Univ. Calif. Press, Berkeley, Calif. USA.

Chapter 5.

Using sensitivity analysis to assess the ambiguity and variability of potential field models of maar-diatremes from the Newer Volcanics Province

T. N. Blaikie, L. Ailleres, P. G. Betts

School of Earth, Atmosphere and Environment, Monash University, Clayton, Victoria, Australia

Cover page: Scoria cones of the Red Rock Volcanic Complex.

Monash University

Declaration for Thesis Chapter 5

Declaration by candidate

In the case of Chapter 5, the nature and extent of my contribution to the work was the following:

Nature of contribution	Extent of contribution (%)
Modelling, analysis, interpretation, preparation of the manuscript	95 %

The following co-authors contributed to the work. If co-authors are students at Monash University, the extent of their contribution in percentage terms must be stated:

Name	Nature of contribution	Extent of contribution (%) for student co-authors only
L. Ailleres	Supervisory role	2.5
P. G. Betts	Supervisory role	2.5

The undersigned hereby certify that the above declaration correctly reflects the nature and extent of the candidate's and co-authors' contributions to this work*.

Candidate's Signature **Date**

Main Supervisor's Signature **Date**

*Note: Where the responsible author is not the candidate's main supervisor, the main supervisor should consult with the responsible author to agree on the respective contributions of the authors.

Abstract

Two and three-dimensional potential field modelling techniques have previously been applied to understand the subsurface morphology of maar volcanoes, and have revealed important details on the geometry of the diatreme, location of vents, and presence of dykes and buried lava flows. However, non-uniqueness is inherent in these interpretations because of uncertainties in the models input variables such as density, magnetic susceptibility and geometry. Sensitivity analyses are applied to determine how the maar-diatreme models would be affected if the input variables deviate from the apriori model. This helped identify which structures in the models were well constrained in terms of their geometry and petrophysical properties, and delineated a range of end-member models that satisfied the geophysical and geologic data.

Results of the sensitivity analyses support previous interpretations of the data, but highlight where the models are more ambiguous, and how their geometry could vary within the bounds of the property constraints. Sensitivity analyses of the two-dimensional forward models indicate that the range of allowable petrophysical properties for a fixed model geometry is relatively small, indicating that the models are well constrained for the given geometry. However, if the properties are varied considerably, even within the bounds of the initial constraints, then the model geometry would also have to vary from the reference model. Three-dimensional geometry inversions are applied to determine the range of variability in the diatreme geometries. Results support the initial geometries modelled, but indicate that the maar-diatremes might be shallower if they are less dense than the reference model, and deeper if they are more dense.

Key Words: gravity, magnetic, modelling, inversion, sensitivity analysis, maar-diatreme

1. Introduction

Forward and inverse modelling of potential field data attempts to predict the distribution of density and/or magnetic susceptibility within the subsurface so that geologic interpretations can be made. However, these interpretations are non-unique, with an infinite number of solutions being able to explain the observed data (Whiting 1986; Valenta *et al.* 1992; Jessell *et al.* 1993). When producing a geophysical model, the modeller must integrate geologic data into the model, and make decisions on suitable geometries and property distributions. This process can result in more reliable solutions than computer generated models as the modeller considers their geologic knowledge, however even when geologic constraints are incorporated into geophysical models, solutions can still be non-unique (Nabighian *et al.* 2005a, b), and a range of models may exist that are consistent with all available information. The ambiguity of an interpretation is often acknowledged when a geophysical interpretation is presented, however; often the 'best fit' model will be presented, and rarely will other potential models be discussed, or the final model critically evaluated to assess its validity.

Sensitivity analyses allow the modeller to evaluate the validity of their preferred solution, and also explore a suite of possible alternate models. This can be achieved by testing how a model's 'calculated' response varies when different parameters within a geophysical model are altered, such as the dip of a particular geologic body, or its petrophysical properties. Observing the range of model parameters that can produce a successful geophysical model can provide an understanding of how different structures contribute to the observed geophysical anomaly, and how sensitive they are to changes in their properties and/or geometry (Blaikie *et al.* 2014b). This will identify how well constrained different elements of the model are, and how much a structure of interest might vary in its geometry when its properties are over or underestimated, which is extremely important if targeting an area for exploration.

Sensitivity analyses have been applied in the past to test a range of allowable properties and geometries of structures within potential field models. For example, Aitken *et al.* (2009) tested the sensitivity of the geometry of shears zones in the Musgrave Province by imposing a range of dips on the faults within two-dimensional forward models. A range of dip variations that would still produce an acceptable model were identified which helped determine which structures were well constrained. A large variation in allowable dips along the plane of a shear zone suggests a structure that is less well constrained than a model that only allowed a small range of dips. McLean and Betts (2003) used two-dimensional sensitivity analysis to test a range of geometries and the sensitivity of the petrophysical properties for models of granite plutons in order to justify their interpretation of a tabular shaped intrusion.

Three-dimensional inversions also allow the geometry/properties of the model to be numerically calculated whilst still incorporating all the available geologic constraints, therefore reducing bias in the model caused by the users' interpretations. Sensitivity analysis using three-dimensional inversions have been applied by Aitken and Betts (2009) and Williams *et al.* (2009) to test the geometry of select structures within their three-dimensional models. In these examples, the density or magnetic susceptibility of select models structures were varied by 10-30% and inverted to identify how much the geometry of that structure could vary and still obtain an acceptable misfit between the observed and calculated data. Armit *et al.* (2014) applied a sensitivity analysis to test multiple different geometry and property variations of a 3D structural model of the Mount Painter Province, South Australia, and through this process recognised that a large, low density source body (interpreted to be a felsic intrusion), was required to reduce the misfit of the model to an acceptable level.

Blaikie *et al.* (2014b) introduced several techniques for conducting a sensitivity analysis, utilising two and a half-dimensional modelling techniques to test an allowable range of petrophysical properties, and three-dimensional inversions to test the upper and lower geometry bounds of maar-diatremes. However, this work only focused on two of the four case studies introduced. In this paper, we expand upon the sensitivity analysis techniques introduced by Blaikie *et al.* (2014b) and conduct further sensitivity analyses of the models from Blaikie *et al.* (2014a, b) to assess ambiguity and calculate a range of models that may satisfy the observed geophysical and geologic data.

2. Introduction to case studies

This study draws upon several geophysical models of maar volcanoes that represent good examples of the variable sizes, eruptive styles and complexities observed in maar volcanoes within the Newer Volcanics Province of south-eastern Australia. The volcanoes have previously been the subject of geophysical and volcanological studies (Blaikie *et al.* 2012; Blaikie *et al.* 2014b). Data is drawn from models of the Red Rock Volcanic Complex, Mount Leura Volcanic Complex, Ecklin maar and the Anakies. Ecklin and Anakie are simple maar volcanoes, with Ecklin consisting of single elliptical craters, and Anakie a small crater nested between several scoria cones. Red Rock and Mount Leura are complex monogenetic volcanoes exhibiting a range of eruptive styles. Red Rock is comprised of at least 40 eruption points that formed several multi-vent maar craters and a scoria cone complex. Mount Leura consists of a coalesced maar and tuff ring crater that was infilled by lava and scoria in the later stages of the eruption.

The geophysical models for each of these volcanic centres were constructed by integrating geophysical and geologic data. Best fit models were obtained by constructing multiple 2.5/2.75D forward models of ground gravity and magnetic data, and were constrained by petrophysical data. The forward models were imported into Gocad (www.gocad.org) where they were used to construct a 3D geological model which was used as a reference model for constrained 3D gravity and magnetic inversions performed within VPmg (Fullagar *et al.* 2004; 2008; Fullagar and Pears 2007). Homogenous, heterogeneous property and geometry inversions were applied to optimise the property distributions and geometry of these models. Further details on the modelling techniques are available in Blaikie *et al.* (2014b).

The Ecklin and Anakie maars have relatively simple geophysical signatures. Long wavelength gravity lows with corresponding magnetic highs are observed across the craters and were reproduced during modelling with the presence of a shallow maar-diatreme structure at Anakie and two coalesced diatreme structures containing a denser/more magnetic central vent at Ecklin. Red Rock and Mount Leura have more complex geophysical signatures, consisting of short wavelength gravity and magnetic highs superimposed on longer wavelength gravity lows. These anomalies are reproduced during modelling with multiple shallow coalesced diatremes containing dykes and magma ponds.

The best fit models of each of these centres, initially presented by Blaikie *et al.* (2014a, b) are examined and subjected to sensitivity analysis in order to assess which aspects of the model are better constrained and demonstrate why these models are the best solution to the data given the current geologic and geophysical constraints available.

3. Model limitations and data uncertainty

Uncertainties in model input data (such as a lack of, or poor quality geologic and geophysical data) must be considered prior to modelling so that a range of geologic models that satisfy the available data whilst considering its uncertainties can be produced. In each of the case studies examined here, errors may arise due to the accuracy of gravity and elevation measurements, whilst uncertainty exists in the data reduction process (e.g., Bouguer correction density) and the accuracy of petrophysical measurements (measured surface and inferred subsurface).

During the field surveys, every care is taken to ensure the accuracy of gravity and magnetic measurements. Differential GPS is used to obtain the elevation of each gravity station to a high precision and any error arising from uncertainty in the vertical position results in an error that is less than the resolution of the gravity meter. The major uncertainty in gravity data arises due to noise in the data, caused by unstable ground in some survey areas. It is assumed that the wavelength of any anomaly arising due to volcanic structures is greater than the gravity station spacing. Any gravity anomaly present that is the result of a single measurement is assumed to be noise and removed from the data by manual deletion or image processing unless a corresponding magnetic anomaly is identified.

There is some uncertainty regarding the appropriate Bouguer and terrain correction density to apply to the acquired gravity data as the density of the surrounding terrain can be highly variable. Different cones and tuff rings within individual volcanic complexes (e.g., Red Rock and Mt Leura), can have different densities depending of the degree of welding and composition of the volcanic deposits. Surrounding the volcanoes there can be a high density contrast between the lava flows of the Newer Volcanics Province and underlying sediments of the Otway Basin. Selecting an inappropriate correction density may result in either over or under correcting for topography in some areas. To overcome the uncertainty that may arise from this, we model the free-air anomaly and include topography in all the models.

Prior to modelling the potential field response, there was some constraint on the overall structure of the maar-diatremes because their geometry is fairly well described in the literature (e.g., Lorenz 1986; White and Ross 2011; Valentine and White 2012). Uncertainty in the geometry of the diatreme arises from not knowing its exact depth, as well as the number and location of vents, although these variables can be somewhat constrained from the deposits in the ejecta rim, and by studying the morphology of the crater. In the early stages of modelling, assumptions had to be made on suitable geometries and property distributions within the models, which could bias the final results. Initially these assumptions were based on the expected structure and available constraints on its properties. The model geometry was then modified based on the assumed density and magnetic susceptibility distribution through the model until an acceptable geophysical model is obtained. The petrophysical properties were constrained by analogue samples from the maars ejecta rims, however the assumption that the composition of the diatreme is similar to surface deposits is another source of uncertainty in our models, which in turn, translates into further uncertainty on the geometry of model. In the absence of any drill-hole data, there is no other option but to infer these properties, however a sensitivity analysis is necessary as it allows us to produce a range of solutions that satisfy the geologic, and geophysical data. This ensures that our final models are consistent with the observed data, but also consider how the uncertainty of that data could have affected the results.

4. Method and Results

The structure of a maar volcano is fairly well understood and described in the literature (e.g., Lorenz 1986; White and Ross 2011; Valentine and White 2012), so they act as good case studies towards testing different techniques for sensitivity analysis. We take several different approaches analysing the reference models, which involve testing the model for its petrophysical and geometric sensitivity. These techniques involve modifying the model properties within the bounds of the constraints and assessing how the calculated model response changes. We also present a range of end-member models, so that potential variations in model geometry from our initial reference models are understood.

4.1 Petrophysical analysis

The geophysical response of a model is the result of the super-position of anomalies arising from structures with different petrophysical properties. By manually manipulating the 2-2.75D models produced in GM-SYS, the geophysical response arising from a particular structure can be isolated and a range of geometric/petrophysical solutions tested (Blaikie *et al.* 2014b). This is achieved by manipulating the properties and geometry of that structure, and examining how the calculated response varies, and the range of model parameters that will still produce an acceptable fit to the data. Initially, the geometry of the models remained constant, but the properties of regions were altered to the upper and lower bounds of the constraints, or were varied within a certain range to test the sensitivity of the models properties. We then alter the geometry while the properties remain fixed to determine how well constrained the structure of the model is. This approach works well for complex models, as well as more simple ones as it allows the geophysical response of select structures to be isolated and examined.

4.1.1 Red Rock Volcanic Complex

Seven two and a half-dimensional models across the Red Rock Volcanic Complex were produced by Blaikie *et al.* (2014a), focussing on the central to north-western region of the complex, including the Lake Werowrap maar which has a complex structure consisting of multiple dykes and magma ponds. A sensitivity analysis of a representative model from this maar is discussed below.

The properties of the diatreme were initially altered to assess how well constrained this region of the model is. Decreasing the diatreme to the minimum expected density causes a maximum variation in the anomaly of -1.5 mGals, or 28 % of the dynamic range (5.29 mGals). Increasing the density causes a maximum change of ~0.75 mGals (14 %), over the southern end of the maar which was initially less dense than the rest of the diatreme, but had little effect elsewhere as the density of reference model was close to the upper bounds of the constraints. This demonstrates that for the geometry of the reference model, a scenario where the diatreme is slightly denser is more plausible. However if the properties of the diatreme were to vary significantly from the reference model, then the geometry of the diatreme would also have to vary in order to obtain a match between the observed and calculated data. This is further examined in section 4.3.

Variations to the magnetic susceptibility of the diatreme to the upper and low bounds of values observed in surface deposits produced similar geophysical responses, however both models produce a magnetic response less than the observed data (maximum deviation of ~750 nT, or 21% of the total dynamic range; 3590 nT). This is because the initial model required that the magnetic susceptibility

	Model	Region altered	Property	Value (SI)	Misfit
Gravity	a	Diatreme	Minimum density	1.84	0.436
	b	Diatreme	Maximum density	2.45	0.386
	c	Dykes	Minimum density	1.92	0.535
	d	Dykes	Maximum density	2.94	0.355
	e	Dykes	Neutral density	2.41	0.333
Magnetics	a	Diatreme	Minimum magnetic susceptibility	0.00018	524.9
	b	Diatreme	Maximum magnetic susceptibility	0.014	499.485
	c	Diatreme	Increased magnetic susceptibilty by an order of magnitude		642.907
	d	Diatreme	Decreased magnetic susceptibilty by an order of magnitude		495.027
	e	Dykes	Minimum magnetic susceptibility	0.00019	785.039
	f	Dykes	Maximum magnetic susceptibility	0.083	569.744
	g	Dykes	Neutral magnetic susceptibility	0.050	659.196

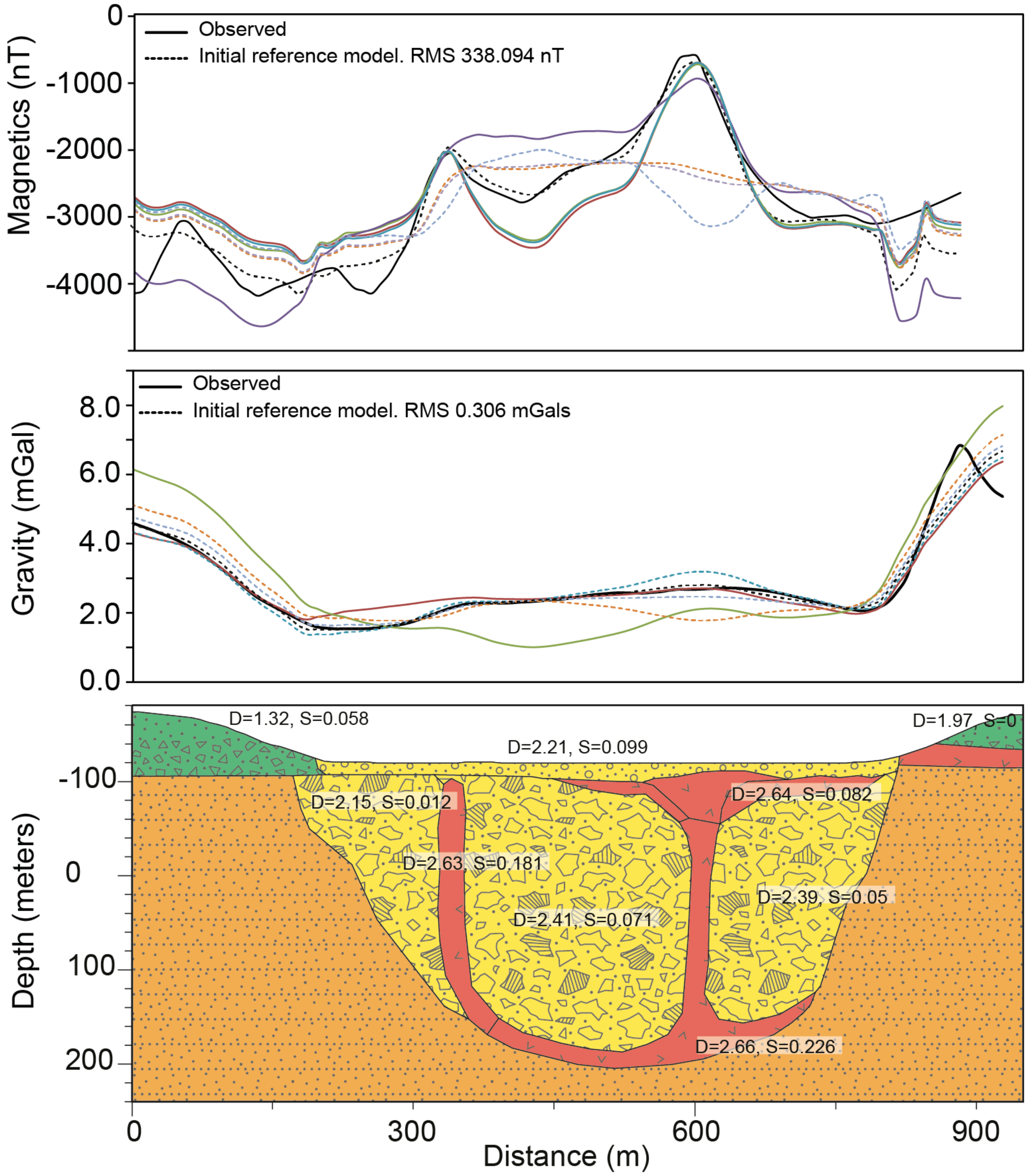

Figure 1. Petrophysical sensitivity analysis of the Lake Werowrap maar of the Red Rock Volcanic Complex showing variations to the calculated gravity and magnetic response and the resulting RMS misfit due to variations in the model parameters listed in the table. Black lines indicate observed data, solid lines variations to the diatreme and dashed lines variations to the dykes. This model was initially presented by Blaikie et al. (2014b).

be increased beyond the observed petrophysical data for ash/scoria deposits, but still within the range observed for basaltic rocks (Clark 1983). This is still a plausible solution since ash/scoria deposits at the surface have been weathered, and the diatreme is interpreted to contain a higher proportion of juvenile material, so the magnetic susceptibility of the diatreme should be higher than that observed for surface deposits.

Altering the properties of the dykes within the model helps to identify what their calculated response is, and allows a comparison of the calculated wavelengths with the observed data. This helps ensure that the geometry of these structures are reasonable with respect to the observed wavelengths, and any errors in the size/position of these structures are not compensated for by altering the properties/geometry of surrounding structures. For example, when the density and magnetic susceptibility of the dykes within the Lake Werowrap diatreme are altered to the bounds of the constraints, although the amplitudes do not match, there is still a generally good agreement between the wavelengths of the observed and the calculated data. This test confirms that the anomalies in the calculated data are reproduced predominantly by the dykes, and not by also manipulating the regions surrounding the dykes to obtain a match for a preferred geometry. Similar to the diatreme, the model required that the magnetic susceptibility be increased beyond the observed petrophysical data to obtain an acceptable match.

These analyses suggest that the allowable range of petrophysical properties for this model is relatively small, indicating that the model is well constrained for the given geometry. However, if the properties are varied considerably, even within the bounds of the initial constraints, then the model geometry would also have to vary from the reference model. A range of solutions for varied geometries is discussed in later sections.

4.1.2 Mount Leura Volcanic Complex

The same technique was applied to test the sensitivity of one of several profiles produced across the Mount Leura Volcanic Complex, with the response of this model being similar to the response described for another profile at Mount Leura by Blaikie *et al.* (2014b). The complex overprinting relationships within the maar are reflected in its complex gravity and magnetic response, with anomalies being the result of superposition from multiple sources. Variations to the density and susceptibility of different model regions such as the dykes and lavas emphasises the wavelengths of these features, which correlate fairly well to the shorter wavelength anomalies in the observed data.

Increasing or decreasing the diatreme density to the upper and lower bounds resulted in the greatest variation to the calculated response over the maar diatreme (~1 – 1.75 mGal; 17 – 30% total dynamic range). There was some variation to the calculated response over the tuff ring, however it was less pronounced than elsewhere in the model (~0.5 – 1 mGal; 9 – 17%), which suggests that the thicker lava flows in this region may be partly masking the signal of the underlying diatreme. Modifying the density of the dykes and lava flows within the model had a variable effect on the calculated response. Increasing the density had little effect since their densities were already close to the upper bound. Decreasing the density of the dykes/lava flow caused a decrease in the gravity response over the centre of the profile, which also resulted in an increase in the gravity response over the maar. This indicates that the relative density of the tuff ring and lava flows must be greater than that of the diatreme in

	Model	Region altered	Property	Value(s)	Misfit
Gravity	a	Diatreme	Minimum density	1.84	1.168
	b	Diatreme	Maximum density	2.45	0.541
	c	Dykes and Lavas	Minimum density	1.92	1.492
	d	Dykes and Lavas	Maximum density	2.94	0.356
	e	Dykes and Lavas	Neutral density	2.41	0.833
Magnetics	a	Diatreme	Minimum magnetic susceptibility	0.00018	388.7
	b	Diatreme	Maximum magnetic susceptibility	0.014	379.4
	c	Dykes and Lavas	Minimum magnetic susceptibility	0.00019	756.8
	d	Dykes and Lavas	Maximum magnetic susceptibility	0.083	575.5
	e	Dykes and Lavas	Maximum model magnetic susceptibility	0.125	586.6

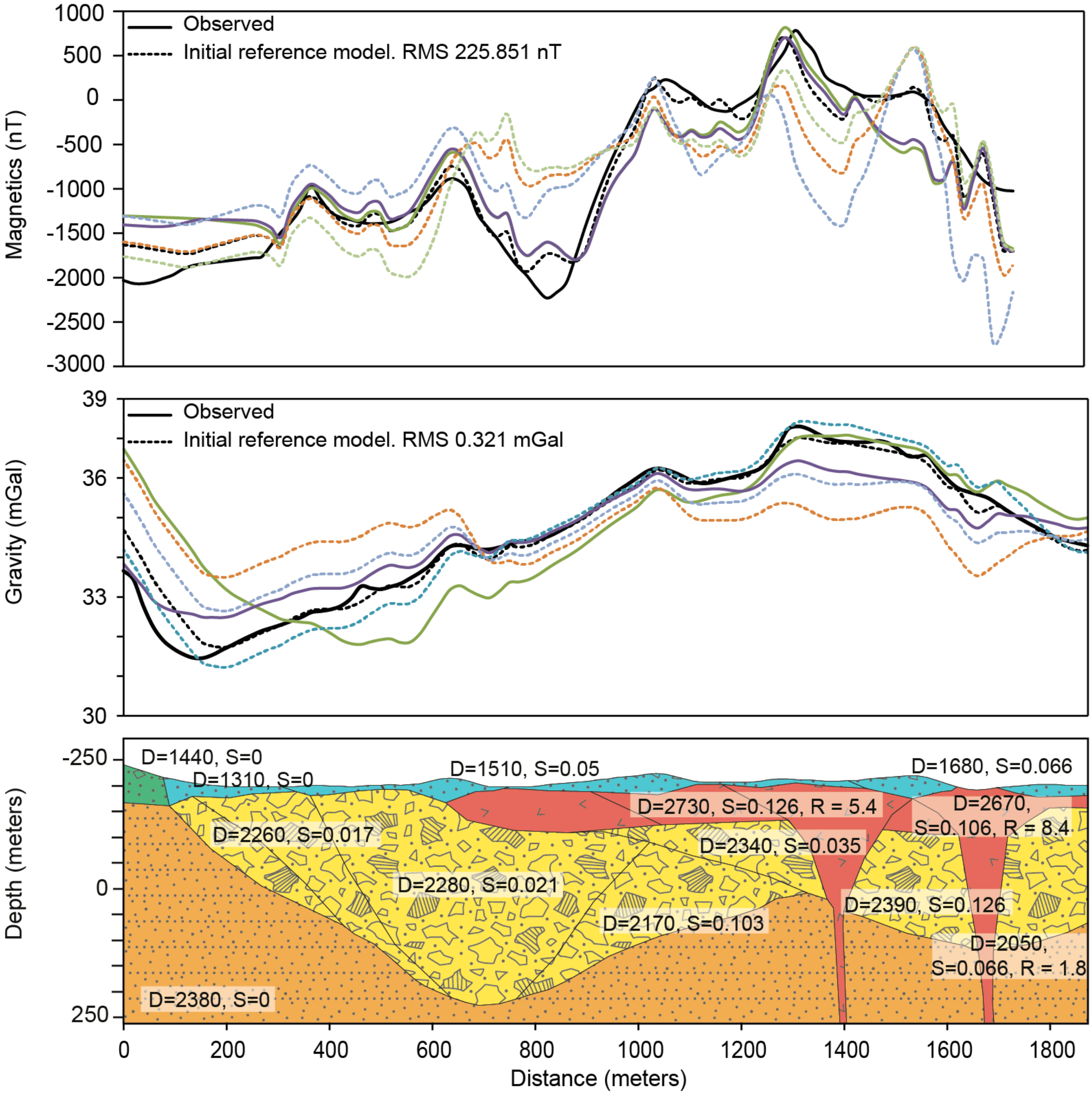

Figure 2. Petrophysical sensitivity analysis of the Mount Leura Voclanic Complex showing variations to the calculated gravity and magnetic response and the resulting RMS misfit due to variations in the model parameters listed in the table. Black lines indicate observed data, solid lines variations to the diatreme and dashed lines variations to the dykes and lava flows. This model was initially presented by Blaikie et al. (2014a).

order to obtain a match between the calculated and observed data.

Variations in the magnetic susceptibility of the model showed there is little difference between the calculated response of the upper and lower susceptibility bounds of the diatreme, suggesting a low sensitivity to variations in susceptibility across this structure. This indicates the geometry of the diatreme is less well constrained by the magnetic data than the gravity, and suggests that most of the magnetic response across the complex is the result of overlying lava and scoria, which due to its higher sensitivity, is better constrained than the underlying diatreme.

The lack of sensitivity to property variations in the regions underlying the lava flows suggests the geometry of these structures are not well constrained by the petrophysics, and could vary from the reference model. This model is however consistent with the present geologic observations, and cannot be further constrained without further information from drill holes or other geophysical data sets.

4.1.3 Ecklin maar

Compared to Mount Leura and Red Rock, Ecklin maar is relatively simple in its structure, consisting of two coalesced diatremes containing denser, more magnetic feeder vents. This simpler geometry, as well as a lack of denser structures such as dykes and overlying lavas results in this model exhibiting a high sensitivity to changes in its petrophysical properties. Variations in the gravity response of up to 1 mGal (27 %) are observed in response to increasing and decreasing the density of the diatreme to the bounds of its constraints which indicates the properties of this model are well constrained for the given geometry. Similarly, we see a deviation from the observed data due to changes in the density of the feeder vents, with the calculated wavelengths being similar to the observed data.

Variations to the models magnetic susceptibility produced some variation to the calculated data, but the amplitudes of the variations (~100 – 250 nT; 18 – 45 %) are less pronounced than at other centres, likely due to the lower susceptibility contrast across the model. This suggests a lower sensitivity to the magnetic data across the model, and that the gravity data is more important in constraining the geometry of this model.

4.1.4 Anakie maar

The geometry of the Anakie maar is relatively simple, consisting of a shallow diatreme structure. Increasing and decreasing the density to the bounds of the constraints showed an equal variation of ~1 mGal from either bound, indicating that for this geometry, the solution lies in the middle of the observed range, and that this model is highly sensitive to property variations. The increased sensitivity of this diatreme compared to others is likely due to its shallow structure and increased contrast with the denser granitic host rock. The gravity data was considered more important in defining the geometry of this volcanic centre as ground magnetic data could not be obtained. Aeromagnetic data was modelled in its place, but the increased flying height and line spacing means that any short wavelength anomalies associated with the volcanoes vents were probably not detected. Sensitivity analysis of this data suggests that similarly to Red Rock and Mount Leura, the susceptibility of this model had to be increased beyond the observed range to obtain an acceptable fit to the data, and remenance added to match the anomaly. These values are an estimate so since there is no remenance data available for this volcanic centre, however results do suggest the model is sensitive to changes in the models susceptibility.

	Model	Region altered	Property	Value(s)	Misfit
Gravity	a	Diatreme	Minimum density	1.84	0.588
	b	Diatreme	Maximum density	2.45	0.511
	c	Vents	Minimum density	1.92	0.588
	d	Vents	Maximum density	2.45	0.143
	e	Vents	Neutral density	2.17	0.200
Magnetics	a	Diatreme	Minimum magnetic susceptibility	0.00018	54.203
	b	Diatreme	Maximum magnetic susceptibility	0.014	108.789
	c	Vents	Minimum magnetic susceptibility	0.00018	61.710
	d	Vents	Maximum magnetic susceptibility	0.014	62.942
	e	Vents	Neutral magnetic susceptibility	0.005	51.325

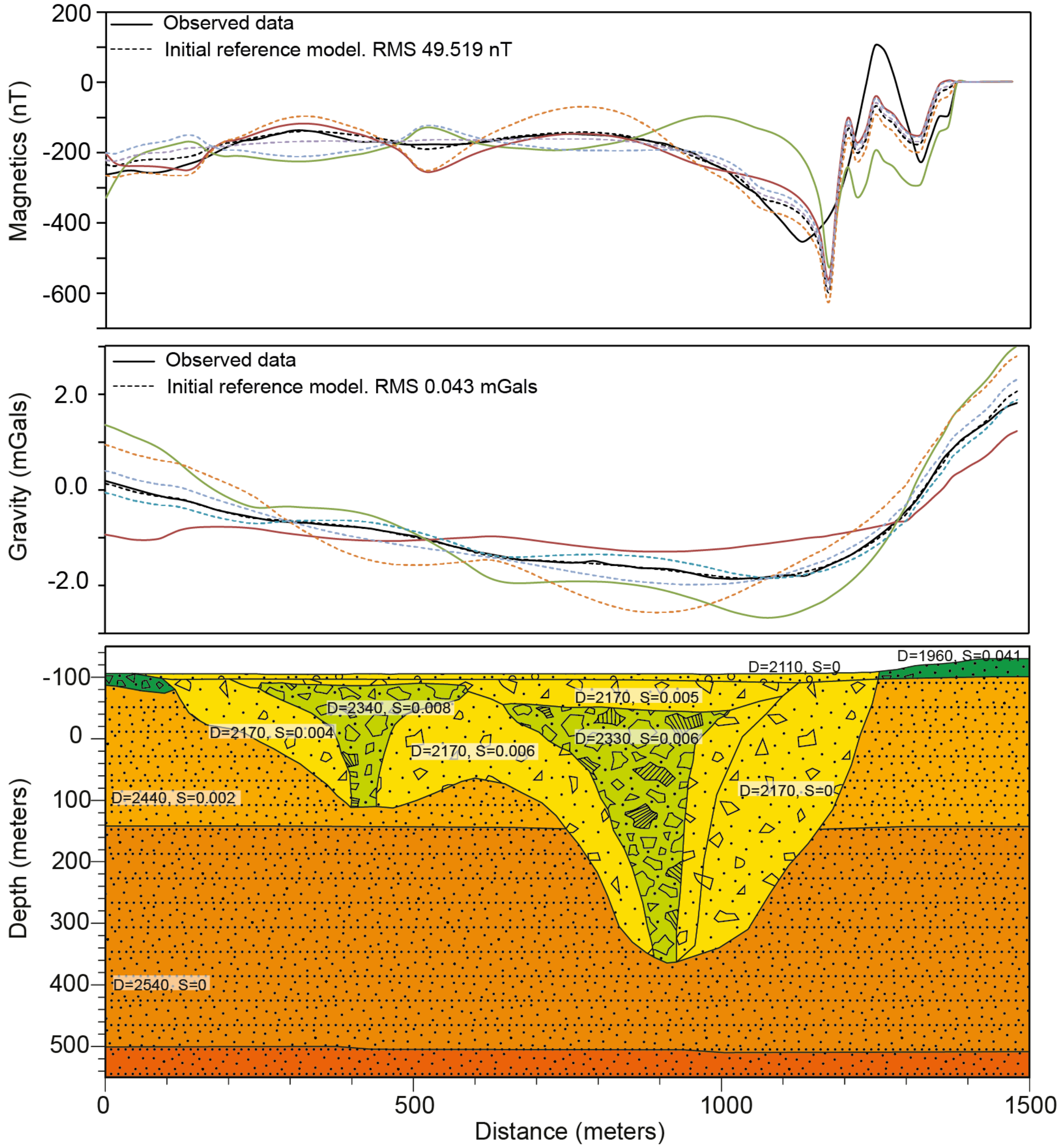

Figure 3. Petrophysical sensitivity analysis of the Ecklin maar showing variations to the calculated gravity and magnetic response and the resulting RMS misfit due to variations in the model parameters listed in the table. Black lines indicate observed data, solid lines variations to the diatreme and dashed lines variations to the vents. This model was initially presented in Blaikie et al. (2014a; b).

	Model	Region altered	Property	Value(s)	Misfit
Gravity	a	Diatreme	Minimum density	1.84	0.400
	b	Diatreme	Maximum density	2.45	0.302
Magnetics	a	Diatreme	Minimum magnetic susceptibility	0.00018	291.052
	b	Diatreme	Maximum magnetic susceptibility	0.014	247.817
	c	Diatreme	Magnetic susceptibility decreased by 0.05 SI	0.04	167.314
	d	Diatreme	Magnetic susceptibility increased by 0.05 SI	0.14	161.764

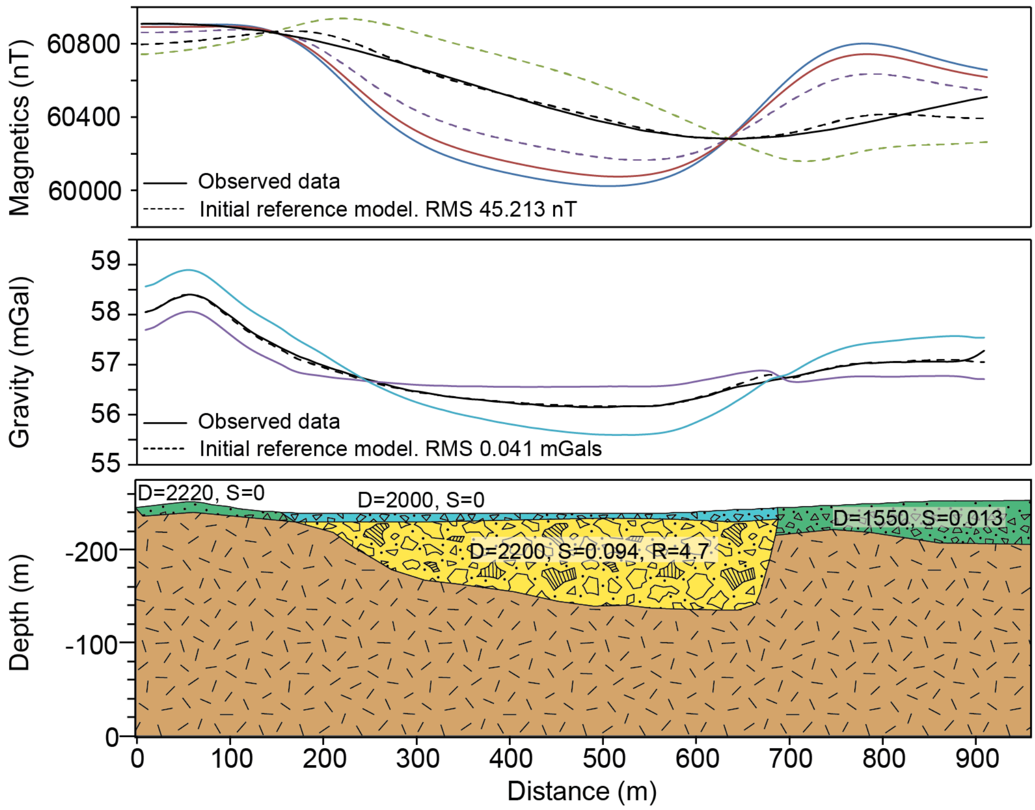

Figure 4. Petrophysical sensitivity analysis of the Anakie maar showing variations to the calculated gravity and magnetic response and the resulting RMS misfit due to variations in the model parameters listed in the table. This model was initially presented by Blaikie et al. (2014a).

4.2 Geometric analysis

The tests described above indicate that although there may be a little variation, the petrophysical properties of the model are fairly well constrained for the given geometry. Here we test how much the geometry of the model may vary while the petrophysical properties remain constant. To achieve this, we increase and decrease the depth of the diatreme by ~20 %. The geometry of modelled structures is consistent with the initial model, although some feeder dykes had to be lengthened/shortened during the modelling process.

Analysis shows that the gravity response of the Lake Werowrap maar diatreme is relatively insensitive to variations in the geometry of the diatreme by ± 20 %. Some variation was observed in the magnetic response, however a negligible change (~0.1 mGal amplitude variation) in the gravity response was observed. The lack of sensitivity in the gravity data to changes in the diatreme geometry is attributed to the low density contrast between the diatreme and the host rock. Although these results suggest the geometry of the diatreme is not well constrained by the gravity data, results are consistent with geologic information (e.g., lithic content observed in pyroclastic deposits). Other aspects of the model, such as the presence of dykes exhibit a higher sensitivity to variations in their properties/geometries and are considered less ambiguous than the diatreme geometry.

Variations of ± 20 % to the geometry of the diatremes at the Mount Leura Volcanic Complex show that an increase in the depth of the diatreme produced little change to gravity and a minor change to the magnetic response. A decrease in model depth produced some variation in both the calculated gravity (0.6 mGal) and magnetic data as the model responds to a lack of mass within the underlying diatreme. Interestingly the region underlying the lava flows which shows a lack of sensitivity in other tests shows the greatest variation in the shallow model. These results suggest the model is unlikely to be much shallower than the reference model, but could potential be deeper, which was previously suggested by Blaikie *et al.* (2014a) following 3D potential field inversions of this model.

The model of Ecklin maar shows some variation in the calculated gravity data after altering the depth of the diatreme by ± 20 % (0.4 mGal deep model, 0.2 mGal shallow model), but little variation in the calculated magnetic data (~40 nT for both models). The greater sensitivity in the gravity response of this model is related to a higher density contrast, while the lower magnetic sensitivity is due to a lower susceptibility contrast across the model. The broader and lower amplitude anomalies of the Ecklin maar mean that smaller variations the models properties and geometry have a greater influence on the model than at Red Rock and Mount Leura which are characterised by shorter wavelength, higher amplitude anomalies. The sensitivity of this model suggests the geometry is fairly well constrained by the gravity data, but less well constrained by the magnetic.

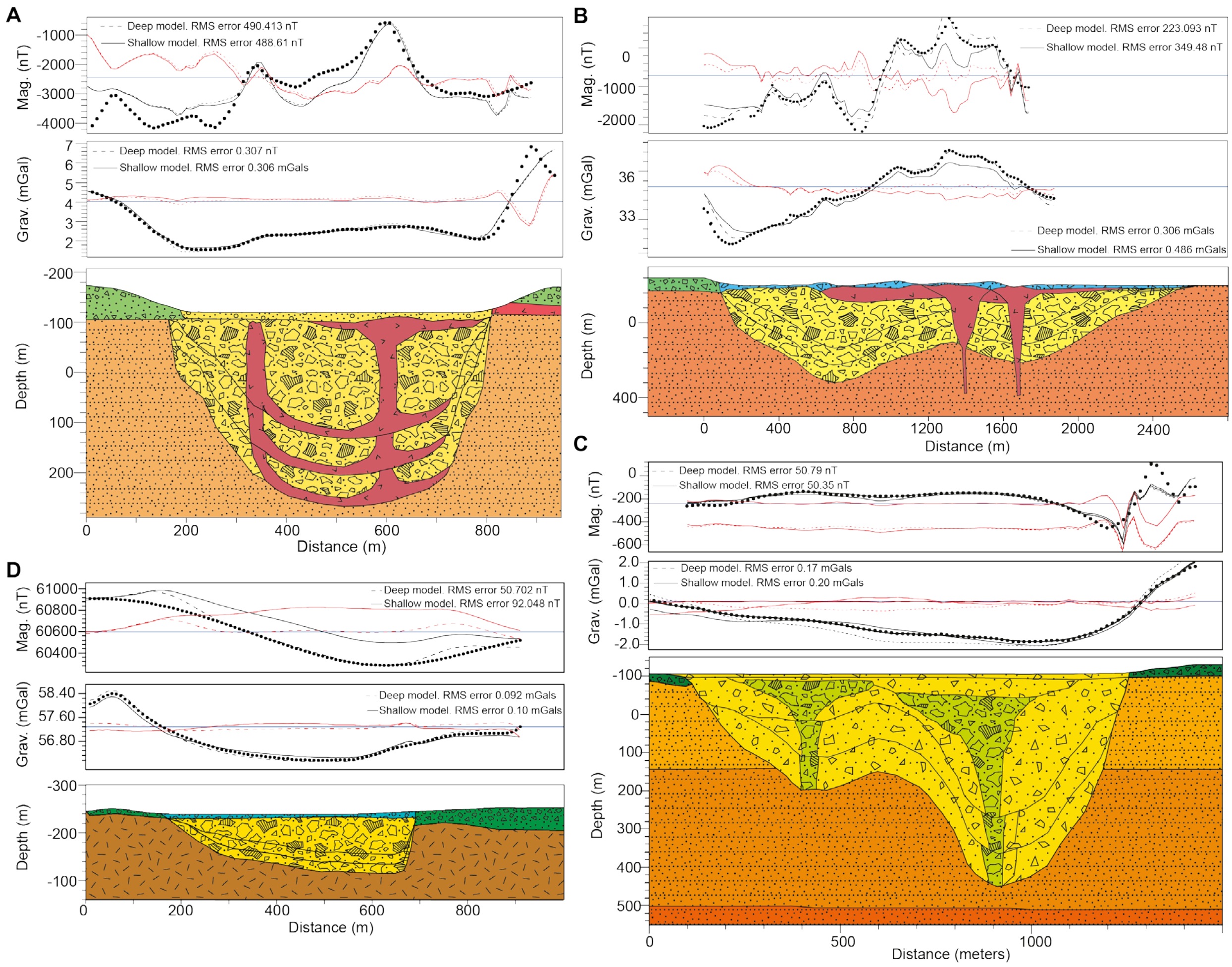

Figure 5. Results of geometric sensitivity analysis where the geometry was altered by ± 20 %. A) Lake Werowrap maar, Red Rock Volcanic Complex, B) Mount Leura Volcanic Complex C) Ecklin maar, D) Anakie maar. Calculated data from the deeper models are indicated by dashed lines, and shallow models by solid lines. Red lines indicate model error.

Anakie shows some variation to the gravity response of both models (0.1 mGal), but only observed a significant variation to the magnetic response (240 nT) for the shallow model. Although the variation in the gravity response is of the same order as that observed at Lake Werowrap, the model is considerably shallower, and also characterised by lower amplitude anomalies. The variation in the calculated gravity and magnetic response of this model suggests it is highly sensitive to changes in its structure, and is therefore geometrically well constrained.

This sensitivity analysis suggest most of these models are geometrically well constrained by at least one data set. However there may be some range of error in some of the modelled diatreme depths, particularly at the Lake Werowrap maar. However, in addition to the petrophysical constraints, these models are constrained with geologic data and we are unable to further improve upon these results without further information from drill holes or other geophysical data sets. Results from this analysis support the initial two-dimensional interpretations of the data by Blaikie *et al.* (2014a, b), but may be further refined through three-dimensional sensitivity analysis.

4.3 Calculating end-member models

Since the maar-diatremes of our case studies are not exposed, the petrophysical properties applied to the geophysical models were based on measurements of surface deposits interpreted to be of a similar composition. However, there could be compositional differences between surface and subsurface deposits, so it is important to assess how the geometry of the geophysical models could vary due to possible variations in the petrophysical properties of the subsurface. The 2D sensitivity analysis provides a good insight into how well constrained different elements of the models are, but determining a range of optimum geometries when the property of a particular structure is varied can be a difficult and time consuming process within GM-SYS. This analysis is easily achieved using the geometry inversion mode within VPmg, which also has the advantage of calculating the optimised geometry in 3D.

This technique was first introduced by Blaikie *et al.* (2014b) where geometry inversions of the Ecklin maar-diatreme were performed using a range of densities between the constraint bounds. This analysis revealed that the maar-diatreme could range between 350 and 1000 m deep (Figure 6), but in each model, the two coalesced vents were still well defined (Blaikie *et al.* 2014b). We perform the same analysis on the maar-diatremes for Mount Leura and Anakie. Attempts were made to apply this analysis to the Lake Werowrap maar, but due to its complexity it was unsuitable for this type of inversion. This is because the lower contact of the diatreme is bound by the dykes and magma pond, so it is not possible to invert the diatreme without also inverting these structures. Compared to the diatreme, the dykes and magma pond have a much higher property contrast with their surroundings, and are preferentially inverted because they can alter the calculated response by the greatest degree. This means the inversion is biased towards modifying these structures, so it is impossible to assess how the geometry of the diatreme would vary if its properties were altered.

The end-member models of the Ecklin, Anakie and Mt Leura maar diatremes (i.e., highest and lowest density) that achieved acceptable inversion results are shown in Figure 6. The inversion parameters that obtained successful results, and the efficiency of each inversion in minimising the misfit and producing a geologically realistic model are summarised in Table 1. In each analysis, the geometry of the maar-diatreme is inverted, and all other model properties/geometries remain fixed during the inversion unless otherwise described below. Since some of these models exhibit complex structures, and are subject to relatively strict model constraints, it is unlikely that an acceptable model will be achieved purely through the geometry inversion of one structure within the model. The purpose of this analysis is to reduce the misfit of the model as much as possible whilst honouring the constraints and ensuring the structure is still geologically plausible. In some cases (outlined in further detail below), obtaining a geologically meaningful result required that the misfit across other structures be minimised prior to geometry inversion, and that the number of iterations the inversion was allowed to perform were restricted. If the target misfit is not reached, then more inversions can then be applied to the resultant model to optimise the property distribution and geometry of other structures in order to further reduce the misfit.

4.3.1 Mount Leura Volcanic Complex

The three-dimensional model of Mt Leura is relatively complex with many regions exhibiting relatively high property contrasts with their surroundings. We focus the sensitivity analysis on the geometry of the maar-diatreme, since the geophysical data does not cover the entire extent of the tuff ring and its geometry is inferred beyond the limits of the data. Prior to testing the variability in the geometry of the maar diatreme, we first had to ensure that any misfit between the observed and calculated gravity response was largely related to the maar-diatreme and not caused by other features within the model. This helps reduce the inversion modifying the geometry of the maar-diatreme to compensate for an error related to another structure. To achieve this, a homogenous inversion was performed initially to optimise the density of every region within the model, and reduced the RMS misfit from an initial value of 1.12 mGals to 0.64 mGals. Next, a heterogeneous inversion was applied to the ejecta rim, scoria deposits, lava flow and the shallow diatreme associated with the tuff-ring which reduced the misfit to 0.58 mGal. The geometry inversions of the maar-diatreme were then performed on the resultant model from these inversions. Each iteration of the inversion was allowed to modify the depth of the diatreme by a maximum of 2.5% and the inversion was allowed to proceed for a maximum of 25 iterations, unless it stalled or a successful model (i.e., target misfit of 0.1 mGal reached) was achieved. Although a target misfit of 0.1 mGal is aimed for during inversion, we consider the model acceptable if a misfit of 0.56 mGal or better is reached, which represents an error less than 10% of the data's total dynamic range.

Decreasing the density of the maar-diatreme from the initial 2.32 g/cm^3 to 1.92 g/cm^3 initially resulted in a misfit increase to 1.09 mGals, but after 25 iterations, was reduced to 0.65 mGals. Although this value is slightly higher than the reference model, the modified geometry can still be considered a valid solution since the misfit was reduced considerably after 25 iterations, and because the solution is geologically reasonable. Inversion results suggest that a diatreme with a density 1.92 g/cm^3 has a have a depth of 250 m, which is much shallower than the reference model. The exception to this is three points along the edge of the diatreme where the inversion rapidly increased the depth of the diatreme to 360 m. Although these features may resemble small vents, they are more likely artefacts of the inversion process caused by noise in the data, or heterogeneities in the diatreme composition. These features are the reason why the number of iterations per inversion is restricted, as allowing the inversion to continue would further amplify their effects.

Increasing the model beyond the reference model density of 2.32 g/cm^3 did not achieve any acceptable results. A maximum density of 2.52 g/cm^3 was tested, and returned a misfit of 0.71 mGal, however the inversion stalled after 1 iteration and could not improve upon the initial model geometry. A geometry inversion of the maar-diatreme, keeping the reference density of 2.32 g/cm^3 was able to reduce the misfit to 0.56 mGals, although stalled after 7 iterations. The optimised geometry supports the initial conclusions of Blaikie *et al.* (2014a), suggesting the diatreme is of a similar geometry but is slightly deeper than the reference model, with a maximum depth of 550 m.

These models are considered the upper and lower bound of acceptable maar-diatreme geometries at the Mt Leura Volcanic Complex. The lower density model is considered slightly more plausible than the higher density model because it is more consistent with the depth of fragmentation determined by accidental lithic fragments in the ejecta rim. However, recent studies suggest that lithic fragments derived from deeper levels are not always represented in the ejecta rim (e.g., Valentine and White 2012; Lefebvre *et al.* 2013; Ross *et al.* 2013), so although less likely, this model is still a plausible solution.

4.3.2 Anakie maar

The Anakie maar is relatively simple, and had a low misfit prior to running any inversions (0.74 mGal, 11% dynamic range). Examining the residual anomaly revealed that the gravity response of the maar-diatreme was mostly accounted for by the present structure, and much of the model misfit was derived from data points outside the extent of the maar. Before running the geometry inversion on the Anakie maar-diatreme, several inversions were performed on the surrounding ejecta rim to minimise the misfit of the data points outside the area of interest. This should prevent large changes to the diatreme geometry in an attempt to accommodate for the misfit beyond the extent of the maar. Initially a homogenous inversion was applied to optimise the properties of the entire model, which was followed by a geometry and heterogeneous inversion of the ejecta rim. This reduced the misfit to 0.40 mGal (6%) prior to the geometry inversions of the maar-diatreme being applied. Trying to invert a model with such low level of misfit can be difficult because there is little residual anomaly to drive the inversion process. However, altering the density of the diatreme should increase the residual anomaly over the maar, and prompt the inversion to modify the geometry.

A geometry inversion of the reference model (130 m deep, density of 2.0 g/cm^3) suggests the Anakie maar has a slightly deeper diatreme (190 m) which is consistent with the results of Blaikie *et al.* (2014a). Lowering the density of the diatreme to 1.90 g/cm^3 initially resulted in a misfit decrease to 0.38 mGals. The inversion modified the diatreme to be 160 m deep, which is slightly shallower than its optimised geometry, but stalled after 6 iterations and only reduced the misfit to 0.37 mGals. Although this is only a minor reduction in the misfit, and the inversion stalled relatively early, the residual gravity anomaly suggests a low level of misfit over the maar, so this result is considered successful.

Increasing the diatreme density to 2.1 g/cm^3 initially increased the misfit to 0.43 mGal. The modified diatreme is deeper (230 m) than the reference model and reduced the misfit to 0.38 mGals before the inversion was terminated after 20 iterations. At densities above 2.1 g/cm^3, the inversion produced results that had a higher misfit, but were geometrically identical to the diatreme with a density of 2.1 g/cm^3. This would suggest that the geometry inversion varied the diatreme by the maximum allowable amount (3% per iteration), but could not lower the misfit before it was terminated at 20 iterations.

Both end-member geometry inversions (Figure 6) resulted in only minor reduction in the overall misfit, which is attributed to the fact that previous inversions had accounted for the misfit over the maar-diatreme, so there was no residual anomaly to drive the inversion. Additionally, because the Anakie maar-diatreme is so small relative to Mt Leura and Ecklin, modifying the properties of the reference model did not have as much as an affect as modifying the properties of a much larger maar-diatreme. Although the misfit of Mt Leura and Ecklin were also initially low, the larger mass of the diatreme means the effect on the gravity response was greater when the model was forced away from an acceptable solution, which therefore prompted the inversion to modify the geometry.

Table 1. Parameters applied during the geometry inversions of the Ecklin, Mount Leura and Anakie maar-diatremes. (E = Efficiency of inversion reducing the model misfit (Low, Medium, High), P = Plausibility of final model geometry (Low, Medium, High))

Model	Reference model		Upper density bound						Lower density bound					
	Density	Misfit	Density	Misfit		Iterations	Efficiency		Density	Misfit		Iterations	Efficiency	
				Initial	Final		E	P		Initial	Final		E	P
Mt Leura	2.32	0.58	2.32	0.58	0.56	7	L	H	1.92	1.09	0.65	25	H	M
Anakie	2.00	0.40	2.10	0.43	0.38	20	M	H	1.90	0.38	0.37	6	L	H
Ecklin	1.94	0.25	2.14	0.49	0.10	44	H	M	1.84	0.34	0.11	22	H	H

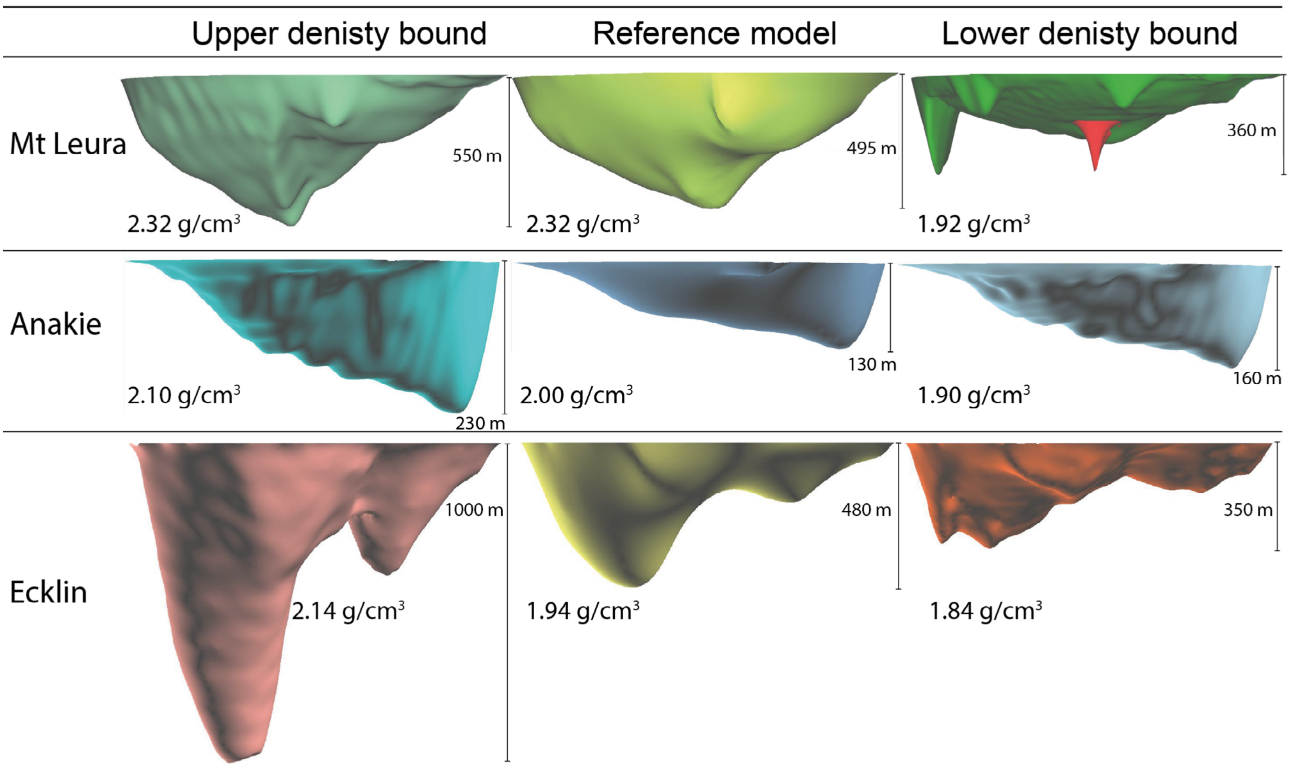

Figure 6. Results of the geometric inversions of the Mt Leura, Anakie and Ecklin maar-diatremes (Ecklin diatreme models are modified from Blaikie et al. 2014b).

5. Discussion

Potential field geophysical models have always suffered from ambiguity because solutions are non-unique (Whiting 1986; Valenta *et al.* 1992; Jessell *et al.* 1993). The ambiguity and any assumptions made during the construction of a geophysical model have been acknowledged for many examples where gravity and magnetic modelling was applied to maar volcanoes (e.g., Schulz *et al.* 2005; Lindner *et al.* 2006; Cassidy *et al.* 2007; Lopez Loera *et al.* 2008; Mrlina *et al.* 2009; Skacelova *et al.* 2010). However, beyond discussing the available geologic constraints, these authors have not conducted (or communicated results of) a sensitivity analyses to demonstrate why their interpretation is more valid than another possible solution. A sensitivity analysis is essential, and should be produced for every potential field model, and the results communicated to demonstrate why a particular solution is the most valid, and also to determine how the models are affected by uncertainty in the input variables such as density, magnetic susceptibility and geometry.

When conducting the sensitivity analysis, we utilised two-dimensional modelling techniques to understand the uncertainties related to the model petrophysics, and three-dimensional modelling techniques to assess uncertainty in the model geometry. The aim of this research is to understand the geometry of maar-diatremes, however, the geometry is dependent on the petrophysical properties applied during modelling. Since petrophysical properties were available to constrain each model, but tended to vary over a range due to variations in composition and vesicularity in the samples measured, there could potentially be a wide range of property values that could be applied to a specific structure in the model. The two-dimensional petrophysical analysis was applied to test how well constrained the model properties of different structures are for the current model geometry, while the three-dimensional analysis calculated a range of model geometries that are possible within the bounds of the constraints.

We consider a structure to be petrophysically well constrained when only narrow range of properties can produce a model with a low level of misfit. If, for the given geometry, a wide range of petrophysical properties can produce an acceptable fit to the data, we consider that model region less well constrained. Results of the two-dimensional analysis suggest these models are generally well constrained for the given geometry, although some structures show greater sensitivity and are therefore better constrained than others. This is perhaps the most evident in the models of the Mt Leura Volcanic Complex, where lava flows have infilled the maar-tuff ring craters. The shallow lava flows are highly sensitivity to variations in their properties but tend to mask the geophysical response of the underlying diatremes. However, when considering these results, it is important to remember that these models are constructed in conjunction with, and also constrained by several other two-dimensional models running perpendicular to the plane of the profile. Some profiles show greater sensitivity than others due to variations in the thickness of lavas for example. A low sensitivity along the plane of a particular model does not necessarily suggest the solution is invalid, as there is some compromise between obtaining a low misfit and achieving results with consistent properties and geometries across multiple profiles.

Three-dimensional geometry inversions can help to optimise the geometry of the diatremes defined by the two-dimensional models, and will usually show greater sensitivity to deeper areas of the model because the inversion considers its 3D geometry, and data off the main profile of the two-dimensional model. The three-dimensional sensitivity analysis was conducted to understand how the geometry of a model could vary within the bounds of the property constraints. This is a good technique for understanding the range of possible model geometries; however, it is limited by the assumption that the residual geophysical anomaly is entirely the result of the geometry of the structure being inverted (in this case the diatreme). The three-dimensional models presented in Figure 6 represent a range of plausible geologic and geophysical solutions to the models described by Blaikie *et al.* (2014a, b). However these models are produced assuming all model misfit is caused by the diatreme. Further analysis could test how the geometry of other model structures could vary, and also if variations to other structures result in further variation to the geometry of the maar-diatreme. For this analysis to be easily achieved, further work is required to automate the inversion process, and perhaps utilise geodiversity techniques (e.g., Lindsay *et al.* 2013). The model suite could then be analysed based on the relationships between different model parameters such as petrophysical properties, depth and volume, which could identify certain characteristics that are required for a successful geophysical model.

5.1 Geologic implications of end-member models

The models presented by Blaikie *et al.* (2014a, b) represent the intermediate between the end-member models calculated in this work, and also integrate the results of geometry and heterogeneous inversion styles to account for property heterogeneities within the subsurface. For this reason, the models from Blaikie *et al.* (2014a, b) are still the preferred solutions, but it is important to recognise that the geometry of those structures could vary between the end-member models in Figure 6 if the properties of the subsurface deviate from what is expected.

If the geometry of the diatreme varied between the end-member models, there would be slightly different implications for processes and hazards occurring during the eruption. Blaikie *et al.* (2014b) discussed the implications of the different end-member models for the Ecklin maar, which would be similar for the different models for Mt Leura and Anakie. Blaikie *et al.* (2014b) suggested that the eruption of a maar and the formation of a shallow maar-diatreme represents a greater hazard than the formation of a deep maar-diatreme because it could potentially eject a higher volume of ash into the atmosphere. This conclusion is drawn from observations of exposed maar-diatremes (e.g., Lefebvre *et al.* 2013) and analogue experiments (e.g., Graettinger *et al.* 2014; Valentine *et al.* 2014) which show that shallow explosions (<200 m) are more likely to eject material from the crater. Deep explosions (>200 m) are confined by the crater and overlying debris, and are less likely to eject material from the crater but will result in the mixing of material through the diatreme fill (Valentine and White 2012; Valentine *et al.* 2014).

5.2 Application of sensitivity analysis to other settings

In the earlier stages of producing two- or three-dimensional models, the modeller must integrate the available geologic data into the geophysical model and make decisions on suitable geometries and property distributions. This can produce more reliable solutions than computer generated models as the modeller considers their geologic knowledge; however ambiguity still exists in these solutions because of uncertainty in the models input variables. A sensitivity analysis should therefore be routinely performed for every geophysical model produced, and the results clearly communicated so the wider geoscience community understands not only the potential that geophysical methods have for understanding the interior of the earth, but also the limitations of using such methods. The methods we have utilised here are not limited to testing the geometry of volcanic structures, and could be easily applied to test the robustness of, and potential geometric variations within other geophysical models, such as those built to understand larger-scale crustal architecture.

The techniques we have demonstrated for assessing model ambiguity are not exclusive to the two- or three-dimensional modelling environment in which they were conducted, and the petrophysical analysis could be conducted in three-dimensions while calculating end-member geometry variations could also be conducted in two-dimensions. The advantage of applying our approach is the ability to rapidly achieve and visualise results. Whilst modifying the petrophysical properties of individual regions of a three-dimensional model, and running a forward model to calculate the misfit is a straightforward process, it requires many steps to set up the model, run the inversion and visualise the results. The same results can be achieved and visualised in real time within GM-SYS in one step.

Modifying the geometry of a two-dimensional model in GM-SYS is also a straightforward process, but it relies on the user manually manipulating the model in an attempt to reduce the misfit. This can be a time-consuming process that relies largely on trial and error as different solutions are tested. It can also lead to biased results caused by a user trying to impose a preferred solution on the model. For this reason, we prefer using three-dimensional inversion techniques to automatically calculate a range of optimum model geometries within the constraints set by the user. The three-dimensional models are also considered more robust than the two-dimensional models because the inversion process considers the whole data set, not just data along the plane of the two-dimensional model. This means lithological boundaries can be better defined because the geophysical response of the structures three-dimensional geometry is accounted for. However, the three-dimensional inversion technique is not without its limitations, and tends to work better on structures with a simple relationship with their surroundings. Successful inversion results becomes much more complex and difficult to achieve when there are lots of intersecting geologic bodies (such as at the Lake Werowrap maar), and in these situations, two-dimensional modelling techniques are the preferred method for testing geometric variations. When optimising the three-dimensional geometry of a model, it is helpful to have a model that already has a relatively low degree of misfit to ensure realistic results and to prevent extreme changes in model geometry, however the misfit should not be so low as to restrict further inversion.

6. Conclusion

The sensitivity analyses were conducted on models previously presented by Blaikie et al. (2014a; b). These models represent the preferred solutions that not only have a low misfit, but are the most consistent with the available geologic data. However, like all potential field models, they suffer from non-uniqueness and required a sensitivity analysis to determine how well the models are constrained, and how they might vary due to uncertainties in the input variables. Results of the two-dimensional analyses suggest these models are fairly well constrained, although shallow structures such as dykes and magma ponds are better constrained than deeper structures such as the diatreme. Since the diatreme showed the greatest degree of ambiguity in the two-dimensional analyses, three-dimensional geometry inversions were applied to understand how the geometry of the diatreme could vary if the density varied from the expected value. Inversion results indicate that a maar-diatreme would be shallower than its reference model if its density was less than, and deeper if its density was greater than the reference model. However, these models are limited in that they assume a homogenous density distribution in the subsurface, and that all model misfit is a result of the structure to be inverted. Further work is required to assess how the maar-diatremes would vary in their geometry if the geometry of other structures in the model were also varied during the inversion.

7. References

Aitken A. R. A. & Betts P. G. 2009. Multi-scale integrated structural and aeromagnetic analysis to guide tectonic models: An example from the eastern Musgrave Province, Central Australia. *Tectonophysics* **476**, 418-435.

Aitken A. R. A., Betts P. G., Weinberg R. F. & Gray D. 2009. Constrained potential field modeling of the crustal architecture of the Musgrave Province in central Australia: Evidence for lithospheric strengthening due to crust-mantle boundary uplift. *J. Geophys. Res.* **114**, B12405.

Armit R. J., Ailleres L., Betts P. G., Schaefer B. F. & Blaikie T. N. 2014. High-heat geodynamic setting during the Palaeozoic evolution of the Mount Painter Province, SA, Australia: evidence from combined field structural geology and potential-field inversions. *Geophysical Journal International* **199**, 253-275.

Blaikie T. N., Ailleres L., Betts P. G. & Cas R. A. F. 2014a. A geophysical comparison of the diatremes of simple and complex maar volcanoes, Newer Volcanics Province, south-eastern Australia. *Journal of Volcanology and Geothermal Research* **276**, 64-81.

Blaikie T. N., Ailleres L., Betts P. G. & Cas R. A. F. 2014b. Interpreting subsurface volcanic structures using geologically constrained 3-D gravity inversions: Examples of maar-diatremes, Newer Volcanics Province, southeastern Australia. *Journal of Geophysical Research-Solid Earth* **119**, 3857-3878.

Blaikie T. N., Ailleres L., Cas R. A. F. & Betts P. G. 2012. Three-dimensional potential field modelling of a multi-vent maar-diatreme - the Lake Coragulac maar, Newer Volcanics Province, south-eastern Australia. *Journal of Volcanology and Geothermal Research* **235-236**, 70-83.

Cassidy J., France S. J. & Locke C. A. 2007. Gravity and magnetic investigation of maar volcanoes, Auckland volcanic field, New Zealand. *Journal of Volcanology and Geothermal Research* **159**, 153-163.

Clark D. A. 1983. Comments on magnetic petrophysics. *Australian Society of Exploration Geophysicists, Bulletin* **14**, 49-62.

Fullagar P. K., Pears G., Hutton D. & Thompson A. D. 2004. 3D gravity and aeromagnetic inversion for MVT lead-zinc exploration at Pillara, Western Australia. *Exploration Geophysics (Melbourne)* **35**, 142-146.

Fullagar P. K. & Pears G. A. 2007. Towards geologically realistic inversion. *In:* Milkereit B. ed. *Proceedings of Exploration 07: Fifth Decennial International Conference on Mineral Exploration*, pp. 444-460.

Fullagar P. K., Pears G. A. & McMonnies B. 2008. Constrained inversion of geologic surfaces--- pushing the boundaries. *The Leading Edge* **27**, 98-105.

Graettinger A. H., Valentine G. A., Sonder I., Ross P. S., White J. D. L. & Taddeucci J. 2014. Maar-diatreme geometry and deposits: Subsurface blast experiments with variable explosion depth. *Geochemistry, Geophysics, Geosystems* **15**, 740-764.

Jessell M. W., Valenta R. K., Jung G., Cull J. P. & Geiro A. 1993. Structural geophysics. *Exploration Geophysics* **24**, 599-602.

Lefebvre N. S., White J. D. L. & Kjarsgaard B. A. 2013. Unbedded diatreme deposits reveal maar-diatreme-forming eruptive processes: Standing Rocks West, Hopi Buttes, Navajo Nation, USA. *Bulletin of Volcanology* **75**, 1-17.

Lindner H., Gabriel G., tze H.-J., rgen, Kaeppler R. & Suhr P. 2006. Geophysical and geological investigation of maar structures in the Upper Lusatia region (East Saxony). *Zeitschrift der Deutschen Gesellschaft fur Geowissenschaften* **157**, 355-372.

Lindsay M. D., Jessell M. W., Ailleres L., Perrouty S., de Kemp E. & Betts P. G. 2013. Geodiversity: Exploration of 3D geological model space. *Tectonophysics* **594**, 27-37.

Lopez Loera H., Aranda-Gomez J. J., Arzate J. A. & Molina-Garza R. S. 2008. Geophysical surveys of the Joya Honda Maar (Mexico) and surroundings; volcanic implications. *Journal of Volcanology and Geothermal Research* **170**, 135-152.

Lorenz V. 1986. On the growth of maars and diatremes and its relevance to the formation of tuff rings. *Bulletin of Volcanology* **48**, 265-274.

McLean M. A. & Betts P. G. 2003. Geophysical constraints of shear zones and geometry of the Hiltaba Suite granites in the western Gawler Craton, Australia. *Australian Journal of Earth Sciences* **50**, 525-541.

Mrlina J., Kampf H., Kroner C., Mingram J., Stebich M., Brauer A., Geissler W. H., Kallmeyer J., Matthes H. & Seidl M. 2009. Discovery of the first Quaternary maar in the Bohemian Massif, Central Europe, based on combined geophysical and geological surveys. *Journal of Volcanology and Geothermal Research* **182**, 97-112.

Nabighian M. N., Ander M. E., Grauch V. J. S., Hansen R. O., LaFehr T. R., Li Y., Pearson W. C., Peirce J. W., Phillips J. D. & Ruder M. E. 2005a. Historical development of the gravity method in exploration. *Geophysics* **70**, 63ND-89ND.

Nabighian M. N., Grauch V. J. S., Hansen R. O., LaFehr T. R., Li Y., Peirce J. W., Phillips J. D. & Ruder M. E. 2005b. The historical development of the magnetic method in exploration. *Geophysics* **70**, 33ND-61ND.

Ross P. S., White J. D. L., Valentine G. A., Taddeucci J., Sonder I. & Andrews R. G. 2013. Experimental birth of a maar–diatreme volcano. *Journal of Volcanology and Geothermal Research* **260**, 1-12.

Schulz R., Buness H., Gabriel G., Pucher R., Rolf C., Wiederhold H. & Wonik T. 2005. Detailed investigation of preserved maar structures by combined geophysical surveys. *Bulletin of Volcanology* **68**, 95-106.

Skacelova Z., Rapprich V., Valenta J., Hartvich F., Sramek J., Radon M., Gazdova R., Novakova L., Kolinsky P. & Pecskay Z. 2010. Geophysical research on structure of partly eroded maar volcanoes; Miocene Hnojnice and Oligocene Rychnov volcanoes (northern Czech Republic). *Journal of Geosciences* **55**, 333-345.

Valenta R. K., Jessell M. W., Jung G. & Bartlett J. 1992. Geophysical interpretation and modelling of three-dimensional structure in the Duchess area, Mount Isa, Australia. *Exploration Geophysics (Melbourne)* **23**, 393-339.

Valentine G. A., Graettinger A. H. & Sonder I. 2014. Explosion depths for phreatomagmatic eruptions. *Geophysical Research Letters*, 2014GL060096.

Valentine G. A. & White J. D. L. 2012. Revised conceptual model for maar-diatremes: Subsurface processes, energetics, and eruptive products. *Geology* **40**, 1111-1114.

White J. D. L. & Ross P. S. 2011. Maar-diatreme volcanoes: A review. *Journal of Volcanology and Geothermal Research* **201**, 1-29.

Whiting T. H. 1986. Aeromagnetics as an aid to geological mapping - a case history from the Arunta Inlier, Northern Territory. *Australian Journal of Earth Sciences* **33**, 271-286.

Williams H. A., Betts P. G. & Ailleres L. 2009. Constrained 3D modeling of the Mesoproterozoic Benagerie Volcanics, Australia. *Physics of the Earth and Planetary Interiors* **173**, 233-253.

Chapter 6.

Summary of results and research implications

Cover page: The Anakie maar and scoria cone complex

1. Introduction

This research presents a method and results for modelling the subsurface architecture of volcanic systems using high-resolution gravity and magnetic data. The research was focussed specifically on modelling the diatremes of several maar volcanoes in the Newer Volcanics Province of south-eastern Australia, and provides new insights into how a diatremes depth and its internal structures relate to its eruptive style.

This final chapter summarises the results and conclusions of the previous research chapters, and relates them to the aims of the research project outlined in chapter 1. The implications of these results for understanding the subsurface structures and volcanic hazards related to maar-volcanoes within south-eastern Australia, and elsewhere are discussed. Our results are also placed in a broader context, and discuss the implications our modelling technique could have for future volcanological studies. Finally, suggestions are made for further research on the volcanic centres examined in this thesis, and in utilising our modelling techniques.

2. Summary of chapter 2: Interpreting volcanic structures using 3D potential field inversions

This chapter was published in the *Journal of Geophysical Research-Solid Earth* (see reference: Blaikie *et al.* 2014b), and presents an interpretation and modelling workflow to understand the subsurface structures of maar volcanoes using potential field data. Techniques for data and image processing, as well as two-dimensional and three-dimensional modelling of the subsurface are discussed. The main points of this chapter are:

- Prior to acquiring geophysical data across the maar volcanoes, some understanding of the wavelength of the gravity anomalies related to the diatreme and its feeder vents was needed so a field survey could be designed with a resolution suitable for imaging those structures. Several synthetic models of maar-diatremes were produced to understand their theoretical gravity response which helped estimate the wavelengths of different structures, and determine the optimum gravity station spacing and location of traverses.
- A workflow for the interpretation and modelling of potential field data was presented. This technique integrates interpretations from gridded data, 2D and 3D modelling, and uses the results of earlier inverse models to drive the next inversion. This produces more robust and constrained models that have the potential to reveal new and more accurate information about the subsurface architecture of volcanic systems.
- High-resolution gravity and magnetic data was acquired over the Ecklin maar, and the Red Rock and Mt Leura Volcanic Complexes. The geophysical surveys reveal gravity lows over the volcanic craters which reflect the lower density lake sediments and pyroclastic debris infilling the crater and diatreme. Superimposed on these gravity lows are short-wavelength positive gravity anomalies with corresponding magnetic anomalies, which were observed at Red Rock and Mt Leura and were interpreted to be dykes with a higher density and magnetic susceptibility than the surrounding diatreme and host rock. Longer-wavelength but lower-amplitude positive anomalies were identified at Ecklin maar, and were interpreted to be caused

by vents with a similar composition to the diatreme, but containing slightly higher proportions of volcanic debris.

- The diatreme geometries were interpreted using 2.5D forward, and 3D inverse modelling techniques and are constrained by geologic information including density and magnetic susceptibility measured from hand samples, surface geology, and the interpretation of digital elevation models and regional scale geophysical data sets. Results suggest these volcanic centres are underlain by shallow, coalesced diatremes that contain complex internal structures which reflect their individual eruptive histories. (Results further summarised in chapter 3 below).
- The geophysical models presented in this chapter represent best-fit models obtained after a series of inversions, however they are non-unique and subject to ambiguity. Sensitivity analyses assessed how well the models were constrained, and how they could vary their properties and geometry within the bounds of the constraints. Results suggest that the Ecklin maar-diatreme could potentially vary between 350 m and 1000 m in depth depending on inversion parameters. This concept is explored further in chapter 4.

3. Summary of chapter 3: A geophysical comparison of simple and complex maar volcanoes

Chapter 3 was published in the *Journal of Volcanology and Geothermal Research* (see reference: Blaikie *et al.* 2014a), and focuses on what was learned about the eruptive history of each maar from the interpretation of geophysical data. The main findings of this chapter are:

- Ecklin maar is characterised by a Bouguer gravity low with a larger amplitude in the southern part of the crater, suggesting the underlying diatreme is deeper in this area of the maar. Two low amplitude gravity highs are superimposed on the gravity low, and correlate with two magnetic high's aligned in the same direction as the long-axis of the maar. Geophysical modelling suggests the diatreme is comprised of two coalesced diatreme structures, with margins that are shallowly sloped and flared in the upper 300 metres, and more steeply dipping below this. Within the centre of the diatreme are two denser zones, interpreted to contain a higher proportion of juvenile material due to the entrainment of debris jets within the diatreme fill.
- The maars contained within the Red Rock Volcanic Complex exhibit complex and highly varied geophysical responses. The Lake Werowrap maar is characterised by a Bouguer gravity high superimposed with several shorter-wavelength, higher-amplitude gravity highs with corresponding magnetic anomalies of a similar wavelength. The Lake Purdigulac maar consists of a Bouguer gravity low, but contains a north-south trending linear gravity anomaly, with a correlating magnetic anomaly which is interpreted to represent the deeper feeder system of the volcanic center. The other maars within the complex have a relatively neutral response, comprised of longer wavelength anomalies. Modelling of the maars identified multiple coalesced diatremes with complex internal structures consisting of dykes and magma ponds. Pyroclastic deposits indicate that the eruption style of the growing maars frequently fluctuated between magmatic and phreatomagmatic explosive activity, suggesting that at some point during the eruption, dykes would have risen through the maar-diatreme to the near surface which is consistent with the geophysical models. Coalesced diatremes suggests lateral vent

migration was frequently occurring during the eruption of the complex.

- The Mt Leura Volcanic Complex exhibits a complex geophysical response that reflects its variable eruption styles. The maar crater in the south of the complex shows a neutral to low gravity response and a magnetic low, reflecting the lower density/magnetic susceptibility of pyroclastic deposits within the maar-diatreme. Modelling of these anomalies suggests that the diatremes underlying the Mt Leura Volcanic Complex are broad and shallow. Confined mostly within the extent of the tuff ring is a Bouguer gravity high, which modelling suggests is the result of the infilling of the tuff ring with denser lava flows, as well as welded spatter and scoria during the effusive and explosive magmatic activity in the later stages of the eruption.
- The Anakie maar has a relatively simple geophysical response, characterised by a gravity and magnetic low. Modelling results suggest a shallow maar-diatreme underlies the crater which is broad with shallowly dipping diatreme walls in the north, becoming more steeply dipping in the south where the diatreme reaches its maximum depth. The simple geometry of the maar diatreme is attributed to a very short lived eruptive phase with relatively stable conduit conditions that prevented lateral and vertical vent migration.
- The diatremes of each case study show similarities in their structure, being generally coalesced, broad and shallow. Coalesced diatremes suggests that lateral vent migration is occurring within the subsurface, and is interpreted to be a result of a weakly lithified host rock collapsing into and blocking the active vent, causing it to migrate elsewhere. Broad, shallow diatremes suggest an eruption where magma-water interaction remained at shallow levels, rather than propagating downwards, and can also be attributed to a water saturated, weakly lithified host rock. Internal structures within the diatremes (vents, dykes and magma ponds) are variable between the different volcanic centres, and reflect differences in the eruptive histories and styles of these volcanoes. For example, the presence of shallow dykes modelled within the diatremes, and the observed fluctuating eruptive styles at the Red Rock Volcanic Complex suggest that explosive fragmentation occurred at varied levels and migrated laterally along irregularly shaped intrusions within the diatremes.

4. Summary of chapter 4: Calculating the total erupted tephra and magma volume of maar volcanoes

This chapter uses results from the geophysical models to estimates the total magma and ejected tephra volumes of the maar volcanoes. The results of these calculations were used to estimate the volcanic explosivity index (VEI) of each eruption. The main conclusions of this chapter are:

- The total volume of erupted tephra at the Red Rock Volcanic Complex is 0.10 x 10^9 m^3, with 0.065 x 10^9 m^3 being derived from phreatomagmatic activity, and 0.037 x 10^9 m^3 from magmatic activity. Based on the componentry of these deposits, the total volume of erupted magma (dense rock equivalent) is 0.029 x 10^9 m^3. The underlying diatremes have a combined volume of 0.38 x 10^9 (excluding intra-diatreme dykes and magma ponds which have a volume of 0.022 x 10^9 m^3). Assuming a similar composition to the ejecta rims, the total subsurface magma volume of the complex is 0.15 x 10^9 m^3. This yields a total magma volume for Red Rock of 0.18 x 10^9 m^3.

- Ecklin maar has a total deposit volume of 0.056 x 10^9 m^3, and a bulk diatreme volume of 0.13 x 10^9 m^3, of which 0.012 x 10^9 m^3 is contained with the two central vents. The subsurface and erupted magma volumes are 0.031 x 10^9 m^3 and 0.012 x 10^9 m^3 respectively, which gives a total volume of approximately 0.043 x 10^9 m^3.
- The diatremes of the Mount Leura Volcanic Complex have a combined bulk volume of 0.58 x 10^9 m^3. The volume of dykes and lava flows infilling the maar-tuff ring craters is 0.095 x 10^9 m^3. The volume of the scoria cone complex is estimated at 0.07 x 10^9 m^3, which equates to a dense rock equivalent magma volume of 0.011 x 10^9 m^3. The total volume of magma contained within the complexes subsurface structures is 0.28 x 10^9 m^3, and the total magma volume for the complex (excluding the ejecta-rim) is 0.29 x 10^9 m^3.
- A VEI magnitude of 2 is assigned to Ecklin maar, and 3 to the Red Rock and Mount Leura volcanic complexes based on the total erupted tephra volumes, and estimates of the eruption column heights by comparison with analogue volcanic centres.

5. Summary of chapter 5: Using sensitivity analysis to assess model ambiguity and variability

Potential field models are non-unique, so this chapter applies a sensitivity analysis to the geophysical models in chapters 2 and 3 to determine how well the models are constrained, where ambiguity lies in the interpretations, and calculate end-member model geometries. The main conclusions of this chapter are:

- Sensitivity analyses assessed how the maar-diatreme models could vary if the input variables deviate from the apriori model. This helped identify which structures in the models were well constrained in terms of their geometry and petrophysical properties, and delineated a range of end-member models that satisfied the geophysical and geologic data.
- Sensitivity analyses of the 2.5D forward models indicate that the models are well constrained for a fixed geometry because the range of allowable petrophysical properties are relatively small. However, some model structures have a low sensitivity, and variations to the properties or geometry produces little variation to the calculated response, which indicates these structures are not as well constrained as the rest of the model. This is either due to a low petrophysical contrast with their surroundings, or because overlying lava flows, or ponded magma mask the geophysical response of underlying structures. This is evident in the models of the Mt Leura Volcanic Complex and Lake Werowrap maar at the Red Rock Volcanic Complex.
- In addition to determining how well constrained a model is, variations to the density and susceptibility of different model regions such as the dykes and lavas emphasise the wavelengths of the anomalies related to these structures. This helps ensure that the calculated anomaly wavelengths are related to the structure of interest, and any errors in the size/position of these structures are not compensated for by altering the properties/geometry of surrounding structures.
- The 3D sensitivity analysis calculated a range of maar-diatreme geometries using 3D gravity inversions to assess how it could vary if the density was over or under estimated. This analysis

revealed that the Ecklin maar-diatreme could potentially range between 350 and 1000 m deep. The Mt Leura maar-diatreme could range between 360 and 550 m deep, while Anakie could range between 160 and 230 m deep. This has implications for the eruptive hazards of the maar, with the shallow maar-diatreme models potentially ejecting a higher volume of ash into the atmosphere compared to the deeper maar-diatreme models.

6. Research implications

The major aims of this thesis were to use geophysical modelling techniques to determine the depth and geometry of the maar-diatreme, and identify what control, if any, the host rock had on its formation. The findings of this research show that although maars are small-volume volcanic eruptions with relatively simple morphologies, they can exhibit great complexities in their subsurface structures and eruptive histories. Geophysical modelling identified that these maar-diatremes are comprised of multiple coalesced vents and contain complex internal structures consisting of dykes, ponded magma, and subvertical zones enriched in juvenile material. Recognising these features has major implications for the application of geophysical techniques in understanding the structure and formation of maar volcanoes, and other volcanic systems. Additionally, this research provides clues about the behaviour of magma in the shallow subsurface as it migrates, fragments and erupts. This knowledge is essential in order to predict the potential range of future eruptive scenarios within the Newer Volcanics Province and elsewhere.

6.1 Application of modelling techniques to other volcanic systems

This research has presented a method for understanding the subsurface morphology of maar volcanoes, by modelling the density and magnetic susceptibility distribution within the subsurface. The novelty of the technique we have applied is the ability to integrate results from geologic observations, image interpretation, two-dimensional, and three-dimensional modelling, all within an environment where the user has control over the model. This process can lead to much more reliable results than computer generated solutions because the modeller can constantly integrate their geologic knowledge into the solution, and ensure results are realistic.

The modelling workflow can be readily applied to other volcanic systems, from smaller scale monogenetic centres, such as is examined in this thesis, to larger scale systems such as calderas, and even their magma chambers provided high resolution data can be obtained by either ground or airborne techniques. It is hoped that with the further application of the techniques presented in this thesis, advances can be made in understanding the subsurface architecture of volcanoes, so that eruptive processes are better understood which will lead to an improved assessment of volcanic hazards.

In addition, aspects of our interpretation technique could also be useful to understand the larger scale structure of volcanic fields by mapping products of volcanism and identifying the location and orientation of faults, which may have been used by magma as a conduit to the surface. Regional scale aeromagnetic and gravity data sets have been used to achieve this (e.g., Lopez Loera *et al.* 2008; Cassidy and Locke 2010; Barde-Cabusson *et al.* 2013), but further application of two- and even three-dimensional modelling can provide a further understanding of crustal structure, which when integrated with geodynamic modelling techniques, could help identify triggers for volcanic activity within monogenetic volcanic fields.

6.2 Implication on the structure, formation and understanding the complexity of maar-diatremes

The complex geometry of the diatreme and its internal structures represent different, but intrinsically linked processes are occurring within the subsurface. These processes include lateral and vertical vent migration, and fluctuations in eruptive style, which are both influenced by the properties of the host rock. The Red Rock Volcanic Complex, Mt Leura Volcanic Complex and the Ecklin maar are all hosted within weakly lithified sediments of the Otway Basin. Broad and shallow diatremes are observed at these volcanic centres, and form because the host rock is unable to sustain steeply dipping diatreme walls, and will collapse and flow into the crater during the eruption (Lorenz 2003; Auer *et al.* 2007; Ross *et al.* 2011). This contributes to the widening of the crater, whilst the collapse of material provides further influx of water into the diatreme to fuel phreatomagmatic explosions (Auer *et al.* 2007). The collapse of the wall rock into the diatreme is also thought to trigger lateral vent migration at these volcanoes as its blocks the active vent and results in the magma migrating laterally as it finds a new pathway to the surface (Sohn and Park 2005).

In some cases, the multiple vents are irregularly distributed within the maar crater (e.g., Lakes Purdigulac and Coragulac, Red Rock), and indicate that dykes may be propagating irregularly through the loose debris of the diatreme fill. Aligned vents are observed in some of the geophysical models, occurring either within the diatreme, or resulting in multiple aligned craters (e.g., Red Rock, Anakie), which would suggest that vent migration is occurring along the length of dyke, which in some cases, appear to be exploiting pre-existing crustal structures as a conduit to the surface.

Chapters two and three discuss the complex eruptive processes of these volcanic centres in more detail, and the implications they have for the currently evolving models for diatreme growth. Our results support the newly revised model for diatreme formation proposed by Valentine and White (2012). This model suggests that phreatomagmatic explosions may occur within any level of the diatreme at any time during the eruption, assuming the diatreme fill is fully saturated with water. Dykes may extend into the fill of the diatreme, which due to its heterogeneous and unconsolidated nature result in irregular shaped intrusions. These dykes form new sites for phreatomagmatic explosions in what is termed an 'intra-diatreme fragmentation zone' (White and Ross 2011). The ejection of material from the maar crater occurs most effectively when explosions are near-surface, and progressive mixing within the diatreme occurs as debris jets transport material upwards through material that is subsiding downwards.

We observe these features in our models in the form of areas of increased density/magnetic susceptibility within the centre of the Ecklin maar-diatreme. These were interpreted to represent a juvenile rich zone which formed as explosions within the root or intra-diatreme fragmentation zones formed debris jets which were progressively mixed upwards into the diatreme fill during the eruption. The presence of dykes and ponded magma within the diatremes, particularly at the Red Rock Volcanic Complex, represent the intra-diatreme fragmentation zones described in the revised diatreme growth model. The presence of these intra-diatreme dykes, and observations of fluctuating eruptive styles, suggest the developing diatremes were not completely saturated with water during the eruption, which allowed to magma to fragment by either magmatic or phreatomagmatic styles when conditions were appropriate.

6.3 Implications for understanding the volume of monogenetic eruptions

Of the total number of eruptions within a volcanic field, maar volcanoes can comprise between 0-10% in arid climates, 20-30% in wetter climates, and up to 70% in partially marine settings (Brown and Valentine 2013). Volumetrically, they are therefore an important component of a volcanic field, however, estimates of the bulk diatreme, total tephra and magma volumes of maar volcanoes are poorly constrained due to uncertainty in the size of their subsurface structures, and rapid erosion of the volcanic edifice (Kereszturi *et al.* 2013). At the scale of an individual eruption, the total tephra and magma volumes are essential parameters for calculating the magnitude and energy budget of a volcanic eruption (e.g., van Otterloo and Cas 2013; Valentine *et al.* 2014). At the scale of a volcanic field, accurate volume estimates are an important constraint for spatio-temporal studies and in understanding long-term magma-flux within the field (Kereszturi *et al.* 2013), and therefore, the magma volume associated with maars and their diatremes should not be neglected. Recently, attempts have been made to estimate the volume of maar-diatremes, and their contribution to the total volume of a volcanic field based on an inverted cone model and their crater dimensions (Kereszturi *et al.* 2013; Lefebvre *et al.* 2013). Our results indicate that, even when the surface morphology is relatively simple, maar-diatremes can have complex geometries and contain multiple vents, and caution is suggested when inferring simple diatreme geometries for volume estimates.

6.4 Volcanic hazards within south-eastern Australia

There is potential for renewed eruptive activity within the Newer Volcanics Province, with the youngest dated eruption recorded at ~4.5 ka at the Mt Gambier Volcanic Complex (van Otterloo and Cas 2013), and an eruption occurring approximately every 10,800 years (Cas *et al.* 2011; Boyce 2013). Other facts such as an increased heat-flow in the region (Graeber *et al.* 2002), and an upwelling of mantle-derived CO_2 in south-eastern South Australia (Chivas *et al.* 1987), and Daylesford in Western Victoria (Cartwright *et al.* 2002) confirm this is still an active volcanic field. This research provides an improved understanding of eruptive processes occurring within maar volcanoes and their subsurface structures, which allows for a better understanding the nature and scale of future eruptions and their associated hazards. While any future eruption in the region will be hazardous, an eruption of a maar volcano poses the greatest threat because it is highly explosive, can develop lethal base surges and pyroclastic flows and distribute large volumes of fine ash in the atmosphere (Lorenz 2007).

This research focussed on the subsurface structure of maar volcanoes and the implications for the eruption, and recognised that some maars within the province are associated with shallow diatremes. This implies that the phreatomagmatic explosions that formed the maar were largely confined to shallow levels. Shallow explosions (<200 m) pose a greater hazard because they have an increased potential of erupting and depositing material in the ejecta rim, whereas deep explosions (>200 m) are unlikely to erupt, but will facilitate mixing of material upwards through the diatreme (e.g., Graettinger *et al.* 2014; Valentine *et al.* 2014). Depending on the energy of these shallow phreatomagmatic explosions, and the height of eruption column, the fraction of tephra dispersed downwind, could in fact, be quite high.

The eruption magnitude of the Red Rock, Mt Leura and Ecklin maars range between 2 and 3 on the Volcanic Explosivity Index. These estimates suggest that the sizes of these eruptions are comparable to the 1977 eruption of the Ukinrek maars in Alaska, which produced eruption columns up to 6 km in height and deposited fine ash at least 160 km from the vent (Self *et al.* 1980). Other eruptions, such as at Mt Gambier, Tower Hill and Lake Purrumbete are volumetrically similar to the eruption of Eyjafjallajokull, Iceland 2010 (van Otterloo and Cas 2013). With winds predominantly coming from the west, a future phreatomagmatic eruption with an intensity similar to any of these eruptions, could significantly affect major cities such as Melbourne, Sydney, Canberra and perhaps even New Zealand by disrupting air travel to and from the region, and impacting upon the health of those living in the area.

7. Suggestions for further research

This research presents a method for understanding the subsurface morphology of volcanoes, and contributed to the understanding of the structure, formation and magma volumes of the Ecklin Maar, Red Rock Volcanic Complex, Mount Leura Volcanic Complex and the Anakies. It has also contributed to a further understanding of the magma volumes of monogenetic volcanoes, and the hazards related to their eruption. However, due to the scope and timeframe of this research project, there is still further opportunity expand upon this work, and further advance our understanding of each of the case studies examined in this thesis, of maar-diatreme volcanism in general, and of the subsurface architecture of volcanoes. Topics of further research include:

- ***The physical volcanology of the Ecklin maar, Red Rock Volcanic Complex, Mt Leura Volcanic Complex and the Anakies.*** There has been some previous research conducted on the stratigraphy, petrology and geochemistry of these volcanic centres (e.g., Shaw-Stuart 2005; Cheesman 2007; Piganis 2011; Roche 2011; Uehara 2011). However, there is further opportunity to expand upon these works, and the research conducted in this thesis to better understand the eruptive histories, triggers for fluctuating eruptive styles, and dispersal of volcanic products. To achieve this, future work could involve more detailed studies on the stratigraphy, petrography and geochemistry to complement previous work, and could include new research on palaeomagnetics, aquifer dynamics and thermodynamic, and eruption plume modelling.
- ***Model uncertainty and geodiversity.*** The sensitivity analysis of the geophysical models identified the upper and lower bounds of possible maar-diatreme geometries. Further analysis could test how the geometry of other model structures could vary, and also if variations to those structures result in further variation to the geometry of the maar-diatreme. For this analysis to be easily achieved, further work is required to automate the inversion process, and perhaps utilise geodiversity techniques (e.g., Lindsay *et al.* 2013) to analyse the model suite based on the relationships between different model parameters such as petrophysical properties, depth and volume. This may help identify certain characteristics that are required for a successful geophysical model, and identify model outliers.
- ***Validation of the geophysical models.*** The geophysical models produced in this thesis were constrained from geologic observations and petrophysical properties collected from the surface. However, maar-diatremes can be highly variable structures, and to further constrain the models we have produced, it is necessary to drill into each of the maar craters. This will provide important petrophysical and componentry data as well as the depth to major boundaries within

the diatreme which will be highly useful in updating the geophysical models. Additionally, other types of geophysical surveys such as ground penetrating radar, seismic, electromagnetic and resistivity could be employed to help constrain the potential field models.

- ***Application of airborne magnetics and gravity gradiometry in monitoring the growth of maar-diatremes.*** The modelling technique we present relies heavily on being able to access the crater of the volcanoes being studies. However this is not always possible in volcanic terrains, which can be very rugged, and may also contain a crater lake. As airborne gravity gradiometry data acquisition improves, it will be possible to rapidly acquire high resolution gravity data across volcanoes that were previously inaccessible for this sort of study. Additionally, it could be possible to monitor the formation of a maar volcano by acquiring airborne magnetic and gravity data across the crater during different stages of the eruption.

8. References

Auer A., Martin U. & Németh K. 2007. The Fekete-hegy (Balaton Highland Hungary) "soft-substrate" and "hard-substrate" maar volcanoes in an aligned volcanic complex - Implications for vent geometry, subsurface stratigraphy and the palaeoenvironmental setting. *Journal of Volcanology and Geothermal Research* **159**, 225-245.

Barde-Cabusson S., Gottsmann J., Martí J., Bolós X., Camacho A. G., Geyer A., Planagumà L., Ronchin E. & Sánchez A. 2013. Structural control of monogenetic volcanism in the Garrotxa volcanic field (Northeastern Spain) from gravity and self-potential measurements. *Bulletin of Volcanology* **76**, 1-13.

Blaikie T. N., Ailleres L., Betts P. G. & Cas R. A. F. 2014a. A geophysical comparison of the diatremes of simple and complex maar volcanoes, Newer Volcanics Province, south-eastern Australia. *Journal of Volcanology and Geothermal Research* **276**, 64-81.

Blaikie T. N., Ailleres L., Betts P. G. & Cas R. A. F. 2014b. Interpreting subsurface volcanic structures using geologically constrained 3-D gravity inversions: Examples of maar-diatremes, Newer Volcanics Province, southeastern Australia. *Journal of Geophysical Research-Solid Earth* **119**, 3857-3878.

Boyce J. 2013. The Newer Volcanics Province of southeastern Australia: a new classification scheme and distribution map for eruption centres. *Australian Journal of Earth Sciences* **60**, 449-462.

Brown R. J. & Valentine G. A. 2013. Physical characteristics of kimberlite and basaltic intraplate volcanism and implications of a biased kimberlite record. *Geological Society of America Bulletin* **125**, 1224-1238.

Cartwright I., Weaver T., Tweed S., Ahearne D., Cooper M., Czapnik K. & Tranter J. 2002. Stable isotope geochemistry of cold CO2-bearing mineral spring waters, Daylesford, Victoria, Australia: sources of gas and water and links with waning volcanism. *Chemical Geology* **185**, 71-91.

Cas R. A. F., Blaikie T., Boyce J., Hayman P., Jordan S., Piganis F., Prata G. & van Otterloo J. 2011. VF01: Factors that influence varying eruption styles (from magmatic to phreato-magmatic) in intraplate continental basaltic volcanic provinces: the Newer Volcanics Province of south-eastern Australia. *IUGG 2011 Fieldtrip guide*.

Cassidy J. & Locke C. A. 2010. The Auckland volcanic field, New Zealand; geophysical evidence for structural and spatio-temporal relationships. *Journal of Volcanology and Geothermal Research* **195**, 127-137.

Cheesman A. 2007. The nature of transitions between magmatic and phreatomagmatic explosive volcanism at the Red Rock Volcanic Complex, Newer Volcanics Province, Southeastern Australia. Masters thesis, Monash University, Australia (unpubl.).

Chivas A. R., Barnes I., Evans W. C., Lupton J. E. & Stone J. O. 1987. Liquid carbon dioxide of magmatic origin and its role in volcanic eruptions. *Nature* **326**, 587-589.

Graeber F. M., Houseman G. A. & Greenhalgh S. A. 2002. Regional teleseismic tomography of the western Lachlan Orogen and the Newer Volcanic Province, southeast Australia. *Geophysical Journal International* **149**, 249-266.

Graettinger A. H., Valentine G. A., Sonder I., Ross P. S., White J. D. L. & Taddeucci J. 2014. Maar-diatreme geometry and deposits: Subsurface blast experiments with variable explosion depth. *Geochemistry, Geophysics, Geosystems* **15**, 740-764.

Kereszturi G., Németh K., Cronin S. J., Agustín-Flores J., Smith I. E. M. & Lindsay J. 2013. A model for calculating eruptive volumes for monogenetic volcanoes — Implication for the Quaternary Auckland Volcanic Field, New Zealand. *Journal of Volcanology and Geothermal Research* **266**, 16-33.

Lefebvre N. S., White J. D. L. & Kjarsgaard B. A. 2013. Unbedded diatreme deposits reveal maar-diatreme-forming eruptive processes: Standing Rocks West, Hopi Buttes, Navajo Nation, USA. *Bulletin of Volcanology* **75**, 1-17.

Lindsay M. D., Jessell M. W., Ailleres L., Perrouty S., de Kemp E. & Betts P. G. 2013. Geodiversity: Exploration of 3D geological model space. *Tectonophysics* **594**, 27-37.

Lopez Loera H., Aranda-Gomez J. J., Arzate J. A. & Molina-Garza R. S. 2008. Geophysical surveys of the Joya Honda Maar (Mexico) and surroundings; volcanic implications. *Journal of Volcanology and Geothermal Research* **170**, 135-152.

Lorenz V. 2003. Maar-Diatreme Volcanoes, their Formation, and their Setting in Hard-rock or Soft-rock Environments. *Geolines* **15**, 72-83.

Lorenz V. 2007. Syn- and posteruptive hazards of maar-diatreme volcanoes. *Journal of Volcanology and Geothermal Research* **159**, 285-312.

Piganis F. 2011. A volcanological investigation of the polymagmatic Red Rock Volcanic Complex and a 3D geophysical interpretation of the subsurface structure and geology of the poly-lobate Lake Purdigulac maar, Newer Volcanics Province, southeastern Australia. Masters thesis, Monash University, Australia (unpubl.).

Roche L. 2011. Volcanological evolution and subsurface structure of a maar. Honours thesis, Monash University, Australia (unpubl.).

Ross P.-S., Delpit S., Haller M. J., Nemeth K. & Corbella H. 2011. Influence of the substrate on maar-diatreme volcanoes; an example of a mixed setting from the Pali Aike volcanic field, Argentina. *Journal of Volcanology and Geothermal Research* **201**, 253-271.

Self S., Kienle J. & Huot J.-P. 1980. Ukinrek Maars, Alaska, II. Deposits and formation of the 1977 craters. *Journal of Volcanology and Geothermal Research* **7**, 39-65.

Shaw-Stuart A. 2005. Transition from phreatomagmatic maar forming explosive activity to magmatic scoria cone complex forming activity in the Pleistocene Mt Leura Volcanic Complex, southeastern Australia. Masters thesis, Monash University, Australia (unpubl.).

Sohn Y. K. & Park K. H. 2005. Composite tuff ring/cone complexes in Jeju Island, Korea: possible consequences of substrate collapse and vent migration. *Journal of Volcanology and Geothermal Research* **141**, 157-175.

Uehara D. 2011. Geophysical and volcanological study on the Mount Leura Volcanic Complex of the Newer Volcanics Province, south western Victoria. Honours thesis, Monash University, Australia (unpubl.).

Valentine G. A., Graettinger A. H. & Sonder I. 2014. Explosion depths for phreatomagmatic eruptions. *Geophysical Research Letters*, 2014GL060096.

Valentine G. A. & White J. D. L. 2012. Revised conceptual model for maar-diatremes: Subsurface processes, energetics, and eruptive products. *Geology* **40**, 1111-1114.

van Otterloo J. & Cas R. F. 2013. Reconstructing the eruption magnitude and energy budgets for the pre-historic eruption of the monogenetic ~5 ka Mt. Gambier Volcanic Complex, south-eastern Australia. *Bulletin of Volcanology* **75**, 1-18.

White J. D. L. & Ross P. S. 2011. Maar-diatreme volcanoes: A review. *Journal of Volcanology and Geothermal Research* **201**, 1-29.

Appendix 1.

Three-dimensional potential field modelling of a multi-vent maar-diatreme. The Lake Coragulac maar, Newer Volcanics Province, south-eastern Australia

Blaikie T. N., Ailleres L., Cas R. A. F. & Betts P. G.

Journal of Volcanology and Geothermal Research, 235-236 (2012);
doi: 10.1016/j.jvolgeores.2012.05.002

Cover page: The Lake Coragulac maar, Red Rock Volcanic Complex.

Journal of Volcanology and Geothermal Research 235–236 (2012) 70–83

Contents lists available at SciVerse ScienceDirect

Journal of Volcanology and Geothermal Research

journal homepage: www.elsevier.com/locate/jvolgeores

Three-dimensional potential field modelling of a multi-vent maar-diatreme — The Lake Coragulac maar, Newer Volcanics Province, south-eastern Australia

Teagan N. Blaikie *, Laurent Ailleres, Ray A.F. Cas, Peter G. Betts

School of Geosciences, Monash University, Clayton, Victoria, 3800, Australia

A R T I C L E I N F O

Article history:
Received 13 December 2011
Accepted 2 May 2012
Available online 14 May 2012

Keywords:
Maar
Diatreme
Gravity
Magnetic
Potential field inversions
Newer Volcanics Province

A B S T R A C T

High resolution gravity and magnetic data have been acquired across Lake Coragulac, a Quaternary maar volcano located in the Newer Volcanics Province of south-eastern Australia. A gravity low is observed across the maar crater, with several local gravity highs identified in the centre of the crater, often with corresponding magnetic anomalies. Geophysical data has been integrated with geologic observations and subjected to 2D forward and 3D inverse potential field modelling. Modelling has revealed a complex subsurface maar structure with four coalesced diatremes and several intrusive dykes identified. The modelled diatremes are shallow (maximum of 290 m deep) with the margins having a similar density to the host rock, while the diatreme centre is often denser, indicating that higher volumes of volcanic debris are present.

Deposits of the maar rim sequence show frequent transitions between phreatomagmatic and magmatic fragmentation styles, a result of fluctuations in magma rise rate and interactions with external water. The complex nature of the underlying maar-diatreme suggests that the maar formed from at least four vents which migrated laterally during the eruption.

1. Introduction

Potential field geophysical modelling can be used to image subsurface geologic features and its application to volcanology may contribute to a better understanding of the internal structure and evolution of a volcanic centre. Maar-diatremes are formed by the interaction of magma with groundwater, with explosive fragmentation occurring at some depth below the surface resulting in the excavation of a volcanic crater in which host rock and pyroclastic debris collapse into (Lorenz, 1975, 1986, 2003). The morphology of maar volcanoes (broad crater surrounded by a gently dipping ring of tephra) are well suited for geophysical surveying compared to cone-shaped volcanoes as the low topographic profiles mean that the effects of terrain on the gravity response are minimal. Understanding the relationships between the eruptive styles of a maar volcano, its deposits, morphology, diatreme geometry and feeder vents are important for an improved understanding of maar-diatreme volcanism.

The Cainozoic Newer Volcanics Province of Western Victoria is an intraplate basaltic volcanic province composed of over 400 monogenetic volcanoes (Joyce, 1975; Cas, 1989; Cas et al., 1993, 2011). Approximately 40 maar volcanoes have been identified, all of which have their original edifice preserved and no exposure of the underlying maar-diatreme (Joyce, 1975). Where no exposure of the diatreme exists, the application of geophysical modelling techniques can provide a method to model the geometry of a maar-diatreme, its feeder dykes and any intrusions (Lindner et al., 2006; Cassidy et al., 2007). Geophysical modelling can be applied to older maar volcanoes where there is some exposure of the diatreme (e.g. Skacelova et al., 2010), however the original edifice is often completely eroded and observations cannot be directly linked with surface deposits preserved in younger maar volcanoes elsewhere. This study illustrates a methodology to improve this knowledge gap by examining the relationships between surface deposits and the subsurface morphology of a maar volcano in order to gain a more complete understanding of maar-diatreme volcanism.

Previously published geophysical studies of maar volcanoes have been able to successfully model different aspects of their subsurface structures using a number of geophysical techniques. Seismic and electrical resistivity data has been utilised to examine the geometry of maar lake sedimentary sequences (e.g. Brunner et al., 1999; Schulz et al., 2005; Buness et al., 2006; Gebhardt et al., 2011), while gravity and magnetic methods have been applied to model the geometry of maar diatremes and/or subsurface basaltic bodies contained within them (e.g. Rout et al., 1993; Schulz et al., 2005; Lindner et al., 2006; Cassidy et al., 2007; Lopez Loera et al., 2008; Mrlina et al., 2009; Skacelova et al., 2010). However, these geophysical models are often not related to volcanological observations made at the surface. Where potential field methods are focussed upon, these studies have also assumed a homogenous density and magnetic susceptibility distribution within the underlying structures which may be unrealistic given the nature of some maar-diatremes. Studies of exposed diatreme structures (e.g. Coombs Hill; McClintock and White, 2006; Ross and White, 2006; Hopi Buttes;

* Corresponding author. [redacted] (T.N. Blaikie), [redacted] (R.AF. Cas), [redacted] (P.G. Betts).

0377-0273/$ – see front matter © 2012 Elsevier B.V. All rights reserved.
doi:10.1016/j.jvolgeores.2012.05.002

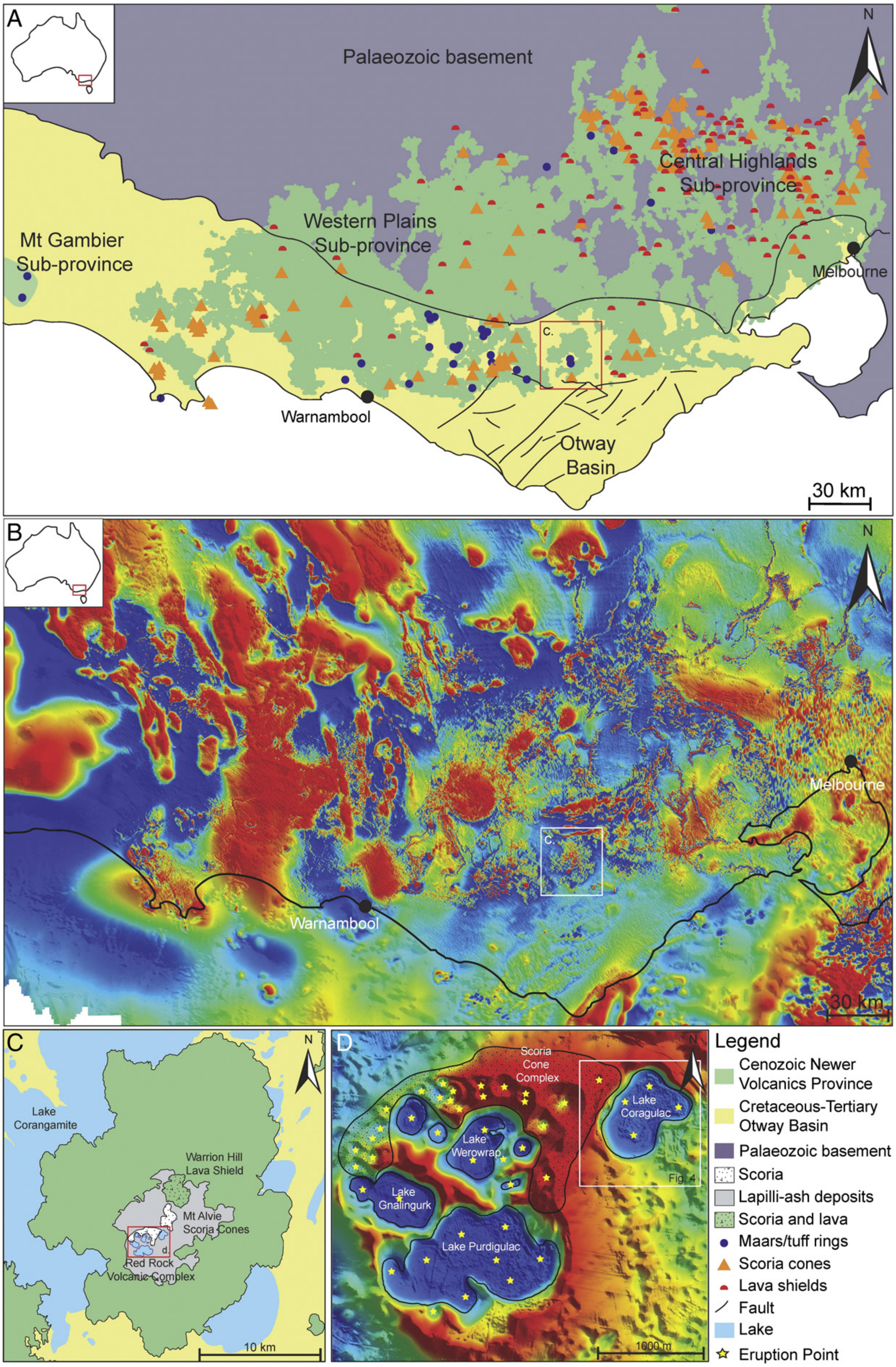

A
Palaeozoic basement
N
Central Highlands Sub-province
Western Plains Sub-province
Mt Gambier Sub-province
Melbourne
c.
Warnambool
Otway Basin
30 km
B
N
Melbourne
c.
Warnambool
30 km
C
N
Lake Corangamite
Warrion Hill Lava Shield
Mt Alvie Scoria Cones
d
Red Rock Volcanic Complex
10 km
D
Scoria Cone Complex
Lake Coragulac
Lake Werowrap
Lake Gnalingurk
Lake Purdigulac
Fig. 4
1000 m
Legend
Cenozoic Newer Volcanics Province
Cretaceous-Tertiary Otway Basin
Palaeozoic basement
Scoria
Lapilli-ash deposits
Scoria and lava
Maars/tuff rings
Scoria cones
Lava shields
Fault
Lake
Eruption Point

White, 1991; White and Ross, 2011) have shown that the internal structure of a diatreme can be highly heterogeneous and consists of irregular zones of poorly sorted pyroclastic rock with different proportions of juvenile and country rock clasts. Large clasts up to several metres in size are common and occurrences of country rock blocks up to 100 m in diameter have also been noted (Ross and White, 2006; White and Ross, 2011). A heterogeneous distribution of volcanic and host rock debris within the diatreme implies that the petrophysical properties within the diatreme are also likely to be heterogeneous and this should be considered during geophysical modelling. This study will focus on modelling the subsurface structures of a maar volcano in two and three dimensions and will utilise 3D potential field inversions to understand property distributions within the maar-diatreme. Inverse modelling has not been applied to previous geophysical models of maar volcanoes because forward modelling has been considered more realistic (Lindner et al., 2006). The method proposed by this study uses forward modelling to initially define the structure of the maar and build the three-dimensional model. Inverse modelling is then applied to refine the geometry of structures in 3D and to understand the distribution of properties in the subsurface.

The Red Rock Volcanic Complex (RRVC) is the most complex volcanic centre within the Newer Volcanics Province (NVP) of South-Eastern Australia, with over 40 eruption points identifiable (Cas et al., 1993, 2011). Lake Coragulac is one of several maars contained within this complex and displays a complex shape with multiple embayments suggesting that perhaps several eruptions occurred and/or the vent migrated during eruption. In order to understand the volcanic evolution of the maar complex and distinguish individual eruption points, gravity and magnetic modelling of high resolution data obtained from ground surveys is combined with a study on the physical volcanology of deposits of the Lake Coragulac maar. Stratigraphic logging, identification of accidental lithic fragments and petrographic analysis are used to help understand the volcanic evolution of the maar and to constrain the geophysical models.

2. Geologic setting

2.1. The Newer Volcanics Province, Western Victoria

The Cainozoic (4.5 Ma–4.5 ka) Newer Volcanics Province (NVP) is an intraplate basaltic plains province composed of over 400 eruptive centres including shield volcanoes, scoria cones, tuff rings, maars, composite volcanoes and extensive lava fields (Fig. 1A) (Cas, 1989). Products of volcanism cover an area of >25 000 km^2 across Western Victoria into South Australia and overlie the Palaeozoic basement rocks of the Lachlan and Kanmantoo Fold Belts in the north and the Mesozoic–Cenozoic sediments of the Otway Basin in the south (Joyce, 1975; Lesti et al., 2008; Cas et al., 2011). Initial periods of volcanism within the NVP consisted of prolonged effusive eruptions forming basaltic pahoehoe and aa lava flows that are dominantly tholeiitic in composition (Price et al., 1997). Later eruptive phases consisted of dominantly explosive eruptions forming numerous scoria cones and maars of a predominantly alkalic composition (Price et al., 1997).

Three different sub-provinces have been identified within the NVP (Fig. 1A) (Nicholls et al., 1989; Cas et al., 1993). The Western Plains is the largest of these provinces, and is characterised by extensive lava plains sourced from lava shields and fissure systems. Superimposed on the flat or hummocky topography of the lava plains are numerous monogenetic volcanic edifices such as maars, tuff rings and scoria cones (Lesti et al., 2008). Overlying a basement of Paleozoic meta-sediments and granites is the Central Highlands sub-province (Nicholls et al., 1989; Cas et al., 1993; Price et al., 2003). Host to over 250 eruptive centres consisting dominantly of lava shields, lava flows and scoria cones, volcanism within this province is dated between 4.5 and 2.0 Ma (Cas et al., 1993; Price et al., 2003). The Mount Gambier sub-province is the smallest of the three sub-provinces and is located 60–80 km west of the main section of the NVP (Fig. 1A). This province is associated with clusters of maars, scoria cones and minor associated lavas which overlie a karst limestone terrain (Nicholls et al., 1989; Sheard, 1990; Cas et al., 1993). Mount Gambier and Mount Schank, located within this province, represent the most recent eruptions within the NVP, about 4.5 ka (Sheard, 1990).

Approximately 40 maars have been identified within the NVP, ranging from small, simple maars several hundred metres across, to more complex maars containing nested scoria cones and large complex maars up to 3 km in diameter (Joyce, 1975). The majority of maar volcanoes are located within the southern parts of the NVP where water-saturated porous aquifers contained within thick sedimentary sequences of the underlying Otway Basin have facilitated phreatomagmatic explosions, at least in the initial phase of each eruption (Joyce, 1975). Several maars have been identified in the northern parts of the province and are hosted in the Paleozoic granites of the Lachlan Fold Belt where groundwater is available in joints and fractures. Maars within the southern region of the NVP are ideal for geophysical modelling, as a high geophysical contrast exists between the lower density (1.9–2.4 g cm^{-3}) and magnetic susceptibility of the host siliciclastic sediments and the higher density (2.6 g cm^{-3}) and magnetic susceptibility (0.005 SI) of the basaltic volcanoes. The region of interest has relatively high resolution aeromagnetic data that enables the imaging of discrete eruptive centres and surrounding lava plains (Fig. 1B). Eruption points typically show up as near-circular magnetic highs and lava flow fields are characterised by magnetic highs with a highly stippled texture. These anomalies are superimposed on the relatively low magnetic, smooth response of the Otway Basin. The data is however of insufficient resolution to image and assess the subsurface structures of individual maars and ground gravity and magnetic data are collected at a higher resolution for modelling.

2.2. Red Rock Volcanic Complex

The Red Rock Volcanic Complex (RRVC) is located within the Western Plains sub-province and forms part of three closely spaced volcanic centres aligned in a NNE direction, thought to have erupted along a major crustal fracture used by magmas as a conduit (Cas et al., 1993, 2011). Warrion Hill is the northern most eruptive centre, lying 3 km NNE of the RRVC. It erupted lavas that extend up to 12.5 km from the vent and underlie the deposits of the Mt. Alvie scoria cones (central volcanic centre) and the RRVC (Fig. 1C) (Cas et al., 1993).

The RRVC is one of the most complex volcanic centres within the NVP involving multiple maar and scoria cone forming eruptions covering an area of 7–8 km^2 (Fig. 1D). Early phases of eruptive activity within the RRVC were dominantly phreatomagmatic forming multiple scalloped shaped maars including Lake Coragulac, Lake Purdigulac, Lake Gnalinegurk and Lake Werowrap. The scalloped shaped margins of each of the maar craters indicate a complex eruptive history involving eruptions from at least 18 vents (Fig. 1D; Cas et al., 2011). Following this phase of dominantly phreatomagmatic volcanism, the eruptive style of the complex shifted to dominantly magmatic, producing a scoria cone complex (22 vents) within the north-east of the complex (Fig. 1D; Cas et al., 2011). Interestingly, the phreatomagmatic fall and surge deposits surrounding the maars are interbedded with strombolian scoria fall deposits, suggesting either the contemporaneous eruption of some of the cones and/or rapidly changing eruption styles of the maars.

Fig. 1. A) The extent of the Cainozoic Newer Volcanics Province of Western Victoria (modified after Joyce, 1975; Hare et al., 2005). B) Psuodocolour aeromagnetic image of Western Victoria. C) Regional geology of the Red Rock Volcanic Complex. D) LIDAR image of the Red Rock Volcanic Complex (courtesy of the Corangamite catchment management authority) showing multiple poly-lobate maars, scoria cone complex and vent locations.

Lake Coragulac is the second largest maar within the RRVC and is the focus of this geophysical study. It was selected because part of the maar rim was exposed by quarrying which provides important constraints on the geophysical models. Consisting of at least three coalescing vents, Lake Coragulac is 800 m long along its longest axis (trending NNE) and 400 m across its shortest axis (trending EW). The maar rim is up to 40 m thick (from the crater floor), with the thickest sequence of deposits occurring along the northern side of the maar, likely due to the prevailing wind direction during the eruption. The maar rim pyroclastic deposits indicate a complex eruptive history involving abrupt transitions between phreatomagmatic and magmatic explosive eruption styles.

2.3. Subsurface stratigraphy and key aquifers

The subsurface stratigraphy and aquifer properties of the region around the RRVC are known from two nearby petroleum exploration wells (Nalangil-1 and Irrewarra-1; Constantine and Liberman, 2001) and are summarised in Fig. 2. The oldest sediments underlying the complex are Mesozoic sandstones, mudstones and conglomerates of the Eumeralla formation (occurring below a depth of 290 m; Fig. 2) which are generally considered to be poor aquifers with a low porosity and permeability due to diagenetic burial, compaction and lithification, however when fractured the group can act as a minor aquifer (Tickell et al., 1991). Overlying the Eumeralla formation are weakly lithified to unconsolidated Tertiary sands, gravels and limestones. The porous quartz rich sandstones and sandy limestones of the Eastern View Formation (238–290 m) have a high hydraulic conductivity and form the major aquifer within the region (Tickell et al., 1991). The Demons Bluff Formation (186–238 m) and Gellibrand Marl (26–186 m), consisting of marls, calcareous clays and silts behave like aquitards, however more sandy facies variants, particularly towards the top of the Gellibrand Marl can act as a minor aquifer (Tickell et al., 1991; Edwards et al., 1996).

3. Volcanological evolution of Lake Coragulac

3.1. Maar rim deposit and facies characteristics

Forty eruption points have been identified from field mapping within the RRVC (Fig. 1D; Cas et al., 1993, 2011), posing significant problems in identifying the source vent for each layer in a sequence of deposits. Detailed stratigraphic logging, sampling and thin section analysis were undertaken in order to reconstruct the eruptive history of the Lake Coragulac maar. Descriptive terms of volcanic deposits used in this paper are based on the guidelines of Cas et al. (2009) while eruptive classifications are based on Walker (1973) and Francis et al. (1990).

Exposures within the maar rim are limited to several abandoned quarries, which exposes approximately 7 m of stratigraphy from the top of the maar rim succession. Two main facies have been identified within these exposed sections of the Lake Coragulac maar (Fig. 3).

The lower facies interval displays frequent and abrupt transitions between thin beds of fine-coarse ash and thicker beds of medium-coarse lapilli sized scoria. Ash beds vary between fine grained, thin, well-sorted and planar stratified to coarser beds that are commonly undulating, planar stratified or display weak cross bedding (Fig. 3). Accidental lithic fragments and quartz xenocrysts form between 20 and 50% (visual estimate) of the ash deposits with poorly vesicular (0–20%) juvenile pyroclasts making up the remainder. The high proportion of country rock debris, fine grainsize, poorly vesiculated juvenile pyroclast population, and the depositional bed forms are consistent

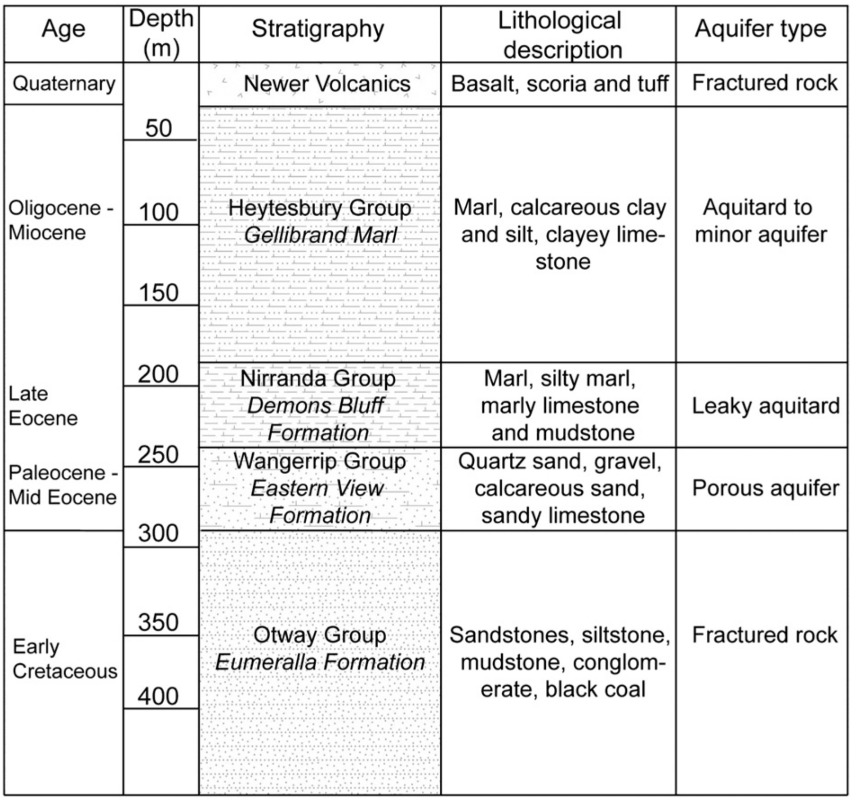

Fig. 2. The subsurface stratigraphy and key aquifers of the region surrounding the RRVC.

with phreatomagmatic explosive activity. The fine grained, poorly vesiculated juvenile pyroclasts suggest that explosive interaction between rising magma and external water occurred before the magma had fully vesiculated, and that quenching of the magma occurred upon contact with groundwater, terminating the growth of vesicles (Houghton and Wilson, 1989). Ash beds were deposited by fallout (well-sorted and planar stratified) and base surge (coarse, undulating or weakly cross-bedded) processes.

Scoria beds are poorly to moderately well sorted and are massive to diffusely stratified with highly vesicular (60–80%) pyroclasts. Scoria deposits within this facies are interpreted to have formed from short-lived, single magmatic explosions consistent with spaced strombolian style activity (Walker, 1973).

The upper facies interval consists dominantly of massive to diffusely stratified medium-coarse lapilli sized scoria deposits (Fig. 3). Scoria deposits are well sorted, consist of highly vesicular (60–85%) scoria clasts and contain low degrees of ash indicating that the eruption was driven by the exsolution and expansion of magma volatiles (e.g. Houghton and Wilson, 1989). These deposits appear to represent fall out deposits from the scoria cone complex which appear from super-position relationships to have become active after the main phase of phreatomagmatic explosive activity. Their transport and dispersal away from the cone complex indicate that a sustained, low buoyant eruption column existed at the time of the eruption. The deposits are texturally similar to Plinian style deposits (massive, well-sorted and highly vesiculated juvenile pyroclasts) however the dispersal is more restricted. The term micro-plinian as defined by Francis et al. (1990) is applied to describe the eruption style during this phase of magmatic explosive volcanism.

Given that over 40 closely spaced eruption points exist within the RRVC (Fig. 1C), it is possible that some if not many of the beds observed within the stratigraphy could be sourced from different vents within the complex. Inter-bedded ash and scoria deposits (lower facies interval) proximal to the inferred vents within Lake Coragulac contain a high abundance of juvenile and lithic ballistic blocks and bombs (Fig. 3) which are less frequent in more distal deposits. The high abundance of ballistic blocks and bombs in all the facies suggests that the deposits were mostly derived from common or closely-spaced source vents within the Lake Coragulac maar and not from other vents within the complex. The minor country rock xenolith and xenocryst content of the scoria beds indicate breaks in phreatomagmatic activity when they were deposited. The frequent alternations between ash beds and scoria deposits in the lower facies interval therefore suggest that constant fluctuations in magma ascent rates and/or changing degrees of explosive interaction between rising magma with external water were occurring in the maar vent system (Houghton et al., 1999). The thick scoria dominated upper facies interval is consistent with derivation from a sustained scoria cone forming phase of activity, most likely from the younger, scoria cone complex vent system adjacent to the Coragulac maar.

3.2. Depth of explosive fragmentation

To provide further constraint to the geophysical models, an analysis of accidental lithic fragments within the pyroclastic deposits was undertaken to ascertain the maximum depth of explosive fragmentation. Lithic clasts observed are of both a volcanic and non-volcanic origin including basalt, marl, limestone, sandstone and siltstone and were derived from the host rocks overlying the point of explosive fragmentation. Comparison of the observed lithic fragments was made with the detailed lithological descriptions of the Otway Basin sediments provided by Tickell et al. (1991) and Edwards et al. (1996).

Lithic clasts observed in the phreatomagmatic fall and surge deposits (lower facies) include clasts of older basalts, fine grained carbonate siltstones, and sandy limestones occasionally containing fossil fragments. Petrographic analysis reveals that sub-angular to rounded silt sized quartz grains are present amongst the fine ash matrix of phreatomagmatic deposits, an indication that fragmentation occurred within weakly lithified sediments (Lorenz, 2003, 2007; Ross et al., 2011). Angular to sub-rounded lithic clasts ranging in size from 0.1 to 1 mm in size, consisting of siltstones, marls and carbonate sandstones are commonly observed throughout all phreatomagmatic beds, generally contributing up to 15% (visual estimation) of each deposit. Fragments of molluscs, gastropods and echinoderms are commonly observed as isolated clasts or contained within sedimentary lithic fragments.

Comparison of the sedimentary lithic fragments and fossil types with descriptions provided by Edwards et al. (1996) indicates that they were derived from the Gellibrand Marl, Nirranda and Eastern View Formations and that phreatomagmatic fragmentation may have occurred up to a maximum depth of 290 m (Fig. 2). Marl and carbonate siltstone lithic fragments are however the most abundant lithic present within the phreatomagmatic fall and surge deposits, suggesting that fragmentation occurred predominantly within or just below the Gellibrand Marl. The low hydraulic conductivity of the Gellibrand Marl formation may have resulted in slow recharge and limited the availability of water during the eruption. Periods where the aquifer in the vicinity of the magma conduit was dry resulted in the magmatic eruptive phases. Thicker ash beds occurring throughout the stratigraphic sequences represent longer, more sustained phreatomagmatic eruptions that may have occurred within a more porous facies variant of the Gellibrand Marl or within deeper aquifers such as the Eastern View Formation.

Lithic fragments common to the upper facies of the Lake Coragulac maar include blocky fragments of basalt and smaller fragments of marl, carbonate sandstones and siltstones. Basaltic fragments are the most abundant lithic, commonly making up between 1 and 10% of the scoria deposits. These lithic clasts, derived from older plains lava flows, are texturally distinct from the basaltic juvenile clasts erupted from Lake Coragulac and the cone complex. Although similar in mineralogy, the basaltic lithic fragments are coarsely crystalline and poorly vesicular, whereas juvenile pyroclasts are glassy and highly vesicular. This indicates that magmatic explosive fragmentation occurred close to the surface within or just below the lava flow and likely propagated downwards into the upper part of the Gellibrand Marl.

4. Geophysical modelling

4.1. Geophysical data acquisition and processing

Gravity and magnetic data were acquired along three traverses across the Lake Coragulac maar, intersecting several of the inferred vent locations (Fig. 4A). The irregular orientation of the traverses is due primarily to the accessibility of the terrain. Swampy conditions in the centre of the crater proved unsuitable for gravity measurements and these areas were avoided.

The gravity station spacing was determined by constructing a hypothetical forward model of a maar-diatreme. This allowed the wavelengths and amplitude of anomalies associated with different maar structures to be identified, and an appropriate station spacing assigned to detect them. A high precision Scintrex CG-3M gravity meter with a resolution of 0.001 mgal was used to acquire data with a station spacing of 20 m inside the maar crater and 50 m elsewhere. 146 measurements were acquired (excluding base stations) with 67, 53 and 31 measurements acquired across traverses A, B and C respectively (Fig. 4A). A local gravity base station was set up within the southern end of maar crater and was re-occupied every 2–3 h to correct for instrument drift.

The position and elevation of each station were determined using a laser theodolite with an accuracy greater than 0.55 m. The estimated uncertainty in the gravity data arising from uncertainties in elevation is ± 0.17 mgal. Tidal, drift, free-air, latitude, Bouguer and terrain corrections (crustal density of 2.10 g cm^{-3}; corrected using the Geosoft Oasis Montaj terrain correction module) were applied to the raw data to correct for any variations in the gravitational field that did not arise from

T.N. Blaikie et al. / Journal of Volcanology and Geothermal Research 235–236 (2012) 70–83

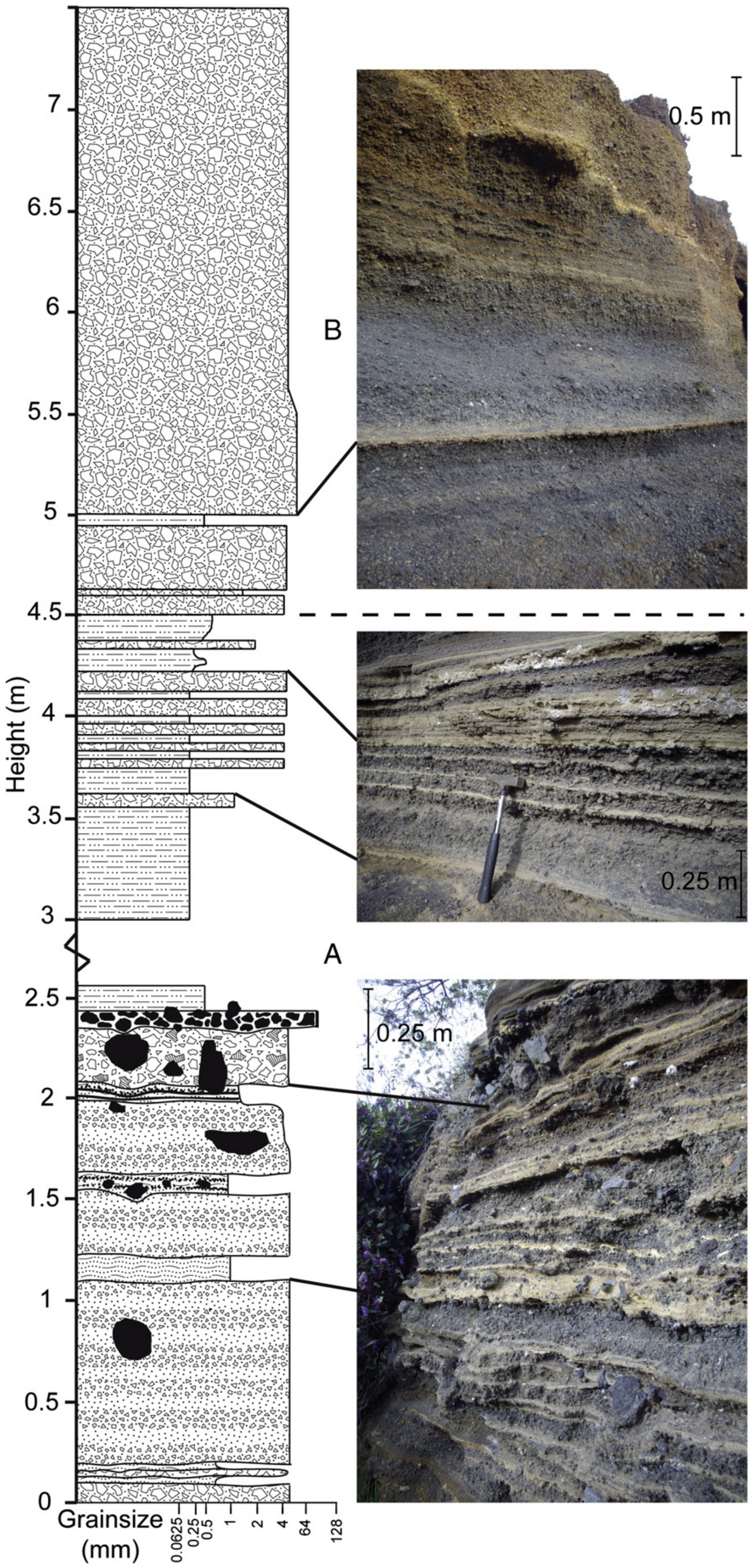

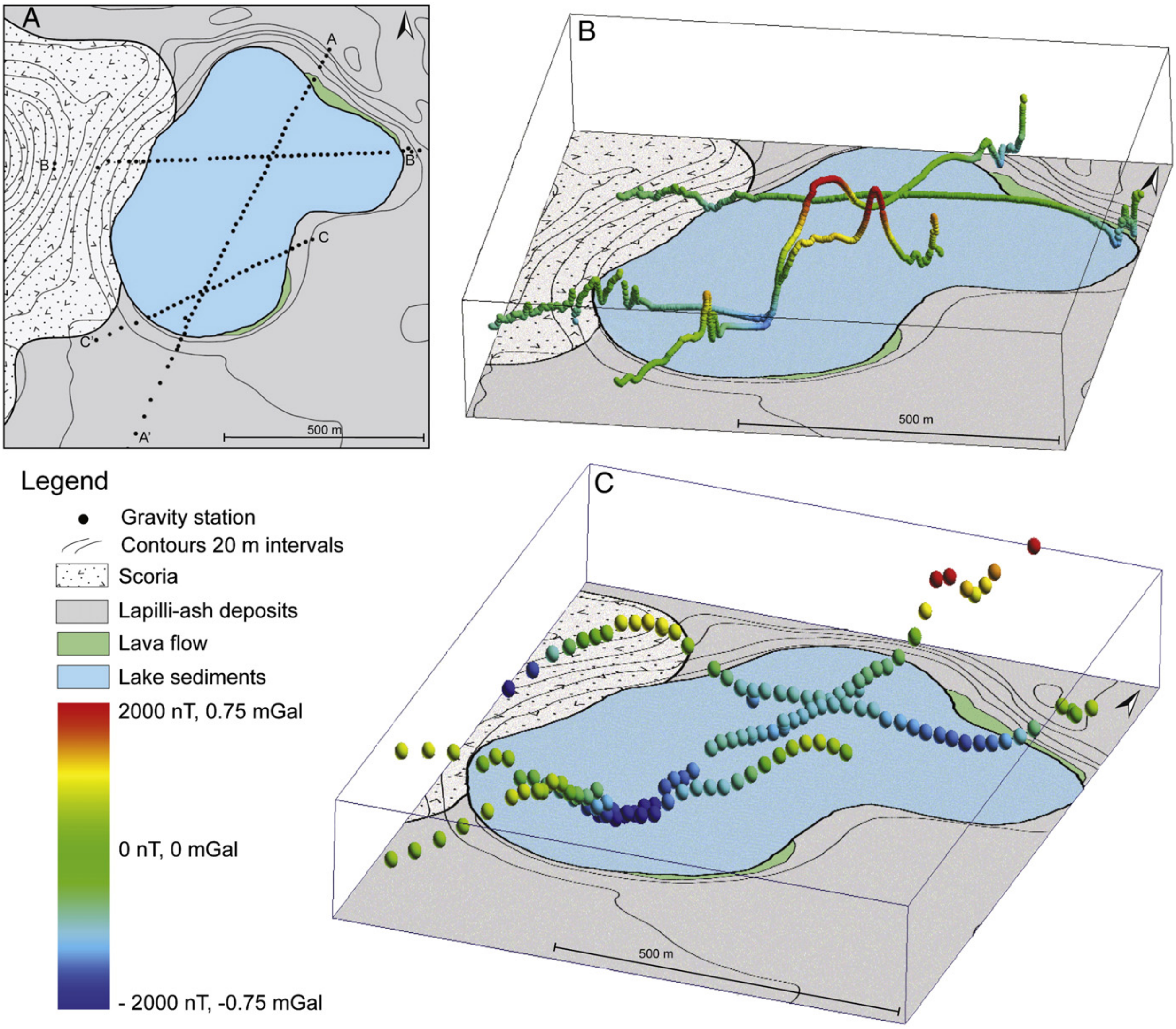

Fig. 4. A) Geologic map of the Lake Coragulac maar showing the location of gravity stations. Magnetic data were collected along the same traverses. B) Magnetic anomaly. C) Bouguer anomaly (correction density of 2.1 g cm^{-3}).

the underlying geology. Free-air gravity data was used for two and three dimensional modelling and the Bouguer and terrain corrections were only necessary for examining the data in gridded form.

Magnetic data were acquired using a G858 Caesium Vapour magnetometer with a sampling rate of 1 s and an accuracy of <2 nT. A G856 Proton Precession magnetometer with a sampling rate of 3 min and accuracy of 0.5 nT was used as a local base station to correct for diurnal variations. An IGRF correction was applied and any noise in the data caused predominately by fences in the survey area was removed by simply deleting large, high frequency spikes and upward continuing the data by 5 m.

4.2. Results and interpretation of potential field data

The processed gravity (Bouguer anomaly terrain corrected to 2.10 g cm^{-3}) and magnetic data (total magnetic intensity (TMI)) are shown in profile form in Fig. 4B and C. A gravity low is observed across the maar crater which is related to the lower density lake sediments and pyroclastic debris infilling the underlying maar-diatreme (Fig. 4C). Within the centre of the maar, several short wavelength gravity highs with corresponding magnetic highs are observed, indicating the presence of a dense magnetic body at depth, potentially remnant feeder vents or dykes (Fig. 4B and C). Short wavelength gravity highs corresponding to the margins of the maar crater observed in the Bouguer gravity data (Fig. 4C) are related to a dense basaltic lava flow belonging to the plains basalts of the NVP which can be observed outcropping in the crater walls.

4.3. Gravity and magnetic 2D forward modelling

Two-dimensional forward modelling allows geologic cross sections to be constructed based upon potential field data (McLean and Betts,

Fig. 3. Stratigraphy of the upper part of the Lake Coragulac maar rim sequence showing the two major lithofacies identified in this region of the complex. The lower facies (A) consists of interbedded phreatomagmatic ash and magmatic scoria deposits with lensoidal layering and ballistic blocks. The upper facies (B) consists of massive to diffusely stratified scoria deposits interbedded with occasional thin layers of ash.

2003). Free-air gravity and TMI data were extracted along the three traverses (A–C) (Fig. 4) from gridded datasets and imported into Geosoft GM-SYS software for forward modelling. Because some of the observed gravity anomalies (e.g. those that correlate to outcropping lava flows and tuff deposits in the crater walls) correlate with topography, free-air gravity data was favoured to the Bouguer gravity as it allowed for the inclusion of topography within the model. Amplitudes of gravity anomalies are between −3 and −6 mgal and correlate with the topography of the maar. Shorter wavelength gravity and magnetic anomalies that do not correlate with topography are observed within the maar. Each forward model was constrained by an understanding of the regional geology, subsurface stratigraphy (Fig. 2) and the petrophysical properties of the rocks which were determined by density (both wet and dry) and magnetic susceptibility measurements of hand samples (tuff, scoria and basalt; Fig. 5). Wet density measurements were applied to units that occurred below the groundwater table and the dry density measurements to units above. Surface deposits were often highly weathered and magnetic susceptibility measurements were increased slightly during forward modelling. Any inferred petrophysical properties are indicated in the legend of Fig. 6.

Australian Geomagnetic Reference Field (AGRF) values were sourced from Geoscience Australia and the magnetic field parameters at the time the ground magnetic survey was conducted (magnitude = 60469 nT, inclination = −69.34 and declination = 11.06) were incorporated into the models. A remanent magnetisation was not applied to maintain model simplicity and because the magnetic anomalies for each profile could be reproduced without applying remanence. During modelling, GM-SYS calculates the effects of topography on the calculated gravity response and the inclination of the earth's magnetic field on the calculated magnetic response. Although GM-SYS does not correct for topography off the line of the traverse, small errors in the geometry/density of the model that may arise from terrain are corrected for by importing a terrain model into VPmg during 3D inverse modelling.

Traverse A–A′ corresponds to the NNE–SSW traverse and intersects two of the maars main lobes (Fig. 6A). Two large diatreme structures were modelled in this section. The northern maar-diatreme is 350 m in diameter and 240 m deep and corresponds to a relatively smooth gravity and magnetic response suggesting that the density and magnetic susceptibility of the underlying rocks are fairly homogenous. The southern maar-diatreme is 400 m in diameter and extends to a depth of 280 m. A short wavelength gravity high with an amplitude of 0.3 mgal and a corresponding magnetic high with an amplitude of 2000 nT is observed in the centre of this diatreme indicating that a dense magnetic body such as a feeder dyke exists in the subsurface. Both the gravity and magnetic anomalies consist of two peaks of similar wavelength, indicating that the source consists of two separate bodies and secondly suggesting that the same sources are contributing to both anomalies. A magnetic gradient of 15 nT/m indicates a steeply dipping source body. Two dense basaltic feeder vents were interpreted in this model to explain the existence of these anomalies.

Traverse B–B′ is oriented in an E–W direction and intersects the northern lobes of the maar (Fig. 6B). This traverse is similar to the first forward model in both geophysical response and the structures modelled. A gravity minimum of −2.4 mgal is observed across the

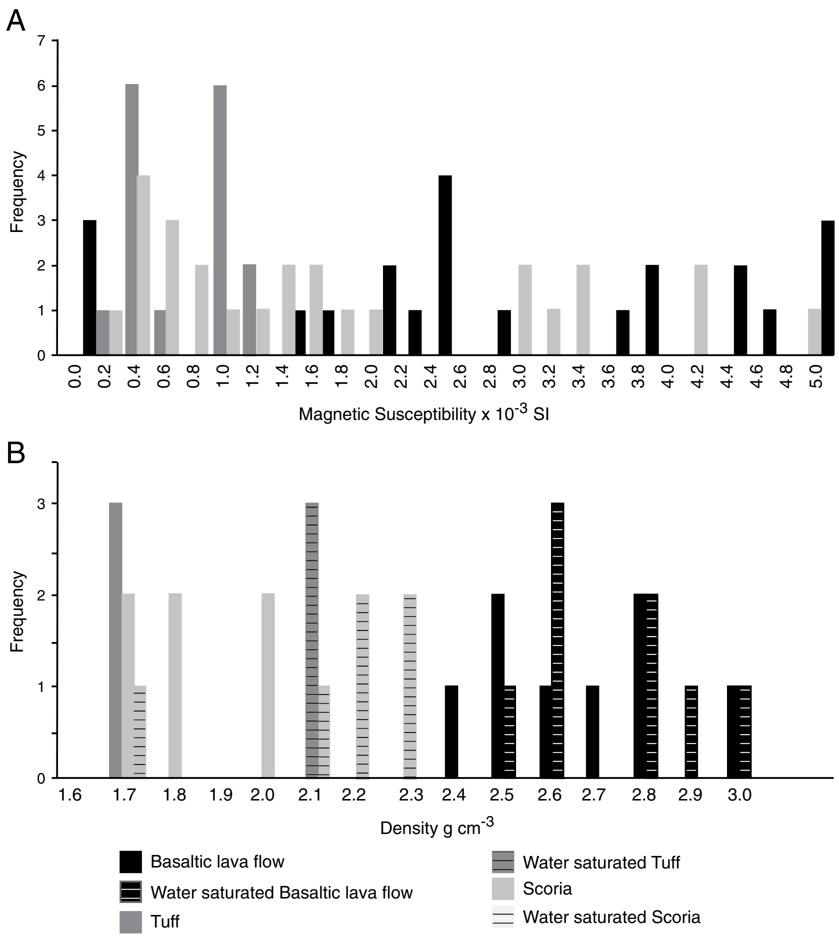

Fig. 5. Histrograms of A) magnetic susceptibility and B) density measurements of hand samples obtained within the stratigraphy of the RRVC.

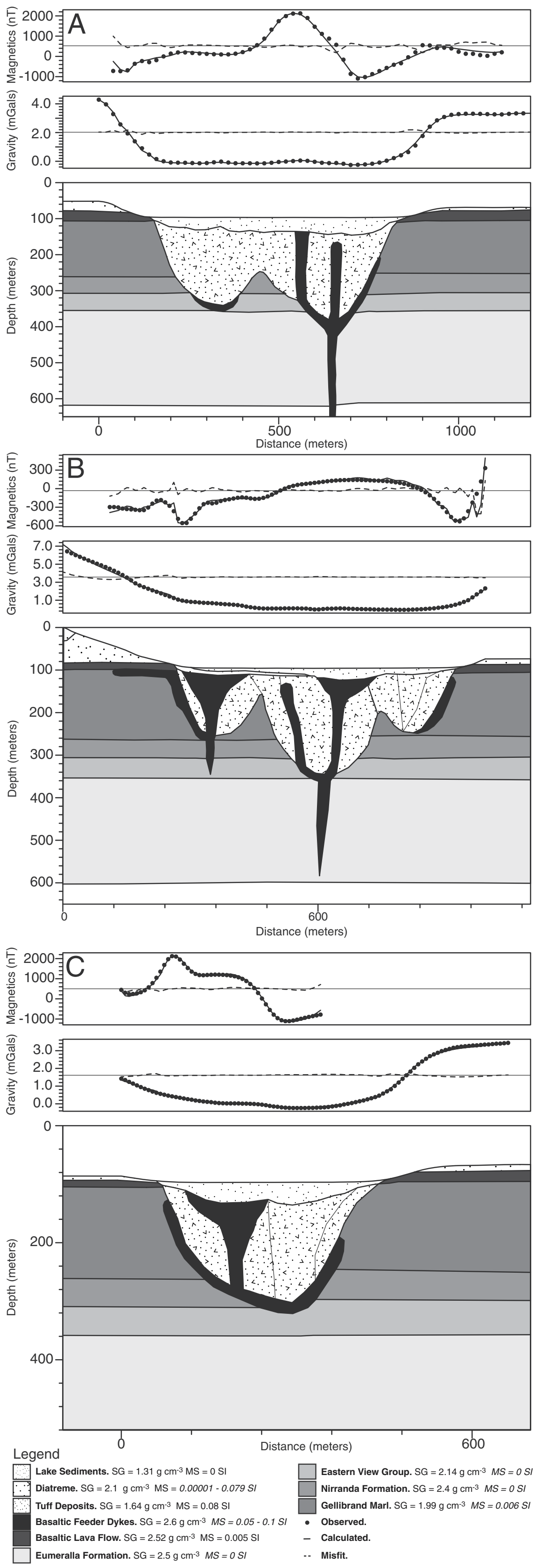

maar crater and is related to the lower density lake sediments observed at the surface which have a maximum thickness of 35 m. Three diatreme structures have been interpreted in this section. Two short wavelength gravity highs with amplitudes of 0.16 mgal are observed above the central diatreme and are interpreted to be a result of a remnant feeder vent and intrusive dyke. A large gravity high with an amplitude of 0.74 mgal is observed directly overlying the easternmost maar-diatreme structure modelled. This anomaly was initially interpreted to be related to the older plains lava flow underlying the complex; however this structure failed to adequately reproduce the observed anomaly. The anomaly indicates that a large dense rock body is present close to the surface and was interpreted to be a result of a feeder vent that formed a magma pond at the surface.

Traverse C–C′ is oriented in a SW–NE direction and intersects the margins of the southern diatreme modelled in A–A′ and has a maximum depth of 200 m (Fig. 6C). A magma pond that formed from a dyke that intrudes along the diatreme margin was interpreted to be the source of the gravity high (amplitude of 0.26 mgal) and the corresponding magnetic anomaly (amplitude of 2300 nT) observed in the north-eastern section of the traverse.

4.4. 3D modelling

A three-dimensional model of the subsurface structures of Lake Coragulac was built from the 2D models produced in GM-SYS (Fig. 7). The 2D models were imported as DXF files into Gocad and served as a framework for creating surfaces within the 3D model (Mallet, 1992, 1997). Each surface within the model defines a lithological contact and was interpolated using a discrete smooth interpolator (DSI) which smoothes the surface whilst honouring fixed data points from the 2D model (Mallet, 1997).

The margins of four coalescing maar-diatremes were defined in the model, the largest of which corresponds to the largest lobe of the maar. The geometry of the maars' feeder dykes was defined based on the 2D forward model interpretations. The dykes are narrow at the base of the diatreme and become wider close to the surface. The larger feeder dykes in the model, some of which formed magma ponds at the surface, are interpreted to represent the main eruptive vents of the maar while the smaller dykes represent later intrusions into the diatreme.

4.5. 3D Potential field inversions

A volumetric (voxet) model was constructed in Gocad which consists of rectangular voxels 20 m by 20 m by 10 m (x, y, z) which have been subdivided into different lithological regions according to the 3D surface model. The different regions represent the host sedimentary rocks, diatreme fill, feeder dykes, tuff deposits and lake sediments and have been assigned relevant petrophysical properties (e.g. density).

Potential field gravity inversions were performed using the VPmg™ software algorithm (Fullagar et al., 2000, 2004, 2008) which can operate within three different inversion modes but relies upon the input model so geologically meaningful results are obtained (Williams et al., 2009). Homogenous and heterogeneous property inversions are designed to optimise the property or property distribution within the model. Geometry inversions manipulate surfaces within the model which define the boundaries between different geologic domains. During the inversion, VPmg™ numerically calculates the optimum property values, property distribution or geometry of the model within the bounds of the applied constraints so that the models calculated geophysical response better fits the observed data.

Fig. 6. Forward models of traverse A) A–A′ (oriented NNE–SSW), B) B–B′ (oriented W–E) and c) C–C′ (oriented NW–SE). Depths indicated on the models are relative to the position of the laser theodolite, inferred petrophysical properties are italicised.

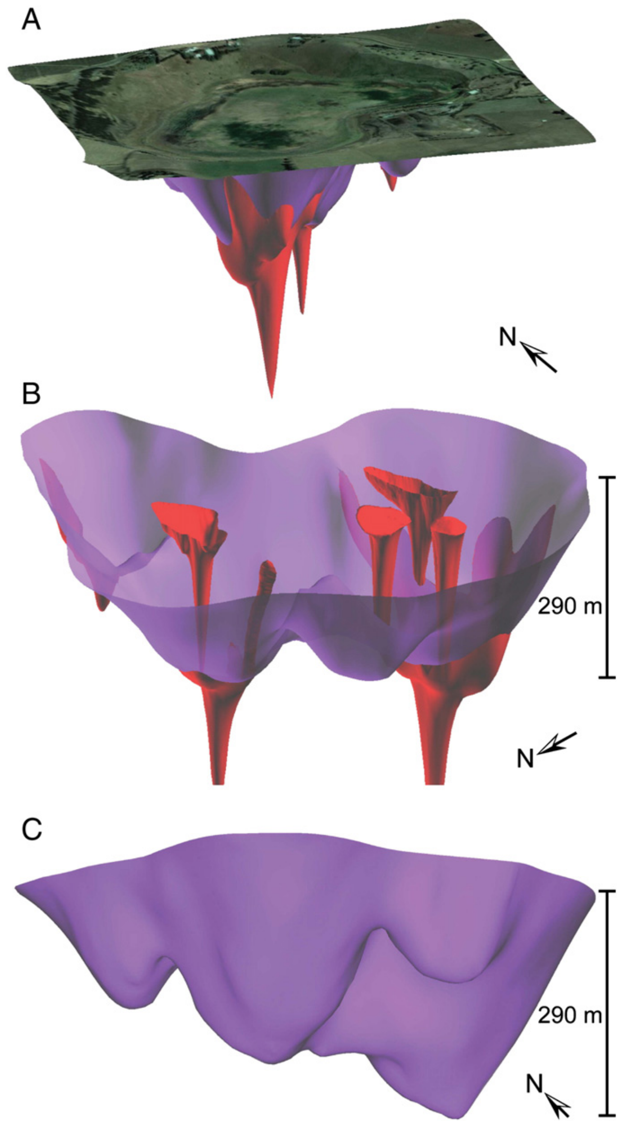

Fig. 7. 3D model of the subsurface structures of the Lake Coragulac maar showing multiple coalesced diatreme structure and intrusive dykes/remnant feeder vents.

Prior to running any inversions, a forward model was calculated to determine the RMS (root mean square) misfit of the reference model. A misfit of 0.23 mgal (3.2% of the dynamic anomaly range) was obtained, with areas of high misfit corresponding to the centre of the diatreme and the location of the modelled dykes indicating that the densities or geometry of structures within this region of the model needed refining (Fig. 8A).

As an initial step to reducing the overall misfit of the model, homogenous property inversions were run to optimise the density value of certain lithological regions. The parameters of the model were set so the diatreme, feeder dykes and the lake sediments were allowed to vary by a maximum of ± 0.5 g/cm^3 whilst all other regions within the model were not altered during the inversion and the properties remained identical to the forward models (refer to legend of Fig. 6). Results of the inversion saw a slight increase in the density of each of the inverted regions as shown in Table 1 and reduced the residual gravity anomaly from 0.23 mgal to 0.19 mgal. The optimised densities were then applied to a new reference model for heterogeneous and geometry inversions.

Heterogeneous inversions with a vertical discretisation of 10 m were applied to gain a better understanding of the density distribution within the subsurface. Similar to the homogenous inversions, the parameters of the model were set so that the properties of the host rock were not altered while the properties of the diatreme, feeder vents and feeder dykes were inverted. Results of these inversions indicate that regions within the centre of the maar-diatreme around the modelled dykes increased in density while the density of the diatreme margins were decreased, reflecting a density similar to that of the host rock (Fig. 8B). These inversion results suggest that a higher volume of dense volcanic rock exists within the centre of the diatreme while the margins of the diatreme contain large volumes of collapsed host sedimentary material.

A geometry inversion applied to the maar-diatreme was used to test the modelled geometry against the data. Results of this inversion suggest that the geometry of the diatreme is fairly similar to the reference model, however the structure may be shallower than the initial model (Fig. 8C and D).

4.6. Limitations of geophysical interpretations

There is a component of ambiguity involved in any geophysical interpretation as there is not one unique solution (Whiting, 1986; Valenta et al., 1992; Jessell et al., 1993; McLean and Betts, 2003). The range of possible solutions can be limited by the inclusion of geologic data and observations within the model. Models of Lake Coragulac were constrained by petrophysical properties determined from field and laboratory measurements. The maximum depth of the maar-diatreme in each model was limited by the maximum depth of phreatomagmatic fragmentation determined from accidental lithic fragments in pyroclastic deposits (290 m).

When building the two and three dimensional models, several key assumptions were made in order to simplify the initial modelling process. During the initial stage of 2D modelling, it was assumed that the observed gravity and magnetic anomalies were related primarily to petrophysical contrasts between the diatreme, intrusive dykes or host rock and were not related to property heterogeneities within each unit. It is assumed that any anomalies created by deeper structures or the surrounding host rock are relatively negligible compared to the anomaly arising from the maar itself. As the pyroclastic debris infilling the maar-diatreme could not be directly sampled, an initial density of 2.1 g cm^{-3} was applied which is similar to scoria and tuff deposits found in the maar rim. Although many maar-diatremes are known to have a heterogenous distribution of pyroclastic and host rock debris (e.g. Coombs Hill; McClintock and White, 2006; Ross and White, 2006; Hopi Buttes; White, 1991; White and Ross, 2011), these assumptions were made to simplify the modelling process by reducing the number of surfaces within the model. It is not possible to model heterogeneous property distribution within a single region using GM-SYS unless this region is subdivided into smaller regions and a different property applied to each. Without any initial constraints (e.g. from drill core) this would just add to the ambiguity of the 2D model.

The variable density distribution within the diatreme is reflected and incorporated into the 3D models during heterogeneous property inversions. The discretisation of the 3D model into voxels with a dimension of 20 m in the X and Y directions and 10 m in the Z direction allowed heterogeneities within the maar-diatreme to be modelled at this scale. This voxel resolution meant that both broader structures related to the geometry of the maar-diatreme and smaller property heterogeneities within it could be modelled.

The process of two and three dimensional forward and inverse modelling creates a set of non-unique solutions, with multiple models satisfying the observed geophysical anomalies (Whiting, 1986; Valenta et al., 1992; Jessell et al., 1993; McLean and Betts, 2003). In order to assess the potential ambiguity and uniqueness of the model and determine the importance of a particular structure to the geophysical response, a

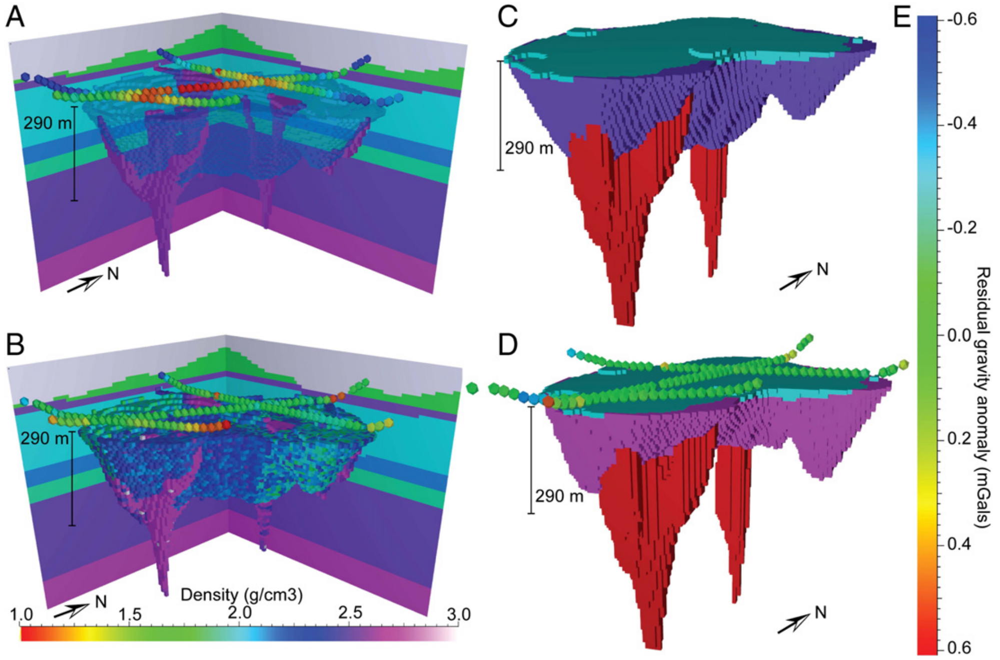

Fig. 8. A) Initial reference model. B) Heterogeneous inversion of the diatreme and feeder dykes. C) Initial and D) inverted geometry of the maar-diatreme. E) Colour bar for the residual gravity anomaly. (Colour of models A–B represents density and C–D lithology. Spheres represent individual gravity readings with the colour indicating the residual gravity anomaly).

sensitivity analysis was performed (e.g. McLean and Betts, 2003; Aitken et al., 2009; Stewart and Betts, 2010). Changes were made to the geometry and petrophysical properties of the model to determine if different model parameters could reproduce the observed data within an acceptable range of error.

A petrophysical sensitivity analysis involved systematically increasing and decreasing the densities of the diatreme and feeder vents to the upper and lower bounds of the constraints. The magnetic susceptibilities of the model were increased and decreased by an order of magnitude. The change in the calculated geophysical response was then compared to the observed data to assess how much of a geophysical influence a particular structure has on the model. Changes to the magnetic susceptibility of the model had only a minor influence on the calculated response, indicating that the model is less constrained by the magnetic data (Fig. 9A). Variations to the magnetic susceptibility would therefore not require a large variation to the geometry of the model to reproduce the observed data within an acceptable range of error. An increase and a decrease in the density of the maar-diatreme (Fig. 9B) had the greatest influence on the calculated gravity response, highlighting the importance of this structure to the model. Variations to the density of the diatreme would require its geometry to be altered significantly in order to maintain an acceptable misfit. Although the density of 2.1 g cm^{-3} applied to the diatreme is inferred because it could not be sampled directly, a significantly lower density is unexpected given that its componentry is likely to be similar to pyroclastic deposits and would have undergone some degree of compaction since the eruption. The effect of altering the density of the feeder dykes was less than that of the diatreme, but changes to this region of the model still had a strong influence on the calculated geophysical response (Fig. 9B).

A geometric sensitivity analysis involved changing the depth/geometry of different structures within the 2D models while the petrophysical properties were not altered to observe if other reasonable geologic solutions are possible. Several different models that were adequately able to reproduce the observed gravity response were produced, suggesting that the model is not highly sensitive to smaller geometric changes in the deeper regions of the maar-diatreme. The lack of sensitivity at depth is attributed partly to the size and resolution of the geophysical survey and also to the low density contrast between the host rock and diatreme margins, making the boundary between them difficult to define. However, results of multiple analyses indicate that a shallow cone-shaped structure produces the best fit to the observed data.

Another sensitivity analysis was applied to test the modelled structure against the structure of a maar within a hard rock setting, which consists of deeper diatremes with steeply dipping walls (Lorenz, 1975, 1986, 2003, 2007). If this structure is applied to Lake Coragulac, with diatreme walls dipping at 80°, then a diatreme depth of up to 750 m for the smaller vents and up to 1300 m for the larger vents would be expected. A 2D geophysical model was used to test this structure and the diatreme was modelled to a maximum depth of 900 m (Fig. 9C), however the calculated response of the model did not match observed data within an acceptable range of error. The modelled depth of 900 m is also considerably deeper than the depth of the diatreme predicted by the lithic content in pyroclastic deposits and is therefore considered geologically unrealistic. The difference between the proposed structure of a maar and the models of Lake Coragulac are attributed to the

Table 1
Initial and optimised densities of the 3D model.

Lithological region	Initial density (g cm^{-3})	Optimised density (g cm^{-3})
Diatreme	2.1	2.121
Feeder vents	2.6	2.699
Feeder dykes	2.6	2.619
Lake sediments	1.31	1.453
Lava flow	2.52	–
Tuff deposits	1.64	–
Gellibrand Marl	1.99	–
Nirranda formation	2.14	–
Eastern view group	1.9	–
Eumeralla formation	2.5	–

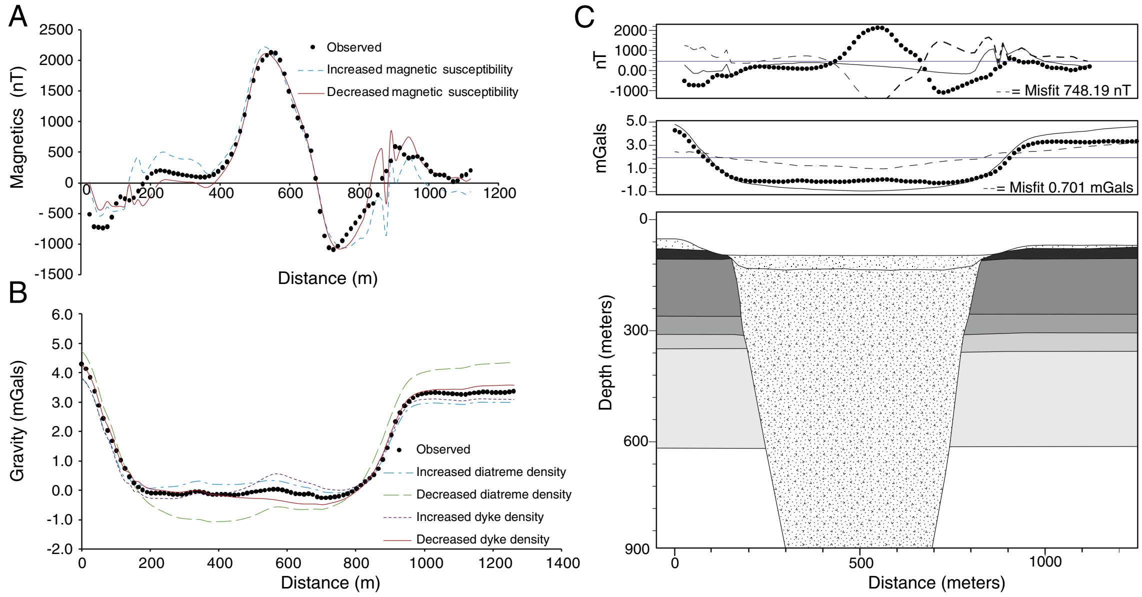

Fig. 9. A) Petrophysical sensitivity analysis of magnetic data increasing and decreasing the magnetic susceptibility of the model by an order of magnitude. B) Petrophysical sensitivity analysis of gravity data. The lower diatreme density limit is 1.7 g cm^{-3}, upper limit is 2.25 g cm^{-3}. Lower feeder vent density limit is 2.1 g cm^{-3}, upper density limit is 3.1 g cm^{-3}. C) Geometric sensitivity analysis of a deeper maar-diatreme.

rheology of the host rock, with Lake Coragulac being hosted in weakly lithified to unconsolidated sediments and the proposed models assuming a hard rock environment.

The results of these analyses highlight the importance of assessing which structures within a model have the most geophysical influence and how sensitive the model is to changes in the geometry and/or properties of those structures. The lack of sensitivity to geometric changes in the deeper parts of these models has important implications for future geophysical modelling of deep maar-diatremes. If for example, geologic evidence suggested that a deep diatreme existed below the Lake Coragulac maar, there would be a very low degree of confidence in a geophysical model of a deep diatreme given the current geophysical data set. Modelling of deeper maar structures may be possible where a greater petrophysical contrast between the host rock and diatreme infill exists, and when the geophysical survey is extended further beyond the maar rim. Deeper structures are associated with longer wavelength anomalies which can be detected with an increased station spacing that extends further from the vent, or alternatively filtering of existing data to remove shorter-wavelength anomalies associated with near-surface structures.

5. Discussion

Geophysical methods are increasingly relied upon to study the subsurface structures of maar volcanoes (e.g. Rout et al., 1993; Brunner et al., 1999; Schulz et al., 2005; Cassidy et al., 2007; Lopez Loera et al., 2008; Mrlina et al., 2009; Gebhardt et al., 2011). Observed geophysical anomalies have been variable, but in general maar volcanoes are characterised by a gravity low with a corresponding magnetic high, related to pyroclastic debris with a low density and high magnetic susceptibility infilling the maar-diatreme. The geophysical response of Lake Coragulac is similar to anomalies observed over other maar volcanoes including the Messel Pit and Baruth Maar in Germany (Schulz et al., 2005), the Pukaki maar in the Auckland Volcanic field (Cassidy et al., 2007), the Joya Honda maar in Mexico (Lopez Loera et al., 2008) and a newly discovered maar in the Bohemian Massif (Mrlina et al., 2009).

The broad, shallow, coalesced diatreme structures suggest that the weakly lithified host sediments influenced the final geometry of the diatreme (Lorenz, 2003; Auer et al., 2007; Ross et al., 2011). The modelled geometry of the diatreme is similar to descriptions of maar volcanoes hosted in a soft substrate (i.e. weakly or unconsolidated sediments), for example the Tatika maar-diatreme (Németh and Martin, 2007) and the Fekete-hegy maar-diatremes in Hungary (Auer et al., 2007), the Ellendale lamproite pipe in Western Australia (Smith and Lorenz, 1989) and Maegok in SE Korea (Kwon and Sohn, 2008). This type of diatreme structure forms as rising magma encounters poorly or unconsolidated sediments with water filled pore spaces. Water is immediately available to react with the magma and consequently prevents the downward migration of phreatomagmatic explosions (Auer et al., 2007). The surrounding substrate is made unstable or even liquefied by intense phreatomagmatic explosions, and water-bearing sediments can collapse or flow into the crater providing a new influx of water (Auer et al., 2007). While shallow maar-diatremes are often described in soft-substrate settings (Auer et al., 2007; Ross et al., 2011), and geologic evidence suggests that a shallow diatreme exists at the Lake Coragulac maar, there are examples of steep-walled maar-diatremes from the Missouri River Breaks, Montana that have formed within weak sedimentary host rocks (Hearn, 1968). Hearn (1968) suggests that the diatreme remained filled to near surface with pyroclastic debris during the eruption which would inhibit collapse of the weak host rock into the diatreme, preventing vent widening.

The geophysical model of Lake Coragulac suggests that numerous narrow dykes, either remnant feeder dykes or intrusions exist within the diatreme and along its margins. The alternating phreatomagmatic and magmatic pyroclastic deposits in the maar rim succession indicate frequent fluctuations in eruption styles. Variations in the style of fragmentation may be a result of periodic fluctuations in water availability within the aquifers, or the magma rise rate (Houghton et al., 1999). When magma–water interaction was inhibited, magma would have risen through the diatreme where it was fragmented at shallow levels by the expansion of magmatic volatiles.

The geophysical model of Lake Coragulac identified four different vents mostly coinciding with the main lobes of the maar. These vents may have erupted simultaneously or shown some temporal progression; however this level of detail could not be determined from geophysical modelling or from the very limited outcrop within the maar rim. Although the coalescence of the feeder dykes below the maar-diatreme could not be modelled due to the low sensitivity of the geophysical models at this depth, given the close proximity of eruption points, it seems likely that the maar was formed either along the length of a dyke or from lateral vent migration during the eruption.

Geophysical modelling has been unable to identify any linear trends in eruption points which might be expected if magma ascent occurred along the length of a dyke. Given the high number of eruption points in close proximity within the Red Rock Volcanic Complex, it is likely that a substantial dyke and sill system exists at depth below the surface and plays some role in determining the location of eruption points. However, given the lack of alignment of vents within the Lake Coragulac maar it is thought that lateral vent migration occurred in the shallow subsurface. This results from the collapse of unstable vent breccias onto the feeder dyke preventing the ascent of magma at that point (Ort and Carrasco-Núñez, 2009). Vent migration is often observed in maars in soft-substrates (e.g. Coombs Hill: White and McClintock, 2001, Tecuitlapa Maar: Ort and Carrasco-Núñez, 2009, Jeju Island: Sohn and Park, 2005) as weakly or unconsolidated sediments cannot sustain vertical walls for long and therefore collapse onto the feeder dyke (Martín-Serrano et al., 2009; Ort and Carrasco-Núñez, 2009; Ross et al., 2011). Alternatively, a slowing of the magma rise rate could result in the magma cooling and solidifying in the vent, forcing the vent to migrate and the magma to rise along a new path. Dykes identified within the maar-diatreme from the geophysical models could represent some of the maars' early vents which later became blocked and prevented further magma ascent at that point.

6. Conclusion

The Lake Coragulac maar of the Red Rock Volcanic Complex shows a complex eruption history, involving lateral vent migration and frequent fluctuations between explosive magmatic and phreatomagmatic fragmentation. Two and three-dimensional modelling of the Lake Coragulac maar revealed detailed information about the geometry of its underlying diatreme and feeder dykes that could otherwise not be detected by simply studying the maar rim pyroclastic deposits. Four broad, shallow coalesced diatreme structures were identified and indicate that soft-sediment behaviour influenced the eruption and final geometry of the diatreme. The modelled diatremes have a maximum depth of 280 m consistent with lithic fragments identified in pyroclastic deposits which suggest that phreatomagmatic fragmentation occurred within the Gellibrand Marl and propagated down to the Eastern View Formation. Multiple eruption points within the maar indicate that the vent migrated during the eruption, likely due to the collapse of country rock debris into the vent/dyke preventing magma ascent at that point. The fluctuations between magmatic and phreatomagmatic fragmentation represent a complex interplay between the magma rise rate and groundwater availability.

Acknowledgements

We wish to acknowledge the assistance provided by Alan Aitken with the geophysical surveys and his advice on data corrections and modelling and Felicity Piganis for her assistance in the field. We are grateful to all the land owners who allowed us to access to their properties to conduct fieldwork. The manuscript was greatly improved by suggestions from Dr Karoly Nemeth and one anonymous reviewer.

Appendix A. Supplementary data

Supplementary data to this article can be found online at http://dx.doi.org/10.1016/j.jvolgeores.2012.05.002.

References

Aitken, A.R.A., Betts, P.G., Weinberg, R.F., Gray, D., 2009. Constrained potential field modeling of the crustal architecture of the Musgrave Province in central Australia: evidence for lithospheric strengthening due to crust–mantle boundary uplift. Journal of Geophysical Research 114 (B12), B12405.
Auer, A., Martin, U., Nemeth, K., 2007. The Fekete-hegy (Balaton Highland Hungary) "soft-substrate" and "hard-substrate" maar volcanoes in an aligned volcanic complex — implications for vent geometry, subsurface stratigraphy and the palaeoenvironmental setting. Journal of Volcanology and Geothermal Research 159 (1–3), 225–245.
Brunner, I., Friedel, S., Jacobs, F., Danckwardt, E., 1999. Investigation of a tertiary maar structure using three-dimensional resistivity imaging. Geophysical Journal International 136 (3), 771–780.
Buness, H.A., Wiederhold, H., Wonik, T., 2006. Seismic reflection patterns of two tertiary maars in Germany. Zeitschrift der Deutschen Gesellschaft fur Geowissenschaften 157 (3), 339–353.
Cas, R.A.F., 1989. Physical volcanology. In: Johnson, R.W., Knutson, J., Taylor, S.R. (Eds.), Intraplate Volcanism in Eastern Australia and New Zealand. Cambridge University Press, pp. 55–88.
Cas, R.A.F., Simpson, C., Sato, H., 1993. Newer Volcanics Province — Processes and Products of Phreatomagmatic Activity. IAVCEI Canberra 1993: excursion guide, September, 1993. Geoscience Australia, Canberra, A.C.T., Australia (93 pp.).
Cas, R.A.F., Porritt, L., Pittari, A., Hayman, P.C., 2009. A practical guide to terminology for kimberlite facies: a systematic progression from descriptive to genetic, including a pocket guide. Lithos 112 (Supplement 1), 183–190.
Cas, R., Blaikie, T., Boyce, J., Hayman, P., Jordan, S., Piganis, F., Prata, G., van Otterloo, J., 2011. VF01: factors that influence varying eruption styles (from magmatic to phreato-magmatic) in intraplate continental basaltic volcanic provinces: the Newer Volcanics Province of south-eastern Australia. IUGG 2011 Fieldtrip guide.
Cassidy, J., France, S.J., Locke, C.A., 2007. Gravity and magnetic investigation of maar volcanoes, Auckland volcanic field, New Zealand. Journal of Volcanology and Geothermal Research 159, 153–163.
Constantine, A., Liberman, N., 2001. Hydrocarbon Prospecivity Package for VIC/O-01(1), VIC/0-01(2) and VIC/O-01(3), Eastern Onshore Otway Basin, Victoria, Australia. 2001 Acreage Release. : Victorian Initiative for Minerals and Petroleum Report, 70. Department of Natural Resources and Environment.
Edwards, J., Leonard, J.G., Pettifer, G.R., McDonald, P.A., 1996. Colac 1:250 000 map geological report. Geological Survey of Victoria Report, 98.
Francis, P.W., Glaze, L.S., Pieri, D., Oppenheimer, C.M.M., Rothery, D.A., 1990. Eruption terms. Nature 346, 519.
Fullagar, P.K., Hughes, N.A., Paine, J., 2000. Drilling-constrained 3D gravity interpretation. Exploration Geophysics 31 (1–2), 17–23.
Fullagar, P.K., Pears, G., Hutton, D., Thompson, A.D., 2004. 3D gravity and aeromagnetic inversion for MVT lead-zinc exploration at Pillara, Western Australia. Exploration Geophysics (Melbourne) 35, 142–146.
Fullagar, P.K., Pears, G.A., McMonnies, B., 2008. Constrained inversion of geologic surfaces - pushing the boundaries. The Leading Edge 27, 98–105.
Gebhardt, A.C., De Batist, M., Niessen, F., Anselmetti, F.S., Ariztegui, D., Haberzettl, T., Kopsch, C., Ohlendorf, C., Zolitschka, B., 2011. Deciphering lake and maar geometries from seismic refraction and reflection surveys in Laguna Potrok Aike (southern Patagonia, Argentina). Journal of Volcanology and Geothermal Research 201 (1–4), 357–363.
Hare, A.G., Cas, R.A.F., Musgrave, R., Phillips, D., 2005. Magnetic and chemical stratigraphy for the Werribee Plains basaltic lava flow-field, Newer Volcanics Province, southeast Australia; implications for eruption frequency. Australian Journal of Earth Sciences 52 (1), 41–57.
Hearn Jr., B.C., 1968. Diatremes with kimberlitic affinities in north-central Montana. Science 159 (3815), 622–625.
Houghton, B.F., Wilson, C.J.N., 1989. A vesicularity index for pyroclastic deposits. Bulletin of Volcanology 51 (6), 451–462.
Houghton, B.F., Wilson, C.J.N., Smith, I.E.M., 1999. Shallow-seated controls on styles of explosive basaltic volcanism: a case study from New Zealand. Journal of Volcanology and Geothermal Research 91 (1), 97–120.
Jessell, M.W., Valenta, R.K., Jung, G., Cull, J.P., Geiro, A., 1993. Structural geophysics. Exploration Geophysics 24 (3–4), 599–602.
Joyce, E.B., 1975. Quaternary volcanism and tectonics in southeastern Australia. Bulletin — Royal Society of New Zealand 13, 169–176.
Kwon, C., Sohn, Y., 2008. Tephra-filled volcanic neck (diatreme) of a mafic tuff ring at Maegok, Miocene Eoil Basin, SE Korea. Geosciences Journal 12 (4), 317–329.
Lesti, C., Giordano, G., Salvini, F., Cas, R., 2008. Volcano tectonic setting of the intraplate, Pliocene–Holocene, Newer volcanic province (southeast Australia); role of crustal fracture zones. Journal of Geophysical Research 113 (B7).
Lindner, H., Gabriel, Gotze, H.J., Kaeppler, R., Suhr, P., 2006. Geophysical and geological investigation of maar structures in the Upper Lusatia region (East Saxony). Zeitschrift der Deutschen Gesellschaft fur Geowissenschaften 157 (3), 355–372.
Lopez Loera, H., Aranda-Gomez, J.J., Arzate, J.A., Molina-Garza, R.S., 2008. Geophysical surveys of the Joya Honda Maar (Mexico) and surroundings; volcanic implications. Journal of Volcanology and Geothermal Research 170 (3–4), 135–152.
Lorenz, V., 1975. Formation of phreatomagmatic maar-diatreme volcanoes and its relevance to kimberlite diatremes. Physics and Chemistry of The Earth 9, 17–27.
Lorenz, V., 1986. On the growth of maars and diatremes and its relevance to the formation of tuff rings. Bulletin of Volcanology 48, 265–274.
Lorenz, V., 2003. Maar-diatreme volcanoes, their formation, and their setting in hard-rock or soft-rock environments. Geolines 15, 72–83.
Lorenz, V., 2007. Syn- and posteruptive hazards of maar-diatreme volcanoes. Journal of Volcanology and Geothermal Research 159 (1–3), 285–312.

Mallet, J.L., 1992. Discrete smooth interpolation in geometric modelling. Computer-Aided Design 24 (4), 178–191.
Mallet, J., 1997. Discrete modeling for natural objects. Mathematical Geology 29 (2), 199–219.
Martín-Serrano, A., Vegas, J., García-Cortés, A., Galán, L., Gallardo-Millán, J.L., Martín-Alfageme, S., Rubio, F.M., Ibarra, P.I., Granda, A., Pérez-González, A., García-Lobón, J.L., 2009. Morphotectonic setting of maar lakes in the Campo de Calatrava Volcanic Field (Central Spain, SW Europe). Sedimentary Geology 222 (1–2), 52–63.
McClintock, M., White, J., 2006. Large phreatomagmatic vent complex at Coombs Hills, Antarctica: wet, explosive initiation of flood basalt volcanism in the Ferrar–Karoo LIP. Bulletin of Volcanology 68 (3), 215–239.
McLean, M.A., Betts, P.G., 2003. Geophysical constraints of shear zones and geometry of the Hiltaba Suite granites in the western Gawler Craton, Australia. Australian Journal of Earth Sciences 50 (4), 525–541.
Mrlina, J., Kampf, H., Kroner, C., Mingram, J., Stebich, M., Brauer, A., Geissler, W.H., Kallmeyer, J., Matthes, H., Seidl, M., 2009. Discovery of the first Quaternary maar in the Bohemian Massif, Central Europe, based on combined geophysical and geological surveys. Journal of Volcanology and Geothermal Research 182 (1–2), 97–112.
Németh, K., Martin, U., 2007. Shallow sill and dyke complex in western Hungary as a possible feeding system of phreatomagmatic volcanoes in "soft-rock" environment. Journal of Volcanology and Geothermal Research 159 (1–3), 138–152.
Nicholls, I.A., Joyce, E.B., Knut son, J., 1989. East Australian volcanic geology: newer volcanics. In: Johnson, R.W., Taylor, S.R. (Eds.), Intraplate Volcanism in Eastern Australia and New Zealand. Cambridge University Press, pp. 137–141.
Ort, M.H., Carrasco-Núñez, G., 2009. Lateral vent migration during phreatomagmatic and magmatic eruptions at Tecuitlapa Maar, east-central Mexico. Journal of Volcanology and Geothermal Research 181 (1–2), 67–77.
Price, R.C., Gray, C.M., Frey, F.A., 1997. Strontium isotopic and trace element heterogeneity in the plains basalts of the Newer Volcanic Province, Victoria, Australia. Geochimica et Cosmochimica Acta 61 (1), 171–192.
Price, R.C., Nicholls, I.A., Gray, C.M., 2003. Cainozoic igneous activity. In: Birch, W.D. (Ed.), Geology of Victoria. : Geological Society of Australia Special Publication, 23. Geological Society of Australia (Victoria Division), pp. 361–375.
Ross, P.-S., White, J.D.L., 2006. Debris jets in continental phreatomagmatic volcanoes; a field study of their subterranean deposits in the Coombs Hills vent complex, Antarctica. Journal of Volcanology and Geothermal Research 149 (1–2), 62–84.
Ross, P.-S., Delpit, S., Haller, M.J., Nemeth, K., Corbella, H., 2011. Influence of the substrate on maar-diatreme volcanoes; an example of a mixed setting from the Pali Aike volcanic field, Argentina. Journal of Volcanology and Geothermal Research 201 (1–4), 253–271.
Rout, D.J., Cassidy, J., Locke, C.A., Smith, I.E.M., 1993. Geophysical evidence for temporal and structural relationships within the monogenetic basalt volcanoes of the Auckland volcanic field, northern New Zealand. Journal of Volcanology and Geothermal Research 57 (1–2), 71–83.
Schulz, R., Buness, H., Gabriel, G., Pucher, R., Rolf, C., Wiederhold, H., Wonik, T., 2005. Detailed investigation of preserved maar structures by combined geophysical surveys. Bulletin of Volcanology 68 (2), 95–106.
Sheard, M.J., 1990. A guide to Quaternary volcanoes in the lower south-east of South Australia. Mines and Energy Review — South Australia 157, 40–50.
Skacelova, Z., Rapprich, V., Valenta, J., Hartvich, F., Sramek, J., Radon, M., Gazdova, R., Novakova, L., Kolinsky, P., Pecskay, Z., 2010. Geophysical research on structure of partly eroded maar volcanoes; Miocene Hnojnice and Oligocene Rychnov volcanoes (northern Czech Republic). Journal of Geosciences 55 (4), 333–345.
Smith, C.B., Lorenz, V., 1989. Volcanology of the Ellendale lamproite pipes, Western Australia. In: Ross, J. (Ed.), Kimberlites and Related Rocks. Geological Society of Australia, Special Publication No. 14, pp. 505–519.
Sohn, Y.K., Park, K.H., 2005. Composite tuff ring/cone complexes in Jeju Island, Korea: possible consequences of substrate collapse and vent migration. Journal of Volcanology and Geothermal Research 141 (1–2), 157–175.
Stewart, J.R., Betts, P.G., 2010. Implications for Proterozoic plate margin evolution from geophysical analysis and crustal-scale modeling within the western Gawler Craton, Australia. Tectonophysics 483 (1–2), 151–177.
Tickell, S.J., Cummings, S., Leonard, I.G. and Withers, J.A., 1991. Colac 1:50 000 map geological report. Geological Survey of Victoria Report, 89.
Valenta, R.K., Jessell, M.W., Jung, G., Bartlett, J., 1992. Geophysical interpretation and modelling of three-dimensional structure in the Duchess area, Mount Isa, Australia. Exploration Geophysics (Melbourne) 23 (1–2), 393–400.
Walker, G., 1973. Explosive volcanic eruptions — a new classification scheme. Geologische Rundschau 62 (2), 431–446.
White, J.D.L., 1991. Maar-diatreme phreatomagmatism at Hopi Buttes, Navajo Nation (Arizona), USA. Bulletin of Volcanology 53, 239–258.
White, J.D.L., McClintock, M.K., 2001. Immense vent complex marks flood-basalt eruption in a wet, failed rift: Coombs Hills, Antarctica. Geology 29 (10), 935–938.
White, J.D.L., Ross, P.S., 2011. Maar-diatreme volcanoes: a review. Journal of Volcanology and Geothermal Research 201, 1–29.
Whiting, T.H., 1986. Aeromagnetics as an aid to geological mapping — a case history from the Arunta Inlier, northern territory. Australian Journal of Earth Sciences 33 (2), 271–286.
Williams, H.A., Betts, P.G., Ailleres, L., 2009. Constrained 3D modeling of the Mesoproterozoic Benagerie Volcanics, Australia. Physics of the Earth and Planetary Interiors 173 (3–4), 233–253.

Appendix 2.

The Red Rock Volcanic Complex

T. Blaikie, F. Piganis, R. Cas, L. Ailleres, P. Betts

In: Cas R. A. F., Blaikie T., Boyce J., Hayman P., Jordan S., Piganis F., Prata G. & van Otterloo J. 2011. VF01: Factors that influence varying eruption styles (from magmatic to phreato-magmatic) in intraplate continental basaltic volcanic provinces: the Newer Volcanics Province of south-eastern Australia. *IUGG 2011 Fieldtrip guide*.

Cover page: Arial photo of the Red Rock Volcanic Complex, viewed from the North-West. (Courtesy of Ray Cas.)

1. Introduction

The Red Rock Volcanic Complex (RRVC), located northwest of the township of Colac, is the most complex volcanic centre within the basaltic Newer Volcanics Province (NVP) of Western Victoria. The RRVC is the southern most of three closely placed volcanic centres, including the Mt. Alvie scoria cones (central) and the Warrion Hill lava shield (north). These closely spaced centres define a north-northeast trending lineament, presumed to reflect a major crustal fracture used by magmas as a conduit (Figure 1).

The surrounding area is typical of the geomorphological character of the NVP and is marked by the numerous rims of maars, tuff rings and scoria cones that overlie the flat to slightly undulating surface relief of extensive plain forming basaltic lava flows. The hummocky topography of the lava plains are marked by two types of lakes: those that have been ponded on the landscape by the damming effects of lava flows blocking pre-existing drainage systems (e.g., Lakes Colac and Corangamite), and those that are the crater lakes of maar, tuff ring or tuff cone volcanic centres (e.g. Lakes Purdigulac, Coragulac, Gnalinegurk and Werowrap (maars)).

The Red Rock Volcanic Complex is a multi-vent volcanic complex, consisting of over 40 identifiable eruption points that have formed multiple poly-lobate maars and scoria cones (Figure 2). Early phases of eruptive activity within the complex were dominantly phreatomagmatic, forming the scalloped shaped maars including Lakes Coragulac, Purdigulac, Gnalingurk and Werowrap. Following the formation of the maars, the eruptive style of the complex shifted to dominantly magmatic, producing the scoria cone complex in the northern region of the RRVC (Figure 2). The superposition of volcanic land forms indicates that the cone complex is later than the maars, however strombolian scoria fall deposits are interbedded with phreatomagmatic fall/surge deposits in the maar rim successions, suggesting that either some of the strombolian cones were active simultaneously with phreatomagmatic maar volcanism, or the maars themselves regularly fluctuated in eruption style from phreatomagmatic to magmatic.

The basement to the Newer Volcanics in this area comprises the Palaeocene-Mid Eocene sandy limestones of the Eastern View Group, overlain by Late Eocene marls of the Demons Bluff Formation and the Oligocene-Miocene calcareous silty clays of the Gellibrand Marl. These are in turn unconformably overlain by the quartzose sediments of the Pliocene Hanson Plain Sand, the Quaternary lavas of the NVP and the components of the three mentioned volcanic centres. Table 1 summarises the major stratigraphic units and key aquifers of the area (Tickell *et al.* 1991; Tabassi 1993). Lithic fragments identified in various maar rim sequences across the RRVC suggest that deepest levels of phreatomagmatic fragmentation occurred within the quartz sands rich aquifer of the Eastern View Formation. This formation occurs at a depth of 290-355, indicating that the maximum depth of maar diatremes below the complex is 355 m (Piganis 2011).

Volcanic eruptions that have occurred in this region, in chronological order are (Leach 1977, Piganis 2011):

1. The earliest phase of Newer Volcanics lavas, which may have dammed the landscape initially to produce the first ancestral lake deposits of the Corangamite system.
2. Eruption of the stony rise lavas from Warrion Hill and the RRVC

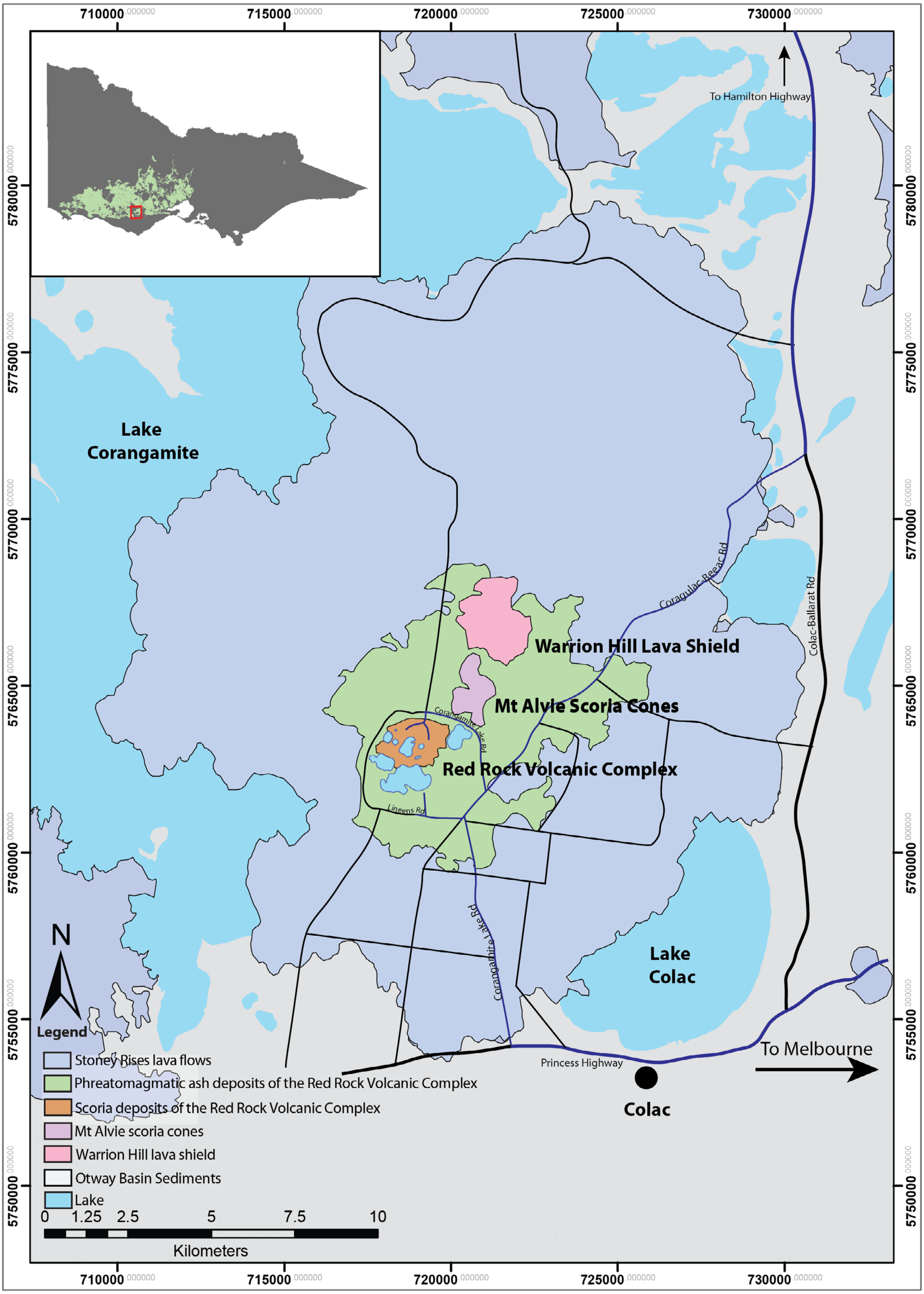

Figure 1. Locality diagram for the Red Rock Volcanic Complex.

3. Warrion Hill scoria and lava eruptions.
4. Final lava eruption from Warrion Hill.
5. Formation of the Mt. Alvie scoria cones.
6. Formation of maars within the RRVC.
7. Formation of the scoria cone complex within the RRVC.

The RRVC has been the focus of several detailed studies on the volcanic history, stratigraphy and geophysics of the region. These works include the unpublished works of Leach (1977), who concentrated on regional stratigraphy and chronology of volcanism, Forster (1983) and Van Tatenhove (1983), who studied in detail the pyroclastic deposits and the modes of formation and deposition around parts of Lake Coragulac and Lake Purdigulac maars respectively. More recent research into the physical volcanology and geophysics of the complex have been conducted by Cheeseman (2007), (Blaikie 2009), Piganis (2011) and Blaikie *et al.* (in prep).

STOP RR1: Red Rock Lookout

Red Rock Lookout - 1 km south of Alvie. From Melbourne drive to Colac via the Geelong-Princes Freeway and Princes Highway. From Colac drive 3km west along the Princes Highway to the Alvie Red-Rock turnoff (Cororooke Rd) on the right. Drive to Coragulac, turn left into Corangamite Lake Road. At Alvie follow signposts to Alvie and Red Rock Lookout (Figs. RR1, RR2). This outstanding vantage point is at the top of the scoria cone complex of the Red Rock Volcanic Complex. Numerous volcanic centres of the NVP can be seen on the skyline on a clear day, including the largest strombolian scoria cone of the NVP, Mt. Elephant to the northwest. To the west of the lookout, Lake Corangamite (the largest permanently wet lake in Australia) is visible.

The earliest volcanic activity within this region was marked by effusive pahoehoe lava flows, thought to have originated from the Warrion Hill lava cone/shield volcano. The products of these flows underlie the entire RRVC and can be seen outcropping at the bottom of the crater walls within Lake Coragulac. The eruption of the Red Rock Volcanic complex can be divided into three discrete phases (Piganis 2011). The oldest phase consisted of minor effusive activity from an unknown vent that produced pahoehoe lava flows, underlying part of the complex. The next eruptive phase was dominantly phreatomagmatic, forming the numerous maars (eg. Lakes Coragulac, Purdigulac, Werowrap and Gnalingurk) and their associated pyroclastic deposits. The eruptive style of the complex then shifted to dominantly magmatic, forming the scoria cone complex in the final phases of the eruption. The controls on these changes will be considered in discussion of Stops RR2. At least 20 vents associated with the formation of the maar craters have been identified by geophysical modelling of the complex (Blaikie et al. in prep, Piganis 2011), and its thought that there are at least another 28 eruption points associated with the scoria cone complex, making the RRVC the most complex volcanic centre within the NVP.

2. Geochemistry

Major and trace element geochemical analysis of deposits suggest that two different magma batches were sourced by the RRVC (Piganis 2011). Geochemical variations can be correlated spatially and stratigraphically across the complex, separating the lower lapilli-ash/tuff sequences of the Lake

Age	Depth (m)	Stratigraphy		Lithological description	Aquifer type
Quanternary			Newer Volcanics	Basalt, scoria and tuff	Fractured rock
Oligocene - Miocene	50 100 150 200	Gellibrand Marl	Heytesbury Group	Marl, calcareous clay and silt, clayey limestone	Aquitard to minor aquifer
Late Eocene	250	Demons Bluff Formation	Nirranda Group	Marl, silty marl, marly limestone and mudstone	Leaky aquitard
Paleocene - Mid Eocene	300	Eastern View Formation	Wangerrip Group	Quartz sand, gravel, calcareous sand, sandy limestone	Porous aquifer
Early Cretaceous	350 400	Eumeralla Formation	Otway Group	Sandstones, siltstone, mudstone, conglomerate, black coal	Fractured rock

Table 1. Stratigraphy and aquifer descriptions of the RRVC's subsurface geology

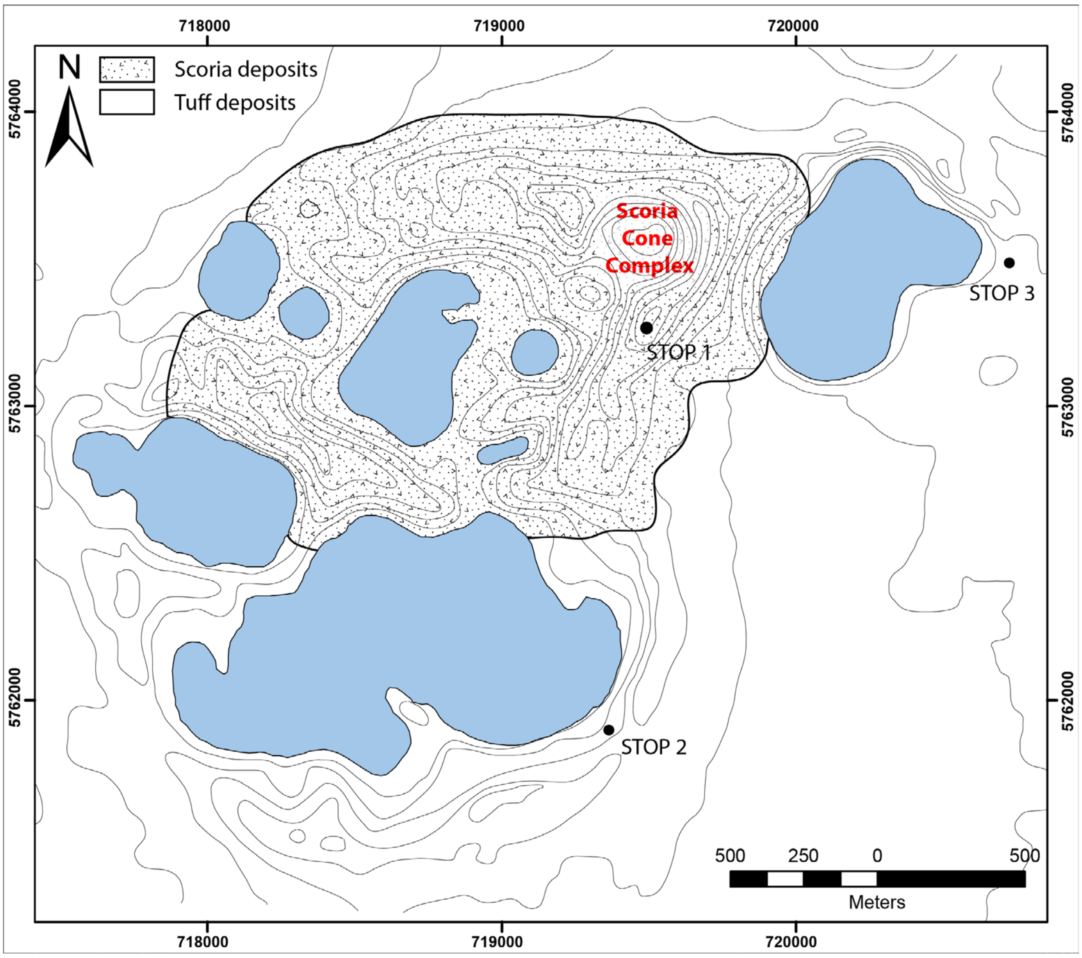

Figure 2. Contour map of the Red Rock Volcanic Complex showing the location of maars and cones. Lobate outlines of maars suggest multiple eruption points.

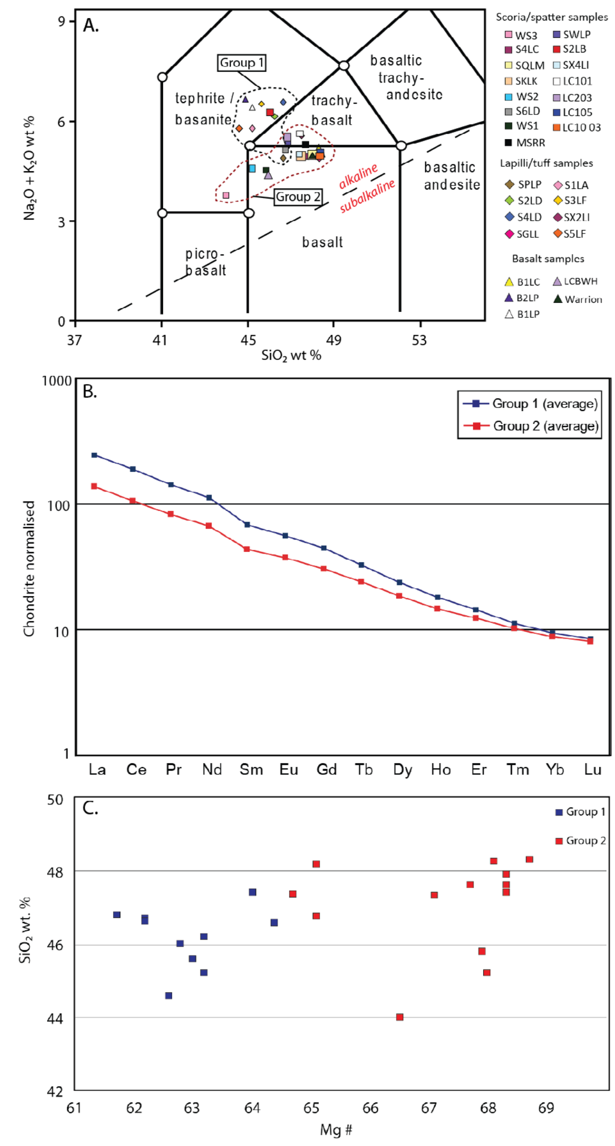

Figure 3. TAS, REE and Mg # vs. SiO_2 plot of geochemical data from various facies within the RRVC (Piganis 2011)

Purdigulac maar in the south of the complex (Group 1) to the upper lapilli-ash/tuff and scoria/spatter sequences of the other maars and scoria cone complex in the north (Group 2). Sequences from group 1 are classified as 'basanites' with a relatively higher total alkalies, REE and incompatible element concentrations compared to Group 2 which are classified as alkali-olivine to trachy-basalts with relatively lower total alkalies, REE and incompatible elements (Figures 3 a & b).

A plot of Mg# vs. SiO_2 wt. % (Figure 3b) distinctly shows that the southern and northern samples form separate magmatic suites. The southern alkaline basalts have lower Mg-numbers (61.7 - 64.4) and with most samples plotting below 46.8 wt. % SiO_2. In comparison, the northern sub-alkaline basalts have higher Mg-numbers (65.1 - 68.7) though similar SiO_2 values. This suggests that the two magmatic suites correspond to two different magma batches. The northern magmatic suite is more LREE enriched but also more primitive (Mg # 66 - 75); the southern basalts originated from a less LREE enriched magma which underwent some degree of crystal fractionation (Mg # <66; Irving and Green, 1976). Results indicate that two geochemically distinct magma batches sourced the explosive eruptions at Red Rock (Piganis 2011).

3. Geophysics

The surface morphology of the maar craters within the RRVC indicates that multiple vents may have coalesced to form the scalloped shape of each of the maars. Outcrop is limited, particularly in the northern part of the complex, so geophysical methods are relied upon to understand the subsurface morphology of the craters. Detailed ground based gravity and magnetic surveys have been conducted across each of the maars within the RRVC, and the data (Figure 4) has been subject to forward and inverse modelling in two and three dimensions (Figure 5).

Gravity and magnetic surveys have revealed contrasting geophysical anomalies between all the maars of the complex even though the surface morphology is similar. This highlights the complex and variable nature of volcanic systems and indicates there is substantial variation in subsurface structure between the maars. Maars with corresponding low gravity and magnetic anomalies suggest an eruption where all available magma interacted with external water. The resulting gravity and magnetic low arise as a result of the low density and magnetic susceptibility of pyroclastic debris and lake sediments infilling the maar diatreme. Maars with corresponding gravity and magnetic highs indicate the presence of a substantial body of basalt within the subsurface, possibly in the form of a plug or resulting from magma ponding at the surface of the vent. This indicates a lack of available groundwater during the eruption which has allowed magma to rise upwards through the maar diatreme. A vertical derivative of the gravity and magnetic data has highlighted frequency anomalies associated with shallow sources. Several local corresponding gravity and magnetic anomalies within the crater of Lake Werowrap can be observed and likely represent individual feeder vents or intrusive dykes within the maar diatreme.

Two-dimensional forward modeling allows geologic cross sections to be constructed based upon potential field data (McLean and Betts 2003). Free-air gravity and reduced to the pole magnetic data was extracted from gridded data and modeled in two dimensions. Two models covering Lake Werowrap and the two small maars in the west of the complex are shown in Figures 5 a & b. The two small maars on the western side of the traverse are characterised by small, shallowly dipping diatremes. The western-most maar does not appear to be characterised by any sizeable gravity or magnetic anomaly. This indicates that there is no substantial body of basalt in the subsurface, suggesting that the eruption was probably dominantly phreatomagmatic with all available magma interacting with water during the eruption. The central maar has a slightly higher gravity response, yet no local maximums are observed within the centre of the crater. A large magnetic anomaly observed across the maar however indicates that there is a substantial basalt body beneath the maar diatreme. Lake Werowrap, the eastern maar and the largest surveyed has a complex geophysical signature. Several local gravity and magnetic highs are observed across the maar and indicate the presence of basaltic intrusions within the maar diatreme, most likely remnant feeder dykes or late stage magma intrusions into the unconsolidated rocks of the newly formed diatreme.

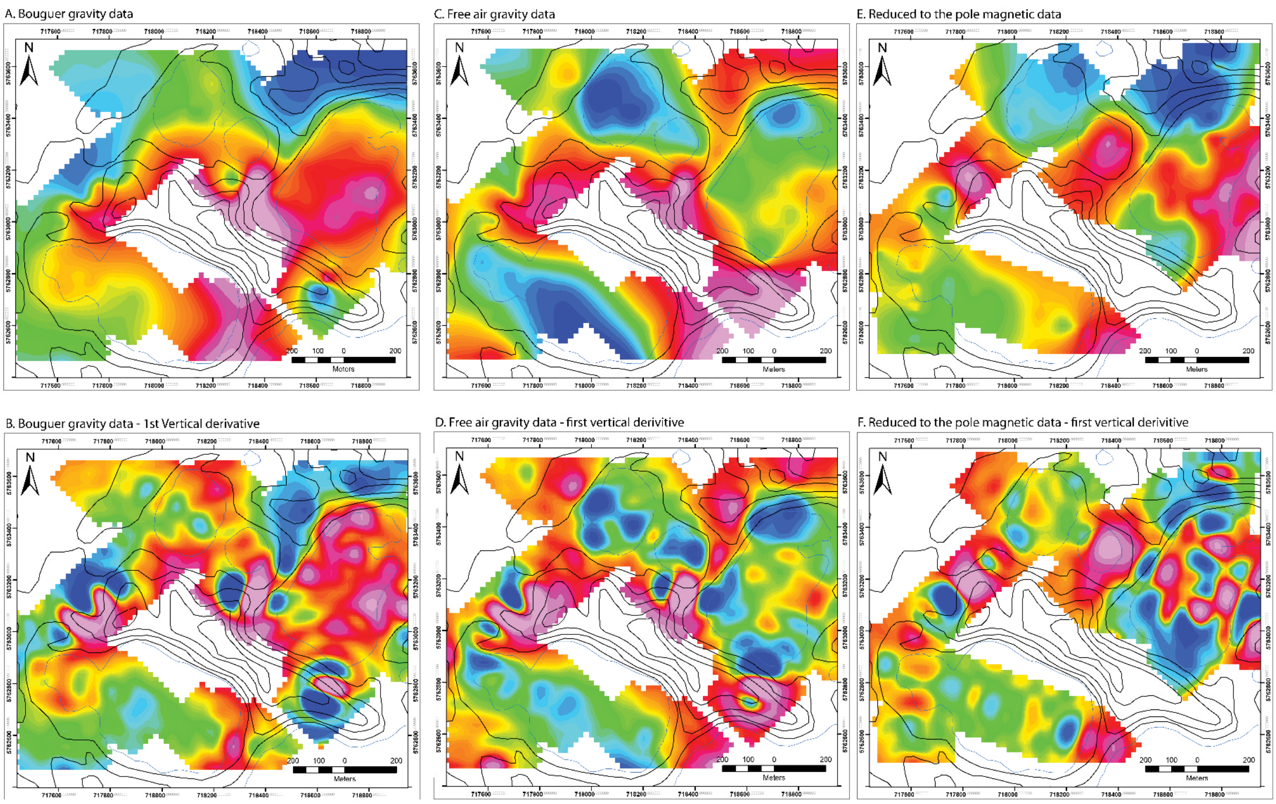

Figure 4. Bouguer, free air and reduced to the pole magnetic data for the north-western to central part of the RRVC showing the complex and variable geophysical signature of the maar volcanoes (Pink–red represents gravity/magnetic highs, blue-green represents gravity/magnetic lows, contours represent topography) (Blaikie *et al.* In prep).

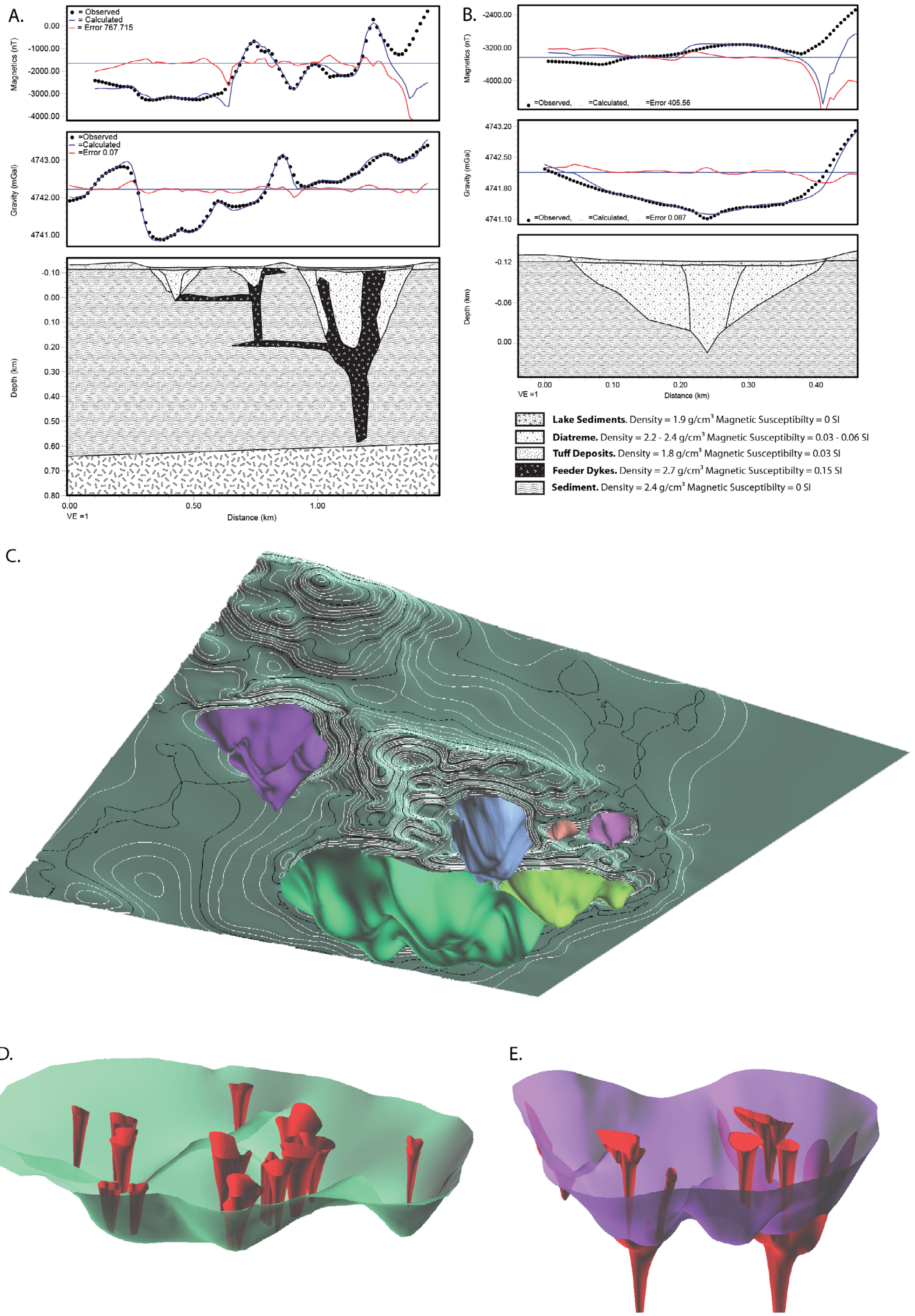

Figure 5. a 2D forward model of an E-W traverse across Lake Werowrap and the small maars in the west of the complex. **b.** 2D forward model of an N-S traverse across the small maar in the west of the complex. **c.** 3D model of multiple, coalesced, maar diatreme structures underlying the RRVC (Blaikie *et al.* In prep). **d & e** Internal structure of the Lakes Purdigulac and Coragulac maars respectively

The three-dimensional subsurface structures of the RRVC, including the geometry of maar diatremes and intrusive dykes have been defined from 16 cross-cutting 2D forward models of the complex. Modelling has revealed that multiple coalesced diatreme structures exist beneath the maar craters, suggesting that the eruption point of the maars frequently migrated. The maar diatremes are shallow and 'bowl' shaped, rather than the steeply dipping, deep pipe-like structures that are commonly observed within maar volcanoes and kimberlite pipes (Lorenz 1975, 1986). The structure of maar diatremes observed at the RRVC are consistent with maar diatremes hosted in soft-sediments (Lorenz 2003; Auer *et al.* 2007), indicating that the weakly lithified Tertiary sediments of the Otway Basin influenced the geometry of maar diatremes. The maximum depth of the diatremes determined by modelling is 350 m, whick is consistent with the depth of diatreme penetration determined from an analysis of accessory lithic fragments in the maar rim successions.

Scientific Questions for discussion

1. What caused the position of eruption points within the RRVC to migrate?
2. What caused the long term change from phreatomagmatic to magmatic explosive activity?
3. What is the significance of two magma batches?
4. What are the constraints and reliabilities of using geophysics to model subsurface maar structures?
5. How is the geometry of the maar diatreme influenced by the host rock?
6. How can understanding the subsurface structures of maar volcanoes improve our understanding of kimberlite emplacement processes?
7. To what degree can young basaltic maar volcanoes be used as analogues to kimberlite volcanoes?

STOP RR2 – Lake Purdigulac

Russell's Pit, Lake Purdigulac Maar, Red Rock Volcanic Centre. From the lookout return to Corangamite Lake Road, turn right and drive back towards Colac. Turn right into Lineen's Road and drive for approximately 1 km. Stop at the farmhouse into Russell's pit/quarry on the right and ask permission. This is private property and permission must be sought. Drive into quarry.

Variable eruption styles and depositional processes are clearly evident within the deposits across of the RRVC. Detailed mapping and logging of deposits across the entire complex have identified ten distinct facies on the basis of variations in grainsize, components and depositional structures. These facies are described in detail in the works of Cheesman (2007) and Piganis (2011) and are sumarised briefly below. A 15 m sequence of the maar rim deposits contained within an abandoned quarry on the southern margin of Lake Purdigulac provides some excellent exposures of many of the facies described below. Several stratigraphic logs from this sequence are shown in Figure 6 as an example.

The products which can be observed within this quarry include phreatomagmatic airfall and surge deposits as well as strombolian-style scoria fall deposits and distinctive ballistic block beds (Figure 6, 7 and Table 2). The alternation of phreatomagmatic deposits with magmatic strombolian-style fall deposits suggests that significant fluctuations in the degree of magma to water interaction have occurred. This is even reflected in the phreatomagmatic deposits by virtue of the variations in grain size, slumping features, and degree of vesiculation of clasts.

Table 2. Description of facies within the RRVC (Cheesman 2007; Piganis 2011)

Facies	Description	Mode of Fragmentation	Transportational and depositional origin
Basalt	Coherent basalt with vesicular upper crust	-	Pahoehoe lava flow
Welded spatter	Variably vesicular welded spatter clasts	Magmatic explosive	Agglutination of erupted magma from late stage Hawaiian fire fountaining
Massive scoria/ lapilli	Massive, unconsolidated, well sorted, variable vesicular (30-70%) scoria clasts 1-2 cm in size	Magmatic explosive	Strombolian fallout
Stratified scoria	Well bedded and sorted, variable vesicular, scoria, interbedded with ash/ tuff and lapill-ash/tuff facies	Magmatic explosive	Air fall
Block and bomb	Ballistic blocks (variably vesicular basalt and sandstone) impacting a fine grained ash/tuff displaying lensoidal layering	Phreatomagmatic	Phreatomagmatic base surges
Massive lapilli-ash/tuff	Lensoidal, clast to matrix supported with poor to moderate sorting of fragmented material	Phreatomagmatic	'Dry' phreatomagmatic base surges
Planar stratified lapilli-ash/tuff	Lensoidal to planar stratified layers of ash/tuff interbedded with coarser grained lapilli/tuff	Phreatomagmatic	'Dry' phreatomagmatic base surges
Cross stratified lapilli-ash/tuff	Well sorted, cross laminated lapilli-ash/ tuff	Phreatomagmatic	'Dry' phreatomagmatic base surges
Planar stratified ash/tuff	Planar, very well sorted, interstratified coarse lapilli/tuff and ash/tuff	Phreatomagmatic	'Wet' phreatomagmatic base surges
Cross stratified ash/tuff	Ash/tuff with gently dipping cross beds	Phreatomagmatic	'Wet' phreatomagmatic base surges

Outcrop 1

A prominent channel structure cut into bedded phreatomagmatic lapilli ashes and filled with bedded ash, lapilli ash and towards the top, scoria beds (Figs. RR7, RR8) occurs at the eastern end of the quarry and has two possible origins: eroded by surges, or eroded by fluvial gullying. The channel base shows no evidence of pre-filling weathering. It is overlain directly by steeply dipping pockets of slumped wet surge deposits rather than fluvial channel deposits, suggesting that a surge origin is likely. The lensoidal pocket of volcanic breccia within the lower part of the channel is problematic. It may be a fluvial lag deposit or a pocket of coarse clasts that were entrained by and deposited by surges. It is conformable with interpreted surge deposits and its top is concave up, both suggesting a surge origin.

Alternations of scoria deposits and phreatomagmatic deposits in the upper parts of the channel fill succession (Figs. RR7, RR8) indicate magma-water ratio variations during a continuous explosive eruption phase.

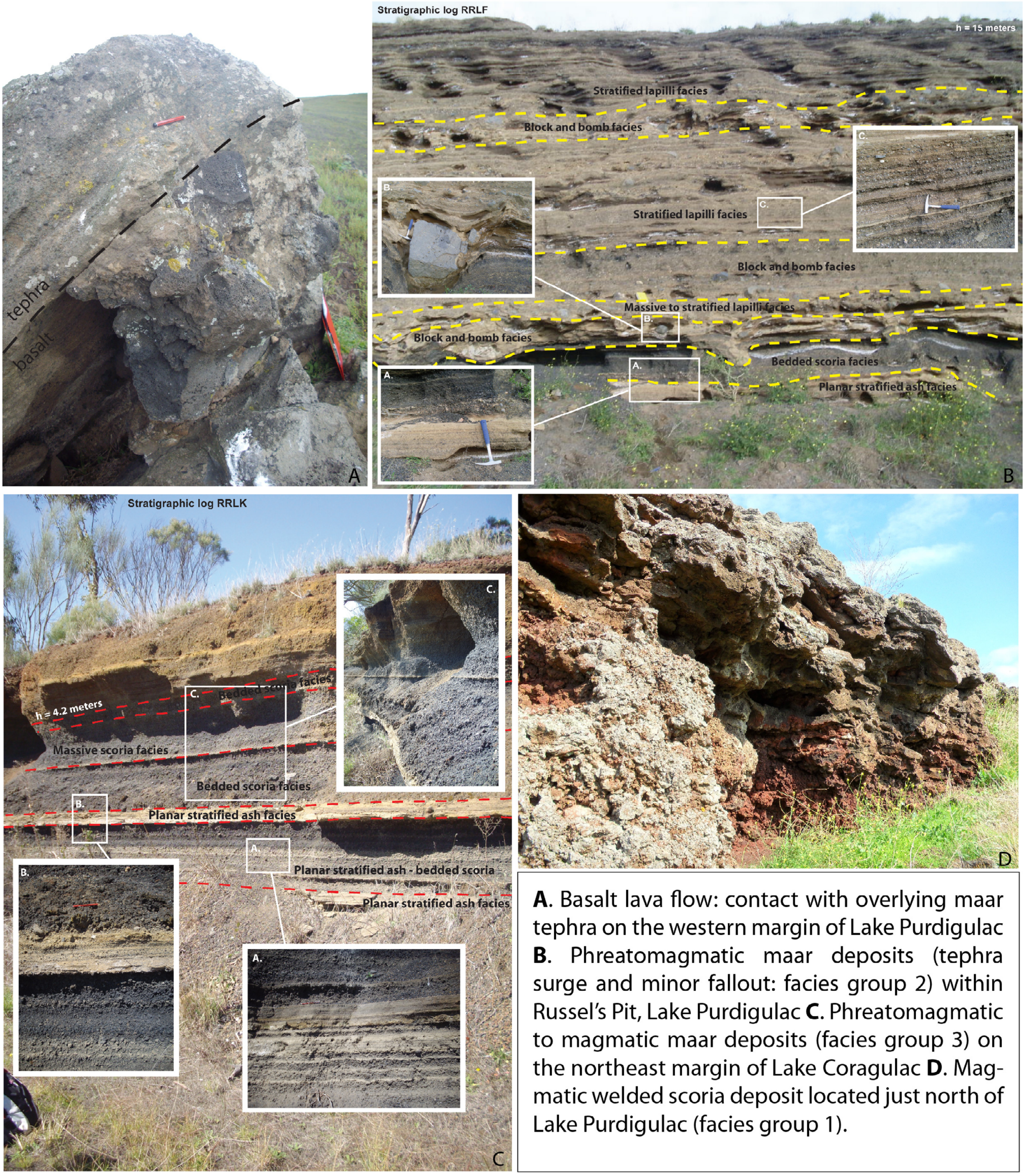

A. Basalt lava flow: contact with overlying maar tephra on the western margin of Lake Purdigulac **B**. Phreatomagmatic maar deposits (tephra surge and minor fallout: facies group 2) within Russel's Pit, Lake Purdigulac **C**. Phreatomagmatic to magmatic maar deposits (facies group 3) on the northeast margin of Lake Coragulac **D**. Magmatic welded scoria deposit located just north of Lake Purdigulac (facies group 1).

Figure 6. Different lithofacies of the RRVC (Piganis 2011)

Scientific questions for discussion:

1. Is the channel fluvial or surge in origin?

Outcrop 2

At the western end of the quarry two distinctive block horizons occur (Figs. RR6, RR8), with the largest blocks being up to 1 m in diameter. Major impact sag structures testify to the ballistic, explosive origin of the blocks. Blocks consist of both basalt and limestone and their eruption corresponds to a change from coarser lapilli-ash surge deposits to fine surge ash deposits. The dual compositional character of the blocks suggests that they originated by vent-wall erosion and therefore correspond to significant

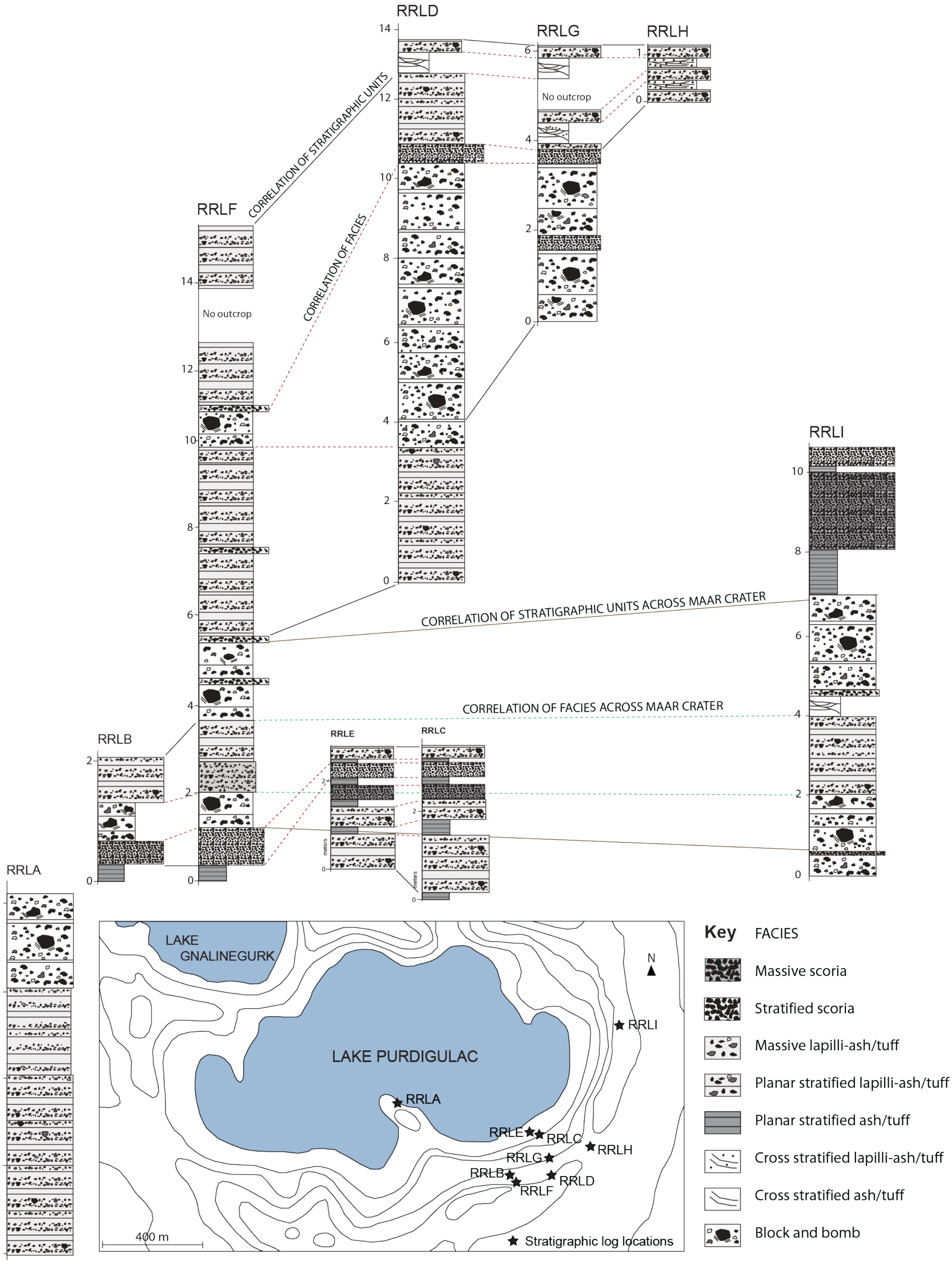

Figure 7. Stratigraphic logs of deposits in and around Russels Pit, Lake Purdigulac (Piganis 2011)

vent widening. The limestones may be representatives of the aquifer in which the phreatomagmatic explosions have occurred.

The distinction between fall and surge deposits is not easy but the principal criteria are: regular continuous layering in fall deposits, especially phreatomagmatic fall deposits; strombolian scoria fall deposits consist of well sorted highly vesicular scoria in massive or only faintly layered, laterally continuous deposits. Surge deposits are most rapidly identified by variably sorted, low angle crossstratification, low-angle truncations, pockets or lenses of pyroclasts, all of which imply the influence of lateral transport processes. In near-vent settings, both fall and base surge transport and deposition may be occurring simultaneously, producing surge-modified fall deposits (Cas 1989). The coarse lapilli-tuffs are considered to be examples of this.

Scientific questions for discussion:

1. Distinguishing between fall and planar stratified surge deposits
2. What has caused the fluctuating explosive eruption styles?

Outcrop 3

The low cutting at the crest of the tuff ring exposed in the road leading out of the quarry contains dune form and low angle cross stratified lapilli tuffs. The cutting is perpendicular to the maar rim, and surge flow directions were clearly away from the maar.

STOP 3: Lake Coragulac

Drive back along Lineens Rd and turn left on Corangamite Lake Rd, heading back towards the lookout. Turn left into the driveway of the Alvie Municipal Garbage Tip. On the right there is driveway leading to a disused quarry. This is a private property, stop at farm house to ask permission.

This old quarry preserves the succession of the eastern part of the Lake Coragulac Maar (Figure 8). Measured sections and lateral tracing indicate that stratigraphic units are laterally continuous, although variations in thickness and grainsize are clearly discernible, particularly in a direction perpendicular to the edge of the maar. The succession consists of layers of scoria ranging from cms to 70 cms thick, alternating with variably vesicular but denser clast lapilli-tuffs, and tuffs some as thin as millimetres. A course block and bomb bed represents the uppermost exposed horizon closest to the maar.

The scoria layers are massive to diffusely

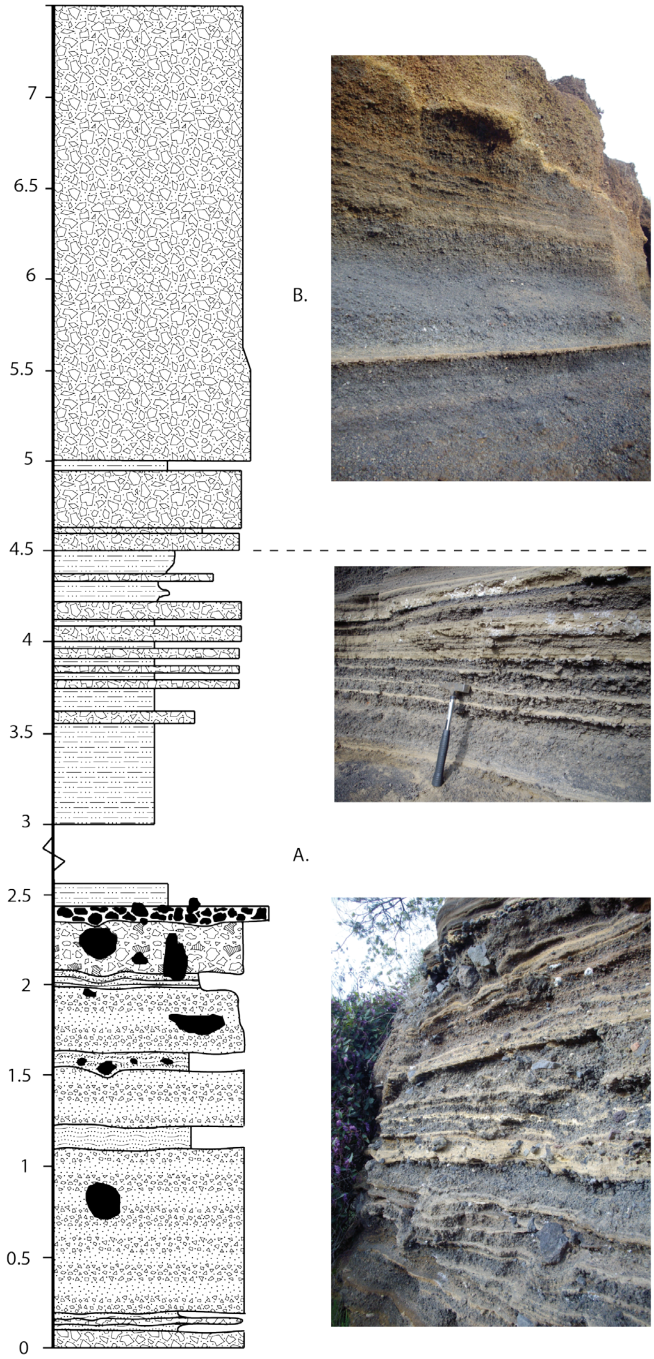

A. Interbedded phreatomagmatic ash and magmatic scoria deposits with lensoidal layering and balistic blocks. **B**. Massive to diffusely stratified scoria deposits with occasional thin interbeds of ash.

Figure 8. Stratigraphic log of the eastern maar rim succession of Lake Coragulac showing frequent alternations between ash and scoria deposits.

layered, are highly vesicular (60%-85%), and were clearly produced by magmatic explosive eruption phases, i.e. driven by exsolution and explosive expansion of magmatic volatiles.

The lapilli-tuff horizons vary from massive, diffusely layered to lensoidal layering with low angle discontinuities. Some clearly contain large ballistics. The vesicularity of juvenile clasts vary from low vesicularity (~ 20%) to high (60 %+). Ballistics include dense accessory basalt blocks (accessory lithics), sedimentary clasts including limestone and sandstone, and juvenile bombs. At the microscopic scale, abundant quartz silt grains are present in the finer ash deposits (Figure 9). This silt size quartz is xenocryst material, and like the larger sedimentary clasts, is derived from the Tertiary part of the Otway Basin. The finer ashes have cryptic accretionary lapilli. Many of these deposits are indurated, and juvenile fragments are palagonitized. These characteristics are consistent with phreatomagmatic explosive eruptive origins. Deposition appears to have been by near-vent base surge deposition, accompanied by fallout processes as evidenced at least by the ballistics. However, so near to vent, other debris in the lapilli-tuffs must also have originated as fall material. Many of the deposits are therefore surge modified fall deposits.

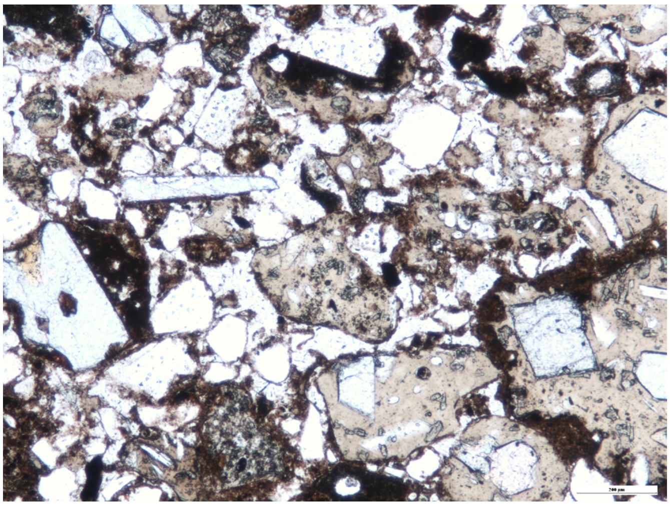

Figure 9. Thin section image of phreatomagmatic ash layer from the sequence at Lake Coragulac showing abundant angular to sub-rounded quartz xenocrysts in PPL.

A discontinuous horizon of accessory lithics, dense juvenile lithics and coarse scoria can be seen occurring as a series of fines depleted lenses. The overlying unit is a fine grained ash and lapilli-ash with undulating layering. Some of the elongate blocks have landed with long axis upright, and partially embedded in the underlying lapilli tuffs. These blocks appear to have been emplaced from ballistic trajectories. However, a ballistic trajectory origin does not explain the lensoidal nature and the regular 1-1.5m wavelength spacing of the lenses.

Two alternative explanations are possible. They may represent a trail of lithics and juvenile debris transported by the overlying surge deposits. Either the lithics segregated to the bottom of the base surge, or the lithics were incorporated into the base of surge from the existing depositional surface, and aggregated into regularly spaced lenses or dunes of debris as the surge passed through a flow regime stage where it began to oscillate.

The preferred interpretation is that the lenses represent a small fines depleted blast deposit. The blast flow would have produced disconnected debris lenses or dunes, much like starved ripple horizons produced by distal turbidites with a low granular sediment budget. The combination of identifiable ballistic blocks, with juvenile dense clasts and scoria, suggest a vulcanian type blast resulting from gas pressure build-up resulting from the development of a congealed lava crust in the vent.

An intriguing aspect of the succession is the alternation between scoriaceous and less vesicular phreatomagmatic layers, in places on a scale of millimetres and centimetres. It is clear that very rapid alternations have occurred in the mechanism driving explosive eruptions, from those driven by explosive expansion of magmatic volatiles to those driven by phreatomagmatic explosive interaction between groundwater and rising basaltic magma. Possible causes for such rapid alternations include slow recharge rates of the aquifer in the sub-surface zone of explosive interaction, or temporary development of, followed by collapse of a lining of impermeable basalt on the margins of the magma conduit. The absence of quartz silt and accessory lithics from the scoria deposits indicate that explosive disruption of the magma did not occur in the subsurface, as for the phreatomagmatic deposits, but in the open vent.

Although scoria fall deposits are usually associated with Strombolian scoria cone eruptions, in this case it would be difficult to imagine the scoria being derived from scoria cone sources, and the phreatomagmatic deposits being derived contemporaneously from the maar, producing such intricate layering. It seems more reasonable to consider the whole succession, including scoria deposits, to have been erupted from the maar, and the alternation of magmatic and phreatomagmatic deposits, to have been produced by variations in magma-water interaction. Scoria layers are therefore not just indicative of Strombolian scoria cone centres. Presumably scoria forming eruptions were too short to produce a cone, or if a small cone did begin to grow in the maar, it may have been destroyed by the next phreatomagmatic explosive burst.

4. Summary

- The deposits of the Red Rock Volcanic Complex record a complex history of phreatomagmatic and magmatic explosive activity. Although magmatic eruptive activity appears to have become dominant towards the later stages of the eruptive history, producing the strombolian scoria cones, it is clear that such strombolian style eruptions were also occurring sporadically as short-lived episodes from the maars, when for whatever reasons, the vent "dried up". Therefore, scoria deposits do not necessarily indicate scoria cone sources.
- Periodic "drying" of the vent occurred either due to low recharge rates in the aquifer, or the walls of the magma conduit were temporarily lined with impermeable basalt.
- Geochemical analysis suggests that two magma batches were sourced during the eruption of the Red Rock Volcanic Complex.
- Geophysical modelling the maar craters has identified multiple coalesced diatreme structures, indicating that the vents frequently migrated during the eruption.

5. References

Auer A., Martin U. & Németh K. 2007. The Fekete-hegy (Balaton Highland Hungary) "soft-substrate" and "hard-substrate" maar volcanoes in an aligned volcanic complex - Implications for vent geometry, subsurface stratigraphy and the palaeoenvironmental setting. *Journal of Volcanology and Geothermal Research* **159**, 225-245.

Blaikie T. 2009. Determining the subsurace structure of a maar volcano, Lake Coragulac, Red Rock Volcanic Complex. Honours thesis, Monash University, Australia (unpubl.).

Cheesman A. 2007. The nature of transitions between magmatic and phreatomagmatic explosive volcanism at the Red Rock Volcanic Complex, Newer Volcanics Province, Southeastern Australia. Masters thesis, Monash University, Australia (unpubl.).

Lorenz V. 1975. Formation of phreatomagmatic maar-diatreme volcanoes and its relevance to kimberlite diatremes. *Physics and Chemistry of The Earth* **9**, 17-27.

Lorenz V. 1986. On the growth of maars and diatremes and its relevance to the formation of tuff rings. *Bulletin of Volcanology* **48**, 265-274.

Lorenz V. 2003. Maar-Diatreme Volcanoes, their Formation, and their Setting in Hard-rock or Soft-rock Environments. *Geolines* **15**, 72-83.

McLean M. A. & Betts P. G. 2003. Geophysical constraints of shear zones and geometry of the Hiltaba Suite granites in the western Gawler Craton, Australia. *Australian Journal of Earth Sciences* **50**, 525-541.

Piganis F. 2011. A volcanological investigation of the polymagmatic Red Rock Volcanic Complex and a 3D geophysical interpretation of the subsurface structure and geology of the poly-lobate Lake Purdigulac maar, Newer Volcanics Province, southeastern Australia. Masters thesis, Monash University, Australia (unpubl.).

Tabassi A. 1993. Well completion report Nalangil-1. Gas and fuel exploration N.L, 1-14.

Tickell S. J., Cummings S., Leonard I. G. & Withers J. A. 1991. Colac 1:50 000 map geological report. *Geological Survey of Victoria Report* **89.**